UNCLASSIFIED

AD NUMBER: AD0064525

LIMITATION CHANGES

TO:

Approved for public release; distribution is unlimited.

FROM:

Distribution authorized to U.S. Government agencies and their contractors; Administrative or operational use; 15 Sep 1954. Other requests shall be referred to U.S. Army Signal Corps Engineering Laboratories, Fort Monmouth, NJ 07703.

AUTHORITY

ST-A USAEC LTR, 9 OCT 1968

THIS PAGE IS UNCLASSIFIED

AD 64525

Armed Services Technical Information Agency

Reproduced by

DOCUMENT SERVICE CENTER

KNOTT BUILDING, DAYTON, 2, OHIO

Because of our limited supply, you are requested to
RETURN THIS COPY WHEN IT HAS SERVED YOUR PURPOSE
so that it may be made available to other requesters.
Your cooperation will be appreciated.

NOTICE: WHEN GOVERNMENT OR OTHER DRAWINGS, SPECIFICATIONS OR OTHER DATA ARE USED FOR ANY PURPOSE OTHER THAN IN CONNECTION WITH A DEFINITELY RELATED GOVERNMENT PROCUREMENT OPERATION, THE U. S. GOVERNMENT THEREBY INCURS NO RESPONSIBILITY, NOR ANY OBLIGATION WHATSOEVER; AND THE FACT THAT THE GOVERNMENT MAY HAVE FORMULATED, FURNISHED, OR IN ANY WAY SUPPLIED THE SAID DRAWINGS, SPECIFICATIONS, OR OTHER DATA IS NOT TO BE REGARDED BY IMPLICATION OR OTHERWISE AS IN ANY MANNER LICENSING THE HOLDER OR ANY OTHER PERSON OR CORPORATION, OR CONVEYING ANY RIGHTS OR PERMISSION TO MANUFACTURE, USE OR SELL ANY PATENTED INVENTION THAT MAY IN ANY WAY BE RELATED THERETO.

UNCLASSIFIED

AD No. 42525
ASTIA FILE COPY

No. 11

DEPARTMENT OF ELECTRICAL ENGINEERING
UNIVERSITY OF MINNESOTA

Final Report

Research and Development on Design Method for Reactors

September 15, 1952 to September 15, 1954

Contract No. DA 36-039 sc-42573
D.A. Proj. No. 3-26-00-602
S.C. Proj. No. 32-2006C

PLACED BY: U.S. ARMY, SIGNAL CORPS ENGINEERING LABORATORIES
FORT MONMOUTH, NEW JERSEY

REGENTS OF THE UNIVERSITY OF MINNESOTA
MINNEAPOLIS, MINNESOTA

Research and Development on Design Method for Reactors

Final Report

September 15, 1952 to September 15, 1954

The object of this research and development program is the establishment of a design method for audio, power, pulse and video reactors in accordance with Squier Signal Laboratory Technical Requirements for PR and C No. 52-ELS/D-3434, dated 3 March 1952.

Contract No. DA 36-039 sc-42573

D.A. Proj. No. 3-26-00-602

S.C. Proj. No. 32-20060

Report prepared by: J.T. Ludwig, P.E.

TABLE OF CONTENTS

		Page
I. Purpose.		1
II. Abstract		2
IIII. Publications, Reports and Conferences.		3
IV. Factual Data		8
A. Theory Section.		8
Chapter 1	Introduction	8
Chapter 2	The Basic Equations.	11
Chapter 3	The Analysis of Inductors. . . .	19
	Analysis with Specified Alternating Voltage Component	19
	Analysis with Specified Current.	23
	Analysis of Resistance	25
Chapter 4	The Design Method for Inductors Limited by Copper Resistance . .	27
	Shape Numbers and General Equations.	27
	Minimum Size Design.	29
	Auxiliary Axes and Variable Stack Heights.	36
	Design with Zero Air Gap	42
	Design with Induction Limitation	44
Chapter 5	The Design Method for Inductors Limited by Copper Loss Heating .	46
	Minimum Size Design.	46
	Auxiliary Axes and Variable Stack Heights.	49
	Design with Zero Air Gap	51
	Design with Induction Limitation	52

Chapter 6 The Design Method for Inductors Limited by Total Resistance. . . 54

General Equations. 54

Design with Equal Copper and Core Loss Resistance. 58

Design Limited by Copper Resistance. 61

Chapter 7 The Design Method for Inductors Limted by Total Loss Heating . . 63

General Equations. 63

Design with Equal Copper and Core Loss. 65

Design Limited by Copper Loss. . 67

Chapter 8 The General Design Method. . . . 70

B. Procedure Section 71a

Chapter 9 Curve Construction 71a

General Data 71a

Chart 1A Construction. 74

Chart 1B Construction. 79

Chart 1C Construction. 79

Chart 2A Construction. 80

Chart 2B Construction. 80

Chart 2C Construction. 82

Chart 3 Construction 83

Chart 3A Construction. 84

Chapter 10 Design Procedures. 85

Reistance Limitation 85

Heating Limitation 91

Core Selection by Charts 1 and 2 97

Winding Calculation. 98

Chapter 11 Analysis Procedures. 100

Voltage Specified. 100

Current Specified. 102

Chapter 12 Examples and Models. 105

C. Additional Data 142

Chapter 13 Inductor Circuits. 142

Specifications 142

Power Filter Inductors 143

Pulse Charging Inductors 143

Audio and Video Inductors. . . . 144

Chapter 14 Measurement and Testing. 146

Inductor Measurements. 146

Material Measurements. 147

Chapter 15 Other Inductive Components . . . 150

Electronic Inductors 150

Inductors with Permanent Magnet Gaps 150

Appendix A Symbols. 152

Appendix B Bibliography 154

V. Conclusions. 166

VI. Recommendation 157

VII. Personnel. 158

VIII. Figures, Charts and Tables 159

Appendix C Armour Report. 228

LIST OF FIGURES

Figure		Page
1.	The Normal Induction Curve and One Symmetrical Major Hysteresis Loop.	159
2.	The Normal Induction Curve and One Unsymmetrical (minor) Hysteresis Loop	160
3.	The Normal Induction Curve With Karapetoff's Air Gap Line to Find d-c Induction in Absence of a-c Induction.	161
4.	The Biased (anhysteretic) Induction Curves with Air Gap Line to Find the Center of the Minor Loop.	162
5.	Incremental Permeability Curves	163
6.	The Normal Induction Curve with Air Gap Line to Find the Upper Tip of the Minor Loop . . .	164
7.	The Incremental Induction Curves with Air Gap Line to Find the Incremental Induction. . . .	165
8.	Core Loss with Biasing Magnetizing Force as a Parameter	166
9.	Core Loss with Maximum Magnetizing Force as a Parameter	167
10.	Scrapless EI Lamination	168
11.	Normal Induction Curve with a Minor Loop Extending Above the "Knee".	169
12.	Map of Synthesis Method	170
13.	Normal Induction Curve.	171
14.	Normal Permeability Curve	172
15.	Incremental Permeability Curves	173
16.	Construction of Incremental Permeability Curves with H_{max} as Parameter	174
17.	Incremental Permeability vs B_{max} with B_{Δ}/B_{max} as Parameter.	175
18.	Incomplete Chart 1A Showing I_{Δ}/I_{max} Points. .	176
19.	Construction of g_{lr}, n_{lr} and S Axes	177

20. Choke Input Filter. 178
21. Capacitor Input Filter. 178
22. Simplified Pulser Circuit 178
23. Charging Inductor Waveforms for Circuit of figure 22 179
24. Shunt Fed Amplifier 180
25. Push-pull Modulator 180
26a. Pulser Power Supply 181
26b. Pulser Trigger Generator. 182
26c. Pulser. 183
27. Hay Bridge. 184
28. Major Minor Waveforms and Loop. 185
29a. High Frequency B-H Looper, Upper Chasis . . . 186
29b. High Frequency B-H Looper, Lower Chassis. . . 187
30. Mechanical Major Minor Loop Generator 188
31. Integrator. 189
32. Low Frequency Integrator. 190
33. Design Models 191

II. ABSTRACT

Methods of analysis are presented for calculating the inductance of inductors when the physical parameters are given. The two methods cover the cases where either the a-c voltage wave or the current wave is known and there is no restriction on the magnitudes of the a-c/d-c components.

Methods of synthesis are presented for designing minimum size inductors when the electrical specifications and the physical shape are given. These methods cover the range from the case of an infinitely small a-c component of current superposed on a d-c component to the case where the current reaches zero once each cycle.

Some principles are given for the sine wave testing of inductors which will operate with non sinusoidal waveforms. Test methods for obtaining incremental data are described.

Areas for further study including iron measurements and new devices are suggested.

III. PUBLICATIONS, REPORTS AND CONFERENCES

Quarterly reports were issued as follows.

Report	Period	Authors
1st Quarterly	September 15 to December 15, 1952	P.A. Cartwright J.T. Ludwig
2nd Quarterly	December 15, 1952 to March 15, 1953	P.A. Cartwright J.T. Ludwig
3rd Quarterly	March 15 to June 15, 1953	P.A. Cartwright J.T. Ludwig G.J. Murphy
4th Quarterly	June 15 to September 15, 1953	P.A. Cartwright J.T. Ludwig G.J. Murphy
5th Quarterly	September 15 to December 15, 1953	P.A. Cartwright J.T. Ludwig G.J. Murphy
6th Quarterly	December 15, 1953 to March 15, 1954	P.A. Cartwright J.T. Ludwig G.J. Murphy

Monthly letter-type reports were issued as follows:

Number	Period	Authors
1	August 15-September 15, 1952	P.A. Cartwright
2	September 16 - October 15, 1952	P.A. Cartwright
3	October 16 - November 15, 1952	P.A. Cartwright
4	December 16, 1952 - January 15,1953	P.A. Cartwright
5	January 16 - February 15, 1953	P.A. Cartwright
6	March 16 - April 15, 1953	P.A. Cartwright
7	April 16 - May 15, 1953	P.A. Cartwright
8	June 16 - July 15, 1953	P.A. Cartwright

Number	Period	Authors
9	July 16 - August 15, 1953	P. A. Cartwright
10	September 16 - October 15, 1953	P. A. Cartwright
11	October 16 - November 15, 1953	P. A. Cartwright
12	December 16, 1953 - January 15, 1954	P. A. Cartwright
13	January 15 - February 15, 1954	P. A. Cartwright
14	March 16 - April 15, 1954	P. A. Cartwright
15	April 16 - May 15, 1954	P. A. Cartwright
16	May 16 - June 15, 1954	J. T. Ludwig

A special report, Discussion of Charging Choke Test Method by J. T. Ludwig, April 30, 1953, was submitted to the Squier Signal Laboratory.

The theory of this design method was published in a thesis, A Study in the Design of Magnetic Circuits Employing Soft Magnetic Materials and Superposed A-C and D-C Magnetization by J. T. Ludwig, July 1954. This thesis was sent to the Squier Signal Laboratory and is to be published on microfilm by University Microfilms, Ann Arbor, Michigan.

Conferences on the general progress of the project were held with Squier Signal Laboratory representatives in Minneapolis as follows:

Date	Signal Corps Personnel
August 19-20, 1952	I. Remis
December 5, 1952	E. Wiler
February 25, 1953	I. Remis and N. Canon

Date	Signal Corps Personnel
May 16, 1953	N. Capon
August 10, 1953	I. Remis
September 9-10, 1953	Wiler (see below, 13th project review meeting)
December 4, 1953	I. Remis
May 17, 1954	I. Remis

Oral Reports were given at the following project review meetings of the Audio, Power and Pulse group of the Coils, Inductors and Transformers Subpanel of the Research and Development Board and the succeeding military advisory group.

Project Review Meeting	Date	Place	University Personnel	Subcontractor Personnel
10th	9/27-28/52	Wright AFB	Cartwright Ludwig	
11th	1/26-27/53	Washington DC	Cartwright Ludwig	
12th	6/1-2/53	Detroit	Cartwright Ludwig Murphy	
13th	9/9-10/53	Minneapolis	Cartwright Ludwig Murphy	Sell
14th	2/8-9/54	Johnsville NADC	Cartwright Ludwig	Sell

Visits were made to the following establishments to obtain information for this project.

Date	Establishment	University Personnel
1/28/53	General Electric Company Transformer and Allied Products Department Holyoke, Massachusetts	P. A. Cartwright J. T. Ludwig
1/29/54	Squier Signal Laboratories Fort Monmouth, New Jersey	P. A. Cartwright J. T. Ludwig
3/16/53	Westinghouse Electric Corporation Transformer Division Greenville, Pennsylvania	J. T. Ludwig
3/17/53	Bell Telephone Laboratories Power Apparatus Department Murray Hill, New Jersey	J. T. Ludwig
3/18/53	Weston Electrical Instrument Corporation Newark, New Jersey	J. T. Ludwig
3/18/53	Squier and Evans Signal Laboratories Fort Monmouth, New Jersey	J. T. Ludwig
3/19/53	General Electric Company Specialty Transformer and Ballast Department Fort Wayne, Indiana	J. T. Ludwig
9/21/53	Armco Steel Corporation Research Laboratories Middletown, Ohio	J. T. Ludwig
9/22/53	Bell Telephone Laboratories Power Apparatus Department Murray Hill, New Jersey	J. T. Ludwig
9/23/53	Squier Signal Laboratories Fort Monmouth, New Jersey	J. T. Ludwig
9/24/53	Ferroxcube Corporation of America Saugerties, New York	J. T. Ludwig

(cont'd)

Date	Establishment	University Personnel
9/25/53	General Electric Company Research Laboratory Schenectady, New York	J. T. Ludwig
9/29/53	Representatives in Chicago: Arnold Engineering Company Marengo, Illinois Magnetics, Inc. Butler, Pennsylvania	J. T. Ludwig
9/30/53	Armour Research Foundation Electrical Engineering Department Chicago, Illinois	J. T. Ludwig
2/9/54	Squier Signal Laboratory Fort Monmouth, New Jersey	P. A. Cartwright

IV Factual Data

A. Theory Section

CHAPTER 1

INTRODUCTION

The problem is that of designing electrical inductors each consisting of a ferromagnetic core interlinking a coil of wire. It is desirable that a method of design proceed from the specified electrical characteristics directly to the physical dimensions of the inductor without the use of trial-and-error methods.

Methods of analysis have been discussed by several writers.* [1 through 13] with various degrees of approximation and trial-and-error procedure. Of particular significance is the method given by Karapetoff in 1911 for finding the induction in a series magnetic circuit when a known d-c magnetomotive force is applied. This method, involving an "air gap" line superposed on the iron normal induction curve requires no trial-and-error procedures as in the ordinary method which requires the assumption of an induction and the calculation of the resulting magnetomotive force for comparison with the given magnetomotive force. The writer will show how Karapetoff's method may be extended, by the use of various induction curves, for the analysis of inductors with superposed a-c and d-c magnetization.

The design of iron core inductors is usually accomplished by use of analysis methods rather than synthesis methods.

* Refer to Bibliography, Appendix B.

The designer usually assumes several physical dimensions and from these he calculates others. He then analyzes the result (by mathematical computation or by measuring a model) and adjusts the assumed physical dimensions in a trial and error process until the required specifications are met. When a good supply of previous designs or experience is at hand, the method of analysis of the assumed solution is a good one because the assumed solution will be very close to the correct one and few trials-and-errors are required. When the supply of designs does not cover the region of a new required design, the trial-and-error process is lengthy and a direct synthesis method is to be preferred.

There are relatively fewer papers on synthesis. Among them are those by Hanna,[14] Crowhurst,[15] Carter and Richards,[16] and Legg.[17] Hanna's method[14] which has widespread usage will determine the best air gap to use for an inductor when the core size is known or assumed. Carter and Richards[16] present an algebraic method of synthesis, and Crowhurst[15] presents a graphical method based on a similar derivation, but both of these assume that the maximum incremental permeability is a simple exponential function of the polarizing magnetizing force, and this is not an entirely satisfactory approximation over the range normally encountered.

Legg[17] has attacked the problem by solving the system of governing equations in such a manner that a design chart may be prepared from the magnetic characteristics of the core material. This chart specifies all the physical dimensions when the electrical requirements are known.

These four methods all are applied to the case of small a-c inductions and the use of copper resistance as the only size-limiting factor. In a d-c power supply filter the chokes following the first capacitor nearly always have these requirements, but most other applications may have requirements limiting the core loss. A design method not subject to these limitations is the objective of this study.

The basic attack on the problem is the simultaneous solution of the pertinent equations relating the electrical, magnetic and physical factors in terms of the iron characteristics. With the electrical specifications known, the physical dimensions and magnetic factors may be found from charts obtained from the iron characteristics.

CHAPTER 2

THE BASIC EQUATIONS

An "ideal" magnetic circuit will be considered in the mathematical analysis. This ideal circuit is one in which the magnetic induction is constant around the circuit, there is no fringing of flux lines at points where the permeability changes as at an air gap. The principal error introduced by this idealization is that a real air gap having the same reluctance as the ideal gap will be physically longer than the ideal gap. In practice the exact spacing of the actual gap, having the same reluctance as the calculated ideal gap may be found by adjusting the gap of a model.

The fundamental equations relating the electrical conditions in the coil to the magnetic conditions in the core will be considered. The magnetomotive force acting in a closed path is defined by

$$m \triangleq \oint \hat{h} \cdot d\hat{\ell} \quad , \qquad (2\text{-}1)$$

where m is the mmf in gilberts,

$\hat{h}$ is the magnetizing force vector (oersteds),

and $d\hat{\ell}$ is the infinitesimal vector element of length along the path (centimeters).

From Ampere's Law,

$$\oint \hat{h} \cdot d\hat{\ell} = .4\pi Ni \quad , \qquad (2\text{-}2)$$

Where N is the number of turns linking the path

and i is the current through the turns in amperes.

Faraday's Law for the induced electromotive force acting in a closed path is,

$$e = -N \frac{d\phi}{dt} \; 10^{-8}, \qquad (2\text{-}3)$$

where e is the induced electromotive force in volts,

N is the number of turns

ϕ is the magnetic flux in maxwells which links every turn,

and t is the time in seconds.

Now the magnetic flux ϕ is related to the magnetic induction b by

$$\phi = \iint \vec{b} \cdot \vec{ds} \qquad (2\text{-}4)$$

where $\vec{b}$ is the magnetic induction vector (gausses) and $\vec{ds}$ is the infinitesimal vector element of area (square centimeters).

It should be noted that a mixed system of units is being used. All the magnetic and spacial units are in the centimeter-gram-second electromagnetic system while the electrical units are in the meter-kilogram-second practical system. This system is used since in U. S. practice nearly all electrical specifications are in mks units and nearly all magnetic material data are in cgs electromagnetic units.

All that remains to complete the system of equations specifying the operation of the magnetic circuit is the relation between b and h, and in the ideal circuit postulated, only the magnitudes of these vectors need by considered.

In a magnetic circuit composed of an iron core with an

air gap, the relationship in the air gap is quite simple, namely,

$$b = h, \qquad (2\text{-}5)$$

where b is the magnetic induction in gausses,

and h is the magnetizing force in oersteds.

In the iron, however, the relationship is very complicated. It is neither linear nor single valued, and it is this complicated relationship that makes the design of magnetic circuits a difficult and esoteric art.

The first relation between the induction b and the magnetizing force h is the normal induction curve and associated with it, the normal permeability. The normal induction curve is the locus of the tips of all symmetrical hysteresis loops and is shown in Figure 1 together with one of the symmetrical hysteresis loops which determine it. The coordinates of any point on the normal induction curve are then the maximum values, B_{max} and H_{max}, for some symmetrical loop. The normal permeability μ for any point on the normal induction curve is defined by,

$$\mu \triangleq \frac{B_{max}}{H_{max}} . \qquad (2\text{-}6)$$

Since μ is a function of either B_{max} or H_{max}, the choice of the independent variable is arbitrary. In the method of analysis it is more convenient to use the direct relation between B_{max} and H_{max} (the normal induction curve) but in the synthesis method it is more convenient to use the normal permeability.

A second relation between b and h is necessary to

describe unsymmetrical hysteresis loops in which the maximum and minimum values are not the equal negatives of each other. Such a loop is shown in figure 2 together with the normal induction curve. The maximum point of this loop lies on the normal induction curve. [16,18,19,20]

An incremental permeability is associated with each unsymmetrical or minor loop. It is usually defined as

$$\mu_\Delta = \frac{\Delta B}{\Delta H} , \qquad (2\text{-}7)$$

where ΔB is the total change of induction in gausses and ΔH is the total change of magnetizing force in oersteds. Alternatively

$$\mu_\Delta = \frac{B_\Delta}{H_\Delta} , \qquad (2\text{-}8)$$

where B_Δ is half the total change of induction in gausses and is called the incremental induction, and H_Δ is half the total change of magnetizing force in oersteds and is called the incremental magnetizing force.

This incremental permeability represents the slope of the minor loop and is a function of any two variables which specify the tips of the minor loop.

The relative "location" of the minor loop is determined by the upper tip which falls on the normal induction curve so the ratio of B_{max} to H_{max} is the normal permeability. Another method of specifying the "location" of the minor loop is by means of the center point whose coordinates are B_b and H_b, the biased induction and the biasing magnetizing force,

describe unsymmetrical hysteresis loops in which the maximum and minimum values are not the equal negatives of each other. Such a loop is shown in figure 2 together with the normal induction curve. The maximum point of this loop lies on the normal induction curve.[16,18,19,20]

An incremental permeability is associated with each unsymmetrical or minor loop. It is usually defined as

$$\mu_\Delta \triangleq \frac{\Delta B}{\Delta H} , \qquad (2\text{-}7)$$

where ΔB is the total change of induction in gausses and ΔH is the total change of magnetizing force in oersteds. Alternatively

$$\mu_\Delta = \frac{B_\Delta}{H_\Delta} , \qquad (2\text{-}8)$$

where B_Δ is half the total change of induction in gausses and is called the incremental induction, and H_Δ is half the total change of magnetizing force in oersteds and is called the incremental magnetizing force.

This incremental permeability represents the slope of the minor loop and is a function of any two variables which specify the tips of the minor loop.

The relative "location" of the minor loop is determined by the upper tip which falls on the normal induction curve so the ratio of B_{max} to H_{max} is the normal permeability. Another method of specifying the "location" of the minor loop is by means of the center point whose coordinates are B_b and H_b, the biased induction and the biasing magnetizing force,

respectively. The relationship between B_b and H_b depends on B_Δ or H_Δ as well as B_b or H_b so the use of this method of locating the minor loop involves one more variable and is therefore not used in this development except where data are already presented in terms of B_b or H_b.

Since the magnetic induction is uniform around the circuit, the development will make use of the permeabilities as functions of the inductions rather than functions of magnetizing forces. In this manner μ will represent $\mu\ (B_{max})$ where B_{max} is the peak induction of a major (symmetrical) or minor (unsymmetrical) loop, and μ_Δ will represent $\mu_\Delta\ (B_{max}, B_\Delta)$.

The integral $\int h \cdot d\ell$ may now be evaluated at the point of maximum current, induction and magnetizing force. In the iron, from (2-6),

$$H_{max} = \frac{B_{max}}{\mu} \quad , \tag{2-9}$$

and the integral $\int H_{max} \cdot d\ell$ in the iron is

$$\int_{\ell_i} H_{max} \cdot d\ell = \frac{B_{max}\, \ell_i}{\mu} \quad , \tag{2-10}$$

where ℓ_i is the iron length in centimeters.

In the air gap from (2-5)

$$H_{max} = B_{max} \tag{2-11}$$

and the integral $\int H_{max}\, d\ell$ in the air is,

$$\int_{a\ell_i} H_{max}\, d\ell = B_{max} a\ell_i \quad , \tag{2-12}$$

where $a\ell_i$ is the length of the air gap in centimeters. The integral around the whole circuit is then,

$$\int_{max} = \oint H_{max} d\ell = B_{max}\, \ell_i \left(\frac{1}{\mu} + a\right), \qquad (2\text{-}13)$$

and by (2-2),

$$B_{max}\, \ell_i \left(\frac{1}{\mu} + a\right) = .4\pi N I_{max}, \qquad (2\text{-}14)$$

where I_{max} is the peak current in amperes.

Solving (2-14) for B_{max} leaves

$$B_{max} = \frac{.4\pi N\, I_{max}}{\ell_i \left(\frac{1}{\mu} + a\right)} \qquad (2\text{-}15)$$

which is a basic equation for the derivation of the design method.

The integral $\oint h d\ell$ may also be evaluated for the incremental variation. Thus

$$\frac{\oint H_{max}\, d\ell - \oint H_{min}\, d\ell}{2} = \oint \frac{H_{max} - H_{min}}{2} \cdot d\ell = H_\Delta d\ell \qquad (2\text{-}16)$$

from the definition of H_Δ.

In the iron, from (2-8),

$$H_\Delta = \frac{B_\Delta}{\mu_\Delta} \qquad (2\text{-}17)$$

and the integral $\int h d\ell$ in the iron is,

$$\int_{\ell_i} H_\Delta\, d\ell = \frac{B_\Delta \ell_i}{\mu_\Delta}. \qquad (2\text{-}18)$$

In the air gap from (2-5),

$$\int_{a\ell_i} H_\Delta d\ell = B_\Delta\, a\ell_i, \qquad (2\text{-}19)$$

and the total integral is,

$$H_\Delta = \oint H_\Delta \cdot d\ell = B_\Delta\, \ell_i \left(\frac{1}{\mu} + a\right), \qquad (2\text{-}20)$$

where M_Δ is the incremental magnetomotive force in gilberts, being half the difference of the maximum and minimum values of magnetomotive force.

Now by (2-2),

$$\frac{M_{max} - M_{min}}{2} = .4\pi N\left(\frac{I_{max} - I_{min}}{2}\right) \qquad (2\text{-}21)$$

and substituting M_Δ and I_Δ for the appropriate quantities

$$M_\Delta = .4\pi N I_\Delta . \qquad (2\text{-}22)$$

from (2-20) and (2-22),

$$B_\Delta \ell_i \left(\frac{1}{\mu_\Delta} + a\right) = .4\pi N I_\Delta , \qquad (2\text{-}23)$$

and solving for B_Δ ,

$$B_\Delta = \frac{.4\pi N I_\Delta}{\ell_i \left(\frac{1}{\mu_\Delta} + a\right)} , \qquad (2\text{-}24)$$

which is the second basic equation for the design method.

The equation for the inductance of a coil linking this magnetic circuit may be derived from the definition of inductance:

$$e = - L \frac{di}{dt} . \qquad (2\text{-}25)$$

where L is the inductance in henries. The back electromotive force is given by (2-3) so this value may be inserted into (2-25).

$$-N \frac{d\phi}{dt} 10^{-8} = - L \frac{di}{dt} \qquad (2\text{-}26)$$

and (2-26) may be solved for L to give

$$L = N \frac{d\phi}{di} \times 10^{-8} . \qquad (2\text{-}27)$$

Assuming approximately linear variation of flux with current the derivative $d\phi/di$ is approximated by $\bar{\phi}_\Delta/I_\Delta$ so that

$$L = N \frac{\bar{\phi}_\Delta}{I_\Delta} 10^{-8} .$$

From (2-4)

$$\bar{\phi}_\Delta = B_\Delta a_i \qquad (2\text{-}28)$$

where a_i is the net cross sectional area of the iron in square centimeters.

Therefore

$$L = \frac{NB_\Delta a_i}{I_\Delta 10^8} , \qquad (2\text{-}29)$$

and substituting B_Δ from (2-24) gives

$$L = \frac{.4\pi N^2 a_i}{\ell_i \left(\frac{1}{\mu_\Delta} + a\right)} 10^{-8} . \qquad (2\text{-}30)$$

This is the basic inductance equation to be used in the derivation.

CHAPTER 3

THE ANALYSIS OF INDUCTORS

A method of analysis, determining the electrical characteristics from the physical configuration, is helpful to the design procedure in providing a check on designs and in evaluating the effect of changes of the various physical dimensions.

Because of the non-linearity of the iron characteristics, the inductance of any iron-core inductor is not a constant but depends upon the electrical conditions under which it is operated. Methods of analysis will be developed for two types of electrical conditions:

1. The biasing current, I_b, and a time varying component of voltage $e'(t)$ which produces a symmetrical time varying current component are specified.
2. The current $i(t)$ is specified.

Analysis With Specified Alternating Voltage Component

When the time varying component of voltage is given it is assumed that the voltage drop across the resistance R_c is small compared to the back electromotive force of the inductance, and the analysis begins with equation (2-3). If it is integrated with respect to time it becomes

$$\int_{t_1}^{t_2} e' \, dt = - N \, 10^{-8} \int_{\phi(t_1)}^{\phi(t_2)} d\phi \qquad (3\text{-}1)$$

and

$$\int_{t_1}^{t_2} e' \, dt = - N \, 10^{-8} \left[\phi(t_2) - \phi(t_1)\right] \qquad (3\text{-}2)$$

If t_1 and t_2 are now chosen points of minimum and maximum $\int e' \, dt$ respectively,

$$\phi(t_1) = \bar{\Phi}_{min} \, , \qquad (3\text{-}3)$$

$$\phi(t_2) = \bar{\Phi}_{max} \, , \qquad (3\text{-}4)$$

and

$$\int_{t_1}^{t_2} e' \, dt = - N \, 10^{-8} \left[\bar{\Phi}_{max} - \bar{\Phi}_{min}\right] . \qquad (3\text{-}5)$$

If

$$\bar{\Phi}_{\Delta} = \frac{\bar{\Phi}_{max} - \bar{\Phi}_{min}}{2} \, , \qquad (3\text{-}6)$$

$$\int_{t_1}^{t_2} e' \, dt = - 2 N \bar{\Phi}_{\Delta} \, 10^{-8} \, , \qquad (3\text{-}7)$$

and substituting $\bar{\Phi}_{\Delta}$ from (2-28) gives

$$\int_{t_1}^{t_2} e' \, dt = -2NB_{\Delta} \, a_1 \, 10^{-8} \, . \qquad (3\text{-}8)$$

The sign of B_{Δ} is irrevelant to the analysis so

$$B_{\Delta} = \frac{\int_{t_1}^{t_2} e' \, dt \, 10^{8}}{2N \, a_1} \, . \qquad (3\text{-}9)$$

When e' is a sinusoidal wave with frequency f and effective value E_{ac},

$$e' = \sqrt{2} \, E_{ac} \cos 2\pi f t \qquad (3\text{-}10)$$

$$\int_{t_1}^{t_2} e' \, dt = \frac{\sqrt{2} \, E_{ac}}{2\pi f} \left(\sin 2\pi f t_2 - \sin 2\pi f t_1\right) \qquad (3\text{-}11)$$

The value of $\int e' \, dt$ is minimum at $-\frac{1}{4f}$ and maximum at $+\frac{1}{4f}$, t_1 and t_2 are set equal respectively to $-\frac{1}{4f}$ and $+\frac{1}{4f}$ and

$$\int_{-\frac{1}{4f}}^{+\frac{1}{4f}} e' \, dt = \frac{\sqrt{2}\, E_{ac}}{nf} \quad . \tag{3-12}$$

Inserting this value into (3-9) gives

$$B_\Delta = \frac{E_{ac} \times 10^8}{\sqrt{2}\ nf\ N\ a_i} \quad , \tag{3-13}$$

or

$$B_\Delta = \frac{E_{ac} \times 10^8}{4.44\ f\ N\ a_i} \quad , \tag{3-14}$$

which is the customary transformer equation.

Karapetoff[5] described a method for finding the induction in a uniform magnetic circuit with air gaps when a known d-c magnetomotive force is applied. First it is assumed that the relation between B and H in the iron is known and plotted as in Figure 3. If the circuit is magnetized by a magnetomotive force $.4\pi NI$, the magnetomotive force equation is

$$.4\pi\ N\ I = H\ \ell_1 + B\alpha\ \ell_1 \quad , \tag{3-15}$$

or alternatively,

$$\frac{.4\pi NI}{\ell_1} = H + B\alpha \quad . \tag{3-16}$$

This is the equation of a straight line on the BH plane having intercepts

$$H = \frac{.4\pi\ N\ I}{\ell_1} \tag{3-17}$$

and

$$B = \frac{.4\pi\ N\ I}{\alpha\ \ell_1} \quad . \tag{3-18}$$

It may be plotted by means of these intercepts or any two points which satisfy (3-16). Such a line is shown in Figure 3. The intersection of this line with the iron BH curve then gives the induction and magnetizing force in the iron. The B value of this point is the induction and magnetizing force in the air gap.

In the analysis of the inductor with specified I_b and $e'(t)$, this method can be applied to find the B_b, H_b point.[21] A set of plots of B_b versus H_b for various B_Δ values is shown in Figure 4. The equation of the Karapetoff line is

$$\frac{.4\pi N I_b}{\ell_1} = H_b + B_b \alpha \,, \tag{3-19}$$

and its intercepts are

$$H_b = \frac{.4\pi N I_b}{\ell_1} \,, \tag{3-20}$$

and

$$B_b = \frac{.4\pi N I_b}{\alpha \ell_1} \,. \tag{3-21}$$

The values of B_b and H_b in the iron may be found at the intersection of this line with the B_bH_b curve for the particular value of B_Δ, already found by (3-9) or (3-14).

One method of presenting incremental permeability data is shown in Figure 5. Several curves show μ_Δ as a function of B_Δ each for a different value of H_b. The values of B_Δ and H_b already found are used to find μ_Δ directly from this graph.

The inductance L may be calculated by

$$L = \frac{.4\pi N^2 a_1}{\ell_1 \left(\frac{1}{\mu_\Delta} + \alpha\right)} \; 10^{-8} \,. \tag{2-36}$$

Thus, when an alternating voltage and a direct current are specified the analysis steps are:

1. Calculate B_Δ from (3-9) or (3-14).
2. Construct Karapetoff line on the biased induction curves (B_b vs. H_b). For the value of B_Δ found above, read B_b and H_b. (3-19), (3-20), (3-21).
3. For B_Δ and H_b found above find μ_Δ from curve, Figure 5.
4. Calculate the inductance from (2-30).

Analysis With Specified Current

When the current, i(t), is specified, a different analysis method is used. First the minimum and maximum values of i(t) are determined and I_Δ is calculated by

$$I_\Delta = \frac{I_{max} - I_{min}}{2} \quad . \tag{3-22}$$

Karapetoff's method is first applied to the normal induction curve such as Figure 6. The equation of the straight line is,

$$\frac{.4\pi N I_{max}}{\ell_i} = H_{max} + B_{max}\alpha \quad . \tag{3-23}$$

and its intercepts are,

$$H_{max} = \frac{.4\pi N I_{max}}{\ell_i} \quad . \tag{3-24}$$

and

$$B_{max} = \frac{.4\pi N I_{max}}{\alpha \ell_i} \quad . \tag{3-25}$$

The intersection of the normal induction curve and the straight line is the H_{max}, B_{max} point of the minor loop since the right

hand (H_{max}, B_{max}) tips of all the minor loops lie on the normal induction curve independently of B_Δ or H_Δ.

Instead of considering the incremental permeability curves as before, the incremental induction (B_Δ vs. H_Δ) curves shown in Figure 7 will be used with another Karapetoff line construction. Each incremental induction curve is associated with one (H_{max}, B_{max}) point on the normal induction curve and the appropriate curve (or interpolated curve) is used for the (H_{max}, B_{max}) value found by the first (normal induction curve) Karapetoff line construction. The line on this incremental induction graph is drawn to fit the equation

$$\frac{.4\pi N I_\Delta}{\ell_i} = H_\Delta + B_\Delta \alpha \, , \qquad (3\text{-}26)$$

which may be derived from Ampere's law equations for I_{max} and I_Δ points. The intercepts are

$$H_\Delta = \frac{.4\pi N I_\Delta}{\ell_i} \, , \qquad (3\text{-}27)$$

and

$$B_\Delta = \frac{.4\pi N I_\Delta}{\alpha \ell_i} \, . \qquad (3\text{-}28)$$

The intersection of this line with the proper incremental induction curve gives H_Δ and B_Δ in the iron and the B_Δ value is also the incremental induction and incremental magnetizing force in the air gap. The inductance L can now be found from

$$L = \frac{N B_\Delta a_i}{I_\Delta} 10^{-8} \, . \qquad (2\text{-}29)$$

Thus, when the current is specified the analysis steps are:

1. Construct Karapetoff line on normal induction curve.

(3-23), (3-24), (3-25). Read B_{max} and H_{max}.

2. Construct Karapetoff line on incremental induction curves. For the value of B_{max} found above, read B_Δ and H_Δ. (3-26), (3-27), (3-28).
3. Calculate the inductance from (2-29).

Analysis of Resistance

In either case the copper resistance R_c is calculated by the usual methods.

The general resistance equation is

$$R_c = \frac{\rho N \ell_c}{a_w} \quad , \qquad (3\text{-}29)$$

where ρ is the resistivity in ohm-centimeters

N is the numbers of turns

ℓ_c is the mean length of turn in centimeters

and a_w is the cross sectional area of the wire in square centimeters.

A more convenient method for the resistance calculation is the use of a wire table for the value of ρ/a_w and the appropriate $N\ell_c$ in the units consistent with the wire table units.

The core loss component of resistance is calculated by use of incremental core loss data as Figure 8 or Figure 9. If the voltage analysis using H_b has been used Figure 8 is more convenient, if the current analysis using H_{max} has been used Figure 9 is more convenient. The total core loss is then

$$W_i = \frac{\text{watts}}{\text{lb}} \quad \text{(weight of core in lb.)}, \qquad (3\text{-}30)$$

and

$$R_1 = \frac{W_1}{I_{rms}^2 - I^2} \quad . \tag{3-31}$$

where I_{rms} is the root-mean-square value of i(t) in amperes and I is the average value of i(t) in amperes.

The denominator of (3-31) is $(I_{rms}^2 - I^2)$, the mean square value of the varying current which is the only component resulting in core losses.

CHAPTER 4

THE DESIGN METHOD FOR INDUCTORS LIMITED BY COPPER RESISTANCE

Shape Numbers and General Equations

In the mathematical formulation of the problem it is convenient to separate size and shape. The spacial quantities of principal importance are:

1. mean iron length in cm. (ℓ_i)
2. mean copper turn length in cm. (ℓ_c)
3. net cross sectional area of copper in cm^2. (a_c)
4. net cross sectional area of iron in cm^2. (a_i)

Now ℓ_i may be arbitrarily chosen as a measure of size and the other three quantities may be related to ℓ_i by means of dimensionless multiplying factors u, v and w such that

$$u \triangleq \ell_c / \ell_i \quad . \tag{4-1}$$

$$v \triangleq a_c / \ell_i^2 \quad . \tag{4-2}$$

and

$$w \triangleq a_i / \ell_i^2 \quad . \tag{4-3}$$

From these definitions

$$\ell_c = u\ell_i \quad . \tag{4-4}$$

and

$$a_c = v\ell_i^2 \quad . \tag{4-5}$$

$$a_i = w\ell_i^2 \quad . \tag{4-6}$$

The numbers u, v and w then describe the "shape" while ℓ_i describes the size of the inductor. It should be noted that the v and w are defined in terms of the "net" cross sectional areas

which include the respective space factors for the copper and iron. In the optimization process, finding the smallest size design, the u, v and w are treated as constants to simplify the solution. This simplification is justified by two reasons. First, it is relatively simple to make several designs with this constant-shape method to compare the advantage of different shapes for the particular specifications to be met. Second, the economic factors are strongly in favor of the "scrapless" EI lamination having the fixed proportions shown in Figure 10. A method of considering various stack heights will be described later.

The general inductance equation (2-30) may now be written in terms of shape numbers by substitution of the value of a_1 from (4-6) to give

$$L = \frac{.4\pi N^2 w \ell_1}{(\frac{1}{\mu_\Delta} + \alpha)} 10^{-8} \qquad (4-7)$$

If the number of turns is increased sufficiently any value of L may be designed for any fixed size. This can be done only by using decreasing sizes of wire as the number of turns is increased so that the total resistance increases rapidly. The copper resistance is the first size limiting factor to be considered.

The turns of the coil must "link" the core and the "window" space in the core limits the size of the coil. If a coil of N turns is placed in a net window area $v\ell_1^2$ the resistance may be found as follows. The cross-sectional area of the conductor is $v\ell_1^2/N$, the length of one turn is $u\ell_1$ so the resistance of one turn is

$$\frac{u\rho N}{v\ell_1} = \text{(resistance of one turn)}, \qquad (4\text{-}8)$$

and since there are N turns,

$$R_c = \frac{u\rho N^2}{v\ell_1} \quad , \qquad (4\text{-}9)$$

where R_c is the resistance of the coil.

Minimum Size Designs

Consider equations (4-7) and (4-9) which respectively give the inductance and copper resistance. Equation (4-7) may be solved for N^2 to give,

$$N^2 = \frac{L(\frac{1}{\mu_\Delta} + \alpha)\ 10^8}{.4\pi\ w\ \ell_1} \quad , \qquad (4\text{-}10)$$

and this value of N^2 may be inserted into (4-9) to give,

$$R_c = \frac{u\rho L(\frac{1}{\mu_\Delta} + \alpha)\ \ 10^8}{.4\pi\ v\ w\ \ell_1^{\,2}} \quad . \qquad (4\text{-}11)$$

Examination of this equation (4-11) shows that the copper resistance varies directly with u, ρ and $(\frac{1}{\mu_\Delta} + \alpha)$ and inversely with v, w and $\ell_1^{\,2}$ for a given inductance. The copper resistance is a dissipative factor which usually must be held under some limit. To make R_c small, the values of u, ρ and $(\frac{1}{\mu_\Delta} + \alpha)$ should be as small as possible and the values of v and w should be as large as possible. Winding the conductor with minimum insulation space around the core will minimize u while the conductor material determines ρ. Minimum internal coil insulation and space-saving winding methods will maximize the copper space factor F_c and shape factor v. Likewise in the core a high

space factor F_i will maximize w.

The factor $(\frac{1}{\mu_\Delta} + \alpha)$ requires detailed consideration since μ_Δ is a function of the operating inductions. When an unsymmetrical magnetomotive force ($H_{max} \neq -H_{min}$) is applied to a ferromagnetic core, a minimum value of $(\frac{1}{\mu_\Delta} + \alpha)$ may occur for a value of α greater than zero due to the decrease in induction as α is increased.[11, 13, 14, 16, 17]

Now the incremental permeability, μ_Δ, is a function of two variables, B_{max} and B_Δ, but it is convenient to consider it as a function of B_{max} alone by fixing the ratio, B_Δ / B_{max}. It is then necessary to consider various values of the B_Δ / B_{max} ratio. The incremental permeability treated in this way, as a function of B_{max} will be symbolized by μ_Δ'. To find the minimum $(\frac{1}{\mu_\Delta'} + \alpha)$ it may be differentiated with respect to α and equated to zero.

$$\frac{d(\frac{1}{\mu_\Delta'} + \alpha)}{d\alpha} = \frac{d(\frac{1}{\mu_\Delta'})}{d\alpha} + 1 \qquad (4\text{-}12)$$

and

$$\frac{d(\frac{1}{\mu_\Delta'})}{d\alpha} = \frac{d(\frac{1}{\mu_\Delta'})}{dB_{max}} \frac{dB_{max}}{d\alpha} . \qquad (4\text{-}13)$$

Now

$$\frac{d(\frac{1}{\mu_\Delta'})}{dB_{max}} = \frac{-1}{\mu_\Delta'^2} \frac{d\mu_\Delta'}{dB_{max}} . \qquad (4\text{-}14)$$

and to evaluate $\frac{dB_{max}}{d\alpha}$ it is convenient to define a fictitious magnetizing force $\bar{H}_{max}$ such that

$$\bar{H}_{max} = \frac{.4\,\pi\,I_{max}}{l_i} . \qquad (4\text{-}15)$$

From (2-15) and (4-15),

$$B_{max} = \frac{\bar{H}_{max}}{\frac{1}{\mu} + \alpha} \quad . \tag{4-16}$$

By differentiation with respect to α,

$$\frac{dB_{max}}{d\alpha} = \bar{H}_{max} \frac{(-1)}{(\frac{1}{\mu} + \alpha)^2} \left(\frac{-1}{\mu^2} \frac{d\mu}{dB_{max}} \frac{dB_{max}}{d\alpha} + 1 \right) . \tag{4-17}$$

and solving for $dB_{max} / d\alpha$ gives

$$\frac{dB_{max}}{d\alpha} = \frac{-1}{\frac{(\frac{1}{\mu} + \alpha)^2}{\bar{H}_{max}} - \frac{1}{\mu^2} \frac{d\mu}{dB_{max}}} \quad . \tag{4-18}$$

Inserting these factors into (4-17) and equating to zero gives,

$$\frac{\frac{1}{\mu_\Delta{}'^2} \frac{d\mu_\Delta{}'}{dB_{max}}}{\frac{(\frac{1}{\mu} + \alpha)^2}{\bar{H}_{max}} - \frac{1}{\mu^2} \frac{d\mu}{dB_{max}}} + 1 = 0 \tag{4-19}$$

and rearranging,

$$\frac{1}{\mu^2} \frac{d\mu}{dB_{max}} + \frac{1}{\mu_\Delta{}'^2} \frac{d\mu_\Delta{}'}{dB_{max}} = \frac{(\frac{1}{\mu} + \alpha)^2}{\bar{H}_{max}} . \tag{4-20}$$

Let

$$D \triangleq \frac{1}{\mu^2} \frac{d\mu}{dB_{max}} + \frac{1}{\mu_\Delta{}'^2} \frac{d\mu_\Delta{}'}{dB_{max}} \tag{4-21}$$

and equation (4-20) becomes

$$D = \frac{(\frac{1}{\mu} + \alpha)^2}{\bar{H}_{max}} \quad . \tag{4-22}$$

Multiplying (4-16) by (4-22) gives

$$B_{max} D = \frac{1}{\mu} + \alpha \tag{4-23}$$

and

$$\alpha = B_{max} D - \frac{1}{\mu} \quad . \tag{4-24}$$

This last equation gives the air gap for minimum $(\frac{1}{\mu_\Delta} + \alpha)$ when B_{max} is known. At this point

$$\frac{1}{\mu_\Delta} + \alpha = B_{max} D - \frac{1}{\mu} + \frac{1}{\mu_\Delta'} \quad . \tag{4-25}$$

Equation (4-16) may be multiplied by (4-23) to give

$$B_{max}^2 D = \bar{H}_{max} \quad . \tag{4-26}$$

which determines the value of B_{max} for which $(\frac{1}{\mu_\Delta'} + \alpha)$ is minimum. It is now necessary to find $\bar{H}_{max}$ in terms of the known requirements so that it may be equated to $B_{max}^2 D$ in (4-26).

From (4-9)

$$N = \sqrt{\frac{v \ell_1 R_c}{u\rho}} \quad . \tag{4-27}$$

Inserting this value of N into (4-15) gives

$$\bar{H}_{max} = .4\pi I_{max} \sqrt{\frac{vR_c}{u\rho \ell_1}} \quad . \tag{4-28}$$

From (4-11)

$$\ell_1^2 = \frac{(\frac{1}{\mu_\Delta'} + \alpha) u\rho L 10^8}{.4\pi v w R_c} \quad . \tag{4-29}$$

or

$$\sqrt{\ell_1} = \sqrt[4]{\frac{(\frac{1}{\mu_\Delta'} + \alpha) u \rho L 10^8}{.4\pi v w R_c}} \quad . \tag{4-30}$$

and inserting this value of ℓ_1 into (4-28) gives

$$\bar{H}_{max} = \sqrt[4]{\frac{(.4\pi)^5 v^3 w I_{max}^4 R_c^3 10^{-8}}{(\frac{1}{\mu_\Delta'} + \alpha) u^3 \rho^3 L}} \tag{4-31}$$

If n_1 is defined as

$$n_1 \triangleq \frac{(.4\pi)^5 \nu^3 w I_{max}^4 R_c^3 10^{-8}}{u^3 \rho^3 L} \quad . \tag{4-32}$$

then

$$\bar{H}_{max} \sqrt[4]{\frac{1}{\mu_\Delta'} + \alpha} = \sqrt[4]{n_1} \quad . \tag{4-33}$$

Substituting the values of $\frac{1}{\mu_\Delta} + \alpha$ and $\bar{H}_{max}$ from (4-25) and (4-26) respectively into (4-33) gives

$$B_{max}^2 D \sqrt[4]{B_{max} D - \frac{1}{\mu} + \frac{1}{\mu_\Delta}} = \sqrt[4]{n_1} \tag{4-34}$$

or equivalently

$$B_{max}^8 D^4 (B_{max} D - \frac{1}{\mu} + \frac{1}{\mu_\Delta'}) = n_1 \tag{4-35}$$

Now these equations (4-34), (4-35) relate B_{max} and the known factors of n_1 since D, μ and μ_Δ' are functions of B_{max} alone. Given an n_1 this equation specifies B_{max} but it is an implicit relationship which cannot be solved directly. It can be solved in the opposite manner by assuming various values of B_{max} and tabulating the values of n_1. These points may then be plotted on a chart with B_{max} ordinates and n_1 abscissas. Generally there is an upper limit beyond which no minimum of $(\frac{1}{\mu_\Delta} + \alpha)$ exists. In practice, the chart will be used the other way around; n_1 may be calculated from the known factors and the chart will give B_{max} for the minimum size design.

It is also necessary to obtain α, ℓ_1 and N to complete the design and points may be added to the chart for this purpose. The equation for α was previously found to be

$$\alpha = B_{max} D - \frac{1}{\mu} \quad . \tag{4-24}$$

This quantity may be calculated and plotted on the chart as a second set of ordinates against the corresponding values of the abscissa n_1.

The square root of (4-29) is

$$\ell_i = \sqrt{\frac{(\frac{1}{\mu_\Delta'} + \alpha)\ u\ \rho\ L\ 10^8}{.4\pi\ v\ w\ R_c}} \quad . \tag{4-36}$$

For computing ℓ_i it is convenient to plot ε_1 which is defined as

$$\varepsilon_1 \overset{\Delta}{=} \sqrt{\frac{1}{\mu_\Delta T} + \alpha)} \tag{4-37}$$

so that

$$\ell_i = \varepsilon_1 \sqrt{\frac{u\ \rho\ 10^8}{.4\pi v\ w}} \sqrt{\frac{L}{R_c}} \quad . \tag{4-38}$$

The maximum value of $\frac{1}{\mu_\Delta'} + \alpha$ was given by (4-25) so for these conditions

$$\varepsilon_1 = \sqrt{B_{max}\ D - \frac{1}{\mu} + \frac{1}{\mu_\Delta'}} \tag{4-39}$$

This quantity can also be calculated and plotted as a third set of ordinates on the chart. From these points ℓ_i may be calculated by (4-38).

Either equation (4-10) or (4-27) will provide the equation for N when the value of ℓ_i from (4-36) has been inserted.

$$N = \sqrt[4]{\frac{(\frac{1}{\mu_\Delta'} + \alpha)\ v\ L\ R_c\ 10^8}{.4\pi\ u\ w\ \rho}} \tag{4-40}$$

and in terms of ε_1

$$K = \sqrt{\varepsilon_1}\ \sqrt{\frac{v\ 10^8}{.4\pi\ n\ w\ \rho}}\ \ \sqrt{L\ R_e} \qquad (4\text{-}41)$$

It should be recalled that the foregoing derivation was based on an additional restriction of a constant B_Δ / B_{max} ratio. Now the B_Δ / B_{max} ratio is not directly specified by the electrical requirements of the inductor so the method and chart developed above will not allow direct design from the electrical specifications. Several sets of calculations, each for a different value of B_Δ / B_{max} ratio will be considered. The corresponding I_Δ / I_{max} ratio may be calculated for each point, and from this information, design curves may be constructed in terms of the I_Δ / I_{max} ratio instead of the B_Δ / B_{max} ratio.

To do this, (2-24) may be divided by (2-15) to give

$$\frac{B_\Delta}{B_{max}} = \frac{I_\Delta}{I_{max}}\ \frac{\frac{1}{\mu} + \alpha}{\frac{1}{\mu_\Delta'} + \alpha} \qquad (4\text{-}42)$$

and

$$\frac{I_\Delta}{I_{max}} = \frac{B_\Delta}{B_{max}}\ \frac{\frac{1}{\mu_\Delta'} + \alpha}{\frac{1}{\mu} + \alpha} \qquad (4\text{-}43)$$

where μ_Δ' has been substituted for μ_Δ. For each point on the chart a B_Δ / B_{max} ratio and a B_{max} value have been assumed; n, ℓ_1, α and ε_1 have been calculated. Now I_Δ / I_{max} can be calculated by (4-43) for each point, and curves of the various ordinates, B_{max}, α and ε_1 can be drawn through their respective points having the same I_Δ / I_{max} ratio. These curves, each labeled with its respective I_Δ / I_{max} value, can then be used for direct design since the I_Δ / I_{max} ratio may be obtained from the electrical requirements. Such a set of

curves are presented in Chart 1A and it should be noted that these curves with n_1 as abscissa and B_{max}, α and ε_1 as ordinates are determined solely by the magnetic characteristics of the core material, independently of the inductor geometry and the resistivity of the coil conductor.

To use the curves the designed must calculate n_1 by (4-32) and having ε_1 he must calculate ℓ_i by (4-38).

Auxiliary Axes and Variable Stack Heights

If many designs are to be made with fixed constant values of u, v, w and ρ the design process may be simplified by adding two new axes to the chart. First consider the function n_{1r} given by,

$$n_{1r} \triangleq \frac{R_c^3 I_{max}^4}{L} \quad . \tag{4-44}$$

From (4-32) and (4-44),

$$n_{1r} = n_1 \frac{u^3 \rho^3 10^8}{(.4\pi)^5 v^3 w} \quad . \tag{4-45}$$

Since the n_1 axis is logarithmic, an n_{1r} axis may be plotted parallel to it to perform the multiplication indicated in (4-45). The designer then need only calculate (4-44) to find n_{1r} and enter the chart at this point on the n_{1r} axis. This factor n_{1r} is the fourth power of Legg's "m_r"[17], and unlike the n_1 axis, the n_{1r} axis is dependent on the shape numbers, u, v and w, and on the resistivity, ρ.

In a similar fashion the calculations of ℓ_i from (4-38) can be simplified. Consider the function ε_{1r} where

$$\ell_{1r} \triangleq \ell_1 \sqrt{\frac{R_c}{L}} \qquad (4\text{–}46)$$

Then

$$\ell_1 = \ell_{1r} \sqrt{\frac{L}{R_c}} \quad . \qquad (4\text{–}47)$$

which is a simpler calculation than (4–38). From (4–38) and (4–46),

$$\ell_{1r} = \ell_1 \sqrt{\frac{u\,\rho\,10^8}{.4\pi\,v\,w}} \quad . \qquad (4\text{–}48)$$

and a ℓ_{1r} axis can be plotted parallel to the ℓ_1 axis to provide ℓ_{1r} directly. This factor ℓ_{1r} is Legg's "ℓ_r".[17] and the ℓ_{1r} axis is dependent on u, v, w and ρ.

From the ℓ_1 or ℓ_{1r} value obtained from the chart the designer can calculate ℓ_i, the length of the core. This ℓ_i may have any value, while laminations are available only in discrete sizes each with a discrete value of ℓ_i. One of the most convenient modifications of the standard shape is the variation of the height of the stack of laminations. In a qualitative manner, a lamination with an ℓ_i too small may be stacked higher to compensate or conversely a lower stack of larger laminations may be used.

A variation in stack height will result in a change in u and w, since both the mean turn length and the net iron cross section area are affected. If s is the ratio of the variable stack height to the standard stack height, the values of u and w will be symbolized generally by u(s) and w(s) and then u(1) and w(1) will be the standard values. The n_{1r} for the standard stack height axis is related to the n_1 axis by the factor $\frac{u^3(1)\,\rho^3\,10^8}{(.4\pi)^5 v^3 w(1)}$ and for variable stack heights to

the factor should be $\frac{u^3(s)\,\rho^3\,10^8}{(.4\pi)^5 v^3 w(s)}$. The n_{1r} axis for these variable stack heights should be shifted a distance of log $\frac{u^3(s)}{u^3(1)}\frac{w(1)}{w(s)}$. By similar arguments the g_{1r} axis for variable stack heights should be shifted a distance of log $\sqrt{\frac{u(s)}{u(1)}\frac{w(1)}{w(s)}}$ from the position of the g_{1r} axis for standard stack height.

A convenient geometrical device for shifting the n_{1r} and g_{1r} axis is a transparent overlay with the n_{1r} and g_{1r} axis ruled on it. The main chart then may have an auxiliary axis s to guide the location of some arbitrary reference point on the transparency. A convenient reference point is the intersection of the n_{1r} and g_{1r} axes. This auxiliary axis is the locus of points whose abcissas are - log $\frac{u^3(s)}{u^3(1)}\frac{w(1)}{w(s)}$ and whose ordinates are - log $\sqrt{\frac{u(s)}{u(1)}\frac{w(1)}{w(s)}}$. This curve can then be graduated with values of s. The transparency is placed over the chart with the corresponding axes parallel and with the intersection of the transparency axes lying on the s axis of the main chart. The n_{1r} and g_{1r} axes on the transparency will then be in correct relationship to the n_1 and g_1 axes and the curves on the chart for the particular value of s indicated on the s axis by the intersection of the n_{1r} and g_{1r} axes at the transparency. It should be noted that the ordinates B_{max} and α are independent of the inductor geometry and are measured on the chart B_{max} and α axes directly. The abscissa (n_{1r}) for these curves must be the one on the transparency for stack heights other than standard.

The designer may use the transparency in either of two ways. If a design is wanted for a stack height other than standard, the transparency is located at the proper point on

the s axis and the chart is read opposite the n_{lr} point on the transparency n_{lr} axis. The B_{max} and α values are read on the chart B_{max} and α axes while the g_{lr} value is read on the transparency g_{lr} axis. If a design results in a value of ℓ_i intermediate between standard lamination sizes, the designer may determine the B_{max}, α and s for the design using standard laminations having ℓ_i smaller or larger than that called for by the particular specifications. He first calculates g_{lr} by (4-46) from the ℓ_i of the standard lamination and marks the n_{lr}, g_{lr} point on the transparency. He then moves the transparency, keeping the axes parallel to those on the main chart and keeping the intersection of the axes on the s axis of the main chart. When the n_{lr}, g_{lr} point on the transparency falls on the g_l curve of the main chart, he can read s from the s axis at the intersection of the transparency n_{lr} and g_{lr} axes. The values of B_{max} and α are found from their respective curves and axes of the main chart. opposite the n_{lr} axis of the transparency.

This method of considering variation in stack height will be derived specifically for the case of "scrapless" EI laminations. Such a lamination with center leg width x is shown in Figure 10. The mean iron length path is shown by the dotted line as a rectangle. Its length is

$$\ell_i = 6\,x \quad . \tag{4-49}$$

This relation for the effective iron length is used by the Allegheny Ludlum Steel Corporation in their specifications.[22]

The mean turn length path as shown by the broken line in

Figure 10 is a rectangle. This path has a length intermediate between that of a bulgeless coil and that of a circular coil. For this path

$$\ell_c = 2(\frac{3x}{2} + \frac{x}{2} + T) \qquad (4\text{-}50)$$

or

$$\ell_c = 4x + 2T. \qquad (4\text{-}51)$$

Now from (4-1) and (4-49)

$$n = \frac{4x + 2T}{6x} \qquad (4\text{-}52)$$

and substituting sx for T,

$$n(s) = \frac{2 + s}{3} \quad . \qquad (4\text{-}53)$$

If F_c is the fractional part of the window area which is copper, the copper area is

$$a_c = \frac{x}{2}\frac{3x}{2} F_c \qquad (4\text{-}54)$$

or

$$a_c = \frac{3x^2}{4} F_c \qquad (4\text{-}55)$$

From (4-2) and (4-49),

$$v = \frac{3x^2 F_c}{4x^2\ 36} \quad , \qquad (4\text{-}56)$$

and

$$v = \frac{F_c}{48} \quad . \qquad (4\text{-}57)$$

The shape number v is independent of s. For commercially wound coils in a wide range of wire sizes for use under 1500

volts, F_c is approximately 30% so for these cases

$$v = \frac{1}{160} = .00625 \qquad (4\text{-}58)$$

The iron area is

$$a_i = x\, T\, F_i \qquad (4\text{-}59)$$

where F_i is the iron space factor. From (4-3) and (4-49)

$$w = \frac{x\, T\, F_i}{36\, x^2} \quad . \qquad (4\text{-}60)$$

and in terms of s,

$$w(s) = \frac{sF_i}{36} \quad . \qquad (4\text{-}61)$$

An iron space factor value commonly realized in practice[22] is 90% so that

$$w(s) = \frac{s}{40} = .025\, s \quad . \qquad (4\text{-}62)$$

For square stacks,

$$s = 1 \quad , \qquad (4\text{-}63)$$

and

$$u(1) = 1 \quad , \qquad (4\text{-}64)$$

and

$$w(1) = .025 \quad . \qquad (4\text{-}65)$$

The constant in (4-45) may now be evaluated

$$\frac{n_{1r}}{n_1} = \frac{u^3\, \rho^3\, 10^8}{(.4\pi)^5\, v^3 w} = \frac{1}{40} \qquad (4\text{-}66)$$

The constant in (4-48) is

$$\frac{\ell_{1r}}{\ell_1} = \sqrt{\frac{u\,\rho\,10^8}{.4\pi\,v\,w}} = 1000 \qquad (4\text{-}67)$$

The negative logarithmic coordinates of the points on the s axis are then

$$\frac{u^3(s)}{u^3(1)}\frac{w(1)}{w(s)} = \frac{(2+s)^3}{27\,s} \quad . \qquad (4\text{-}68)$$

and

$$\sqrt{\frac{u(s)}{u(1)}\frac{w(1)}{w(s)}} = \sqrt{\frac{2+s}{3\,s}} \quad . \qquad (4\text{-}69)$$

Such an axis is shown in chart 1A.

Designs With Zero Air Gap

The method developed thus far provides a direct means of design when I_{max}, I_Δ, L and R_c are specified. One limitation of this method is that there is no restriction on the sign of α, and for low values of n_1, the indicated air gap length does become negative. For these specifications the optimum design is the one with zero air gap since a negative air gap cannot be physically realized.

Previously the system of equations (2-15) (4-7) and (4-9) was solved for a relation between B_{max} and ℓ_1, (4-34), such that $(\frac{1}{\mu_\Delta} + \alpha)$ was a minimum. Now for the zero air gap case, the system of equations (2-15), (4-7) and (4-9) will be solved together with

$$\alpha = 0 \quad . \qquad (4\text{-}70)$$

Equations (4-16) and (4-33) were derived from (2-15), (4-7), and (4-9) and they result in

$$B_{max} = \frac{\sqrt[4]{n_1}}{(\frac{1}{\mu} + \alpha)\sqrt[4]{\frac{1}{\mu_\Delta'} + \alpha}} \quad . \tag{4-71}$$

Applying (4-70),

$$\frac{B_{max}}{\mu\sqrt[4]{\mu_\Delta'}} = \sqrt[4]{n_1} \tag{4-72}$$

or

$$\frac{B_{max}^4}{\mu^4 \mu_\Delta'} = n_1 \quad . \tag{4-73}$$

These last two equations give the relation between B_{max} and the known requirements contained in n_1 since the μ's are functions of B_{max}. These equations are analogous to (4-34) and (4-35) and a design chart relating n_1 and B_{max} can be set up in the same way as Chart 1A was constructed. From (4-37) and (4-70)

$$\varepsilon_1 = \sqrt{\frac{1}{\mu_\Delta'}} \quad . \tag{4-74}$$

Equations (4-38) and (4-42) still apply for calculating ε_1 and (4-41) still applies for N.

This design chart has curves of B_{max} and ε_1 versus n_1 for various I_Δ / I_{max} ratios. Axes for n_{1r}, ε_{1r} and s are identical to those of Chart 1A. This chart, for $\alpha = 0$, is shown as Chart 1B.

Normally the designer would first calculate n_1 or n_{1r} and consult Chart 1A. If the value of n_1 or n_{1r} was too small to be found on Chart 1A, he would consult Chart 1B for the $\alpha = 0$ design which is the optimum design when the air

gap is negative for the "minimum size" design.

Design With Induction Limitation

Another limitation of the "minimum size" method of Chart 1A is that the B_{max} may be too large for the linearity or core loss requirements of the inductor. The specification and mensuration of "linearity" and "non-linearity" is a very complicated question, especially when the waveforms of current and voltage are of unlimited shapes. One useful measure, though, is B_{max}. If B_{max} is above the "knee" of the induction curve, minor loops at large B_Δ will generally bend around the knee as shown in Figure 11. It is useful to then have the design curves for various limiting values of B_{max}. If the limiting value of B_{max} is below the optimum value found in Chart 1A, the "B_{max}-limited" design will generally be larger. If the limiting value of B_{max} is above the optimum value found in Chart 1A, the optimum design of Chart 1A should be used.

For this B_{max}-limited method consider the simultaneous solution of (2-15), (4-7), (4-9) and

$$B_{max} = \text{(constant)}. \tag{4-75}$$

Previously the simultaneous solution of (2-15), (4-7) and (4-9) was found to be

$$B_{max} = \frac{\sqrt[4]{n_1}}{(\frac{1}{\mu} + \alpha)\sqrt[4]{\frac{1}{\mu_\Delta'} + \alpha}} \quad . \tag{4-76}$$

Substituting α from (4-37) gives

$$B_{max} = \frac{\sqrt[4]{n_1}}{(\varepsilon_1^2 - \frac{1}{\mu_\Lambda} + \frac{1}{\mu})\sqrt{\varepsilon_1}} \tag{4-77}$$

and rearranging (4-77) results in

$$B_{max} \sqrt{\varepsilon_1} \left(\varepsilon_1^2 - \frac{1}{\mu_\Delta} + \frac{1}{\mu}\right) = \sqrt[4]{n_1} \qquad (4\text{-}78)$$

or

$$B_{max}^4 \varepsilon_1^2 \left(\varepsilon_1^2 - \frac{1}{\mu_\Delta} + \frac{1}{\mu}\right)^4 = n_1 \qquad (4\text{-}79)$$

For a constant B_{max} this equation can be tabulated in a "reverse" manner similar to (4-34) or (4-72). First a value of B_{max} is assumed for the particular chart under construction. Then for various B_Δ / B_{max} ratios, various values of ε_1 are assumed and the resulting n_1 values calculated by (4-78) or (4-79). From (4-37),

$$\alpha = \varepsilon_1^2 - \frac{1}{\mu_\Delta} \qquad (4\text{-}80)$$

which can be used to calculate α for every point. For each point the I_Δ / I_{max} ratio can be found by (4-43) and curves of ε_1 and α versus n_1 can be drawn for the various I_Δ / I_{max} ratios. This is Chart 1C. The n_{1r}, ε_{1r} and s axes are identical to those on Chart 1A and 1B. There is a Chart 1C for B_{max} values of 1, 2, 4 and 10 kilogauss.

If the B_{max} from Chart 1A for a given set of specifications is too large, the designer would use the appropriate Chart 1C. Equations (4-38) and (4-47) still apply for calculating L_1 and (4-41) still applies to H.

CHAPTER 5

THE DESIGN METHOD FOR INDUCTORS LIMITED BY COPPER LOSS HEATING

Minimum Size Design

In some cases the circuit requirements limiting the resistance are so loose that the only factor limiting the resistance of the inductor is the heating of the inductor by the current through its copper resistance. For these cases it is convenient to prepare charts for the design of inductors subject only to the limitation of their own heating.

The average rate of heat generation in the copper resistance is $I^2_{rms}R_c$. The deterioration or destruction of the inductor is a function of the temperature which in turn is a function of the density of thermal power passing through the surface of the unit. For units of the same shape the surface area may be expressed by

$$S = p\, \ell_1^2 \,. \tag{5-1}$$

where S is the surface area in square centimeters and p is a dimensionless constant for the particular shape under consideration. The thermal power density is then given by

$$K_c = \frac{I^2_{rms} R_c}{p\, \ell_1^2} \,. \tag{5-2}$$

where K_c is the termal power density in watts per square centimeter. Substituting the value of R_c from (2-2) gives

$$K_c = \frac{u\, \rho\, N^2\, I^2_{rms}}{p\, v\, \ell_1 3} \,. \tag{5-3}$$

Substituting N^2 from (4-10) gives

$$K_c = \frac{u\,\rho\,L\,I_{rms}^2\,(\frac{1}{\mu_\Delta} + \alpha)10^8}{.4\pi\,p\,v\,w\,\ell_i^4} \quad . \tag{5-4}$$

This equation is similar to (4-11) in the location of the various factors in numerator and denominator. And the optimum design is again that for which $(\frac{1}{\mu_\Delta} + \alpha)$ is minimum. Equation (4-26) specifies the point of minimum $(\frac{1}{\mu_\Delta} + \alpha)$ and it is necessary to calculate the value of $\bar{H}_{max}$ from the thermal power density equations to arrive at the equations from which design charts may be made. From (5-3)

$$N = \sqrt{\frac{p\,v\,\ell_i^3\,K_c}{u\,\rho\,I_{rms}^2}} \quad . \tag{5-5}$$

Inserting this value of N into (4-15) gives

$$\bar{H}_{max} = .4\pi\,I_{max}\sqrt{\frac{p\,v\,\ell_i\,K_c}{u\,\rho\,I_{rms}^2}} \quad . \tag{5-6}$$

From (5-4)

$$\ell_1 = \sqrt[8]{\frac{(\frac{1}{\mu_\Delta} + \alpha)\,u\,\rho\,L\,I_{rms}^2\,10^8}{.4\pi\,p\,v\,w\,K_c}} \quad , \tag{5-7}$$

and inserting this value of ℓ_i into (5-6) gives

$$\bar{H}_{max} = \sqrt{\sqrt[8]{\frac{(\frac{1}{\mu_\Delta} + \alpha)(.4\pi)^7 p^3 v^3 L\,I_{max}^8 K_c^3\,10^8}{u^3\,w\,\rho^3\,I_{rms}^6}}} \quad . \tag{5-8}$$

If n_2 is defined as

$$n_2 \overset{\Delta}{=} \frac{(.4\pi)^7\,p^3\,v^3\,L\,I_{max}^8\,K_c^3\,10^8}{u^3\,w\,\rho^3\,I_{rms}^6} \quad , \tag{5-9}$$

then

$$\frac{\bar{H}_{max}}{\sqrt[8]{\frac{1}{\mu_\Delta} + \alpha}} = \sqrt[8]{n_2} \quad . \tag{5-10}$$

Substituting the values of $(\frac{1}{\mu_\Delta} + \alpha)$ and $\bar{H}_{max}$ from (4-25) and (4-26) respectively gives

$$\frac{B_{max}^2 \; D}{\sqrt[8]{B_{max} D - \frac{1}{\mu} + \frac{1}{\mu_\Delta}}} = \sqrt[8]{n_2} \; . \qquad (5\text{-}11)$$

or equivalently

$$\frac{B_{max}^{16} \; D^8}{B_{max} D - \frac{1}{\mu} + \frac{1}{\mu_\Delta}} = n_2 \; . \qquad (5\text{-}12)$$

These equations are analogous to (4-34) and (4-35) for setting up a design chart. For various B_{max} values n_2 can be calculated and a plot of B_{max} vs. n_2 can be made in a manner similar to that of Chart 1A.

A curve for α can also be added to the chart by use of (4-24). From (5-7)

$$\ell_i = \sqrt[4]{\frac{(\frac{1}{\mu_\Delta} + \alpha) \; u \; \rho \; L \; I_{rms}^2 \; 10^8}{.4\pi \; p \; v \; w \; K_c}} \; . \qquad (5\text{-}13)$$

so that it is convenient to plot a factor g_2 defined by

$$g_2 \triangleq \sqrt[4]{\frac{1}{\mu_\Delta} + \alpha} \; . \qquad (5\text{-}14)$$

With this definition,

$$\ell_i = g_2 \sqrt[4]{\frac{u \; \rho \; 10^8}{.4\pi \; p \; v \; w}} \sqrt[4]{\frac{L \; I_{rms}^2}{K_c}} \; . \qquad (5\text{-}15)$$

The maximum value of $(\frac{1}{\mu_\Delta} + \alpha)$ was given by (4-25) so

$$g_2 = \sqrt[4]{B_{max} D - \frac{1}{\mu} + \frac{1}{\mu_\Delta}} \; . \qquad (5\text{-}16)$$

This quantity can also be computed and added to the chart and then (5-15) can be used to compute ℓ_i.

Either (4-10) or (5-5) will provide the formula for H when the value of ℓ_i from (5-13) has been inserted. Thus,

$$N = \sqrt[8]{\frac{\left(\frac{1}{\eta_\Delta} + \alpha\right)^3 p\, v\, L^3\, K_c\, 10^{24}}{(.4\pi)^3\, u\, w^3\, \rho\, I_{rms}^2}} \quad . \tag{5-17}$$

and in terms of ε_2.

$$N = \varepsilon_2^{3/2} \sqrt[8]{\frac{p\, v\, L^3\, K_c\, 10^{24}}{(.4\pi)^3\, u\, w^3\, \rho\, I_{rms}^2}} \quad . \tag{5-18}$$

From (5-2) the copper resistance may be calculated.

$$R_c = \frac{p\, \ell_1^2\, K}{I_{rms}^2} \quad . \tag{5-19}$$

Inserting into (5-19) the value of ℓ_1 from (5-15) gives

$$R_c = \varepsilon_2^2 \sqrt{\frac{p\, u\, \rho\, 10^8}{.4\pi\, v\, w}} \sqrt{\frac{L\, K_c}{I_{rms}^2}} \quad . \tag{5-20}$$

The chart can be set up in terms of the I_Δ / I_{max} ratios in a manner similar to Chart 1A. The result is then Chart 2A.

Auxiliary Axes And Variable Stack Height

For designing with particular values of u, v, w and ρ it is convenient to set up additional axes similar to the n_{1r} and ε_{1r} axes used in the resistance limited design charts. First consider

$$n_{2r} \triangleq \frac{L\, I_{max}^8\, K_c^3}{I_{rms}^6} \quad . \tag{5-21}$$

From (5-9) and (5-21)

$$n_{2r} = \frac{u^3\, w\, \rho^3\, 10^{-8}}{(.4\pi)^7\, p^3\, v^3}\, n_2 \quad . \tag{5-22}$$

An n_{2r} axis can be laid out parallel to the n_2 axis to perform the multiplication indicated in (5-22). The designer calculates n_{2r} by (5-21) and enters the chart at the corres-

ponding point of the n_{2r} axis. The calculation of n_{2r} by (5-21) is simpler than the calculation of n_2 by (5-9) but the n_2 axis on the chart is a function only of the magnetic properties of the material (5-21) while the n_{2r} axis is dependent upon u, v, p, w and ρ.

For simplifying the ℓ_i calculation another function g_{2r} is defined.

$$g_{2r} \triangleq \ell_i \sqrt[4]{\frac{K_c}{L I_{rms}^2}} . \tag{5-23}$$

Then

$$\ell_i = g_{2r} \sqrt[4]{\frac{L I_{rms}^2}{K_c}} , \tag{5-24}$$

which is a simpler calculation than (5-15). From (5-15) and (5-23)

$$g_{2r} = g_2 \sqrt[4]{\frac{u \rho 10^8}{.4\pi p v w}} . \tag{5-25}$$

and a g_{2r} axis can be laid out parallel to the g_2 axis to do this operation directly.

The constants in (5-22) and (5-25) may be evaluated for the scrapless EI low voltage case as were the constants in the resistance limited design. For cases such as the standard military line,

$$p = 1.3 \tag{5-26}$$

From (5-22),

$$\frac{n_{2r}}{n_2} = \frac{u^3 w \rho^3 10^{-8}}{(.4\pi)^7 p^3 v^3} = 5 \times 10^{-22} \tag{5-27}$$

and from (5-25),

$$\frac{g_{2r}}{g_2} = \sqrt[4]{\frac{u \rho 10^8}{.4\pi p v w}} = 30 \tag{5-28}$$

As in the resistance limited charts an s axis may be set up to facilitate the design for various stack heights. The negative logarithmic coordinates of the s axis points are

$$\frac{u^3(s)\,w(s)}{u^3(1)\,w(1)} = \frac{(2+s)^3\,s}{27} \tag{5-29}$$

and

$$\sqrt[4]{\frac{u(s)\,w(1)}{u(1)\,w(s)}} = \sqrt[4]{\frac{2+s}{3s}} \tag{5-30}$$

provided that the case area factor p is a constant over the range of s variation considered. Such an axis is shown in Chart 2A. It is used in the same manner as the s axis of Charts 1A, 1B and 1C for designing inductors with $s \neq 1$.

Design With Zero Air Cap

As in the copper resistance limited case the minimum value of $(\frac{1}{\mu_\Delta} + \alpha)$ may occur for a negative value of α so a chart for the $\alpha = 0$ designs is necessary. From (4-16) and (5-10)

$$B_{max} = \frac{\sqrt[8]{n_2}\ \sqrt[8]{\frac{1}{\mu_\Delta'} + \alpha}}{\frac{1}{\mu} + \alpha} \,. \tag{5-31}$$

Letting

$$\alpha = 0 \,, \tag{5-32}$$

$$\frac{B_{max}\sqrt[8]{\mu_\Delta'}}{\mu} = \sqrt[8]{n_2} \tag{5-33}$$

or

$$\frac{B_{max}^8\,\mu_\Delta'}{\mu^8} = n_2 \,. \tag{5-34}$$

These equations are analogous to (4-51) and (4-52) in relating B_{max} to the known requirements and they form the basis of the new chart for $\alpha = 0$ designs. A chart with n_2 as abscissa and B_{max} as ordinate can be made. From (5-14) and (5-32)

$$\varepsilon_2 = \sqrt[4]{\frac{1}{\mu_\Delta'}} \tag{5-35}$$

and a curve of ε_2 vs. n_2 can be added to the chart.

Equation (5-15), (5-18) and (5-20) still apply for calculating ℓ_1, N and R_c respectively. Axes of n_{2r}, ε_{2r} and s may be added in a manner identical to that of Chart 2A. The result is Chart 2B.

Normally the designer, in designing a temperature limited inductor, would first calculate n_2 or n_{2r} and consult Chart 2A. If this value of n_2 or n_{2r} was too small to be found on the curves of Chart 2A this would indicate that the minimum value of $(\frac{1}{\mu_\Delta} + \alpha)$ occurs for negative α. The best physically realizable design is that for which $\alpha = 0$ and so Chart 2B is used.

Design With Induction Limitation

Another limitation applies to large values of n_1, the value of B_{max} may be too high for the required degree of linearity or $(\frac{1}{\mu_\Delta} + \alpha)$ may not have a minimum. For such cases charts for the optimum design with fixed B_{max} values are useful.

By previous derivation,

$$B_{max} = \frac{\sqrt[8]{n_2}\ \sqrt[8]{\frac{1}{\mu_\Delta'} + \alpha}}{\frac{1}{\mu} + \alpha} \quad . \tag{5-31}$$

Equation (5-14) may be solved for α.

$$\alpha = \varepsilon_2^4 - \frac{1}{\mu_\Delta^2} \tag{5-36}$$

Inserting this α into (5-31) and rearranging gives,

$$\frac{B_{max}\left(\varepsilon_2^4 - \frac{1}{\mu_\Delta^2} + \frac{1}{\mu}\right)}{\varepsilon_2} = s\sqrt{n_2} \tag{5-37}$$

or

$$\frac{B_{max}^s\left(\varepsilon_2^4 - \frac{1}{\mu_\Delta^2} + \frac{1}{\mu}\right)^s}{\varepsilon_2^4} = n_2 \tag{5-38}$$

These equations are tabulated by assuming a constant B_{max} value for the particular chart under construction. Then for various B_Δ / B_{max} ratios, various values of ε_2 are assumed and the resulting n_2 values calculated by (5-37) or (5-38). Curves with n_2 as abscissas and ε_2 as ordinates can then be plotted with I_Δ / I_{max} as a constant by the method use for previous charts. By means of (5-36) curves of α versus n_2 can be constructed. Such a chart is called Chart 2C. This also has the n_{2r}, ε_{2r} and s axes identical to those of Charts 2A and 2B. There is a Chart 2C for each value of B_{max}. 1, 2, 4 and 10 kilogauss.

Chart 2C would normally be used after the designer had used Chart 2A and found the B_{max} value to be too high. He would then use the appropriate Chart 2C. Equations (5-15), (5-18) and (5-20) are used to calculate ℓ_i, N and R_c respectively.

CHAPTER 6

THE DESIGN METHOD FOR INDUCTORS LIMITED BY TOTAL RESISTANCE

General Equations

Chapter IV considered the problem of synthesis of inductors where only the copper resistance was specified. In any iron core inductor there is core loss when the induction or magnetizing force is varying with time. This core loss is generally a function of the induction wave (including frequency waveforms and amplitude) and the volume of the iron having this waveform. For the type of core materials considered here the core loss for a fixed frequency is expressed approximately by

$$W_i = \gamma B_\Delta^2 w \ell_i^3 \quad . \tag{6-1}$$

where γ is a constant for a given frequency and waveform.

This loss is supplied by the time varying components of current and voltage so that in computing the resistance that this loss presents in the circuit, the mean square current used must not include the d-c component. The equation relating loss and resistance is then,

$$(I_{rms}^2 - I^2) R_i = W_i \quad . \tag{6-2}$$

where I_{rms} is the root-mean-square value of the current in amperes, including the d-c component,

I is the d-c component of current in amperes

and R_i is the core loss component of resistance in ohms.

Solving (6-2) for R_i gives

$$R_i = \frac{W_i}{I_{rms}^2 - I^2} \quad . \tag{6-3}$$

and when W_i from (6-1) is inserted, (6-3) becomes

$$R_i = \frac{\gamma B_\Delta^2 w \ell_i^3}{I_{rms}^2 - I^2} \quad . \tag{6-4}$$

From (2-24)

$$B_\Delta \ell_i = \frac{.4\pi N I_\Delta}{(\frac{1}{\mu_\Delta} + \alpha)} \quad , \tag{6-5}$$

and from (2-29) by substituting $w \ell_i^2$ for a_i.

$$B_\Delta w \ell_i^2 = \frac{I_\Delta L 10^8}{N} \quad . \tag{6-6}$$

Multiplying (6-5) and (6-6) gives

$$B_\Delta^2 w \ell_i^3 = \frac{.4\pi I_\Delta^2 L 10^8}{\frac{1}{\mu_\Delta} + \alpha} \quad , \tag{6-7}$$

and inserting this value of $B_\Delta^2 w \ell_i^3$ into (6-4) gives

$$R_i = \frac{.4\pi\gamma I_\Delta^2 L 10^8}{(I_{rms}^2 - I^2)(\frac{1}{\mu_\Delta} + \alpha)} \quad , \tag{6-8}$$

The total resistance to the time varying component of current is

$$R_{ac} = R_c + R_i \quad . \tag{6-9}$$

where R_{ac} is the total effective resistance in ohms.

The values of R_c and R_i from (4-11) and (6-8) result in

$$R_{ac} = \frac{\rho L 10^8 (\frac{1}{\mu_\Delta} + \alpha)}{.4\pi v w \ell_i^2} + \frac{.4\pi \gamma I_\Delta^2 L 10^8}{(I_{rms}^2 - I^2)(\frac{1}{\mu_\Delta} + \alpha)} \quad . \tag{6-10}$$

This equation is of the form

$$R_{ac} = Qy + \frac{q}{y} \quad . \tag{6-11}$$

where

$$y = \left(\frac{1}{\mu_\Delta} + \alpha\right) \quad . \tag{6-12}$$

$$Q = \frac{n \rho L 10^8}{.4\pi \nu w \ell_1^2} \tag{6-13}$$

and

$$q = \frac{.4\pi \gamma I_\Delta^2 L 10^8}{(I_{rms}^2 - I^2)} \quad . \tag{6-14}$$

Functions of the form (6-11) are hyperbolas having a minimum value at the point where

$$Qy = q \quad . \tag{6-15}$$

or

$$y^2 = \frac{q}{Q} \quad . \tag{6-16}$$

If there is no other restriction on the value of $\left(\frac{1}{\mu_\Delta} + \alpha\right)$, the minimum R_{ac} occurs at the point where

$$R_c = R_1 = \frac{R_{ac}}{2} \quad . \tag{6-17}$$

and

$$\left(\frac{1}{\mu_\Delta} + \alpha\right)^2 = \frac{(.4\pi)^2 \nu w \gamma \ell_1^2 I_\Delta^2}{n\rho (I_{rms}^2 - I^2)} \quad . \tag{6-18}$$

In Chapter IV it was shown that $\left(\frac{1}{\mu_\Delta} + \alpha\right)$ has a minimum value which is a function of the magnetic core material and the electrical specifications, L, I_{max}, I_Δ and R_c. This minimum value of $\left(\frac{1}{\mu_\Delta} + \alpha\right)$ may be less than, equal to, or greater than the value given by (6-18) for minimum R_{ac}. If the minimum value of $\left(\frac{1}{\mu_\Delta} + \alpha\right)$ is greater than the value given by (6-18), the minimum R_{ac} condition expressed by (6-17) and (6-18) can not be realized and from (6-9) and (6-10) it is apparent that

$$R_1 < \frac{R_{ac}}{2} < R_c < R_{ac} \quad . \tag{6-19}$$

On the other hand if the minimum value of $(\frac{1}{\mu_\Delta} + \alpha)$ is less than or equal to the value give by (6-18) the minimum R_{ac} condition, (6-17) and (6-18) can be realized.

Consider the case in which the optimum value of $(\frac{1}{\mu_\Delta} + \alpha)$ can be realized. The value of $(\frac{1}{\mu_\Delta} + \alpha)$ from 6-18) can be inserted into (4-11), (6-8) and (6-17) to give

$$R_c = R_i = \frac{R_{ac}}{2} = \frac{L\,10^8}{\ell_i}\sqrt{\frac{u\,\rho\,\gamma\,I_\Delta^2}{\gamma\,w(I_{rms}^2 - I^2)}}. \qquad (6\text{-}20)$$

This equation may be solved for ℓ_i.

$$\ell_i = \frac{2L\,10^8}{R_{ac}}\sqrt{\frac{u\,\rho\,\gamma\,I_\Delta^2}{\gamma\,w(I_{rms}^2 - I^2)}}\ . \qquad (6\text{-}21)$$

Inserting this value of ℓ_i into (6-18) gives

$$\frac{1}{\mu_\Delta} + \alpha = \frac{.4\pi\,\gamma\,I_\Delta^2\,L\,10^8}{(I_{rms}^2 - I^2)\,R_{ac}\,/\,2}\ . \qquad (6\text{-}22)$$

This equation may be used with Chart 1A (or 1B or 1C where their respective conditions apply) to determine in which case any given specifications lie. The value of n_1 (or n_{1r}) may be calculated from the known specifications and

$$R_c = \frac{R_{ac}}{2}\ . \qquad (6\text{-}23)$$

From the chart the value of g_1 is read from the appropriate curve. From (4-37)

$$\frac{1}{\mu_\Delta} + \alpha = g_1^2\ . \qquad (6\text{-}24)$$

and this equation can be used to calculate the minimum value of $(\frac{1}{\mu_\Delta} + \alpha)$ for the given specifications and the condition of (6-23). Equation (6-22) can be used to calculate the value of $(\frac{1}{\mu_\Delta} + \alpha)$ for minimum R_{ac}. This value will be symbolized by θ_1^2 so that

$$G_1^2 = \frac{.4\pi \gamma I_\Delta^2 L 10^8}{(I_{rms}^2 - I^2) R_{ac}/2} \quad . \tag{6-25}$$

A comparison of ϵ_1^2 and G_1^2 will immediately indicate under which case the design will fall. If

$$G_1^2 < \epsilon_1^2 \quad . \tag{6-26}$$

the value of $(\frac{1}{\mu_\Delta} + \alpha)$ for minimum R_{ac} can not be reached and the optimum design will be one of the copper resistance limited designs given by Chart 1A, 1B or 1C, the specific details to be given later. If

$$\epsilon_1^2 \leq G_1^2 \quad . \tag{6-27}$$

the value of $(\frac{1}{\mu_\Delta} + \alpha)$ for minimum R_{ac} can be reached and the design is made around this value. When (6-27) is an equality the design is identical to the copper resistance limited design for the condition of (6-23). When it is an inequality the resulting design will not be identical to any copper resistance limited design.

Design With Equal Copper and Core Loss Resistance

For the case in which (6-27) is satisfied, (6-21) will provide the iron length, ℓ_1. A plot of $\frac{u(s)}{v(s)} \frac{v(1)}{u(1)}$ is shown in Chart 3a for convenience in calculating (6-21) for various stack heights after an initial calculation of square stack has been made. Equation (6-18) may be rearranged to give

$$\frac{\frac{1}{\mu_\Delta} + \alpha}{\ell_1} = .4\pi \sqrt{\frac{v w \gamma I_\Delta^2}{u \rho (I_{rms}^2 - I^2)}} \tag{6-28}$$

and this value may be inserted into (4-10) to give

$$N^2 = L\,10^8 \sqrt{\frac{v\,\gamma\,I_\Delta^2}{u\,w\,\rho(I_{rms}^2 - I^2)}} \quad . \tag{6-29}$$

and

$$N = \sqrt{L\,10^8} \sqrt[4]{\frac{v\,\gamma\,I_\Delta^2}{u\,w\,\rho(I_{rms}^2 - I^2)}} \quad . \tag{6-30}$$

An equation for B_Δ can be obtained by inserting the values of N, ℓ_1 and $(\frac{1}{\mu_\Delta} + \alpha)$ from (6-26), (6-21) and (6-22) respectively into (2-24) .

$$B_\Delta = (\frac{R_{ac}}{2})^2 \sqrt[4]{\frac{v^3\,w(I_{rms}^2 - I^2)^5}{u^3\,\rho^3\,\gamma^5\,I_\Delta^6 (L\,10^8)^6}} \quad . \tag{6-31}$$

The above equations formulate all the important quantities of the design except α, B_{max}, μ and μ_Δ. To find these consider (4-42). By definition

$$G_1^2 \overset{\Delta}{=} \frac{1}{\mu_\Delta} + \alpha \tag{6-32}$$

for this $R_c = R_1$ case. Substituting α from (6-32) into (4-42) gives

$$\frac{B_\Delta}{B_{max}} = \frac{I_\Delta}{I_{max}} \quad \frac{G_1^2 - \frac{1}{\mu_\Delta} + \frac{1}{\mu}}{G_1^2} \quad . \tag{6-33}$$

Rearranging,

$$\frac{B_\Delta\,I_{max}\,G_1^2}{I_\Delta} = B_{max}\,G_1^2 - B_{max}(\frac{1}{\mu_\Delta} - \frac{1}{\mu}) \quad . \tag{6-34}$$

and

$$B_{max}\,(\frac{1}{\mu_\Delta} - \frac{1}{\mu}) = B_{max}\,G_1^2 - \frac{B_\Delta\,I_{max}\,G_1^2}{I_\Delta} \quad . \tag{6-35}$$

This equation may be solved by a graphical method. For each of several values of B_Δ the left hand side may be plotted as a function of B_{max}. Such a plot is Chart 3. All the quantities

on the right hand side are known except B_{max}. This right hand side represents a straight line on Chart 3 whose slope is G_1^2 and whose B_{max} axis intercept is

$$B_{max} = \frac{B_\Delta I_{max}}{I_\Delta} \quad . \tag{6-36}$$

This line may be constructed for each design and its intersection with the curve of Chart 3 is the solution of (6-35). There may be two intersections each indicating an allowable operating point. Generally the lower one would be chosen from the standpoint of linearity, etc. Since B_{max} and B_Δ are now known, μ_Δ can be obtained from the original iron μ_Δ curves and from (6-32)

$$\alpha = G_1^2 - \frac{1}{\mu_\Delta} \quad . \tag{6-37}$$

Alternatively, μ may be obtained from the original iron curves and used in the following equation derived from (4-42).

$$\alpha = \frac{B_\Delta I_{max}}{B_{max} I_\Delta} G_1^2 - \frac{1}{\mu} \quad . \tag{6-38}$$

The design process began by use of (6-23) to enter Chart 1A, 1B or 1C. Next G_1^2 was calculated by (6-25) and compared with g_1^2 from the chart. Having found that (6-27) applied the designer calculated ℓ_1 by (6-21), $(\frac{1}{\mu_\Delta} + \alpha)$ by (6-22), N by (6-30) or (4-10) and B_Δ by (6-31) or (2-24). He constructed the straight line on Chart 3 representing the right hand side of (6-35) and then found B_{max} and α.

Design Limited By Copper Resistance

If (6-26) was found to describe the order of G_1 and g_1, a different attack is necessary. Equation (6-9) may be solved for $(\frac{1}{\mu_\Delta} + \alpha)$.

$$\frac{1}{\mu_\Delta} + \alpha = \frac{.4\pi \gamma I_\Delta^2 L 10^8}{(I_{rms}^2 - I^2) R_1} \tag{6-39}$$

From (6-9)

$$R_1 = R_{ac} - R_c \tag{6-40}$$

and inserting this into (6-39) and substituting G_{1*}^2 for $(\frac{1}{\mu_\Delta} + \alpha)$ gives

$$G_{1*}^2 = \frac{.4\pi \gamma I_\Delta^2 L 10^8}{(I_{rms}^2 - I^2)(R_{ac} - R_c)} . \tag{6-41}$$

From the equation for n_1 (4-32),

$$R_c = \frac{u \rho}{v} \sqrt[3]{\frac{L n_1 10^8}{(.4\pi)^5 w I_{max}^4}} . \tag{6-42}$$

Inserting this value of R_c into (6-41) gives

$$G_{1*} = \sqrt{\frac{.4\pi \gamma I_\Delta^2 L 10^8}{(I_{rms}^2 - I^2)\left[R_{ac} - \frac{u \rho}{v}\sqrt[3]{\frac{L n_1 10^8}{(.4\pi)5 w I_{max}^4}}\right]}} \tag{6-43}$$

For a particular set of specifications this quantity might be plotted as a curve on Chart 1A and its intersection with the g_1 curve would be the design point from which the design would be made according to Chapter IV.

This is a very complicated function to compute and an approximate method will be satisfactory in most cases. From (6-19) the limiting values that R_c can have are $R_{ac}/2$ and R_{ac}. Calculations can be made for these two points as follows:

$$\text{Let } R_c' = \frac{R_{ac}}{2} \quad . \tag{6-44}$$

Calculate n_1' corresponding to R_c' by (4-32). Read ε_1' corresponding to n_1'. Calculate, from (6-8) and (4-37)

$$R_i' = \frac{.4\pi\ \gamma\ I_\Delta^2\ L\ 10^8}{(I_{rms}^2 - I^2)\ \varepsilon_1'^2} \quad . \tag{6-45}$$

$$\text{Calculate } R_{ac}' = R_c' + R_i' \ . \tag{6-46}$$

$$\text{Let } R_c'' = R_{ac} \quad . \tag{6-47}$$

In the same manner as before calculate n_1'', read ε_1'', calculate R_i'' and R_{ac}''. By consideration of (6-10) and (6-26) it is seen that

$$R_i' < R_c \quad . \tag{6-48}$$

so that

$$R_{ac}' < R_{ac} \quad . \tag{6-49}$$

$$\text{As long as } I_\Delta \neq 0, \tag{6-50}$$

$$\text{and } \gamma \neq 0, \tag{6-51}$$

$$R_i'' > 0, \tag{6-52}$$

so that

$$R_{ac}'' > R_{ac} \tag{6-53}$$

These are then two points on either side of the point where the inductor design will have the proper R_{ac}. Linear interpolations may be used to find the approximate design point. Thus,

$$\frac{n_1 - n_1'}{n_1'' - n_1'} = \frac{R_{ac} - R_{ac}'}{R_{ac}'' - R_{ac}'} \quad . \tag{6-54}$$

CHAPTER 7

THE DESIGN METHOD FOR INDUCTORS LIMITED BY TOTAL LOSS HEATING

General Equations

As copper loss heating was considered in Chapter V, heating by the total resistance will be considered now.

The thermal power density resulting from the copper resistance was derived as

$$K_c = \frac{u \rho I_{rms}^2 L 10^8 \left(\frac{1}{\mu_\Delta} + \alpha\right)}{.4\pi v w \ell_1^4} \quad . \tag{5-4}$$

The core loss was given by (6-1) and by inserting (6-7) into (6-1),

$$W_i = \frac{.4\pi \gamma I_\Delta^2 L 10^8}{\frac{1}{\mu_\Delta} + \alpha} \quad . \tag{7-1}$$

Since the surface area is $p\ell_1^2$, the thermal power density resulting from the core loss is,

$$K_i = \frac{.4\pi \gamma I_\Delta^2 L 10^8}{p \ell_1^2 \left(\frac{1}{\mu_\Delta} + \alpha\right)} \quad . \tag{7-2}$$

where K_i is the thermal power density resulting from the core loss, in watts per square centimeter. These two power density terms (5-4) and (7-2) may be added to give the total power density, K_{ac} in watts per square centimeter.

$$K_{ac} = \frac{u\rho I_{rms}^2 L 10^8 \left(\frac{1}{\mu_\Delta} + \alpha\right)}{.4\pi p v w \ell_1^4} + \frac{.4\pi \gamma I_\Delta^2 L 10^8}{p \ell_1^2 \left(\frac{1}{\mu_\Delta} + \alpha\right)} \tag{7-3}$$

This equation is of the same form as (6-10) and will be treated in the same way. If $\left(\frac{1}{\mu_\Delta} + \alpha\right)$ is not otherwise resistricted, K_{ac} is a minimum when

$$K_c = K_i \quad , \tag{7-4}$$

and

$$\left(\frac{1}{\mu_\Delta} + \alpha\right)^2 = \frac{(.4\pi)^2 \, v \, w \, \gamma \, \ell_i^{\,2} \, I_\Delta^{\,2}}{u \, \rho \, I_{rms}^2} \quad . \tag{7-5}$$

Substituting this value of $\left(\frac{1}{\mu_\Delta} + \alpha\right)$ into (5-4) and (7-2) gives

$$K_c = K_i = \frac{K_{ac}}{2} = \frac{I_{rms} \, I_\Delta \, L \, 10^8}{p \, \ell_i^{\,3}} \sqrt{\frac{u \, \rho \, \gamma}{v \, w}} \quad . \tag{7-6}$$

Solving (7-6) for ℓ_i,

$$\ell_i = \sqrt[3]{\frac{I_{rms} \, I_\Delta \, L \, 10^8}{p \, K_{ac}/2} \sqrt{\frac{u \, \rho \, \gamma}{v \, w}}} \quad , \tag{7-7}$$

and substituting (7-7) into (7-5) gives

$$\frac{1}{\mu_\Delta} + \alpha = .4\pi \sqrt[3]{\frac{v \, w \, \gamma^3 \, I_\Delta^{\,4} \, L \, 10^8}{pu\rho \, I_{rms}^2 \, K_{ac}/2}} \quad . \tag{7-8}$$

This equation can be used for comparison with Chart 2A (or 2B or 2C when they apply) to determine whether this value of $\left(\frac{1}{\mu_\Delta} + \alpha\right)$ can be realized. From (5-9) n_2 may be calculated for the condition that

$$K_c = \frac{K_{ac}}{2} \tag{7-9}$$

where K_{ac} is determined by the allowable temperature rise. The Chart will then give g_2 and from (5-14),

$$\frac{1}{\mu_\Delta} + \alpha = g_2^{\,4} \quad , \tag{7-10}$$

the minimum value of $\left(\frac{1}{\mu_\Delta} + \alpha\right)$ is obtained for the condition (7-9). Equation (7-8) will be used to calculate the value of $\left(\frac{1}{\mu_\Delta} + \alpha\right)$ required for minimum R_{ac} and this value will be symbolized by $G_2^{\,4}$ so that

$$G_2^{\,4} = .4\pi \sqrt[3]{\frac{v \, w \, \gamma^3 \, I_\Delta^{\,4} \, L \, 10^8}{p \, u \, \rho \, K_{ac}/2 \, I_{rms}^2}} \quad . \tag{7-11}$$

The quantities $g_1^{\,4}$ and $G_1^{\,4}$ may now be compared. If

$$\mathcal{C}_2^4 < \mathcal{E}_2^4 \quad . \tag{7-12}$$

the value of $(\frac{1}{\mu_\Delta} + \alpha)$ for minimum K_{ac} can not be reached and the optimum design will be one of the copper loss limited designs of Chart 2A, 2B or 2C. If

$$\mathcal{E}_2^4 \leq \mathcal{C}_2^4 \quad . \tag{7-13}$$

the value of $(\frac{1}{\mu_\Delta} + \alpha)$ for minimum K_{ac} can be realized and used for the design. If (7-13) is an equality the design will be identical to the copper loss heating limited design, but if (7-13) is an inequality the design may be different from any copper loss limited design.

Design With Equal Copper And Core Loss

In either situation for which (7-13) is satisfied, equation (7-7) will provide the formula for ℓ_1. A plot of $\sqrt[6]{\frac{u(s)}{v(s)}\frac{v(1)}{u(1)}}$ is shown in Chart 3a for convenience in calculating (7-7) for various stack heights after an initial calculation for a square stack has been made. Equation (7-5) may be rearranged to give,

$$\frac{\frac{1}{\mu_\Delta} + \alpha}{\ell_1} = .4\pi \sqrt{\frac{v\, w\, \gamma\, I_\Delta^2}{u\, \rho\, I_{rms}^2}} \quad . \tag{7-14}$$

and this value may be inserted into (4-10) so that

$$N^2 = L\, 10^8 \sqrt{\frac{v\, \gamma\, I_\Delta^2}{u\, w\, \rho\, I_{rms}^2}} \quad . \tag{7-15}$$

and

$$N = \sqrt{L\, 10^8} \sqrt[4]{\frac{v\, \gamma\, I_\Delta^2}{u\, w\, \rho\, I_{rms}^2}} \quad . \tag{7-16}$$

An equation for B_Δ can be obtained by inserting the values of N, ℓ_1, and $(\frac{1}{\mu_\Delta} + \alpha)$ from (7-16), (7-7) and (7-8) respectively into (2-24).

$$B_\Delta = \sqrt[12]{\frac{p^6 \, v \, (K_{ac}/2)^6}{u \, w^5 \, \rho \, \gamma^7 \, I_\Delta{}^2 \, I_{rms}^2 \, (L \, 10^6)^2}} \qquad (7\text{-}17)$$

The other unknowns, α, B_{max}, μ and μ_Δ can be found by a method similar to that for the total resistance limited case. By definition

$$G_2{}^4 \triangleq \frac{1}{\mu_\Delta} + \alpha \qquad (7\text{-}18)$$

for the $K_c = K_1$ case. Substituting α from (7-18) into (4-42) gives

$$\frac{B_\Delta}{B_{max}} = \frac{I_\Delta}{I_{max}} \quad \frac{G_2{}^4 - \frac{1}{\mu_\Delta} + \frac{1}{\mu}}{G_2{}^4} \; . \qquad (7\text{-}19)$$

Rearranging,

$$\frac{B_\Delta I_{max} \, G_2{}^4}{I_\Delta} = B_{max} \, G_2{}^4 - B_{max} \left(\frac{1}{\mu_\Delta} - \frac{1}{\mu}\right) \; . \qquad (7\text{-}20)$$

and

$$B_{max} \left(\frac{1}{\mu_\Delta} - \frac{1}{\mu}\right) = B_{max} \, G_2{}^4 - \frac{B_\Delta \, I_{max} \, G_2{}^4}{I_\Delta} \qquad (7\text{-}21)$$

Chart 3 can be used to solve this equation in the same way as it was used for (6-35). The construction line is now a line with slope, $G_2{}^4$, and with B_{max} axis intercept

$$B_{max} = \frac{B_\Delta I_{max}}{I_\Delta} \; . \qquad (7\text{-}22)$$

The intersection of this line and the appropriate curve is the solution of (7-21). The value of B_{max} is now known and μ or μ_Δ can be obtained from the basic iron data.

From (7-18)

$$\alpha = G_2{}^4 - \frac{1}{\mu_\Delta} \; . \qquad (7\text{-}23)$$

and from (4-42),

$$\alpha = \frac{B_\Delta I_{max}}{B_{max} I_\Delta} \quad G_2^4 - \frac{1}{\mu} \quad . \tag{7-24}$$

Either of these equations can be used to find α.

The copper resistance of the choke may be derived from (5-20) by inserting $K_{ac}/2$ for K_c.

$$R_c = G_2^3 \quad \frac{p\, u\, \rho\, L\, 10^8\, K_{ac}/2}{.4\pi\, v\, w\, I_{rms}^2} \tag{7-25}$$

The iron loss component of resistance may be derived from (6-8) as

$$R_i = \frac{.4\pi\, \gamma\, I_\Delta^2\, L\, 10^8}{G_2^4 (I_{rms}^2 - I^2)} \quad . \tag{7-26}$$

Design Limited By Copper Loss

All the dimensions of the design under the condition of (7-13) have been found so it is next necessary to consider the case where (7-12) applies. This design will be one of the copper loss heating limited designs such that

$$K_i < \frac{K_{ac}}{2} < K_c < K_{ac} \tag{7-27}$$

and the particular one for smallest size will be found in a manner analogous to the second case in Chapter VI. Equation (7-2) may be solved for $(\frac{1}{\mu_\Delta} + \alpha)$,

$$\frac{1}{\mu_\Delta} + \alpha = \frac{.4\pi\, \gamma\, I_\Delta^2\, L\, 10^8}{p\, \ell_i^2\, K_i} \quad . \tag{7-28}$$

Since K_{ac} is the sum of K_i and K_c,

$$K_i = K_{ac} - K_c \quad . \tag{7-29}$$

and this value may be inserted into (7-28) to give

$$G_{2e}{}^4 = \frac{.4\pi\ \gamma\ I_\Delta{}^2\ L\ 10^8}{p\ \ell_1{}^2\ (K_{ac} - K_c)} \qquad (7\text{-}30)$$

where $G_{2e}{}^4$ has been substituted for $(\frac{1}{\mu_\Delta} + \alpha)$ from (5-14).

From (5-15)

$$\ell_1{}^2 = g_2{}^2 \sqrt{\frac{u\ \rho\ I_{rms}^2\ L\ 10^8}{.4\pi\ p\ v\ w\ K_c}} \quad . \qquad (7\text{-}31)$$

and this may be substituted into (7-30) to give

$$G_{2e}{}^4 = \frac{\gamma\ I_\Delta}{g_2{}^2\ I_{rms}\ (K_{ac} - K_c)} \sqrt{\frac{(.4\pi)^3\ v\ w\ K_c\ L\ 10^8}{p\ u\ \rho}} \quad . \qquad (7\text{-}32)$$

From the equation for n_2 (5-9)

$$K_c = \frac{u\ \rho}{p\ v} \sqrt[3]{\frac{n_2\ w\ I_{rms}^6}{(.4\pi)^7\ L\ I_{max}^8\ 10^8}} \quad . \qquad (7\text{-}33)$$

Inverting (7-33) into (7-31) gives

$$G_{2e}{}^4 = \frac{w\ \gamma\ I_\Delta}{g_2{}^2 p (K_{ac} - \frac{u\rho}{pv} \sqrt[3]{\frac{n_2 w\ I_{rms}^6}{(.4\pi)^7\ I_{max}^8 L\ 10^8}})} \sqrt[6]{\frac{(.4\pi)^2 n_2 (L10^8)^2}{L_{max}^8}} \quad . \qquad (7\text{-}34)$$

For a particular set of specifications, this quantity might be plotted on the chart (2A, 2B, or 2C) with G_{2e} being plotted to the same scale as g_2. The intersection of this curve with the g_2 curve is then the point where the specified, K_{ac} figure will just be met and therefore this point represents the minimum size design. As in the second case of Chapter VI this is a very complicated function and linear interpolation may be used to good advantage in most problems. From (7-27) the limiting values of K_c are $K_{ac}/2$ and K_{ac}. Let

$$K_c{}' = \frac{K_{ac}}{2} \quad . \qquad (7\text{-}35)$$

Calculate $n_2{}'$ corresponding to $K_c{}'$ by (5-9). Read the corresponding $g_2{}'$ from the chart. Calculate $\ell_1{}'$ from (5-15) and K_1

from

$$K_i' = \frac{.4\pi\ \gamma\ I_\Delta^2\ L\ 10^8}{p\ 4_1^2\ (\varepsilon_2')^4} \qquad (7\text{-}36)$$

which was derived from (5-14) and (7-2). Calculate

$$K_{ac}' = K_c' + K_i' \quad . \qquad (7\text{-}37)$$

Make similar calculations for

$$K_c'' = K_{ac} \quad . \qquad (7\text{-}38)$$

These will lead to a value of K_{ac}''. From (7-27) it is seen that

$$K_i' \quad K_c' \quad , \qquad (7\text{-}39)$$

so that

$$K_{ac}' < K_{ac} \quad . \qquad (7\text{-}40)$$

If

$$I_\Delta \neq 0 \quad , \qquad (7\text{-}41)$$

and

$$\gamma \neq 0 \quad , \qquad (7\text{-}42)$$

then

$$K_i'' > 0 \qquad (7\text{-}43)$$

and

$$K_{ac}'' > K_{ac} \quad . \qquad (7\text{-}44)$$

These two points are therefore on either side of the point with the specified value of K_{ac} and linear interpolation between them will give the approximate design point.

CHAPTER 8

THE GENERAL DESIGN METHOD

Specific methods of synthesis were developed in Chapters 4, 5, 6, and 7. Figure 12 shows the use and order of the various parts. Where the circuit imposes a resistance limitation, the design method follows the course in the upper part of the map. In the general case, the total resistance R_{ac} would be given and the method of design would be chosen by the inequalities (6-26) and (6-27). In some cases only the copper resistance R_c is specified and the R_c-limited design method would be used.

Within the R_c-limited area there are several charts. Normally Chart 1A is used first since it specifies the minimum size design otherwise unrestricted. It has a lower limit below which the air gap should be negative and in this range Chart 1B will specify the zero air gap design which is the best physically realizable design. Chart 1A has upper limits where a minimum ceases to exist and in many cases considerations of linearity may restrict the maximum induction to be used. For design in these ranges the Charts 1C provide designs.

Within the $R_c = R_i$ design area, the design method involves more algebraic equations and fewer curves than the R_c-limited area.

When the design has been made to meet a specified resistance figure, the thermal power density (which determines the temperature rise) should be checked. If the thermal power density of the design is too high or if there is no circuit

requirement on the allowable resistance, the design should be made in the thermal power density limited area shown in the lower portion of Figure 12.

The map of this area is similar to the map for specified resistance. Normally the designer would determine the specific method by means of the inequalities (7-12) and (7-13) although in the case of a small alternating current and large direct current, he would use the K_c-limited design immediately. There are several charts within the K_c-limited area and these are analogous to the charts in the R_c-limited area. The design method within the $K_c = K_i$ area is similar to the method in the $R_c = R_i$ area and uses the same Chart 3.

In most cases the design synthesized by the method will be subject to a winding calculation taking into account the actual wire size, local winding methods, etc.

The general method, in so far as the basic ideas are concerned, may also be used for transformers with superposed a-c and d-c magnitization. When so used, all the currents should be referred to one winding and the design can then be based on the magnitizing current and the open circuit inductance requirements. The heating effects must be based on the total magnetizing and load currents. The copper area factor v must be that for the reference winding alone. In a two winding transformer, the value of v would approximately be half of the value used in the inductor design for the same winding methods since each coil should occupy half the window.

B. Procedure Section

CHAPTER 9

Procedure for Construction of Curves

In this chapter a method of constructing the charts from the iron characteristics is presented. This method was used to construct the charts in this report. It does, however, involve graphical interpolation techniques which may introduce errors. A more accurate scheme would be to set up many more points and carry out the computations by means of digital computers.

The normal induction data is commonly given in two ways; the normal induction curve Figure 13, and the normal permeability curve 14.

Since

$$\mu = \frac{B_{max}}{H_{max}} \quad . \tag{9-1}$$

either of these curves may be used to plot the other on a point-by-point basis by making use of (9-1) at each point.

The analysis method makes use of the normal induction curve while the synthesis curves are constructed by use of the permeability curve. The incremental data is usually furnished by curves such as Figure 15. A number of points on these curves are arbitrarily chosen. After the calculations for these initial points have been made it may be necessary to make additional calculations to fill in "vacant" areas of the resulting curves.

For each point

$$H_{\Delta} = \frac{B_{\Delta}}{\mu_{\Delta}} \tag{9-2}$$

$$H_{max} = H_{\Delta} + H_{b} \tag{9-3}$$

and

$$H_{max} = \frac{B_{\Delta}}{\mu_{\Delta}} + H_{b} \quad . \tag{9-4}$$

From this value of H_{max} the corresponding value of B_{max} may be found from the normal induction curve, Figure 13. The ratio B_Δ/B_{max} may now be calculated.

An optional intermediate step is the plotting of μ_Δ versus B_Δ with H_{max} and B_{max} as constant parameters for each curve. Such a chart is shown in Figure 54 in Lee's book [7] although his curve data was obtained by use of Spooner's [20; 23] empirical formula for μ_Δ. Figure 16 shows the original μ_Δ curves with the values of H_{max} marked along each curve and the curves of constant H_{max} (and B_{max}) superposed. Whether or not this optional μ_Δ chart is constructed, the original points may now be tabulated.

Each of the points may now be plotted on coordinates of B_{max} and μ_Δ, each point being labeled with its B_Δ/B_{max} ratio. Curves may now be drawn for various values of the B_Δ/B_{max} value and being interpolated between points having close B_Δ/B_{max} values. Such a set of points and the resulting curves are shown in Figure 17. (See Table 1) It should be noted that the B_Δ/B_{max} ratio is always less than the final I_Δ/I_{max} ratio so that for designs in which the current never reverses,

$$\frac{I_\Delta}{I_{max}} \doteq 1/2 \qquad (9\text{-}5)$$

$$\frac{B_\Delta}{B_{max}} < 1/2 \qquad (9\text{-}6)$$

and no points for which

$$B_\Delta/B_{max} > 1/2 \qquad (9\text{-}7)$$

need to be computed. When the incremental permeability is considered as a function of B_{max}, for a given B_Δ/B_{max} ratio, it will be symbolized by μ'_Δ.

These curves of μ and μ'_Δ are the basis for the design charts. Both the values of the μ's and the derivatives of them will be needed in the construction of the design charts so a means of finding the derivative is necessary. The simplest methods is that of finite differences. Two points on the curve are chosen. The difference in their ordinates (vertical axis values) divided by the difference in their abscissas (horizontal axis values) gives the approximate derivative. The points chosen must be far enough apart so that these differences can be found with some accuracy. If they are too far apart an error from the curvature will result. This method is illustrated in Figure 17.

Construction of Chart 1A

The construction of Chart 1A will be described first. The following equations were previously derived or defined.

$$D = \frac{1}{\mu^2}\frac{d\mu}{dB_{max}} - \frac{1}{\mu'^2_\Delta}\frac{d\mu'_\Delta}{dB_{max}} \qquad (4\text{-}21)$$

$$\alpha = B_{max} D - \frac{1}{\mu} \qquad (4\text{-}24)$$

$$\frac{I_\Delta}{I_{max}} = \frac{B_\Delta}{B_{max}} \frac{\left(\frac{1}{\mu_\Delta} + \alpha\right)}{\left(\frac{1}{\mu} + \alpha\right)} \qquad (4\text{-}43)$$

For Chart 1A

$$n_1 = B_{max}^{.6} D^{.4} \left(B_{max} D - \frac{1}{\mu} + \frac{1}{\mu'_\Delta}\right) \qquad (4\text{-}35)$$

$$\epsilon_1 = \sqrt{B_{max} D - \frac{1}{\mu} + \frac{1}{\mu'_\Delta}} \qquad (4\text{-}39)$$

These quantities may now be calculated and tabulated for various points on the μ versus B_{max} and μ'_Δ versus B_{max} curves. Table -2 is such a tabulation.

For low values of B_{max} the value of α will be negative. For a given B_Δ/B_{max} ratio the point where α equal zero will be a lower limit beyond which points need not be computed nor plotted.

It may be found that for points with a given B_Δ/B_{max} ratio n_1 will increase as B_{max} is increased up to some point, and above this point n_1 will decrease as B_{max} is increased further. This point is than an upper limit for this B_Δ/B_{max} ratio and no points for greater values of B_{max} should be calculated or plotted for this B_Δ/B_{max} ratio.

Logarithmic coordinates are used for the chart. The abscissa (horizontal axis variable) is n_1 and the three ordinates (vertical axis variables) are B_{max}, α and ϵ_1.

A different spacing for the abscissa and ordinates is convenient because of the ranges involved. Each use of Table -2 gives a point for B_{max}, a point for α, and a point for ε_1. These three points are plotted on the chart in a vertical line above the corresponding n_1 value and each is labeled with the corresponding I_Δ/I_{max} ratio value.

When all these points have been plotted curves of B_{max}, α and ε_1 are drawn through (or interpolated between) points having the same I_Δ/I_{max} ratio. Such curves are shown in Figure 18 and the finished set of curves will be Chart 1A when the auxiliary axes are added.

Equations (4-45) and (4-48) govern the auxiliary axes.

$$n_{1r} = n_1 \frac{u^3 \rho^3 10^8}{(.4\pi)^5 v^3 w} \tag{4-45}$$

$$\varepsilon_{1r} = \varepsilon_1 \sqrt{\frac{u\rho 10^8}{.4\pi vw}} \tag{4-48}$$

The coefficients on the right hand side of (4-45) and (4-48) must be evaluated for the particular shape of inductors built by the particular local manufacturing technique.

$$u = \frac{\ell_c}{\ell_1} \tag{4-1}$$

$$v = \frac{a_c}{\ell_1^2} \tag{4-2}$$

$$w = \frac{a_1}{\ell_1^2} \tag{4-3}$$

The a_c and a_i are "net" areas and include the respective space factors. The resistivity ρ is determined by the conductor material (usually copper) and by the average operating temperature. For constructing the charts a resistivity figure for the highest average temperature may be used.

Having values for u, v, w and ρ, the coefficients on the right side of (4-45) and (4-48) may be computed. Logarithmic axes with the same spacings respectively as the g_1 and n_1 axes drawn parallel to the g_1 and n_1 axes such that all points on these new axes have values equal to the values of corresponding point on the g_1 and n_1 axes multiplied by the coefficients in (4-48) and (4-45) respectively.

The s axis may next be constructed. Some reference point is arbitrarily chosen. The charts in this report use the intersection of the g_{1r} and n_{1r} axes although any other point would do as well. At this point lay out a horizontal construction axis have the same spacing as the n_1 and n_{1r} axis and having the unity calibration point at the reference point. Similarly lay out a vertical construction axis having the same spacings as the g_1 and g_{1r} axes and having the unity calibration point at the reference point. Figure 19 shows these construction axes.

It is next necessary to compute the values of u, v, and w as functions of s, the stack height ratio.

It is assumed here that s is the ratio of stack height to the standard stack height from which the u, v and w were calculated. These values of u, v and w where computed for scrapless EI laminations and nominal space factors in (4-53), (4-58) and (4-62).

$$u(s) = \frac{2 + s}{3} \tag{4-53}$$

$$v(s) = .00625. \tag{4-58}$$

(a constant independent of s)

$$w(s) = .025s. \tag{4-62}$$

The s axis is constructed on a point-by-point basis plotting each point by use of the auxiliary construction axes. From (4-68) and (4-69) the positive logarithmic coordinates are abscissa (horizontal)

$$\frac{27s}{(2 + s)^3}$$

and ordinates (vertical)

$$\sqrt{\frac{3s}{2 + s}}\ .$$

Several values of s are assumed and for each value the abscissa and ordinate are calculated and the point is plotted and labeled with the value of s from which it was calculated. A curved s-axis line may then be drawn through all these points. Chart 1A shows the complete set of curves and axes.

For Charts 1B, 1C, 2A, 2B, and 2C the procedure is similar although the equations are different.

Construction of Chart 1B

Chart 1B, for the condition that $\alpha = 0$, requires no curves of α, only curves for B_{max} and ε_1. The equations are

$$n_1 = \frac{B_{max}^4}{\mu^4 \mu_\Delta'} \quad . \tag{4-73}$$

and

$$\varepsilon_1 = \frac{1}{\sqrt{\mu_\Delta'}} \quad . \tag{4-74}$$

The current ratio equation (4-43) becomes

$$\frac{I_\Delta}{I_{max}} = \frac{B_\Delta}{B_{max}} \frac{\mu}{\mu_\Delta'} \quad . \tag{9-6}$$

These quantities may now be tabulated as in Table -3.

Logarithmic coordinates are laid out with n_1 as abscissa and ε_1 and B_{max} as ordinates. For each use of Table -3 a point of ε_1 and a point for B_{max} are plotted at the appropriate n_1 point and are labeled with the corresponding I_Δ/I_{max} ratio.

Curves of B_{max} and ε_1 are now drawn for various I_Δ/I_{max} ratios in a similar manner to the method for Chart 1A. The auxiliary axes n_{1r}, ε_{1r} and s are identical to those of Chart 1A.

Construction of Chart 1C

Chart 1C, for the condition of a B_{max} limitation, requires no curves of B_{max}. Instead, a separate chart is

made for each B_{max} limitation. The equations are

$$n_1 = B_{max}^4 \varepsilon_1^2 \left(\varepsilon_1^2 - \frac{1}{\mu'_\Delta} + \frac{1}{\mu}\right)^4 \qquad (4\text{-}79)$$

$$\alpha = \varepsilon_1^2 - \frac{1}{\mu'_\Delta} \qquad (4\text{-}80)$$

$$\frac{I_\Delta}{I_{max}} = \frac{B_\Delta}{B_{max}} \frac{\left(\frac{1}{\mu'_\Delta} + \alpha\right)}{\left(\frac{1}{\mu} + \alpha\right)} \qquad (4\text{-}43)$$

These quantities may be tabulated as in Table 4.

Logarithmic coordinates are laid out with n_1 as abscissa and ε_1 and α as ordinates. For each use of Table 4, a point for ε_1 and a point for α are plotted as the appropriate n_1 point and are labeled with the corresponding I_Δ/I_{max} ratio. Curves of α and ε_1 are drawn for various I_Δ/I_{max} ratios in a manner similar to the method for Chart 1A. The auxiliary axes — n_{1r}, ε_{1r}, and s — are identical to those of Chart 1A.

Construction of Chart 2A

The equations for the construction of Chart 2A are

$$n_2 = \frac{B_{max}^{16} D^8}{B_{max} D - \frac{1}{\mu} + \frac{1}{\mu_\Delta}} \qquad (5\text{-}12)$$

$$\varepsilon_2 = \sqrt[4]{B_{max} D - \frac{1}{\mu} + \frac{1}{\mu_\Delta}} \qquad (5\text{-}16)$$

$$\alpha = \varepsilon_2^4 - \frac{1}{\mu_\Delta} \qquad (5\text{-}14)$$

$$\frac{I_\Delta}{I_{max}} = \frac{B_\Delta}{B_{max}} \frac{(\frac{1}{\mu_\Delta} + \alpha)}{(\frac{1}{\mu} + \alpha)} \qquad (4\text{-}43)$$

Table -5 is a tabulation for construction of Chart 2A.

Logarithmic coordinates are used for the chart. The abscissa is n_2 and the three ordinates are B_{max}, α, and ε_2. The points where α are negative are not plotted and there is no need for calculating beyond these points. Each use of Table -5 gives a point for B_{max}, α, and ε_2 with the corresponding value of n_2.

For the auxillary axes,

$$n_{2r} = n_2 \frac{u^3 w \rho^3}{(.4\pi)^7 p^3 v^3} \qquad (5\text{-}22)$$

$$\varepsilon_{2r} = \varepsilon_2 \sqrt[4]{\frac{up10^8}{.4\pi pvw}} \qquad (5\text{-}25)$$

The auxiliary axes are constructed in the same manner as in Chart 1A. The s axis is also constructed in a similar manner but the equations are different. They are $\frac{(2+s)^3 s}{27}$ for the abscissa, and $\sqrt[4]{\frac{2+s}{3s}}$ for the ordinates, in a positive sense. Several values of s are assumed and for each value the abscissa and ordinate are calculated and the point is plotted and labeled with the value of s from which it is was calculated. The spacing for plotting the s axis uses the spacing of the corresponding abscissa and ordinate of the n_{2r} and ε_{2r} axes.

Construction of Chart 2B

Chart 2B, for the condition that $\alpha = 0$ requires not curves of α, only curves of B_{max} and ε_1. The equations are

$$n_2 = \frac{B^{\varepsilon}_{max}\mu'_{\Delta}}{\mu^{\varepsilon}} \tag{5-34}$$

$$\varepsilon_2 = \sqrt[4]{\frac{1}{\mu'_{\Delta}}} \tag{5-35}$$

$$\frac{I_{\Delta}}{I_{max}} = \frac{B_{\Delta}\mu}{B_{max}\mu'_{\Delta}} \tag{9-8}$$

These quantities are tabulated as in Table -6.

Logarithmic coordinates are laid out with n_2 as abscissa and ε_2 and B_{max} as ordinates. For each use of Table -6 a point for ε_2 and a point for B_{max} are plotted at the appropriate n_2 point and are labeled with the corresponding I_{Δ}/I_{max} ratio. Curves of B_{max} and ε_2 are drawn for various I_{Δ}/I_{max} ratios in a similar manner to the method for Chart 1A. The auxiliary axes, n_{2r}, ε_{2r}, and s are identical to those of Chart 2A.

Construction of Chart 2C

Chart 2C, for the condition of a B_{max} limitation, requires no curves of B_{max}. Instead, a separate chart is made for each B_{max} limitation. The equations are

$$n_2 = \frac{B_{max}^{8}\left(\varepsilon_2^{4} - \frac{1}{\mu_\Delta T} + \frac{1}{\mu}\right)^{8}}{\varepsilon_2^{4}} \qquad (5\text{-}34)$$

$$\alpha = \varepsilon_2^{4} - \frac{1}{\mu_\Delta^{1}} \qquad (5\text{-}32)$$

$$\frac{I_\Delta}{I_{max}} = \frac{B_\Delta}{B_{max}} \quad \frac{\left(\frac{1}{\mu_\Delta} + \alpha\right)}{\left(\frac{1}{\mu} + \alpha\right)} \qquad (4\text{-}43)$$

These quantities are tabulated as in Table -7.

Logarithmic coordinates are laid out with n_2 as abscissa and ε_2 and α as ordinates. For each use of Table 7, a point for ε_2 and a point for α are plotted at the appropriate n_2 point and are labeled with the corresponding I_Δ/I_{max} value. Curves of α and ε_2 are drawn for various I_Δ/I_{max} ratios in a manner similar to that of Chart 1A. The auxiliary axes, n_{2r}, ε_{2r}, and s are identical to those of Chart 2A.

Construction of Chart 3

The construction of Chart 3 involves the use of Fig. 14 and 17. Each curve of Chart 3 is for a particular value of B_Δ. The first step is choosing a set of different values for B_Δ. For each B_Δ tabulate the values of B_{max} that can be obtained from Fig. 17. Thus, for a B_Δ = 100 gauss, the B_{max} values that can be used are 2000 gauss and 500 gauss for the B_Δ/B_{max} curves of .05 and .2, respectively. The number of points on any B_Δ curve of Chart 3 will depend upon the number of B_Δ/B_{max} curves of Fig. 17.

The value of μ_Δ is obtained from Fig. 17 and the value of μ from Fig. 14. The reciprocals are calculated. The abcissa is the difference of permeability reciprocals, $1/\mu_\Delta - 1/\mu$, multiplied by B_{max}. Table 8 is a tabulation of the necessary steps and calculations to get the values for abcissas and ordinates of Chart 3.

Construction of Chart 3a

The ordinates on Chart 3a are the core length factors given by $\sqrt{\frac{2+s}{3s}}$ for curve (1) and $\sqrt[6]{\frac{2+s}{3s}}$ for curve 2. The values of s make up the abcissa points. The ordinate is linear and the abcissa is logarithmic. This semi-log spacing is used for ease in construction and reading. Several values are assumed for s and points determined for curves 1 and 2. A tabulation listing the three values would be helpful in construction as it was in the construction of the other charts.

Chapter 10

Design Procedures

In the specifications of the reactor it is assumed that L, i(t), and either R_c or R_{ac} are given. Linearity and heating will place some sort of restriction on B_{max} and K_c or K_{ac}, respectively. The calculation of power density (K_c or K_{ac}) from temperature rise or vice versa is shown in two Armour reports [24, 25] and in the extracted portion contained in the appendix to this report. To show how the charts are used, the following procedure begins by knowledge of L, R_c, I_{max}, and I_Δ. This is an example of the resistance limited case. The other possible cases then follow in the step-by-step procedure.

1. Resistance Limitation

Calculate n_1 from

$$n_1 = \frac{(.4\pi)^5 \gamma^3 w I_{max}^4 R_c^3 \, 10^{-8}}{u^3 \rho^3 L} \qquad (4\text{-}32)$$

or n_{1r} from

$$n_{1r} = \frac{R_c^3 I_{max}^4}{L} \qquad (4\text{-}44)$$

if the standard shape is to be used for laminations. If the value of n_1 or n_{1r} falls on Chart 1A and B_{max} is not too large, use Chart 1A. If n_1 or n_{1r} falls above Chart 1A or if B_{max} as read on Chart 1A is too large, use Chart 1C.

1.1 Chart 1A If n_1 or n_{1r} is on the scales of Chart 1A, enter Chart 1A at the n_1 or n_{1r} value.

1.1.1 Read the intersection of the n_1 or n_{1r} line and the ε_1, α, and B_{max} curves of the proper I_Δ/I_{max} ratio for ε_1, α,

and B_{max}.

1.1.2 Calculate the mean path length of the core by

$$\ell_i = g_1\sqrt{\frac{up10^8}{.4\pi vw}}\sqrt{\frac{L}{R_c}} \qquad (4\text{–}38)$$

or by

$$\ell_i = g_{1r}\sqrt{\frac{L}{R_c}} \qquad (4\text{–}47)$$

1.1.3 Knowing ℓ_i select the core, part 3.

1.1.4 Calculate the total air gap length from

$$\ell_a = \alpha\ell_i \qquad (10\text{–}1)$$

where ℓ_i is the length of the core selected.

1.1.5 Calculate the number of turns from

$$N = \sqrt{g_1\sqrt{\frac{v10^8}{.4\pi w\rho}}\sqrt{LR_c}} \qquad (4\text{–}41)$$

1.1.6 Calculate the size of wire from

$$a_w = \frac{v\ell_i^2}{N} \qquad (10\text{–}2)$$

1.1.7 Choose the wire size and make a complete winding calculation, part 4.

1.2 Chart 1B. If n_1 or n_{1r} is below the left hand limit of Chart 1A, enter Chart 1B ($\alpha = 0$) at the n_1 or n_{1r} value.

1.2.1 On Chart 1B at the intersection of the n_1 or n_{1r} line and the B_{max} and g_1 curves for the proper I_Δ/I_{max} ratio, read B_{max} and g_1, respectively.

1.2.2 Calculate the mean path length of the core by

$$\ell_i = g_1\sqrt{\frac{up10^8}{.4\pi vw}}\sqrt{\frac{L}{R_c}} \qquad (4\text{–}38)$$

or by

$$\ell_i = \varepsilon_{1r}\sqrt{\frac{L}{R_c}} \qquad (4\text{-}47)$$

1.2.3 Knowing ℓ_i, select the core, part 3.

1.2.4 Calculate the number of turns from

$$N = \sqrt{\varepsilon_1}\sqrt{\frac{v10^8}{.4\pi w\rho}}\sqrt{LR_c} \qquad (4\text{-}41)$$

1.2.5 Calculate the size of wire from

$$a_w = \frac{v\ell_i^2}{N} \qquad (10\text{-}2)$$

1.2.6 Choose the wire size and make a complete winding calculation, part 4.

1.2.7 Using Chart 1B there is no air gap.

1.3 Chart 1C. If n_1 or n_{1r} is beyond the right hand limit of Chart 1A or if B_{max} is greater than linearity requirements allow, enter Chart 1C at the n_1 or n_{1r} value.

1.3.1 Select the 1C Chart with the appropriate B_{max} value.

1.3.2 Enter the chart at the given n_1 or n_{1r} value.

1.3.3 Read the corresponding values of α and g_1 from the intersection of the n_1 or n_{1r} line and the α and g_1 curves of the proper I_Δ/I_{max} ratio.

1.3.4 Calculate ℓ_i from

$$\ell_i = g_1\sqrt{\frac{\rho 10^8}{.4\pi v}}\sqrt{\frac{L}{R_c}} \qquad (4\text{-}38)$$

or from

$$\ell_i = \varepsilon_{1r}\sqrt{\frac{L}{R_c}} \qquad (4\text{-}47)$$

1.3.5 Knowing ℓ_i select the core, part 3.

1.3.6 Calculate the total air gap length from

$$\ell_a = \alpha\ell_i \qquad (10\text{-}1)$$

where ℓ_1 is the length of the core selected.

1.3.7 Calculate the number of turns from

$$N = \sqrt{g_1 \sqrt{\frac{v10^8}{.4\pi w\rho}}} \sqrt{LR_c} \qquad (4\text{-}41)$$

1.3.8 Calculate the size of wire from

$$a_w = \frac{v\ell_1^2}{N} \qquad (10\text{-}2)$$

1.3.9 Choose the wire size and make a complete winding calculation, part 4.

1.4 For cases with appreciable incremental (alternating) current the total resistance R_{ac} will usually be specified rather than the copper resistance R_c. A design in this case requires a comparison with the R_c case.

1.4.1 Calculate the value of g_1^2 using the procedure given in part 1. For R_c use the value

$$R_c = \frac{R_{ac}}{2} \qquad (10\text{-}3)$$

1.4.2 Calculate G_1^2 from

$$G_1^2 = \frac{.4\pi\gamma I_\Delta^2 L 10^8}{(I_{rms}^2 - I^2)\frac{R_{ac}}{2}} \qquad (6\text{-}25)$$

1.4.3 If $G_1^2 < g_1^2$, then use the previous method after determining the value to use for R_c.

1.4.3.1 Calculate n_1' by (4-32) or (4-44) for

$$R_c = \frac{R_{ac}}{2}\ ' \qquad (10\text{-}4)$$

and n''_1 for

$$R_c = R_{ac}\ '' \qquad (10\text{-}5)$$

Read g'_1 and g''_1 from the same chart that g_1^2 was determined from in part 1.1, 1.2, 1.3.

1.4.3.2 Calculate R'_1 and R''_1 from

$$R'_1 = \frac{.4\pi\gamma I^2 L 10^8}{(I^2_{rms} - I^2)\, g'^2_1} \qquad (6\text{-}45)$$

knowing g'_1 and g''_1 from above.

1.4.3.3 Calculate

$$R'_{ac} = R'_c + R'_1 \qquad (10\text{-}6)$$

$$R''_{ac} = R''_c + R''_1 \qquad (10\text{-}7)$$

1.4.3.4 Calculate

$$n_1 = \frac{(R_{ac} - R'_{ac})(n''_1 - n'_1)}{(R''_{ac} - R'_{ac})} + n'_1 \qquad (10\text{-}8)$$

1.4.3.5 Calculate R_c from (4-32) or (4-44) knowing n_1 or n_{1r}, I_{max}, and L.

1.4.3.6 For this value of n_1 read g_1, α, and B_{max} from Chart 1A, 1B, or 1C and proceed with the design as outlined in the previous part corresponding to the chart used.

1.4.4 If $g_1^2 \doteq G_1^2$ then calculate ℓ_1 from

$$\ell_1 = \frac{2L10^8}{R_{ac}} \sqrt{\frac{u\rho\gamma I^2_\Delta}{vw(I^2_{rms} - I^2)}} \qquad (6\text{-}21)$$

and select the core from part 3.3.

1.4.4.1 Calculate the number of turns from

$$N = \sqrt{L10^8} \sqrt[4]{\frac{v\gamma I^2_\Delta}{uw\rho\,(I^2_{rms} - I^2)}} \qquad (6\text{-}30)$$

1.4.4.2 Calculate the wire size from

$$a_w = \frac{v\ell_i^2}{H} \qquad (10\text{-}2)$$

1.4.4.3 Choose the wire size and make a complete winding calculation, part 4.

1.4.4.4 To get the air gap, use chart 3.

1.4.4.4.1 Calculate

$$B_\Delta = \frac{(R_{ac})^2}{2} \sqrt[4]{\frac{v^3 w (I_{rms}^2 - I^2)^5}{u^3 \rho^3 \gamma^5 I_\Delta^6 (L10^8)^6}} \qquad (6\text{-}31)$$

1.4.4.4.2 On chart 3 draw a line whose slope is G_1^2 and whose B_{max} intercept is given by

$$B_{max} = \frac{B_\Delta I_{max}}{I_\Delta} \qquad (6\text{-}36)$$

1.4.4.4.3 Choose the lowest intersection of the line and the appropriate B_Δ curve and read B_{max}.

1.4.4.4.4 Knowing B_Δ and B_{max}, obtain μ_Δ from original iron curves. (Figure 17)

1.4.4.4.5 Calculate α from

$$\alpha = G_1^2 - \frac{1}{\mu_\Delta} \qquad (6\text{-}37)$$

1.4.4.4.6 Calculate the total air gap length from

$$\ell_a = \alpha \ell_i \qquad (10\text{-}1)$$

where ℓ_i is the length of the core selected.

1.5 The method so far covered evolves a core and coil. It is possible that the heating of this reactor may be excessive if the copper and core losses are large in proportion to the radiating area.

1.5.1 For excessive copper heating only, a limiting value of K_c is determined. Calculate a new K_c from

$$K_c = \frac{I_{rms}^2 R_c}{p \ell_1^2} \qquad (5\text{-}2)$$

using ℓ_1 obtained from the previous resistance limited case.

1.5.1.1 If the calculated K_c is within the limits of heating, the previous design is suitable.

1.5.1.2 If the calculated K_c is greater than the limiting value of K_c, part 2 must be employed.

2. Heating Limitation

Calculate n_2 or n_{2r} from

$$n_2 = \frac{(.4\pi)^7 p^3 v^3 LI_{max}^8 K_c^3 10^8}{u^3 w \rho^3 I_{rms}^6} \qquad (5\text{-}9)$$

or from

$$n_{2r} = \frac{LI_{max}^8 K_c^3}{I_{rms}^6} \qquad (5\text{-}21)$$

If the value of n_2 or n_{2r} falls on Chart 2A and B_{max} is not too large, use Chart 2A. If n_2 or n_{2r} falls below the left hand limit of Chart 2A, use Chart 2B. If n_2 or n_{2r} f lls above the right hand limit of Chart 2A or if B_{max} as read on Chart 2A is too large, use Chart 2C.

2.1 Chart 2A If n_2 or n_{2r} line with the ε_2, α, and B_{max} curves of the proper I_Δ / I_{max} ratio, read ε_2, α, and B_{max}.

2.1.2 Calculate ℓ_1 from

$$\ell_1 = \varepsilon_2 \sqrt[4]{\frac{u\rho 10^8}{.4\pi p v w}} \sqrt[4]{\frac{LI_{rms}^2}{K_c}} \qquad (5\text{-}15)$$

or from

$$\ell_i = \varepsilon_{2r} \sqrt[4]{\frac{LI^2_{rms}}{K_c}} \qquad (5\text{-}24)$$

2.1.3 Knowing ℓ_i select the core, part 3.

2.1.4 Calculate the total air gap from

$$\ell_a = a\ell_i \qquad (10\text{-}1)$$

where ℓ_i is the length of the core selected.

2.1.5 Calculate the number of turns from

$$N = \varepsilon_2^{3/2} \sqrt[8]{\frac{\rho v L^3 K_c 10^{24}}{(.4\pi)^3 w^3 I^2_{rms}}} \qquad (5\text{-}18)$$

2.1.6 Calculate the size of wire from

$$a_w = \frac{v\ell_i^2}{N} \qquad (10\text{-}2)$$

2.1.7 Choose the wire size and make a complete winding calculation, part 4.

2.2 <u>Chart 2B</u> If n_2 or n_{2r} is below the left hand limit of Chart 2A, enter Chart 2B($\alpha = 0$) at the n_2 or n_{2r} point.

2.2.1 At the intersection of the n_2 or n_{2r} line with the B_{max} and ε_2 curves of the proper I_Δ / I_{max} ratio read B_{max} and ε_2.

2.2.2 Calculate ℓ_i from

$$\ell_i = \varepsilon_2 \sqrt[4]{\frac{w\rho 10^8}{.4\pi pvw}} \sqrt[4]{\frac{LI^2_{rms}}{K_c}} \qquad (5\text{-}15)$$

or from

$$\ell_i = \varepsilon_2 \sqrt[4]{\frac{LI^2_{rms}}{K_c}} \qquad (5\text{-}24)$$

2.2.3 Knowing ℓ_i select the core, part 3.

2.2.4 Calculate the number of turns from

$$N = g_2^{3/2} \sqrt[8]{\frac{\rho v L^3 K_c 10^{24}}{(.4\pi)^3 u_w^3 \rho I_{rms}^2}} \qquad (5\text{-}18)$$

2.2.5 Calculate the wire size from

$$a_w = \frac{v\ell_i^2}{N} \qquad (10\text{-}2)$$

2.2.6 Choose the wire size and make a complete winding calculation, part 4.

2.2.7 There is no air gap.

2.3 Chart 2C If n_2 or n_{2r} is beyond the right hand limit of Chart 2A or B_{max} is greater than linearity allows, enter Chart 2C at the n_2 or n_{2r} point.

2.3.1 Select the 2C chart with the appropriate B_{max} value.

2.3.2 Enter the chart at the given n_2 or n_{2r} value.

2.3.3 Read the corresponding value of α and g_2 from the intersection of the n_2 of n_{2r} line and the α and g_2 curves of proper I_Δ / I_{max} ratio.

2.3.4 Calculate ℓ_i from

$$\ell_i = g_2 \sqrt[4]{\frac{u\rho 10^8}{.4\pi\rho v w}} \sqrt[4]{\frac{LI_{rms}^2}{K_c}} \qquad (5\text{-}15)$$

or from

$$\ell_i = g_2 \sqrt[4]{\frac{LI_{rms}^2}{K_c}} \qquad (5\text{-}24)$$

2.3.5 Knowing ℓ_i select the core, part 3.

2.3.6 Calculate the total air gap from

$$\ell_a = \ell_i \qquad (10\text{-}1)$$

2.3.7 Calculate the number of turns from

$$N = g_2^{3/2} \sqrt[8]{\frac{\rho v L^3 K_c 10^{24}}{(.4\pi)^3 u_w^3 \rho I_{rms}^2}} \qquad (5\text{-}18)$$

2.3.8 Calculate the wire size from

$$a_w = \frac{v\ell_i^2}{N} \qquad (10\text{-}2)$$

2.3.9 Choose the wire size and make a complete winding calculation, part 4.

2.4 Generally, the total heating of the copper and core will be specified by K_{ac} having a limit rather than copper heating alone. A design in this case requires a comparison with the previous case of copper heating only.

2.4.1 Calculate g_2^4 using the procedure of 2.1, 2.2, or 2.3 and having

$$K_c = \frac{K_{ac}}{2} \qquad (10\text{-}8)$$

where a limiting value of K_{ac} is known.

2.4.2 Calculate G_2^4 from

$$G_2^4 = .4\pi \sqrt[3]{\frac{vw\gamma^2}{u\rho \frac{K_{ac}}{2}} \frac{I_\Delta^4 LIO^8}{\rho I_{rms}^2}} \qquad (7\text{-}11)$$

2.4.3 If $G_2^4 < g_2^4$ then use the previous method of 2.1, 2.2, or 2.3 after determining the value of K_c to use.

2.4.3.1 Calculate n'_2 for

$$K_c = \frac{K_{ac}}{2} \qquad (10\text{-}8)$$

and n''_2 for

$$K_c = K_{ac} \tag{10-9}$$

Read g'_2 and g''_2 from the same chart that g_2^4 was determined from in the above step.

2.4.3.2 Calculate K'_i and K''_i from

$$K'_i = \frac{.4\pi\gamma I_\Delta^2 L 10^8}{p\ell_i^2 (\epsilon'_2)^4} \tag{7-36}$$

knowing g'_2 and g''_2. (Calculate the ℓ_i for the corresponding g_2 from (5-15) or (5-24)).

2.4.3.3 Calculate

$$K'_{ac} = K'_c + K'_i \tag{10-10}$$

$$K''_{ac} = K''_c + K''_i \tag{10-11}$$

2.4.3.4 Calculate n_2 from

$$n_2 = \frac{(K_{ac} - K'_{ac})(n''_2 - n'_2)}{(K''_{ac} - K'_{ac})} + n'_2 \tag{10-12}$$

2.4.3.5 Calculate K_c from (5-9) or (5-21) knowing all other factors.

2.4.3.6 For this value of n_2 and K_c read g_2, α, and B_{max} from chart 2A, 2B, or 2C and proceed with the design as outlined in 2.1, 2.2, or 2.3.

2.4.4 If $g_2^4 \leq G_2^4$ then calculate ℓ_i from

$$\ell_i = \sqrt[3]{\frac{I_{rms} I_\Delta L 10^8}{p \frac{K_{ac}}{2}}} \sqrt{\frac{u\rho\gamma}{vw}} \tag{7-7}$$

2.4.4.1 Knowing ℓ_i select the core, part 3.3.

2.4.4.2 The number of turns is calculated from

$$N = \sqrt{L10^8} \sqrt[4]{\frac{\nu V I_\Delta^2}{u_w \rho I_{rms}^2}} \qquad (7\text{-}16)$$

2.4.4.3 The size of wire is calculated from

$$a_w = \frac{\nu \ell_i^2}{N} \qquad (10\text{-}2)$$

2.4.4.4 Choose the wire size and make a complete winding calculation, part 4.

2.4.4.5 To get the air gap, use chart 3.

2.4.4.5.1 Calculate B_Δ from

$$B_\Delta = \sqrt[12]{\frac{p^8 \nu (K_{ac}/2)^8}{u_w^5 \rho \gamma^7 I_\Delta^2 I_{rms}^2 (L10^8)^2}} \qquad (7\text{-}17)$$

2.4.4.5.2 On chart 3 draw a line whose slope is G_2^2 and whose B_{max} intercept is given by

$$B_{max} = \frac{B_\Delta I_{max}}{I_\Delta} \qquad (7\text{-}22)$$

2.4.4.5.3 Choose the lowest intersection of the line and the appropriate B_Δ curve and read B_{max}.

2.4.4.5.4 Obtain μ_Δ from the original iron curve, Figure 17, knowing B_Δ and B_{max}.

2.4.4.5.5 Get α from

$$\alpha = G_2^4 - \frac{1}{\mu_\Delta} \qquad (7\text{-}18)$$

2.4.4.5.6 Calculate the total air gap length from

$$\ell_a = \alpha \ell_i \qquad (10\text{-}1)$$

where ℓ_i is the length of the core selected.

3. Core Selection

3.1 For the laminations with the same shape numbers as used in calculating, select the core size with ℓ_1 equal to the calculated or derived ℓ_1.

3.2 If the calculated size is not available, the stack height may be changed for a core lamination which is available. To alter the stack height for calculated ℓ_1's using formulas (6-21) or (7-7) use step 3.3 only. To alter the stack height for all other calculated values of ℓ_1 using charts 1 and 2, the auxillary s axis in the lower left corner of the charts is used.

3.2.1 Use of auxillary s axis. Calculate g_{1r} or g_{2r} for the available lamination nearest the calculated design value of g_{1r} or g_{2r}.

3.2.2 Place a transparency over the given chart 1 or 2 with two axes parallel to the n_{1r} and g_{1r} and g_{2r} axes of the chart. Have the axes on the transparency intersect over the point 1 on the s axis of the chart.

3.2.3 On the transparency mark a point whose abcissa is equal to the design value of n or n_r and whose ordinate is equal to the g_r value of the available lamination. This point will lie above or below the g curve. A point lying on the curve means that the square stack (s = 1) is correct for the available lamination.

3.2.4 Slide the transparency point such that the intersection of the axes on the transparency follows the s curve, until the point marked in 3.2.3 crosses the g curve of the proper I_Δ / I_{max} ratio. Read g on the chart axis corresponding

to the g_r point on the transparency. Use this value of ℓ in calculating the number of turns. Read α on the chart axis corresponding to the g_r point on the transparency. Read s, on the s curve, at the intersection of the transparency axes. This is the new stacking factor.

3.2.5 For ℓ_a and a_w formulas, use ℓ_i of the available core as chosen in 3.2.1.

3.3 Use of chart 3a. Knowing the calculated ℓ_i, choose the core with the core length nearest the calculated value. Determine the core length factor by

$$\text{Core length factor} = \frac{\text{available core length}}{\text{calculated core length from (6-21) or (7-7)}}$$

On chart 3a, the intersection of curve 1 and the core length factor gives the stack height ratio for core length calculated from (6-21). The intersection or curve 2 and the core length factor gives the stack height ratio for core lengths calculated for (7-7).

3.3.1 Subsequent formulas of N and B_Δ will use values of u and w as calculated from (4-53) and (4-61), respectively, knowing s from step 3.3.

4. Winding Calculation

4.1 Determine the layer thickness.

4.1.1 Determine the wire thickness, outside diameter.

4.1.2 Determine the insulation thickness.

4.1.3 $$\text{Layer thickness} = \frac{\text{wire thickness + one thickness of insulation}}{\text{space factor}}$$

4.2 Number of layers.

4.2.1 From size of window determine the usable length for

the winding making the necessary allowance for ends near the core.

4.2.2 Divide the usable winding length by the diameter of wire to get the number of turns per layer.

4.2.3 Divide the total number of turns by the number of turns per layer to get the number of layers.

4.3 Check to see if the total winding height will fit into the core window.

4.3.1 If not, try a different insulation thickness that is still satisfactory for breakdown potential.

Chapter 11

Analysis Procedures

The analysis of a reactor will follow one of two procedures depending upon the specified variables. All factors of the reactor — core dimensions, number of turns, and air gap — are known.

1 Analysis of reactor when an alternating voltage and direct current are specified.

1.1 Calculate B_Δ from

$$B_\Delta = \frac{\int_0^p e' dt 10^8}{2 N a_i} \qquad (3\text{-}9)$$

where e' is integrated over one period or if the applied voltage is sinusiodal with effective value E_{ac} and frequency of

$$B_\Delta = \frac{E_{ac}}{4.44 f N a_i} \qquad (3\text{-}14)$$

1.1.1 a_i is net cross sectional area of iron.

1.2 Construct a Karapetoff type line on the biased induction curve, Figure 4, B_b vs H_b.

1.2.1 Equation of the line

$$\frac{.4\pi N I_b}{\ell_i} = H_b + B_b \alpha \qquad (3\text{-}19)$$

1.2.2 H_b intercept

$$H_b = \frac{.4\pi N I_b}{\ell_i} \qquad (3\text{-}20)$$

1.2.3 B_b intercept

$$B_b = \frac{.4\pi NI_b}{\alpha \ell_1} \tag{3-21}$$

1.2.4 Read the intersection of curve and line to get B_b and H_b.

1.3 Using B_b and H_b from above, and B_Δ from calculation read μ_Δ from Figure 5.

1.4 Calculate the inductance from

$$L = \frac{.4\pi N^2 a_1 10^{-8}}{\ell_1 (\frac{1}{\mu_\Delta} + \alpha)} \tag{2-30}$$

1.5 Copper loss calculation

1.5.1 Calculate the rms value of the variational component, I'_{rms}.

1.5.1.1 For a non-sinusoidal wave

$$i' = \frac{1}{L} \int e'dt + C \tag{11-1}$$

where C is chosen such that

$$\int_0^P i'dt = 0 \tag{11-2}$$

and

$$(I'_{rms})^2 = \frac{1}{P} \int_0^P i'^2 dt \tag{11-3}$$

1.5.1.2 For a sinusoidal wave

$$I'_{rms} = \frac{E_{ac}}{2\pi fL} \tag{11-4}$$

1.5.2 Calculate I^2_{rms}

$$I^2_{rms} = (I'_{rms})^2 + I^2_b \qquad (11\text{-}5)$$

1.5.3 Calculate the copper loss knowing R_c and I^2_{rms} from

$$W_c = I^2_{rms} R_c \qquad (11\text{-}6)$$

1.6 Core loss calculation

1.6.1 Knowing H_b and B_Δ from previous steps, read the core loss in watts per pound from Figure 8.

1.6.2 The weight of iron is given by

$$M_i = \ell_i a_i \Sigma_i \qquad (11\text{-}7)$$

where ℓ_i is in cm, a_i in cm^2, and Σ_i in lbs/cm^3.

1.6.3 Calculate the core loss from

$$W_i = \left(\frac{\text{watts}}{\text{lb}}\right) M_i \qquad (11\text{-}8)$$

2 Analysis of a reactor when the current is specified.

2.1 Calculate I_Δ

$$I_\Delta = \frac{I_{max} - I_{min}}{2} \qquad (3\text{-}22)$$

2.2 Construct a Karapetoff type line on the normal induction curve, B_{max} vs H_{max}, Figure 6.

2.2.1 Equation of the line

$$\frac{.4\pi N I_{max}}{\ell_i} = H_{max} + B_{max}\alpha \qquad (3\text{-}23)$$

2.2.2 H_{max} intercept

$$H_{max} = \frac{.4\pi NI_{max}}{\ell_i} \qquad (3\text{-}24)$$

2.2.3 B_{max} intercept

$$B_{max} = \frac{.4\pi NI_{max}}{a\ell_i} \qquad (3\text{-}25)$$

2.2.4 Read the intersection of the curve and line to get B_{max} and H_{max}.

2.3 Construct a Karapetoff type line on the incremental induction curve, B_Δ vs H_Δ, Figure 7.

2.3.1 Equation of line

$$\frac{.4\pi NI_\Delta}{\ell_i} = H_\Delta + B_\Delta a \qquad (3\text{-}26)$$

2.3.2 H_Δ intercept

$$H_\Delta = \frac{.4\pi NI_\Delta}{\ell_i} \qquad (3\text{-}27)$$

2.3.3 B_Δ intercept

$$B_\Delta = \frac{.4\pi NI_\Delta}{a\ell_i} \qquad (3\text{-}28)$$

2.3.4 Read the intersection of the curve and line to get B_Δ.

2.4 Calculate the inductance from

$$L = \frac{NB_\Delta a_i 10^{-8}}{I_\Delta} \qquad (2\text{-}29)$$

2.5 Copper loss calculation.

2.5.1 Calculation of I^2_{rms}

2.5.1.1 For a specified current of non-sinusoidal nature, calculate I^2_{rms} from

$$I^2_{rms} = \frac{1}{P}\int_0^P i^2 dt \qquad (11\text{-}9)$$

where i^2 is integrated over one period, P.

2.5.1.2 For a current waveform consisting of a d-c component, I_b, and a sinusoidal component having an effective value I'_{rms}, calculate the total rms value from

$$I^2_{rms} = I^2_b + (I'_{rms})^2 \qquad (11\text{-}5)$$

2.5.2 Calculate W_c knowing I^2_{rms} and R_c from

$$W_c = I^2_{rms} R_c \qquad (11\text{-}6)$$

2.6 Core loss calculation

2.6.1 Knowing B_{max} and B_Δ from previous steps, read the core loss in watts per pound from Figure 9.

2.6.2 The weight of iron is given by

$$M_i = \ell_i a_i \Sigma_i \qquad (11\text{-}7)$$

where ℓ_i is in cm, a_i in cm^2 and Σ_i in lb/cm^3.

2.6.3 Calculate the core loss from

$$W_i = \left(\frac{\text{watts}}{\text{lb}}\right) M_i \qquad (11\text{-}8)$$

CHAPTER 12

EXAMPLES AND MODELS

To exemplify this method of inductor design, a set of examples are given. These examples were worked by a young engineer having no background or file of previous design experience to draw upon. Models of these designs were built by the subcontractor without individual air-gap adjustments and were measured by the bridge or pulse methods of Chapter 14. These models however do not constitute an exact evaluation of the method because their cores were not individually measured for comparison with the assumed iron characteristics. They do show that the method has practical merit in spite of the iron variation.

This general methos of synthesis is applied to each example, and then each result is analyzed. It should be recalled that these design charts were constructed by graphical methods which may cause some discrepancy between the specified values synthesized and the analysis of these results.

The specifications for each example are given in the form most convenient for use in this method. The designer will not always be given the specifications in this form but he may always calculate these quantities from the circuit equations.

Each example is broken into three parts: specifications, design and analysis. The numbers proceeding the design and analysis calculations are the step numbers in the

procedure sections as given in Chapters 10 and 11, respectively. Design step numbers refer only to Chapter 10; analysis step numbers refer only to Chapter 11.

In all these examples there is enough allowance of window space to give a filled window when completed. The figures for layer thickness, core weights and case areas, are taken from average practice. The 0.9, in every inductance calculation multiplying the core area, reduces the figure to the net iron area.

Choke A

specs: $L = 15$ hy

$R_c = 250$ ohms

$I_{max} = .1$

$\frac{I_\Delta}{I_{max}} = 0$

design:

1* $$n_{1r} = \frac{R_c^3 \, I_{max}^4}{L} \qquad (4\text{-}44)$$

$$= \frac{(250)^3(.1)^4}{15} = 1.04 \times 10^2$$

1.1 enter Chart 1A (refer to chart section at the end of report)

1.1.1 $\mathcal{E}_{1r} = 75$

$\alpha = .31\%$

$B_{max} = 9300$ gausses

* These numbers agree with Chapter 10.

1.1.2 $\ell_i = g_{1r}\sqrt{\frac{L}{R_c}}$ (4-47)

$= 75\sqrt{\frac{15}{250}} = 18.4$ cm.

$= 7.24$ inches

3.2 available cores

EI - 125 $\ell_i = 19.05$ cm, 7.5 in. $a_i = 10.07$ cm^2

EI - 112 $\ell_i = 17.15$ cm, 6.75 in. $a_i = 8.19$ cm^2

3.2.1 Use EI - 125 $\ell_i = 19.05$ cm.

For this lamination

$$g_{1r} = \frac{i}{\sqrt{\frac{L}{R_c}}} \qquad (4\text{-}47)$$

$$= \frac{19.05}{\sqrt{\frac{15}{250}}} = 78$$

3.2.4 From the chart by means of Chapter 19 part 3.2
$s = .9$

$g_1 = .075$

$\alpha = .0031$

EI - 125 $\ell_i = 19.05$ cm. $g_{1r} = 78$ $a_i = 10.07 \times .9$
$= 9.06$ cm^2

1.1.4 $\ell_a = \alpha \ell_i$

$= .0031 \times 7.5$

$= .0232$ in. total air gap

1.1.5 $$N = \sqrt{g_1\sqrt{\frac{v10^8}{.4\pi w_o}}\sqrt{LR_c}} \qquad (4\text{-}41)$$

(g_1 from step 3.2.4)

$$N = \sqrt{7.5 \times 10^{-2}\sqrt{\frac{6.25 \times 10^{-3} \times 10^8}{1.256 \times 1 \times 2.5 \times 10^{-2} \times 1.72^4 \times 110^{-6}}}\sqrt{15 \times 250}}$$

$= 3950$ turns

1.1.6 $$a_w = \frac{\nu \ell_i^2}{N} \qquad (10\text{-}2)$$

$$= \frac{6.25 \times 10^{-3} \times (7.5)^2}{3950}$$

$$= .0000885 \text{ in.}^2$$

#29 wire

4.1.1 wire thickness .0122 in.

4.1.2 insultation thickness .0015 in.

4.1.3 $$\text{layer} = \frac{.0122 + .0015}{.91} = .0151 \text{ in.}$$

4.2.1 winding length = 1.562 in.

4.2.2 $$\text{turns/layer} = \frac{1.562}{.0122} = 128$$

4.2.3 $$\text{layers} = \frac{3950}{128} = 31 \text{ layers}$$

4.3 winding height = 31 x .0151 = .468 in.

nominal build up = .565 in.

<u>analysis:</u>

$\ell_i = 19.05$ cm. $a_i = 9.06$ cm^2.

$\alpha = .0031$ $N = 3950$

*1.1 $B_\Delta \cong 0$ since $I_\Delta = 0$

1.2.2 $$H_b = \frac{.4\pi N I_b}{\ell_i} \qquad (3\text{-}20)$$

$$= \frac{.4\pi \times 3950 \times .1}{19.05} = 26 \text{ oersteds}$$

1.2.3 $$B_b = \frac{.4\pi \times 3950 \times .1}{19.05 \times .0031} = 8400 \text{ gausses}$$

1.2.4 $H_b = 1.1$ oersteds

$B_b = 8200$ gausses

* These numbers agree with Chapter 11.

1.3 $\mu_\Delta = 550$ (a limiting value)

1.4 $$L = \frac{14\pi N^2 a_i 10^{-8}}{\ell_i \left(\frac{1}{\mu_\Delta} + \alpha\right)} \qquad (2\text{-}30)$$

$$= \frac{.4\pi \times (3950)^2 \times 9.06 \times .9}{19.05 \left(\frac{1}{550} + .0031\right)}$$

$$= 16.9 \text{ hy}$$

1.5.2 $$I_{rms}^2 = I_{rms}'^2 + I_b^2 \qquad (11\text{-}5)$$

$$= 0 + .1^2$$

1.5.3 $$W_c = I_{rms}^2 R_c \qquad (11\text{-}6)$$

$$= .1^2 \times 250$$

$$= 2.5 \text{ watts}$$

1.6.3 no core loss

case area = 75.44 in^2

$$\text{total watts/in}^2 = \frac{2.5}{75.44} = \frac{.0332 \text{ watts}}{in^2}$$

Measurements:

Choke A was built and assigned the number A8744. It was measured on the Hay bridge under 60 cycle sine wave conditions at specified ratings. The inductance measured 17.2 henries and R_c measured 177.7 ohms.

Choke B

specs: $L = 3$ hy

$R_{ac} = 40$ ohms

$I_{max} = .1$

$I_\Delta / I_m = .5$ (resonant charging)

$B_{max} = 10$ Kilogausses

<u>design:</u>

1.4.1 $R_c = \frac{R_{ac}}{2}$ (10-3)

$= \frac{40}{2}$

$= 20$

$n_{1r} = \frac{R_c^3 I_{max}^4}{L}$ (4-44)

$= \frac{20^3 \times .1^4}{3} = 2.66 \times 10^{-1}$

1.3.1 Use Chart 1C B_{max} = 10 Kilogausses

1.3.3 $\epsilon_{1r} = 39$ $\alpha = .0008$

$\epsilon_1 = .039$

$\epsilon_1^2 = 15.2 \times 10^{-4}$

1.4.2 $G_1^2 = \frac{.4\pi \gamma I_\Delta^2 L 10^8}{(I_{rms}^2 - I^2)\frac{R_{ac}}{2}}$ (6-25)

$= \frac{.4\pi \times 20 \times 10^{-12} \times .05^2 \times 3 \times 10^8}{(.0707^2 - .0636^2) \times 20}$

$= 9.4 \times 10^{-4}$

1.4.3.1 $n_{1r}' = \frac{R_c'^3 I_{max}^4}{L}$ (4-44)

$= \frac{20^3 \times .1^4}{3} = 2.66 \times 10^{-1}$

$n_{1r}'' = \frac{R_c''^3 I_{max}^4}{L}$ (4-44)

$= \frac{40^3 \times .1^4}{3} = 2.13$

$\epsilon_1' = .039$

$\epsilon_1'' = .045$

1.4.3.2 $$R'_1 = \frac{.4\pi \gamma I_\Delta^2 L 10^8}{(I_{rms}^2 - I^2)\varepsilon'^2_1} \quad (6\text{–}45)$$

$$= \frac{.4\pi \times 20 \times 10^{-2} \times .05^2 \times 3 \times 10^8}{(.0707^2 - .0636^2) \times .039^2}$$

$$= 12.4$$

$$R''_1 = \frac{.4\pi \gamma I_\Delta^2 L 10^8}{(I_{rms}^2 - I^2)\varepsilon''^4_1} \quad (6\text{–}45)$$

$$= \frac{.4\pi \times 20 \times 10^{-12} \times .05^2 \times 3 \times 10^8}{(.0707^2 - .0636^2) \times .045^2}$$

$$= 9.4$$

1.4.3.3 $$R'_{ac} = R'_c + R'_1 \quad (10\text{–}6)$$

$$= 20 + 12.4 = 32.4$$

$$R''_{ac} = R_c^4 + R''_1 \quad (10\text{–}7)$$

$$= 40 + 9.4 = 49.4$$

1.4.3.4 $$n_{1r} = \frac{(R_{ac} - R'_{ac})(n''_{1r} - n'_{1r})}{(R''_{ac} - R'_{ac})} + n'_{1r} \quad (10\text{–}8)$$

$$= \frac{(40 - 32.4)(2.13 - .266)}{(49.4 - 32.4)} + .266$$

$$= 1.1$$

1.4.3.5 $$R_c = \sqrt[3]{\frac{L\, n_{1r}}{I_{max}^4}} \quad (4\text{–}44)$$

$$= \sqrt[3]{\frac{3 \times 1.1}{.1^4}}$$

$$= 32$$

1.4.3.6 Chart 1C B_{max} = 10 kilogausses

$\varepsilon_1 = .043$

$\varepsilon_{1r} = 43$

$\alpha = .0012$

1.3.4 $\ell_i = g_{1r}\sqrt{\frac{L}{R_c}}$ (4-47)

$= 43\sqrt{\frac{3}{32}}$

$= 13.2$ cm

$= 5.2$ in.

1.3.5 EI = 11 $\ell_i = 13.34$ cm $a_i = 4.97$ cm^2

close enough to use square stack

s = 1

1.3.6 $\ell_a = a\ell_i$ (10-1)

$= .0012 \times 5.25$

$= .0063$ in.

1.3.7 $N = \sqrt{g_1\sqrt{\frac{v\ 10^8}{.4\pi\ u\ w\ \rho}}\sqrt{LR_c}}$ (4-41)

$= \sqrt{.042\sqrt{\frac{6.25 \times 10^{-3} \times 10^8}{.4\pi x1x2.5x10^{-2}x1.72x10^{-6}}}\sqrt{3 \times 32}}$

$= 1200$ turns

1.3.8 $a_w = \frac{v\ \ell_i^2}{N}$ (10-2)

$= \frac{6.25 \times 10^{-3} \times (5.25)^2}{1200}$

$= .000143$ in^2 #27 wire

4.1.1 wire thickness = .0152 in.

4.1.2 insulation thickness = .0015 in.

4.1.3 layer thickness = $\frac{.0152 + .0015}{.91}$

$= .0184$ in.

4.2.1 winding length = 1.06 in.

turns/layer = $\frac{1.06}{.0152} = 70$

4.2.2 $\text{layers} = \frac{1200}{70} = 18$

4.3 winding height = 18 x .0184

= .33 in.

nominal build up = .395 in.

analysis: $\ell_1 = 13.34$ cm $a_1 = 4.97$ cm^2

$\alpha = .0012$ $N = 1200$

2.1 $I_\Delta = .05$ in.

2.2.2 $$H_{max} = \frac{.4\pi N I_{max}}{\ell_1} \qquad (3\text{-}24)$$

$$= \frac{.4\pi \times 1200 \times .1}{13.34} = 11.2 \text{ oersteds}$$

2.2.3 $$B_{max} = \frac{.4\pi N I_{max}}{\alpha \ell_1} \qquad (3\text{-}25)$$

$$= \frac{.4\pi \times 1200 \times .1}{.0012 \times 13.34} = 9400 \text{ gausses}$$

2.2.4 $B_{max} = 8500$ gausses

$H_{max} = 1.2$ oersteds

2.3.2 $$H_\Delta = \frac{.4\pi N I_\Delta}{\ell_1} \qquad (3\text{-}27)$$

$$= \frac{.4\pi \times 1200 \times .05}{13.34} = 5.6$$

2.3.3 $$B_\Delta = \frac{.4\pi N I_\Delta}{\alpha \ell_1} \qquad (3\text{-}28)$$

$$= \frac{.4\pi \times 1200 \times .05}{.0012 \times 13.34} = 4700 \text{ gausses}$$

2.3.4 $B_\Delta = 3900$ gausses

2.4 $$L = \frac{N B_\Delta a_1 10^{-8}}{I_\Delta} \qquad (2\text{-}29)$$

$$= \frac{1200 \times 3900 \times 4.79 \times .9 \times 10^{-8}}{.05}$$

$$= 4.2 \text{ hy.}$$

2.5.1.1 $$I_{rms}^2 = (.707 \times .1)^2$$

2.5.2 $$w_c = I_{rms}^2 R_c \qquad (11\text{-}6)$$

$$= (.707 \times .1)^2 \times 32 = .16 \text{ watt}$$

2.6.1 core loss = .2 watts/lb

2.6.2 wt = 1.05 lb

2.6.3 core loss = .2 x 1.05

= .2 watt

total loss = .36 watts

case area = 35.35 in^2

total watts/in^2 = .0105 watts/in^2

Measurements:

Choke B was built and assigned the number A8745. It was measured on the Hay bridge under 60 cycle sine wave conditions at specified ratings. The inductance measured 2.13 henries and R_{ac} measured 42.3 ohms.

Choke C

specs: L = 1 hy

R_c = 100 ohms

I_{max} = .2

$\frac{I_\Delta}{I_{max}}$ = .25

design:

1. $$n_{lr} = \frac{R_c^3 I_{max}^4}{L} \qquad (4\text{-}44)$$

$$= \frac{100^3 \times .2^4}{1}$$

$$= 1.6 \times 10^3$$

1.3 Chart 1C

1.3.1 use B_{max} = 10 liogausses

1.3.3 $g_l = .08$

$g_{lr} = 80$

$\alpha = .006$

1.3.4 $$\ell_i = g_{lr}\sqrt{\frac{L}{R_c}} \qquad (4\text{-}36)$$

$$= 80\sqrt{\frac{1}{100}} = 8 \text{ cm}$$

$$= 3.14 \text{ in.}$$

3.2.1 closest core

EI - 625 ℓ_i = 9.53 cm, 3.75 in. g_{lr} = 95.3

$a_l = 2.52 \text{ cm}^2$

3.2.4 $s = .65$ $a_i = 1.64 \text{ cm}^2$ $\alpha = .006$ $g_l = 80 \times 10^{-3}$

1.3.6 $$\ell_a = \alpha \ell_i \qquad (10\text{-}1)$$

$$= .006 \times 3.75 = .0225 \text{ in.}$$

1.3.7 $$N = \sqrt{g_l \sqrt{\frac{v\, 10^8}{.4\pi\, u\, w\, \rho}}\ \sqrt{L\, R_c}} \qquad (4\text{-}41)$$

$$= \sqrt{.08\sqrt{\frac{6.25 \times 10^{-3} \times 10^8}{.4\pi \times 1 \times 2.5 \times 10^{-2} \times 1.72 \times 10^{-6}}}\sqrt{1 \times 100}}$$

$$= 1800 \text{ turns}$$

1.3.8 $$a_w = \frac{\nu \ell_i^2}{N} \qquad (1\text{-}2)$$

$$= \frac{6.25 \times 10^{-3} \times 3.75^2}{1800}$$

$$= .0000487 \text{ in}^2$$

use #32 wire

4.1.1 wire thickness = .0087 in.

4.1.2 insulation thickness = .0010 in.

4.1.3 $$\text{layer} = \frac{.0087 + .0010}{.91} = .0107 \text{ in.}$$

4.2.1 winding length = .69 in.

4.2.2 $$\text{turns/layer} = \frac{.69}{.0087} = 23$$

4.3 winding height = 23 x .0107 in = .246 in.

nominal build up = .280 in.

<u>analysis:</u>

ℓ_i = 9.53 cm N = 1800

α = .006 a_i = 1.64 cm^2

2.1 $I_\Delta = .051$

2.2.2 $$H_{max} = \frac{.4\pi N I_{max}}{\ell_i} \qquad (3\text{-}24)$$

$$= \frac{.4\pi \times 1800 \times .2}{9.53}$$

$$= 47.6 \text{ oersteds}$$

2.2.3 $$B_{max} = \frac{.4\pi N I_{max}}{\alpha \ell_i} \qquad (3\text{-}25)$$

$$= \frac{.4\pi \times 1800 \times .2}{.006 \times 9.53}$$

$$= 7930 \text{ gausses}$$

2.2.4 $B_{max} = 7930$ gausses

2.3.2 $$H_\Delta = \frac{.4\pi N I_\Delta}{\ell_1} \qquad (3\text{-}27)$$

$$= \frac{.4\pi \times 1800 \times .051}{9.53}$$

$$= 12.7 \text{ oersteds}$$

2.3.3 $$B_\Delta = \frac{.4\pi N I_\Delta}{\alpha \ell_1} \qquad (3\text{-}28)$$

$$= \frac{.4\pi \times 1800 \times .051}{.006 \times 9.53}$$

$$= 2010 \text{ gausses}$$

2.3.4 $B_\Delta = 2000$ gausses

2.4 $$L = \frac{N B_\Delta a_i 10^{-8}}{I_\Delta} \qquad (2\text{-}29)$$

$$= \frac{1800 \times 2000 \times 1.64 \times .9 \times 10^{-8}}{.051}$$

$$= 1.04$$

2.5.1.2 $I'_{rms} = .0358$

$I_b = .149$

$I^2_{rms} = I_b^2 + .0358^2$

$= 235 \times 10^{-4}$

2.5.2 $$w_c = I_{rms}^2 R_c \qquad (11\text{-}6)$$

$= 235 \times 10^{-4} \times 100$

$= 2.35$ watts

2.6.1 core loss = .06 watts/lb

2.6.2 weight = .392 lb

2.6.3 core loss = .06 x .392

= .03 watts

total loss = 2.38 watts

case area = 13.27 in^2

watts/in^2 = .13 watts/in^2

Measurements:

Choke C was built and assigned the number A8746. It was measured on the Hay bridge under 60 cycle sine wave conditions at specified ratings. The inductance measured 1.27 henries and R_c measured 73.6 ohms.

Choke D

specs: $L = .05$ hy

$R_c = .4$ ohms

$I_{max} = 6$

$\frac{I_\Delta}{I_{max}} = .12$

design:

1. $$n_{1r} = \frac{R_c^3 \, I_{max}^4}{L} \qquad (4\text{-}44)$$

$$= \frac{.4^3 \times 6^4}{.05}$$

$$= 1.67 \times 10^3$$

1.3 chart 10

1.3.1 use B_{max} = 10 kilogausses

1.3.3 $g_1 = .08$ $\qquad g_{1r} = 80$

$\alpha = .006$

1.3.4 $$\ell_1 = g_{1r}\sqrt{\frac{L}{R_c}} \qquad (4\text{-}47)$$

$$= 80\sqrt{\frac{.05}{.4}}$$

ℓ_i = 27.4 cm

= 11.1 in.

3.2.1 closest core

EI - 175 ℓ_i = 26.67 cm = 10.5 in.

a_i = 19.76 cm^2 B_{1r} = 75

3.2.4 s = 1.3 a_i = 25.7 cm^2 α = .006 B_1 = 80 x 10^{-3}

1.3.7
$$N = \sqrt{B_1 \sqrt{\frac{v\ 10^8}{.4\pi\ u\ w\ \rho}}\ \sqrt{L\ R_c}} \qquad (4\text{-}41)$$

$$= \sqrt{.080 \sqrt{\frac{6.25 \times 10^{-3} \times 10^8}{.4\pi \times 1 \times 2.5 \times 10^{-2} \times 1.724 \times 10^{-6}}}\ \sqrt{.05 \times .4}}$$

= 190 turns

1.3.6
$$a_w = \frac{v\ \ell_i^2}{N} \qquad (10\text{-}2)$$

$$= \frac{6.25 \times 10^{-3} \times 10.5^2}{190}$$

= .00362 $in.^2$

use # 13 wire

4.1.1 wire thickness = .0741 in.

4.1.2 insulation thickness = .010 in.

4.1.3 layer = $\frac{.0741 + .010}{.89}$ = .094 in.

4.2.1 winding length = 2.25 in.

4.2.2 turns/layer = $\frac{2.25}{.0741}$ = 30

4.2.3 layers = $\frac{190}{30}$ = 7

4.3 winding height = 7 x .094

= .66 in.

nominal build up = .79 in.

analysis: $\ell_1 = 26.67$ cm $\quad a_1 = 5.7$ cm^2

$\alpha = .006 \qquad N = 190$

2.1 $\quad I_\Delta = .745$

2.2.2 $\quad H_{max} = \dfrac{.4\pi\, N\, I_{max}}{\ell_1}$ (3-24)

$= \dfrac{.4\pi \times 190 \times 6}{26.67} = 53.5$ oersteds

2.2.3 $\quad B_{max} = \dfrac{.4\pi\, N\, I_{max}}{\alpha\, \ell_1}$ (3-25)

$= \dfrac{.4\pi \times 190 \times 6}{26.67 \times .006} = 8900$ gausses

2.2.4 $\quad B_{max} = 8800$ gausses

2.3.2 $\quad H_\Delta = \dfrac{.4\pi\, N\, I_\Delta}{\ell_1}$ (3-27)

$= \dfrac{.4\pi \times 190 \times .745}{26.67}$

$= 6.65$ oersteds

2.3.3 $\quad B_\Delta = \dfrac{.4\pi\, N\, I_\Delta}{\alpha\, \ell_1}$ (3-28)

$= \dfrac{.4\pi \times 190 \times .745}{.006 \times 26.67}$

$= 1100$ gausses

2.3.4 $\quad B_\Delta = 1100$ gausses

2.4 $\quad L = \dfrac{N\, B_\Delta\, a_1\, 10^{-8}}{I_\Delta}$ (2-29)

$= \dfrac{190 \times 1100 \times 25.7 \times .9 \times 10^{-8}}{.745}$

$= .065$ hy

2.5.1.2 $I'_{rms} = .707 \times .745$

$= .527$

$I_b = 5.3$

$I_{rms}^2 = .527^2 + 5.3^2$

$= 28.28$

2.5.2 $W_c = I_{rms}^2 R_c$ (11-6)

$= 28.28^2 \times .4$

$= 11.4$ watts

2.6.1 core loss = .02 watts/lb.

2.6.2 weight = 11.2 lbs

2.6.3 $W_i = .02 \times 11.2$

$= .224$ watts

total loss = 11.6 watts

core area = 132.96 in^2

watts/in^2 = .087 watts/in^2

Measurements:

Choke D was built and assigned the number A8747. It was measured on the Hay bridge under 60 cycle sine wave conditions at specified ratings. The inductance measured .0715 henries and R_c measured .337 ohms.

Choke E

specs: $L = 10$ hy

$R_{ac} = 60$ ohms

$I_{max} = .104$

$\frac{I_\Delta}{I_{max}} = .5$ (resonant charging)

$B_{max} = 10$ kilogausses

design:

1.4.1 $R_c = \frac{R_{ac}}{2}$ (10-3)

$= \frac{60}{2}$

$= 30$

1 $n_{1r} = \frac{R_c^3 I_{max}^4}{L}$ (4-44)

$= \frac{30^3 \times (.104)^4}{10}$

$= 3.16 \times 10^{-1}$

1.3.1 use Chart 1C B_{max} = 10 kilogausses

1.3.3 $g_{1r} = 40 \quad g_1 = .04$

$g_1^2 = 16 \times 10^{-4}$

1.4.2 $G_1^2 = \frac{.4\pi \gamma I_\Delta^2 L 10^8}{(I_{rms}^2 - I^2) \frac{R_{ac}}{2}}$ (6-25)

$= \frac{.4\pi \times 20 \times 10^{-12} \times .052^2 \times 6.2 \times 10^{-8}}{[(.707 \times .104)^2 - (.636 \times .104)^2] 30}$

$= 12.9 \times 10^{-4}$

1.4.3.1 $n_{1r}' = \frac{R'^3_c I_n^4}{L}$ (4-44)

$= \frac{30^3 \times .104^4}{10}$

$= .316$

$n_{1r}'' = \frac{R''^3_c I_m^4}{L}$ (4-44)

$= \frac{60^3 \times .104^4}{10}$

$= 2.53$

$\varepsilon'_1 = .041$

$\varepsilon''_1 = .045$

1.4.3.2 $$R'_i = \frac{.4\pi\ \gamma\ I_\Delta^2\ L\ 10^8}{(I_{rms}^2 - I^2)\ \varepsilon'^2_1} \qquad (6\text{-}45)$$

$$= \frac{.4\pi \times 20 \times 10^{-2} \times .052^2 \times 6.2 \times 10^8}{\left[(.707 \times .104)^2 - (.636 \times .104)^2\right] \times .04^2}$$

$$= 24.4$$

$$R''_i = \frac{.4\pi\ \gamma\ I_\Delta^2\ L\ 10^8}{(I_{rms}^2 - I^2)\ \varepsilon''^2_1} \qquad (6\text{-}45)$$

$$= \frac{.4\pi \times 20 \times 10^{-12} \times .052^2 \times 6.2 \times 10^8}{\left[(.704 \times .104)^2 - (.636 \times .104)^2\right] \times .045^2}$$

$$= 19.4$$

1.4.3.3 $$R'_{ac} = R'_c + R'_i \qquad (10\text{-}6)$$

$$= 30 + 24.4 = 54.4$$

$$R''_{ac} = R''_c + R''_i \qquad (10\text{-}7)$$

$$= 60 + 19.4 = 79.4$$

1.4.3.4 $$n_{1r} = \frac{(R_{ac} - R'_{ac})(n''_1 - n_1)}{(R''_{ac} - R'_{ac})} + n'_1 \qquad (10\text{-}8)$$

$$= \frac{60 - 54.4}{79.4 - 54.4}(2.53 - .31) + .31 = .81$$

1.4.3.5 $$R_c = 3\sqrt{\frac{L\ n_{1r}}{I_{max}^4}} \qquad (4\text{-}44)$$

$$= 3\sqrt{\frac{6.2 \times .81}{(.104)^4}}$$

$$= 35$$

1.4.3.6 Chart 10 $B_{max} = 10$ kilogausses

$\varepsilon_1 = .043 \quad \varepsilon_{1r} = 43$

$\alpha = .0013$

1.3.4 $$\ell_1 = \varepsilon_{1r}\sqrt{\frac{L}{R_c}} \qquad (4\text{-}47)$$

$$= 43\sqrt{\frac{6.2}{35}}$$

$$= 18 \text{ cm} \triangleq 7.1 \text{ in.}$$

3.2.1 nearest lamination

EI - 112 $\ell_1 = 17.15$ cm $a_1 = 8.19$ cm^2

$= 6.75$ in. $\varepsilon_{1r} = 41$

3.2.4 $s = 1.2$ $a_1 = 9.8$ cm^2 $\varepsilon_1 = .0043$ $\alpha = .0013$

1.3.6 $$\ell_a = \alpha\, \ell_1$$

$= .0013 \times 6.75 = .0088$ in.

1.3.7 $$I = \sqrt{\varepsilon_1}\sqrt{\frac{v \times 10^8}{.4\pi\, u\, w\, \rho}}\sqrt{L\, R_c} \qquad (4\text{-}41)$$

$$= \sqrt{.043}\sqrt{\frac{6.25 \times 10^{-3} \times 10^8}{.4\pi \times 1 \times 2.5 \times 10^{-2} \times 1.724 \times 10^{-6}}}\sqrt{6.2 \times 35}$$

$= 1470$ turns

1.3.8 $$a_w = \frac{v\, \ell_1^2}{N} \qquad (10\text{-}2)$$

$$= \frac{6.25 \times 10^{-3} \times (6.75)^2}{1470}$$

$= .000194$ in.^{2}

26 wire

4.1.1 wire thickness = .017 in.

4.1.2 insulation thickness = .002 in.

4.1.3 $$\text{layer thickness} = \frac{.017 + .002}{.9} \times .021 \text{ in.}$$

4.2.1 winding length = 1.375 in.

$$\text{turns/layer} = \frac{1.375}{.017} = 81$$

4.2.2 $\text{layers} = \frac{1470}{81} = 19 \text{ layers}$

4.3 winding height = 19 x .021 = .398 in.

nominal build up = .505 in.

analysis: $\ell_1 = 17.15$ cm $\quad a_1 = 9.8$ cm^2

$\alpha = .0013 \quad N = 1470$

2.2.2 $$H_{max} = \frac{.4\pi N I_{max}}{\ell_1} \qquad (3\text{-}24)$$

$$= \frac{.4\pi \times 1470 \times .104}{17.15} = 11.2 \text{ oersteds}$$

2.2.3 $$B_{max} = \frac{.4\pi N I_{max}}{\alpha \ell_1} \qquad (3\text{-}25)$$

$$= \frac{.4\pi \times 1470 \times .104}{.0013 \times 17.15} = 9000 \text{ gausses}$$

2.2.4 $B_{max} = 8100$ gausses

2.3.2 $$H_\Delta = \frac{.4\pi N I_\Delta}{\ell_1} \qquad (3\text{-}27)$$

$$= \frac{.4\pi \times 1470 \times .052}{17.15} = 5.6 \text{ oersteds}$$

2.3.3 $$B_\Delta = \frac{.4\pi N I_\Delta}{\ell_1} \qquad (3\text{-}28)$$

$$= \frac{.4\pi \times 1470 \times .052}{.0013 \times 17.15} = 4500 \text{ gausses}$$

2.3.4 $B_\Delta = 3700$ gausses

2.4 $$L = \frac{N B_\Delta a_1 10^{-8}}{I_\Delta} \qquad (2\text{-}29)$$

$$= \frac{1470 \times 3700 \times 9.8 \times .9 \times 10^{-8}}{.052}$$

$$= 9.2 \text{ hy}$$

2.5.1.1 $I_{rms}^2 = (.707 \times .104)^2$

2.5.2 $W_r = I_{rms}^2 R_c$ (11-6)

$= (.707 \times .104)^2 \times 35$

$= 1.9$ watts

2.6.1 core loss = .3 watts/lb

2.6.2 wt. = 2.7 lb.

2.6.3 $W_l = 2.7 \times .3 = .81$ watt

total loss = 2.71 watts

total case area = 62.2 in^2

watts/in^2 = .0436 watts/in^2

Measurements:

Choke E was built and assigned the number A8748. It was measured on the Hay bridge under 60 cycle sine wave conditions at specified ratings. The inductance measured 6.12 henries and R_{ac} measured 94.6 ohms.

Choke F

specs: L = 10 hy

R_c = 85 ohms

I_{max} = .25

$\frac{I_\Delta}{I_{max}} = 0$

design:

1. $n_{1r} = \frac{R_c^3 I_{max}^4}{L}$ (4-44)

$= \frac{85^3 \times .25^4}{10}$

$= 2.4 \times 10^2$

1.1

1.1 enter Chart 1A

1.1.1 $\mathcal{E}_{lr} = 80$

$\alpha = .004$

$B_{max} = 10000$ gausses

1.1.2 $$\ell_i = \mathcal{E}_{lr}\sqrt{\frac{L}{R_c}} \qquad (4\text{-}47)$$

$$= 80\sqrt{\frac{10}{85}}$$

$$= 27.5 \text{ cm} = 10.8 \text{ in.}$$

1.1.3 EI - 175 $\mathcal{E}_{lr} = 78$ $\ell_i = 26.67$ cm $= 10.5$ in.

$a_i = 19.79 \text{ cm}^2$

use square stack

1.1.4 $$\ell_a = \alpha\, \ell_i$$

$$= .04 \times 10.5 = .042 \text{ in.}$$

1.1.5 $$N = \sqrt{\mathcal{E}_l}\sqrt{\frac{v\ 10^8}{.4\pi\ u\ w\ \rho}}\sqrt{L\ R_c} \qquad (4\text{-}41)$$

$$= \sqrt{.08}\sqrt{\frac{6.25 \times 10^{-3} \times 10^8}{.4\pi \times 1 \times 2.5 \times 10^{-2} \times 1.724 \times 10^{-6}}}\sqrt{10 \times 85}$$

$$= 2820 \text{ turns}$$

1.1.6 $$a_w = \frac{v\ \ell_i^2}{N} \qquad (10\text{-}2)$$

$$= \frac{6.25 \times 10^{-3} \times 10.5^2}{2820}$$

$$= .000244 \text{ in}^2$$

use # 25 wire

4.1.1 wire thickness = .0191 in.

4.1.2 insulation thickness = .002 in.

4.1.3 $\text{layer} = \dfrac{.0191 + .002}{.91} = .023$ in.

4.2.1 winding length = 2.375 in.

4.2.2 $\text{turns/layer} = \dfrac{2.375}{.0191} = 125$

4.2.3 $\text{layer} = \dfrac{2820}{125} = 23$

4.3 winding height = 23 x .023 = .53 in.

nominal build up = .79 in.

analysis: $\ell_i = 26.67$ cm $\quad a_i = 19.76$ cm^2

$\alpha = .004 \quad N = 2820$

1.1 $B_\Delta = 0$

1.2.2 $H_b = \dfrac{.4\pi N I_b}{\ell_i}$ (3-20)

$= \dfrac{.4\pi \times 2820 \times .25}{26.67} = 33.2$ oersteds

1.2.3 $B_b = \dfrac{.4\pi N I_b}{\alpha \ell_i}$ (3-21)

$= \dfrac{.4\pi \times 2820 \times .25}{.004 \times 26.67} = 8300$ gausses

1.2.4 $H_b = 1.1$ oersteds

$B_b = 8200$ gausses

1.3 $\mu_\Delta = 550$

1.4 $L = \dfrac{.4\pi N^2 a'_i 10^{-8}}{\ell_i (\frac{1}{\mu_\Delta} + \alpha)}$ (2-30)

$= \dfrac{.4\pi \times 2820^2 \times 19.76 \times .9 \times 10^{-8}}{26.67 (\frac{1}{550} + .004)}$

$= 11.4$ hy

1.5.2 $I_{rms}^2 = I_b^2$

1.5.3 $W_c = I_{rms}^2 R_c$

$= .25^2 \times 85$

$= 5.3$ watts

1.6.3 no core loss

total watts = 5.3

case area = 149.47 in^2

watts/in^2 = .0354

Measurements:

Choke F was built and assigned the number A8749. It was measured on the Hay bridge under 60 cycle sine wave conditions at specified ratings. The inductance measured 10.2 henries and R_c measured 69.6 ohms.

Choke G

specs: $L = 28$ hy

$R_c = 670$

$I_{max} = .12$

$\frac{I_\Delta}{I_{max}} = .5$ resonant charging

design:

1 $n_{lr} = \frac{R_c^3 I_{max}^4}{L}$ (4-44)

$= \frac{670^3 \times .12^4}{28}$

$= 2.23 \times 10^3$

1.3 Chart 1C

1.3.1 Use B_{max} = 10 kilogausses

1.3.3 $\ell_{1r} = 77$

$\alpha = .0057$

1.3.4 $$\ell_i = \ell_{1r}\sqrt{\frac{L}{R_c}} \qquad (4\text{-}47)$$

$$= 77\sqrt{\frac{28}{270}}$$

$$= 15.7 \text{ cm} = 6.2 \text{ in.}$$

1.3.2 closest core EI - 12 $\ell_i = 15.25$ cm = 6 in.

$\ell_{1r} = 75$

use square stack

1.3.6 $$\ell_a = \alpha\,\ell_i \qquad (10\text{-}1)$$

$$= .0057 \times 6 = .0342 \text{ in.}$$

1.3.7 $$N = \sqrt{\ell_1\sqrt{\frac{v\,10^8}{.4\pi\,u\,w\,\rho}}\sqrt{L\,R_c}} \qquad (4\text{-}41)$$

$$= \sqrt{.075\sqrt{\frac{6..5 \times 10^{-3} \times 10^8}{.4\pi x1x2.5x10^{-2}x1.724x10^{-6}}}\sqrt{28 \times 670}}$$

$$= 5900 \text{ turns}$$

1.3.8 $$a_w = \frac{v\,\ell_i^2}{N} \qquad (10\text{-}2)$$

$$= \frac{6..5 \times 10^{-3} \times 6^2}{5900}$$

$$= .0000382 \text{ in}^2$$

use # 33 wire

4.1.1 wire thickness = .0077 in.

4.1.2 insulation thickness = .001 in.

4.1.3 $$\text{layer} = \frac{.007^{\circ} + .001}{.91} = .0096 \text{ in.}$$

4.2.1 winding length = 1.25 in.

4.2.2 $$\text{turns/layer} = \frac{1.25}{.0077} = 162$$

4.2.3 $$\text{layers} = \frac{5900}{162} = 37$$

4.3 winding height = 37 x .0096 = .355 in.

nominal build up = .45 in.

analysis: $\ell_i = 15.25$ cm $\quad a_i = 6.45$ cm^2

$\alpha = .0057 \quad N = 5900$

2.1 $I_\Delta = .06$

2.2.2 $$H_{max} = \frac{.4\pi N I_{max}}{\ell_i} \qquad (3\text{-}24)$$

$$= \frac{.4\pi \times 5900 \times .12}{15.25}$$

$$= 58.3 \text{ oersteds}$$

2.2.3 $$B_{max} = \frac{.4\pi N I_{max}}{\alpha \ell_i} \qquad (3\text{-}25)$$

$$= \frac{.4\pi \times 5900 \times .12}{.0057 \times 15.25}$$

$$= 10200 \text{ gausses}$$

2.2.4 $B_{max} = 9500$ gausses

2.3.2 $$H_\Delta = \frac{.4\pi N I_\Delta}{\ell_i} \qquad (3\text{-}27)$$

$$= \frac{.4\pi \times 5900 \times .06}{15.25}$$

$$= 29 \text{ oersteds}$$

2.3.3 $$B_\Delta = \frac{.4\pi N I_\Delta}{\alpha \ell_i} \qquad (3\text{-}28)$$

$$B_\Delta = \frac{.4\pi \times 5900 \times .06}{.0057 \times 15.25}$$

$= 5100$ gausses

2.3.4 $B_\Delta = 4600$ gausses

2.4 $$L = \frac{N B_\Delta a_1 10^{-8}}{I_\Delta} \qquad (2\text{-}29)$$

$$= \frac{5900 \times 4600 \times 6.45 \times .9 \times 10^{-8}}{.06}$$

$= 26.3$ hy

2.5.1.2 $I_{rms} = .707 \times .12$

$= .085$

2.5.2 $w_c = (.085)^2 \times 670$

$= 4.8$ watts

2.6.1 core loss = .4 watts/lb.

2.6.2 weight = 1.7 lb

2.6.3 core loss = $1.7 \times .4 = .68$

total loss = 5.48 watts

case area = 52.08

watts/in^2 = .105 watts/in^2

Measurements:

Choke G was built and assigned the number A8750. It was measured on the Hay bridge under 60 cycle sine wave conditions at specified ratings. The inductance measured 31 henries and R_{ac} measured 676 ohms.

Choke H

specs: L = 5 hy

R_{ac} = 800

$I_{max} = .35$

$\frac{I_\Delta}{I_{max}} = .5$ resonant charging

$B_{max} = 10$ kilogausses

$K_{ac} = .056$ watts/cm^2 = .362 watts/in^2

design:

2.4.1 $K_c = \frac{K_{ac}}{2}$ (10-8)

$= \frac{.056}{2}$

$= .028$

2 $n_{2r} = \frac{L\, I_{max}^{\,8}\, K_c^{\,3}}{I_{rms}^{\,6}}$ (5-21)

$= \frac{5 \times (.35)^8 \times (.028)^3}{(.247)^6}$

$= 1.1 \times 10^{-4}$

2.3 use Chart 2C

2.3.1 use B_{max} = 10 kilogausses

2.3.3 $g_2 = .3$

$g_2^{\,4} = 8.1 \times 10^{-3}$

2.4.2 $G_2^{\,4} = .4\pi \sqrt[3]{\frac{\tau\, w\, \gamma^2}{u\, \rho\, \frac{K_{ac}}{2}} \frac{I_\Delta^{\,4}\, L\, 10^8}{\rho\, I_{rms}^{\,2}}}$ (7-11)

$= .4\pi \sqrt[3]{\frac{6.25\times10^{-3}\times2.5\times10^{-2}\times(20\times10^{-12})^2}{1 \times 1.724 \times 10^{-6} \times \frac{.056}{2}} \frac{(.175)^4 5\times10^8}{1.3 \times (.247)^2}}$

$= 2.49 \times 10^{-4}$

2.4.3.1 $n'_{2r} = \frac{L\, I_{max}^{\,8}\, (K'_c)^3}{I_{rms}^{\,6}}$ (5-21)

$$n'_{2r} = \frac{5 \times (.35)^8 \times (.028)^3}{(.247)^6}$$

$$= 1.1 \times 10^{-4}$$

$$n''_{2r} = \frac{L\, I_{max}^{\,8}\, (K''_c)^3}{I_{rms}^{\,6}} \qquad (5\text{-}21)$$

$$= \frac{5 \times (.35)^8 \times (.056)^3}{(.247)^6}$$

$$= 8.75 \times 10^{-4}$$

$$\varepsilon'_2 = .3$$

$$\varepsilon'_{2r} = 9$$

$$\varepsilon''_2 = .325$$

$$\varepsilon''_{2r} = 9.75$$

2.4.3.2 $$K'_i = \frac{.4\pi\, \gamma\, I_\Delta^{\,2}\, L\, 10^8}{p(\ell'_i)^2(\varepsilon'_2)^4} \qquad (7\text{-}36)$$

$$\ell'_i = \varepsilon'_{2r} \sqrt[4]{\frac{L\, I_{rms}^{\,2}}{K'_c}} \qquad (5\text{-}24)$$

$$= 9 \sqrt[4]{\frac{5 \times .247^2}{.028}}$$

$$= 16.4$$

$$K'_i = \frac{.4\pi \times 20 \times 10^{-12} \times .175^2 \times 5 \times 10^8}{1.3 \times (16.4)^2 \times (.3)^4}$$

$$= 13.5 \times 10^{-5}$$

$$K''_i = \frac{.4\pi\, \gamma\, I_\Delta^{\,2}\, L\, 10^8}{p(\ell''_i)^2(\varepsilon''_2)^4} \qquad (7\text{-}36)$$

$$\ell''_i = \varepsilon''_{2r} \sqrt[4]{\frac{L\, I_{rms}^{\,2}}{K''_c}} \qquad (5\text{-}24)$$

$$\ell''_i = 9.75 \sqrt[4]{\frac{5 \times .247^3}{.056}}$$

$$= 14.9$$

$$K''_i = \frac{.4\pi \times 20 \times 10^{-12} \times .175^3 \times 5 \times 10^8}{1.3 \times (14.9)^3 \times (.325)^4}$$

$$= 12 \times 10^{-5}$$

2.4.3.3 $K'_{ac} = K'_c + K'_i$ (10-10)

$$= .028 + .000135$$

$$= .028135$$

$K''_{ac} = K''_c + K''_i$ (10-11)

$$= .056 + .00012$$

$$= .05612$$

2.4.3.4 $n_{2r} = \frac{(K_{ac} - K'_{ac})}{(K''_{ac} - K'_{ac})} (n''_{2r} - n'_{2r}) + n'_{2r}$ (10-12)

$$= \frac{(.056 - .028135)}{(.05612 - .028135)} (8.75 \times 10^{-4} - 1.1 \times 10^{-4}) + 1.1 \times 10^{-4}$$

$$= 8.75 \times 10^{-4}$$

2.4.3.5 $K_c = \sqrt[3]{\frac{I_{rms}^6 \, n_{2r}}{L \, I_{max}^8}}$ (5-21)

$$= \sqrt[3]{\frac{.247^6 \times 8.75 \times 10^{-4}}{5 \times .35^8}}$$

$$= .056$$

$\varepsilon_2 = .325$

2.3.3 $\varepsilon_{2r} = 9.75$

$\alpha = .01$

2.3.4 $\ell_i = \varepsilon_{2r} \sqrt[4]{\frac{L \, I_{rms}^2}{K_c}}$ (5-24)

$$\ell_i = 9.75 \sqrt[4]{\frac{5 \times .247^2}{.056}}$$

$$= 14.9$$

3.2.2 available core EI - 12

ℓ_i = 15.25 cm = 6 in.

ε_{2r} = 9.9 a_i = 6.45 cm²

3.2.6 s = .85 ε_2 = .332 α = .01

a_i = .85 x 6.45 = 5.5 cm²

2.3.6 $\ell_a = \alpha \ell_i$

= .01 x 6

= .06 in.

2.3.7 $$N = \varepsilon_2^{3/2} \sqrt[8]{\frac{p\, v\, L^3\, K_c\, 10^{24}}{(.4\pi)^3\, u\, w^3\, \rho\, I_{rms}^2}} \qquad (5\text{-}18)$$

$$= (.33)^{3/2} \sqrt[8]{\frac{1.3 \times 6.25 \times 10^{-3} \times 5^3 \times .056 \times 10^{24}}{(.4\pi)^3 \times 1 \times (2.5 \times 10^{-2})^3 \times 1.724 \times 10^{-6} \times (.247)^2}}$$

= 3610 turns

2.3.8 $$a_w = \frac{v\, \ell_i^2}{N} \qquad (10\text{-}2)$$

$$= \frac{6.25 \times 10^{-3} \times (6)^2}{3610}$$

= .0000624 in²

31 wire

4.1.1 wire thickness = .0097 in.

4.1.2 insulation thickness = .001 in.

4.1.3 $$\text{layer thickness} = \frac{.0097 + .001}{.91} = .0118 \text{ in.}$$

4.2.1 winding thickness = 1.19 in.

$$\text{turns/layer} = \frac{1.19}{.0097} = 123$$

4.2.2 $\text{layers} = \dfrac{3610}{123} = 30$

4.3 winding height = 30 x .0118

= .354 in.

nominal build up = .45 in.

analysis: $\ell_1 = 15.25$ cm $\quad a_1 = 5.5$ cm^2

$\alpha = .01 \quad N = 3610$

2.1 $I_\Delta = .175$

2.2.2 $$H_{max} = \frac{.4\pi N I_{max}}{\ell_1} \qquad (3\text{-}24)$$

$$= \frac{.4\pi \times 3610 \times .35}{15.25} = 104 \text{ oersteds}$$

2.2.3 $$B_{max} = \frac{.4\pi N I_{max}}{\alpha \ell_1} \qquad (3\text{-}25)$$

$$= \frac{.4\pi \times 3610 \times .35}{.01 \times 15.25} = 10400 \text{ gausses}$$

2.2.4 $B_{max} = 10000$ gausses

2.3.2 $$H_\Delta = \frac{.4\pi N I_\Delta}{\ell_1} \qquad (3\text{-}27)$$

$$= \frac{.4\pi \times 3610 \times .175}{15.25} = 52 \text{ oersteds}$$

2.3.3 $$B_\Delta = \frac{.4\pi N I_\Delta}{\alpha \ell_1} \qquad (3\text{-}28)$$

$$= \frac{.4\pi \times 3610 \times .175}{.01 \times 15.25} = 5200 \text{ gausses}$$

2.3.4 $B_\Delta = 5000$ gausses

2.4 $$L = \frac{N B_\Delta a_1 10^{-8}}{I_\Delta} \qquad (2\text{-}29)$$

$$L = \frac{3610 \times 5000 \times 5.5 \times .9 \times 10^{-8}}{.175}$$

$$= 5.08 \text{ hy}$$

2.5.1.2 $I_{rms} = .707 \times .35$

$$= .247$$

2.5.2 $$R_c = \frac{\rho N \ell_c}{a_w} \qquad (3\text{-}29)$$

$$= \frac{1.724 \times 10^{-6} \times 3610 \times 14.5}{4.08 \times 10^{-4}} = 222 \text{ ohms}$$

$$I_{rms}^2 R_c = .247^2 \times 222$$

$$= 13.5 \text{ watts}$$

2.6.1 core loss = .5 watts/lb

2.6.2 wt. = 1.45 lb

2.6.3 core loss = .5 x 1.45 = .72 watts

total loss = 14.2 watts

case area = 45.56 in^2

watts/in^2 = .312 watts/in^2 = .05 watts/cm^2

Measurements:

Choke H was built and assigned the number A8786. It was measured on the Hay bridge under 60 cycle sine wave conditions at specified ratings. The inductance measured 7.2 henries and R_{ac} measured 240 ohms.

Choke I

specs: L = 28 hy

R_c = 370

I_{max} = .12

$\frac{I_\Delta}{I_{max}}$ = .5 resonant charging

design:

1 $$n_{1r} = \frac{R_c^3 \, I_{max}^4}{L} \qquad (4\text{-}24)$$

$$= \frac{370^3 \times .12^4}{23} = 4.62 \times 10^2$$

1.3 Chart 1C

1.3.1 use B_{max} = 10 kilogausses

1.3.3 $g_1 = .068 \quad g_{1r} = 68$

$\alpha = .005$

1.3.4 $$\ell_i = g_{1r}\sqrt{\frac{L}{R_c}} \qquad (4\text{-}47)$$

$$= 68\sqrt{\frac{23}{370}}$$

$$= 17 \text{ cm}$$

1.3.5 closest core EI - 112 ℓ_i = 17.15 cm = 6.75 in.

g_{1r} = 69 use square stack a_i = 8.19 cm²

1.3.6 $$\ell_a = \alpha \, \ell_i \qquad (10\text{-}1)$$

$$= .005 \times 6.75 = .0338 \text{ in.}$$

1.3.7 $$N = \sqrt{g_1\sqrt{\frac{v \, 10^8}{.4\pi \, u \, w \, \rho}}\;\sqrt{L \, R_c}} \qquad (4\text{-}43)$$

$$= \sqrt{.068\sqrt{\frac{6.25 \times 10^{-3} \times 10^8}{.4\pi \times 1 \times 2.5 \times 10^{-2} \times 1.724 \times 10^{-6}}}\;\sqrt{23 \times 370}}$$

$$= 4650 \text{ turns}$$

1.3.8 $$a_w = \frac{v \, \ell_i^2}{N} \qquad (10\text{-}2)$$

$$= \frac{6.25 \times 10^{-3} \times 6.75^2}{4650}$$

$$= .0000612 \text{ in}^2 \qquad \#31 \text{ wire}$$

4.1.1 wire thickness = .0097 in.

4.1.2 insulation thickness = .001 in.

4.1.3 $$\text{layer} = \frac{.0097 + .001}{.91} = .0118 \text{ in.}$$

4.3.1 winding length = 1.375 in.

4.2.2 $$\text{turns/layer} = \frac{1.375}{.0097} = 142$$

4.2.3 $$\text{layers} = \frac{4650}{142} = 33$$

4.3 winding height = 33 x .0118 x .39 in.

nominal build up = .505 in.

analysis: $\ell_i = 17.15$ cm $\quad a_i = 8.19$ cm^2

$\alpha = .005 \quad N = 4650$

2.1 $I_\Delta = .06$

2.2.2 $$H_{max} = \frac{.4\pi N I_{max}}{\ell_i} \qquad (3\text{-}24)$$

$$= \frac{.4\pi \times 4650 \times .12}{17.15}$$

$$= 40.9 \text{ oersteds}$$

2.2.3 $$B_{max} = \frac{.4\pi N I_{max}}{\alpha \ell_i} \qquad (3\text{-}25)$$

$$= \frac{.4\pi \times 4650 \times .12}{.005 \times 17.15}$$

$$= 8200 \text{ gausses}$$

222.4 $B_{max} = 8000$ gausses

2.3.3 $$H_\Delta = \frac{.4\pi N I_\Delta}{\ell_i} \qquad (3\text{-}27)$$

$$H_\Delta = \frac{.4\pi \times 4650 \times .06}{17.15}$$

$$= 20 \text{ oersteds}$$

2.3.3 $$B_\Delta = \frac{.4\pi N I_\Delta}{\alpha \ell_i} \qquad (3\text{-}28)$$

$$= \frac{.4\pi \times 4650 \times .06}{.005 \times 17.15} = 4100 \text{ gausses}$$

2.3.4 $B_\Delta = 3900$ gausses

2.4 $$L = \frac{N B_\Delta a_i 10^{-8}}{I_\Delta} \qquad (2\text{-}29)$$

$$= \frac{4650 \times 3900 \times 8.19 \times .9 \times 10^{-8}}{.06}$$

$$= 22.2 \text{ hy}$$

2.5.1.2 $I_{rms} = .707 \times .12$

2.5.2 $W_c = I_{rms}^2 R_c \qquad (11\text{-}6)$

$$= (.707 \times .12)^2 \times 370$$

$$= 2.66 \text{ watts}$$

2.6.1 core loss = .2 watts/lb

2.6.2 wt. = 2.24 lb.

2.6.3 $W_i = .2 \times 2.24$

$$= .45 \text{ watts}$$

total loss = 3.1 watts

case area = 62.2 in^2

watts/in^2 = .05 watts/in^2

Measurements:

Choke I was built and assigned the number A8752. It was measured on the Hay bridge under 60 cycle sine wave conditions at specified ratings. The inductance measured 27.5 henries and R_c measured 307.7 ohms.

C. Additional Data

CHAPTER 13

TYPICAL CIRCUITS USING INDUCTORS

The electrical specification for an inductor should include the following:

Inductance

Voltage: magnitude, ffequency and waveform

Current: magnitude, frequency and waveform

Resistance Limits, if any.

Usually upper limits for the copper resistance or for the total (copper and iron) resistance are specified. The total resistance may be specified by specifying a figure of merit $Q = \frac{2\pi fL}{R_{ac}}$ at a specified frequency which is not always the same as the fundamental frequency of the operating voltage and current.

Linearity Requirements, if any.

Distributed Capacitance

Additional operating conditions, each containing the above items may be specified. Ideally, these items should be furnished by the circuit engineer. In practice the specifications may be incomplete, requiring the design engineer to calculate some items and to make "educated guesses" about others. Sometimes a schematic diagram may be submitted in lieu of the electrical specifications. Either of these circumstances requires the design engineer to understand the circuit in which the inductor is to be used. For detailed exposition of circuits, the reader is referred

to the many books on them and to the circuit portions of the radio engineering handbooks such as FTR,[3] RCA,[26] Terman.[12]

Power Filter Inductors

These inductors are used to remove the a-c components present in the output of rectifier circuits. The detailed analyses of these filters are given in the handbooks and texts. From the inductor design point of view, it is important to distinguish two cases. In the inductance input filter, Figure 20, the first (input) inductor is subject to appreciable a-c components of current and voltage which must be considered in the design. On the other hand if the inductors are beyond the first capacitor there are negligibly small a-c components and the condition $I_\Delta/I_{max} = 0$ will be nearly correct. This also applies to the first inductor of a capacitance input filter shown in Figure 21 and $I_\Delta/I_{max} = 0$ can be assumed.

Charging Inductors

In a line-type pulser a pulse forming network is charged from a power supply and discharged into the load. A charging inductor carries the charging current during the charging portion of the cycle and isolates the power supply during the discharging time. A typical circuit is shown in Figure 22. A detailed discussion is given in Glasoe and Lebacqz.[4]

Typical current waveforms are shown in Figure 23 for linear, resonant, and diode charging. For resonant and diode

charging the current falls to zero and therefore

$$\frac{I_\Delta}{I_{max}} = \frac{1}{2} \qquad (13\text{-}1)$$

For linear charging the ratio I_Δ/I_{max} is less than one-half and approaches zero as the charging current is more nearly constant.

The voltage wave form may be steep enough to require surge type construction. The turns in the outer winding layer may be spaced apart to prevent turn-to-turn breakdown as the voltage wavefront propagates along the winding. In use, this end of the winding is connected to pulse forming network.

Audio and Video Inductors

Inductors in these catagories are used principally to carry direct current to an ungrounded signal-voltage point from a power supply grounded for signal frequencies. Usually the signals may consist of any frequencies within some range or band, in which case the overall performance will have to be evaluated over this band. The required low frequency performance will affect the inductance specification and the required high frequency performance will affect the total resistance specification and the distributed capacitance specification. For additional information the reader is referred to the GE report on audio transformers.[27] Two typical circuits are shown in Figure 24 and Figure 25.

Figure 24 shows a shunt-fed amplifier in which the inductor carries the direct component of amplifier plate current without "shorting" the signal. Figure 25 shows a push-pull audio modulator stage "plate modulating" a class C radio frequency amplifier. This circuit produces an amplitude modulated radio frequency wave. In this case the inductor carries the direct component of the radio frequency amplifier plate current. (sine wave)

CHAPTER 14

MEASUREMENT AND TESTING

Inductor Measurements

To determine the suitability of particular inductor for its ultimate use, the best method is the connection of the inductor to a test circuit identical with that in which it is to be used. The complexity and expense of this procedure preclude its use except as a last resort when no other method is available. A second choice would be to apply the operating voltage or current wave to the unit and observe and measure the voltage and current waves. This would require a "universal" signal generator which is not too practical. Sine wave signals, however, are easily obtained by use of electronic oscillators, rotating alternators and electric utility power; also sine waves may be used without distortion by many types of bridges and impedance measuring circuits which would distort other wave forms. However, there are several important limitations inherent in sine wave testing which must be recognized when the test wave form is different from the operating wave form.

The actual operating inductance can best be obtained when the magnetic circuit operates along the same minor loop under testing and operating conditions. This means the I_{max}, I_{min} and I_{Δ} should have the same values under the test procedure as in operation. When a sine wave plus d-c test is set up accordingly, the losses will generally

be different from those in actual operation.

Figures 26a, 26b, and 26c show a pulse charging circuit set up for testing charging inductors. This device was assembled from parts at hand and therefore its components are not consistant in ratings, etc.

Figure 27 shows a Hay bridge for testing inductors with sine waves plus direct current. The non-linearity of the inductor under test results in harmonics in the detector which do not vanish at the fundamental balance and the selective detector is used to eliminate these harmonics. The inductance obtained in this manner will not necessarily be the same as found bu other methods because of the non-linearities present.

Material Measurements

One of the weak points of magnetic circuit analysis is the lack of precise knowledge of the iron BH characteristics, particularly in the area of superposed a-c and d-c excitation where the BH loops are asymmetrical. The values of B corresponding to the values of H must be known for various ranges of H_{dc} and H_{ac} or, in other words, the minor hysteresis loops with various amplitudes and displacements must be known.

If ring (toroidal) samples with large radius to radial thickness ratio are available, they may be wound with two coils of wire, one to be used as the magnetizing winding and one as a sensing winding. The current through the magnetizing winding is proportional to H since the to-

tal magnetomotive force in on the iron (no air gap). The sensing coil voltage is proportional to dB/dt and this voltage may be time integrated to give B plus a constant.

If ring samples are not available or of it is desired to measure straight samples or actual cores, the magnetizing current is not proportional to H because of the presence of air gaps. H can be obtained however by a Chattock magnetic potentiometer, a small uniformly wound air core coil with the end turns in intimate contact with the specimen. This coil gives a voltage proportional to dH/dt which may be time integrated to give H plus a constant.

When B (or H) is to be obtained by integrating its time derivative there are two problems concerned with the constant component. First if the integrating circuit is ideal, giving an output proportional to the time integral of the input from the start of the process, the starting point must be known to determine the constant of integration. This may be done by demagnetizing the sample specimen through successively smaller cycles of alternating magnetization. The starting condition would then be $H = 0$, $B = 0$.

If resistance-capacitance circuits are used for integration at audio frequencies, the integration is not ideal since the integrator exponentially "forgets" about the input previously received and the low frequency and constant components are lost. If the B and H voltages are presented on an oscilloscope, the origin and axes are not indicated or known. This difficulty may be over-

core by cyclically magnetizing the material along a major symmetrical loop in addition to the minor loop. Such a wave form and the corresponding hysteresis loop are shown in Figure 28. The midpoint of the line joining the tips of the major loop would be the origin. Two means of generating this major-minor waveform were used experimentally. An electronic switching circuit, Figures, 29a and 29b was constructed, but it was superceded by a synchronous commutator circuit, Figure 30, which had better output waveform.

At very low frequencies almost ideal integration can be realized by the system shown in Figure 31. This system may be considered in a simplified manner. When an output current i_o flows in response to an input signal e_i the mutual inductor M generates a feed-back voltage e_f equal to $M\, di_o/dt$. This feedback voltage will approximately cancel the input signal e_i if the gain of the d-c amplifier is large. The output current is then proportional to the flux linked by the search coil. Two such systems (when H is obtained by means of magnetic potentiometer) may drive the two channels of a two-coordinate plotter to produce the BH curves directly on paper. A schematic of the integrator is shown in Figure 32. This circuit was developed by the Weston Electrical Instrument Corporation.

CHAPTER 15

OTHER INDUCTIVE COMPONENTS

Electronic Inductors

For some applications components other than conventional may be preferred. One such component is an electronic filter reactor developed by CBS-Hytron. It is shown in detail on the data sheet included in this report. This circuit has not been tested or evaluated by the contractor under this contract, but mention of it is made here to indicate a possible line of attack on component problems.

Inductors with Permanent Magnet Gaps

Another possible line of attack on the general inductors problem is that of inserting slabs of permanent magnet ferrites into the magnetic circuit in place of air gaps. Such a device would be magnetized in the direction opposite to the induction produced by the operating biasing current I_b, and it would move the center of the minor loop closer to the origin which would increase the incremental permeability and lead to size reduction. Some limitations are apparent. The component would have to bear polarity marks and would have to be connected accordingly but this should present no more difficulty than in the case of electrolytic capacitors. Fault currents or switching transient currents can demagnetize the permanent magnet portion reducing the inductance.

CBS-HYTRON TYPE 6216
FILTER REACTOR TUBE



The CBS-Hytron type 6216 is an electron tube of beam power design and has miniature 9-pin construction.

When used in appropriate circuits, it replaces the iron-core filter choke, particularly in airborne and vehicular electronic equipments, thus materially reducing the weight and space normally required by the iron-core choke. It is equivalent in performance to a 12-henry filter choke of 100 ma and 350 ohm ratings.

The mechanical design of the 6216 is such that it can withstand shocks up to 700 g. It is also extremely resistant to the vibrations encountered in present high-speed military aircraft.

Its electrical design is such that it has an extremely low tube drop and very high plate resistance. For this reason, it outperforms such tubes as the 6W6GT, 25L6GT and 50C5 in applications where high circuit efficiencies are required. A detailed circuit and application information for the 6216 used as a typical filter reactor is included elsewhere in this bulletin.

The CBS-Hytron 6216 has many unique features among which are:

1. Ruggedized construction
2. Resistance to vibration
3. Resistance to interface formation
4. Very high perveance
5. Extreme power sensitivities

It may be used in Class A, Class B, and Class C amplifier applications, as a passing tube in electronic voltage-regulated power supplies, in wide-band video amplifiers, and in passive switching applications.

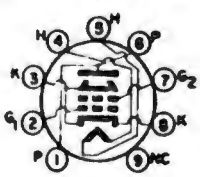
MECHANICAL DATA

Coated unipotential cathode

Bulb	T6½
Base	9-pin miniature
Maximum diameter	1⅛"
Maximum overall height	2⅝"
Maximum seated height	2⅜"

Terminal Connections

Pin connections



Pin 1: Plate
Pin 2: Grid No. 1
Pin 3: Cathode
Pin 4: Heater
Pin 5: Heater
Pin 6: Plate
Pin 7: Grid No. 2
Pin 8: Cathode
Pin 9: No connection

Mounting position	any
Shock	48°

ELECTRICAL DATA

Direct interelectrode capacitances*

Grid to plate: (g1 to p) max.	0.370	μμf
Input: g1 to (h+k+g2+g3+b.p.+b.s.+l.s)	12.3	μμf
Output: p to (h+k+g2+g3+b.p.+b.s.+l.s)	6.7	μμf

*Without shield.

Ratings Design-Center Values

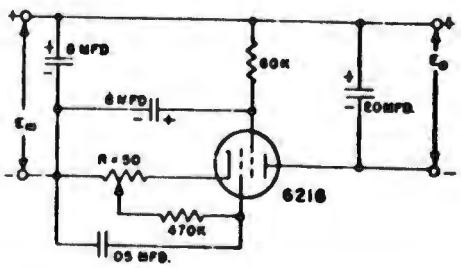
Heater voltage (nominal) (ac or dc)	6.3	volts
Maximum heater-cathode voltage	150	volts
Maximum plate voltage	300	volts
Maximum grid #2 voltage	200	volts
Maximum positive dc grid #1 voltage	0	volts
Maximum plate dissipation	10	watts
Maximum grid #2 dissipation	1.0	watts
Maximum cathode current	110	ma
Maximum bulb temperature at any point	210	°C
Max. grid #1 circuit resistance (fixed bias)	0.1	megohm
Max. grid #1 circuit resistance (self bias)	0.5	megohm

Average Characteristics — Filter Reactor

Heater voltage	6.3	volts
Heater current	1.2	ampere
Plate voltage	100	volts
Grid #2 voltage	100	volts
Grid #1 voltage	-3	volts
Grid #1 resistor	.1	megohm
Plate resistance (approx.)	18,500	ohms
Transconductance	12,800	μmhos
Plate current	72	ma
Grid #2 current	3	ma
Grid #1 voltage (approx.) for Ib=50 ua	-25	volts

Typical Operation — Filter Reactor (See Circuit)

Heater		
Voltage ac-dc	6.3	volts
Current	1.2	amps
D.C. Plate supply voltage (input to filter)	400	volts
D.C. Plate voltage (plate to cathode)	60	volts
D.C. Grid #2 voltage	100	volts
D.C. Grid #1 voltage	-1	volts
D.C. Output voltage (output from filter)	335	volts
D.C. Cathode current (load current)	100	ma d-c
RMS Ripple voltage (in output) (Note 1)	210	millivolts



PREPARED BY COMMERCIAL ENGINEERING DEPT. CBS-HYTRON A Division of Columbia Broadcasting System, Inc.
DANVERS, MASSACHUSETTS
Bulletin 2E-190
February 26, 1953

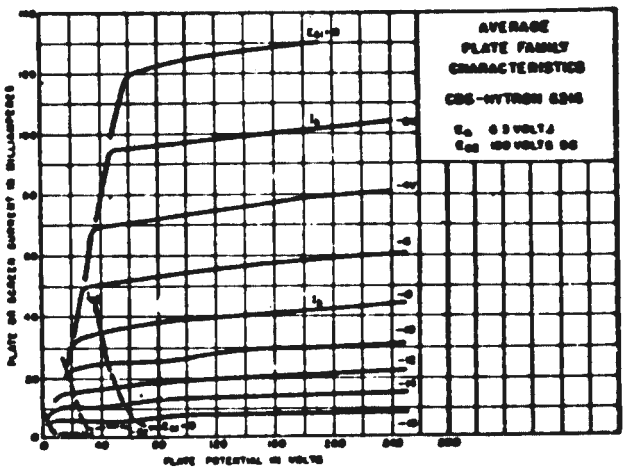
CBS-HYTRON TYPE 6216

FILTER REACTOR TUBE

ELECTRICAL DATA (Cont'd)

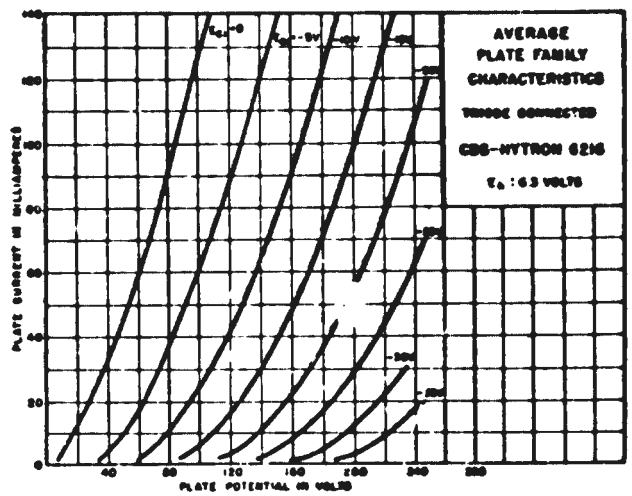
Typical Operation — Class A Audio Amplifier

Plate voltage	200	volts
Grid #2 (screen) voltage	100	volts
Grid #1 (control grid) voltage	-6	volts
Peak AF Grid #1 voltage	6	volts
Zero signal plate current	47	ma
Max. signal plate current	51	ma
Zero signal Grid #2 current	2.0	ma
Max. signal Grid #2	4.0	ma
Plate resistance	38,800	ohms
Transconductance	8,800	umhos
Load resistance	4,500	ohms
Total harmonic	10%	
Max. signal power output	3.8	watts



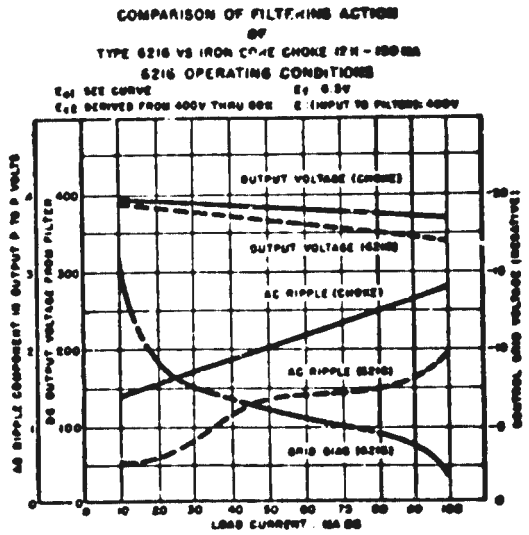
Typical Operation — Class C Oscillator-Amplifier — 50 MC

D.C. Plate voltage	300	volts
D.C. Grid #2 voltage	150	volts
D.C. Grid #1 voltage**	-50	volts
	22,000	ohms
Peak R. F. Grid #1 voltage	65	volts
D.C. Plate current	63	ma
D.C. Grid #2 current	8.0	ma
D.C. Grid #1 current	2.0	ma
Grid #1 driving power (approx.)	0.3	watts
Useful power output	8.8	watts



Typical Operation — Frequency Multiplier — Doubler

D.C. Plate voltage	300	volts
D.C. Grid #2 voltage†		
D.C. Grid #1 voltage**	-75	volts
	25,000	ohms
Peak R. F. Grid #1 voltage (approx.)	95	volts
D.C. Plate current	50	ma
D.C. Grid #2 current	6	ma
D.C. Grid #1 current (approx.)	1	ma
Grid #1 driving power	0.6	watts
Useful power output	4.0	watts



**Obtained from fixed source or grid resister of value shown.

†From 300 volt supply through 25,000 ohms dropping resistor.

NOTE 1: When the 6216 is used in the circuit shown above, the potentiometer R should be adjusted for minimum a-c output voltage across the Eo terminals. The curve shown in the appendix represents adjustment for minimum a-c output voltage at 100 ma d-c load current.

APPENDIX A

LIST OF SYMBOLS

Certain values of the time variable quantities--b,h,i, m, and ϕ--will be designated by capital letters as follows, where s is the general variable and P is the period:

no subscript: time average, $Z = (1/P)\int_0^P s\,dt$

subscript b: biased, $(Z_{max} + Z_{min})/2$
subscript Δ: incremental, $(Z_{max} - Z_{min})/2$
Subscript max: Maximum value during a cycle
subscript min: minimum value during a cycle
subscript rms: root-mean-square, $Z_{rms} = \sqrt{(1/P)\int_0^P s^2\,dt}$
prefix Δ: total change, $\Delta Z = Z_{max} - Z_{min} = 2Z_\Delta$

Certain values of some quantities below are distinguished by ' and ".

a_c is the net copper cross sectional area in cm^2
a_i is the net iron core cross sectional area in cm^2
a_w is the net wire corss sectional area in cm^2
α is the ratio of effective air gap length ot iron length, ℓ_a/ℓ_i
b is the time variable induction in gausses

D is the function $(1/\mu^2)d\mu/dB_{max} - (1/\mu_\Delta^2)d\mu_\Delta/dB_{max}$

E_{ac} is the sine wave effective voltage in volts
e is the time variable voltage in volts
f is the frequency in cyclesper second
F_c is the copper space factor
F_i is the iron space factor
G_1 and G_{1*} are particular values of g_1

g_1 is a design factor, $\sqrt{1/\mu_\Delta + \alpha}$

g_{1r} is a design factor, $\ell_i\sqrt{R_c/L}$

G_2 and G_{2*} are particular values of g_2

g_2 is a design factor, $\sqrt[4]{1/\mu_\Delta + \alpha}$

g_{2r} is a design factor, $\ell_i\sqrt[4]{\frac{K_c}{LI_{rms}^2}}$

g_r is a generalized design factor
h is the time variable magnetizing force in oersteds
H_{max} is a ficticious magnetizing force in oersteds, $.4\pi NI_{max}/\ell_i$

i is the time variable current in amperes
K_{ac} is the total power density in watts per cm^2, $(W_c + W_i)/S$
K_c is the copper loss power density in watts per cm^2, W_c/S
K_i is the iron core loss power density in watts per cm^2, W_i/S
ℓ_a is the effective air gap length in cm
ℓ_c is the mean copper turn length in cm
ℓ_i is the mean iron core length in cm
L is the inductance in henries
m is the time variable magnetomotive force in gilberts
μ is the normal permeability in gausses per oersted
μ_Δ is the incremental permeability in gausses per oersted
μ_Δ is the incremental permeability as a function of B_{max} alone for a fixed B_Δ/B_{max} ratio

n_1 is a design factor $(.4\pi)^5 v^3 w I_{max}^4 R_c^3 10^{-8}/(u^3\rho^3 L)$

n_{1r} is a design factor $I_{max}^4 R_c^3/L$

n_2 is a design factor $(.4\pi)^7 p^3 v^3 L I_{max}^8 K_c^3 10^8/(u^3 w \rho^3 I_{rms}^6)$

n_{2r} is a design factor $L I_{max}^8 K_c^3/I_{rms}^6$

n_r is a generalized design factor
p is the dimensionless ratio of surface area to the square of the mean iron length, S/ℓ_i^2
ϕ is the time variable magnetic flux in maxwells
Q and q are dummy constants in Chapter VI
R_{ac} is the total resistance in ohms, $R_c + R_i$
R_i is the core loss component of resistance in ohms
R_c is the copper resistance in ohms
ρ is the resistivity in ohm-centimeters
S is the surface area in cm^2
s is the ratio of stack height to center leg width
t is the time in seconds
T is the stack height in cm
u is the dimensionless ratio of mean turn length to mean iron length, ℓ_c/ℓ_i
v is the dimensionless ratio of net copper cross sectional area to the square of the mean iron length, a_c/ℓ_i^2
W_c is the copper loss in watts
W_i is the iron core loss in watts
w is the dimensionless ratio of net iron core cross sectional area to the square of the mean iron length, a_i/ℓ_i
x is the lamination center leg width in cm
y is a dummy variable in Chapter VI

APPENDIX B

BIBLIOGRAPHY

1 Allegheny Steel Co., Magnetic Core Materials Practice, Brackenridge, Penna., 1937, Part III, pp 66-86.

2 F. C. Connelly, Transformers, Their Principles and Design for Light Electrical Engineers, London, 1950, pp 405-415.

3 Federal Telephone and Radio Corp., Reference Data For Radio Engineers, Third Edition, New York, 1949, pp 194-195.

4 G. N. Glasoe and J. V. Lebacqz, Pulse Generators, Volume 5, MIT Radiation Laboratory Series, New York, 1948, pp 372-380.

5 V. Karapetoff, The Magnetic Circuit, New York, 1911, p 29 Prob.11.

6 F. W. Lanchester, "The Air Gap Transformer and Choke", Journal of the IEE, October 1933, v. 73, pp 413-418.

7 R. Lee, Electronic Transformers and Circuits, New York, 1947, pp 66-77.

8 MIT EE Staff, Magnetic Circuits and Transformers, New York, 1943, pp 68-81 and 197-241.

9 J. Minton and I. G. Maloff, "Design Methods for Soft Magnetic Materials in Radio", Proceddings IRE, June 1929, v 17, pp 1021-33.

10 G. F. Partridge, "The Inductance of Iron-cored Coils Carr ying Direct Current", Philosophical Magazine, 1937, v 23, pp 99-106.

11 H. C. Roters, Electromagnetic Devices, New York, 1941, pp 102-105.

12 F. E. Terman, Radio Engineers' Handbook, New York, 1943, pp 97-107.

13 V. G. Welsby, The Theory and Design of Inductance Coils, London, 1950, pp 82-85.

14 C. R. Hanna, "Design of Reactances and Transformers Which Carry Direct Current", Journal AIEE, February 1927, v 46, pp 128-133.

15 W. H. Crowhurst, "Design of Iron Cored Inductances Carrying D.C.", Electronic Engineering, December 1950, v 22, pp 516-523.

16 R. O. Carter and D. L. Richards, "Incremental Magnetic Properties of Silicon-Iron Alloys with Particular Reference to the Design of Air-Gapped Smoothing Chokes", Proceedings of the IRE, April 1950, v 97, Part II, pp 199-214.

17 V. E. Legg, "Optimum Air Gap for Various Magnetic Materials in Cores of Coils Subject to Superposed Direct Current", Transactions of the AIEE, 1945, v 64, pp 709-712.

18 F. Brailsford, Magnetic Materials, London, 1948, pp 10-12.

19 Y. Niwa and J. Sugiura and J. Matura, "Further Study on the Magnetic Properties of Electrical Sheet Steel under Superposed Alternating Field and Unsymmetrical Hysteresis Losses", Researches of the Electrotechnical Laboratory, No. 144, Tokyo, Japan, p 19.

20 T. Spooner, "Effect of a Superposed Alternating Field on Apparent Magnetic Permeability and Hysteresis Loss", Physical Review, 1925, v 25, pp 527-540.

21 H. C. Roters, op. cit., footnote 6, page 104.

22 Allegheny Ludlum Steel Corp., Transformer Laminations, EM 3, Fifth Edition, Pittsburgh, Penna., 1952.

23 T. Spooner, "Permeability", Transactions of the AIEE, 1923, v 42, pp 340-348.

24 Armour Research Foundation, Design and Development of Miniature Hermetically Sealed Power Transformers, Report #24, ARF Project #90-686E, Illinois Institute of Technology, Chicago 16, Illinois, February, 1951.

25 Armour Research Foundation, Research and Development of New Design Method for Power Transformers, Report #21, ARF Project #E017-0, Illinois Institute of Technology, Chicago 16, Illinois, February 1953.

26 F. Langford-Smith, Radiotron Designer's Handbook, Fourth Edition, RCA Victor Division, Harrison, New Jersey, 1954.

27 General Electric Research Laboratory, Transformer Design Criteria and Data, Report #RL-417, Schenectady, New York, June, 1954.

V. CONCLUSIONS

The mathematical relations developed provide a method of constructing design charts directly from the magnetic material characteristics. Those charts may then be used for the design (synthesis) of inductors without the usual trial-and-error or "guestimation" procedures for the first design.

The method is limited by the quantity and quality of the magnetic data available. No complete set of incremental data has been avaiable from any one steel manufacturer in recent years nor is the range of variation of these data available. To utilize the method fully, the design curves should be constructed for all the core materials whose use is contemplated, and then direct comparison will show which material will result in the smallest unit for a given set of specifications.

A secondary use of the method is that of providing a quick size estimate for the equipment designer who may need to weigh inductor specifications and size against the specifications and size of other components with which the inductor is connected.

VI. RECOMMENDATIONS

Because of the general lack of comprehensive magnetic data including incremental permeability and incremental core loss, it is recommended that these data be obtained for all the available core materials and that the design charts be constructed for them. Such investigations should cover the variation of characteristics on a statistical basis, so that quantity production performance may be predicted.

New technique such as the use of permanent magnet ferrites to "depolarize" a d-c inductor and substitute devices such as the electronic filter reactor should be studied to determine their areas of applicability.

VII. PERSONNEL

The following personnel were employed on this contract for the percentage time shown (based on a two year period).

Name	Title	Time
P. A. Cartwright	Assistant Professor	25%
J. T. Ludwig	Research Fellow	100%
G. J. Murphy	Instructor	20%
J. K. Shimada	Teaching Assistant	5%
C. O. Persons	Laboratory Technical Assistant	7%
E. W. Reed, Jr.	Electronics Mechanic	55%
W. C. Timm	Electronics Mechanic	30%
A. J. Lane	Clerk-typist	1%
C. E. Machacek	Clerk-typist	3%
Y. Tamekuni	Clerk-typist	10%

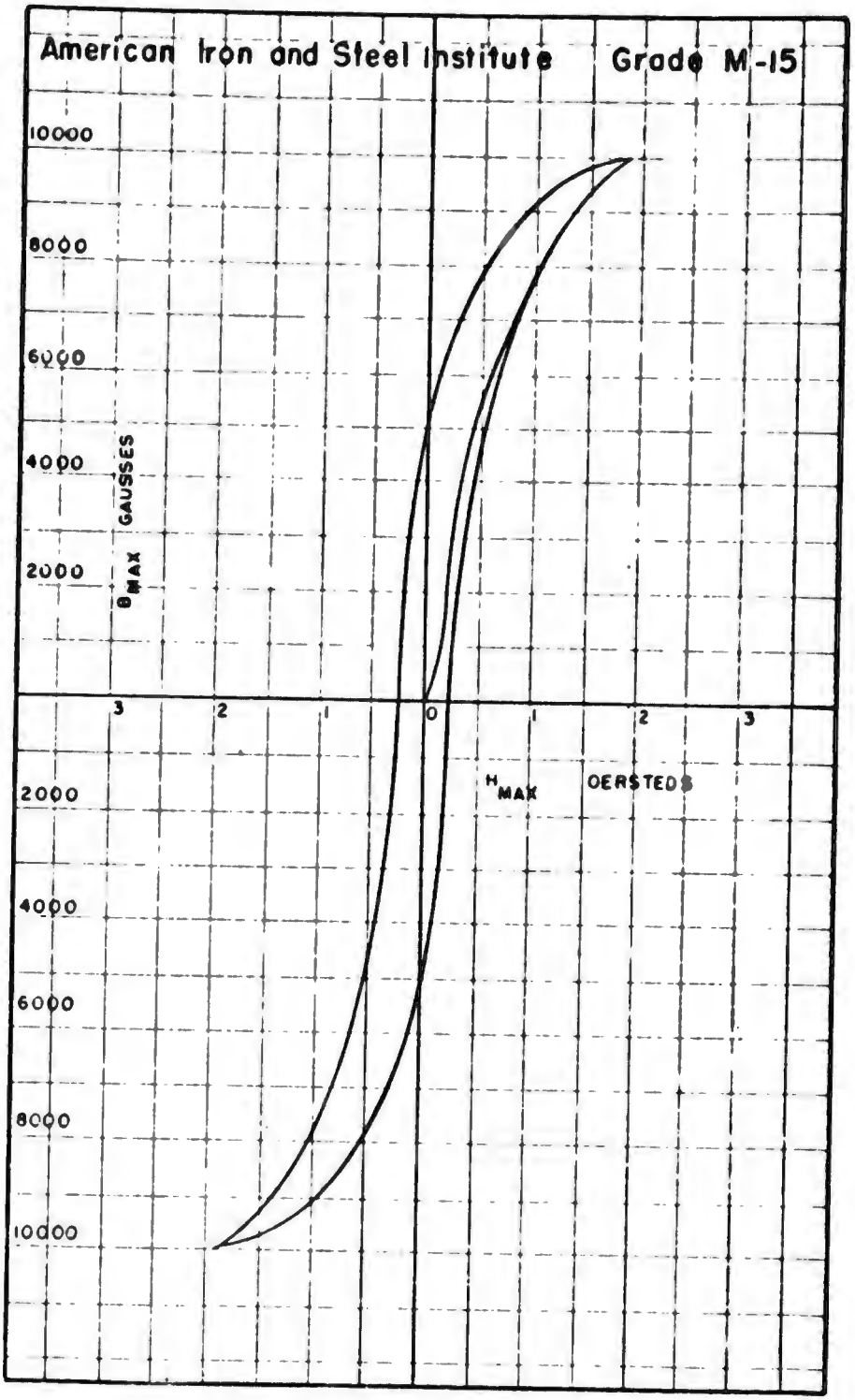


Fig.1 The normal induction curve and one symmetrical major hysteresis loop.

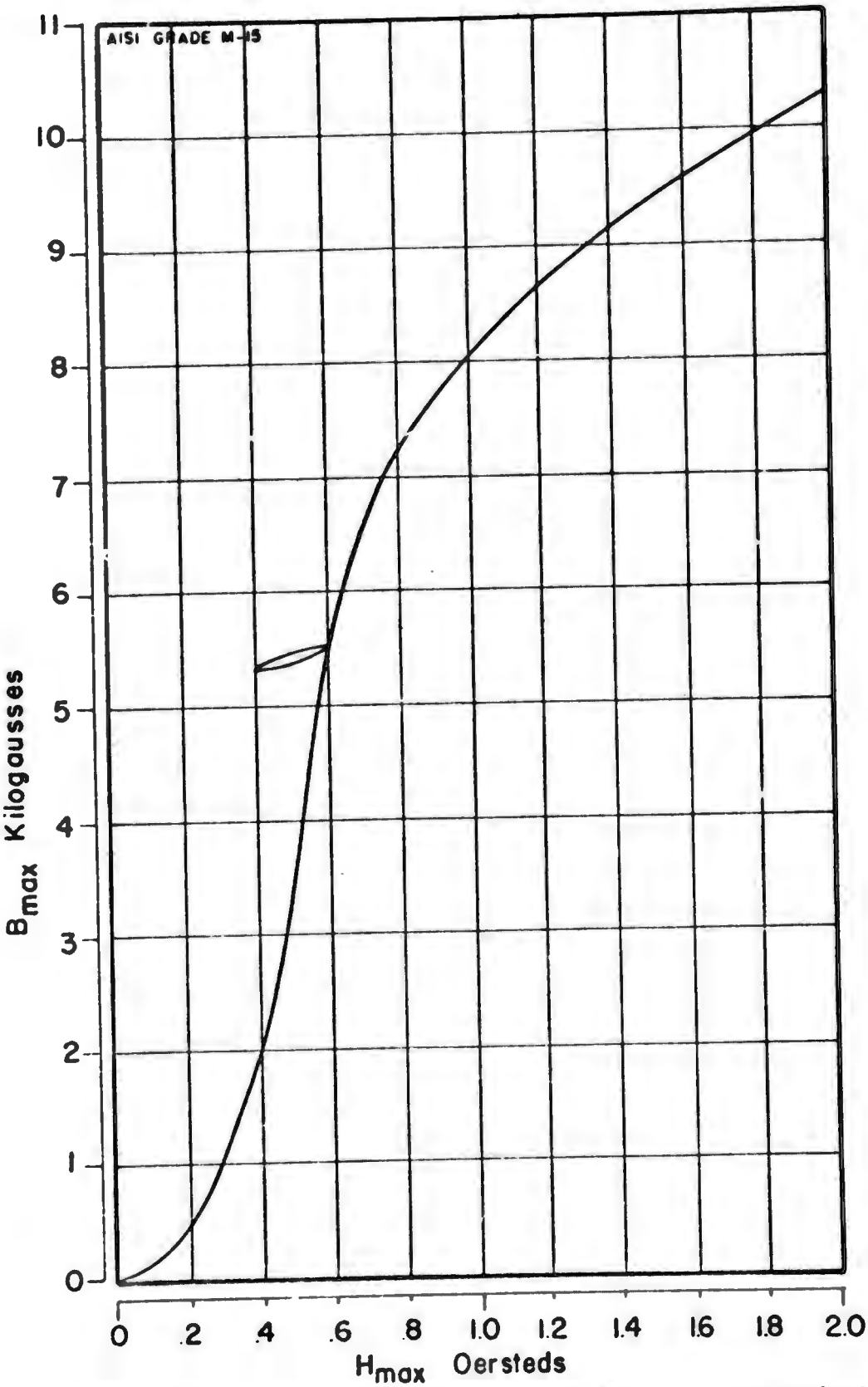


Fig. 2 The normal induction curve and one unsymmetrical (minor) hysteresis loop.

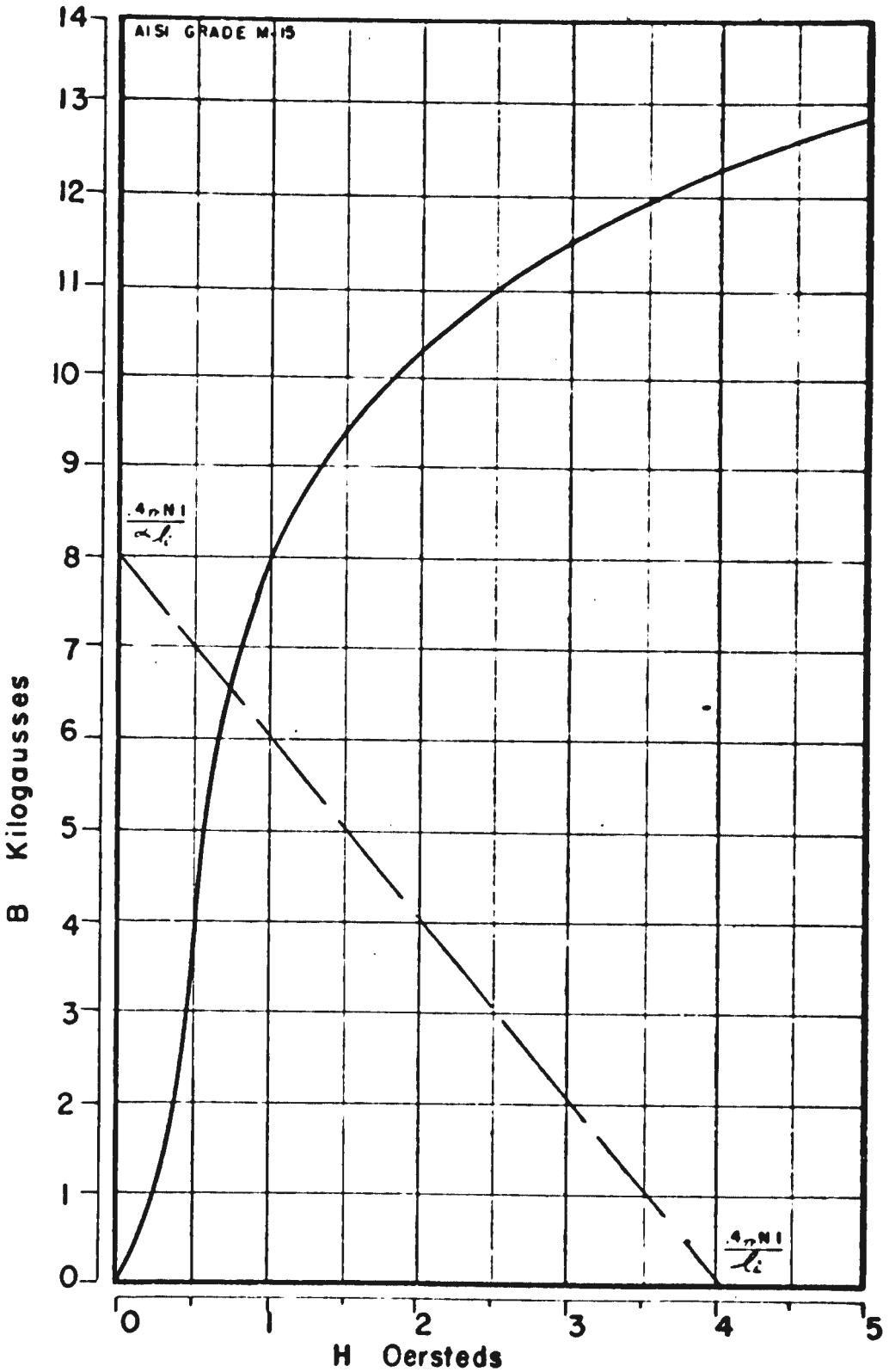


Fig.3 The normal induction curve with Karapetoff's air gap line to find d-c induction in absence of a-c induction.

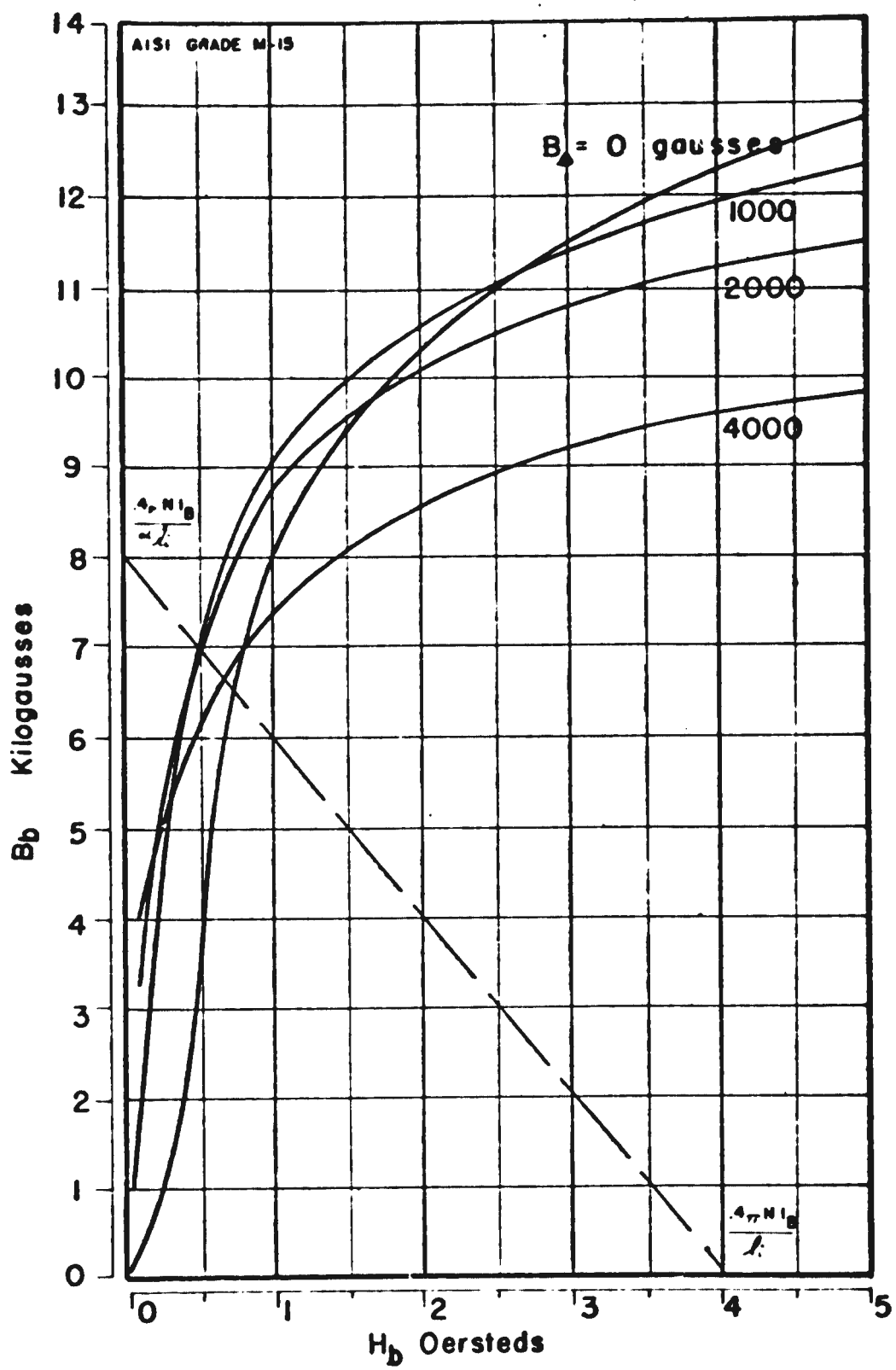


Fig. 4 The biased (anhysteretic) induction curves with air gap line to find the center of the minor loop.

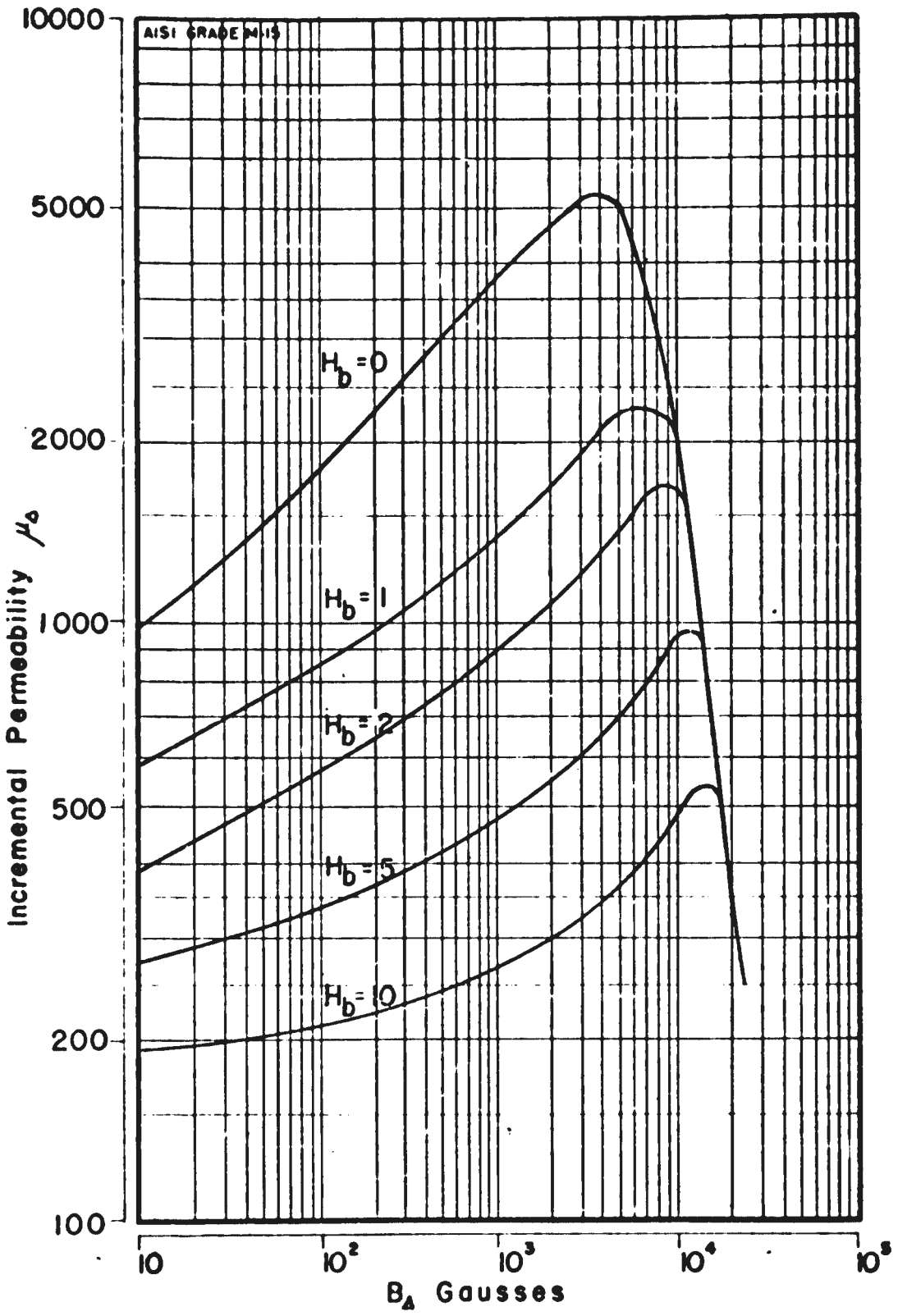


Fig. 5 Incremental permeability curves.

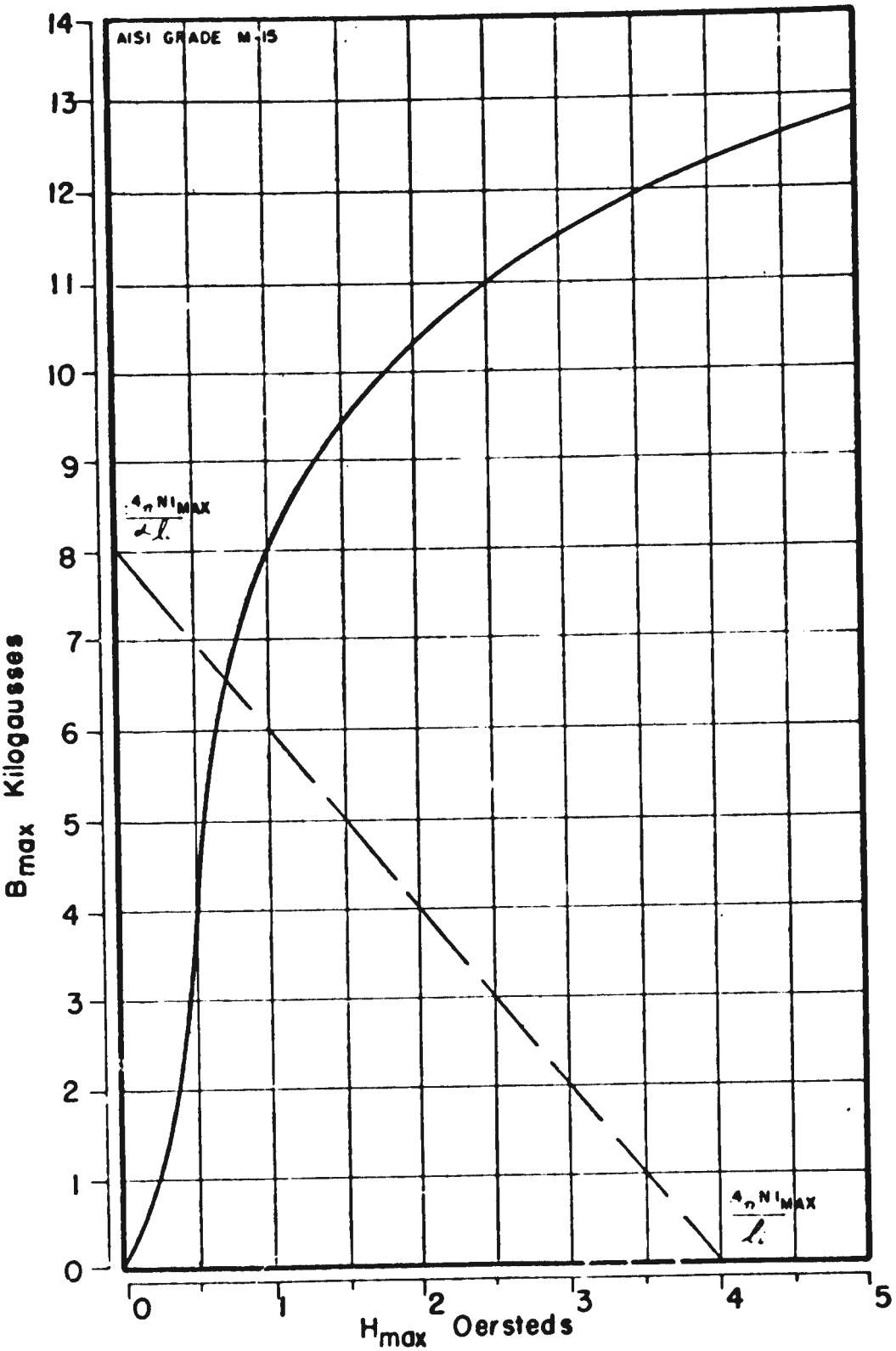


Fig. 6 The normal induction curve with air gap line to find the upper tip of the minor loop.

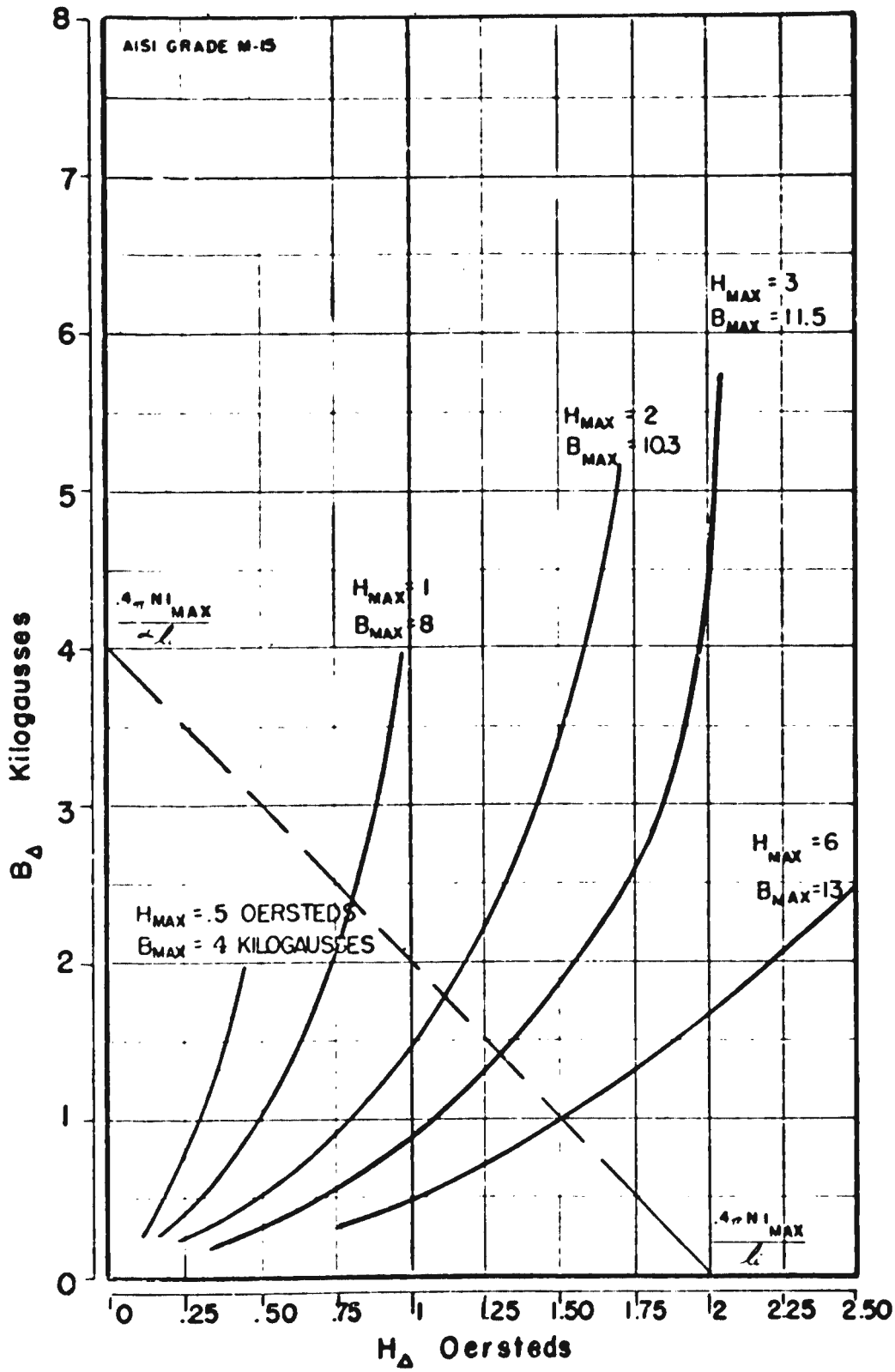


Fig. 7 The incremental induction curves with air gap line to find the incremental induction.

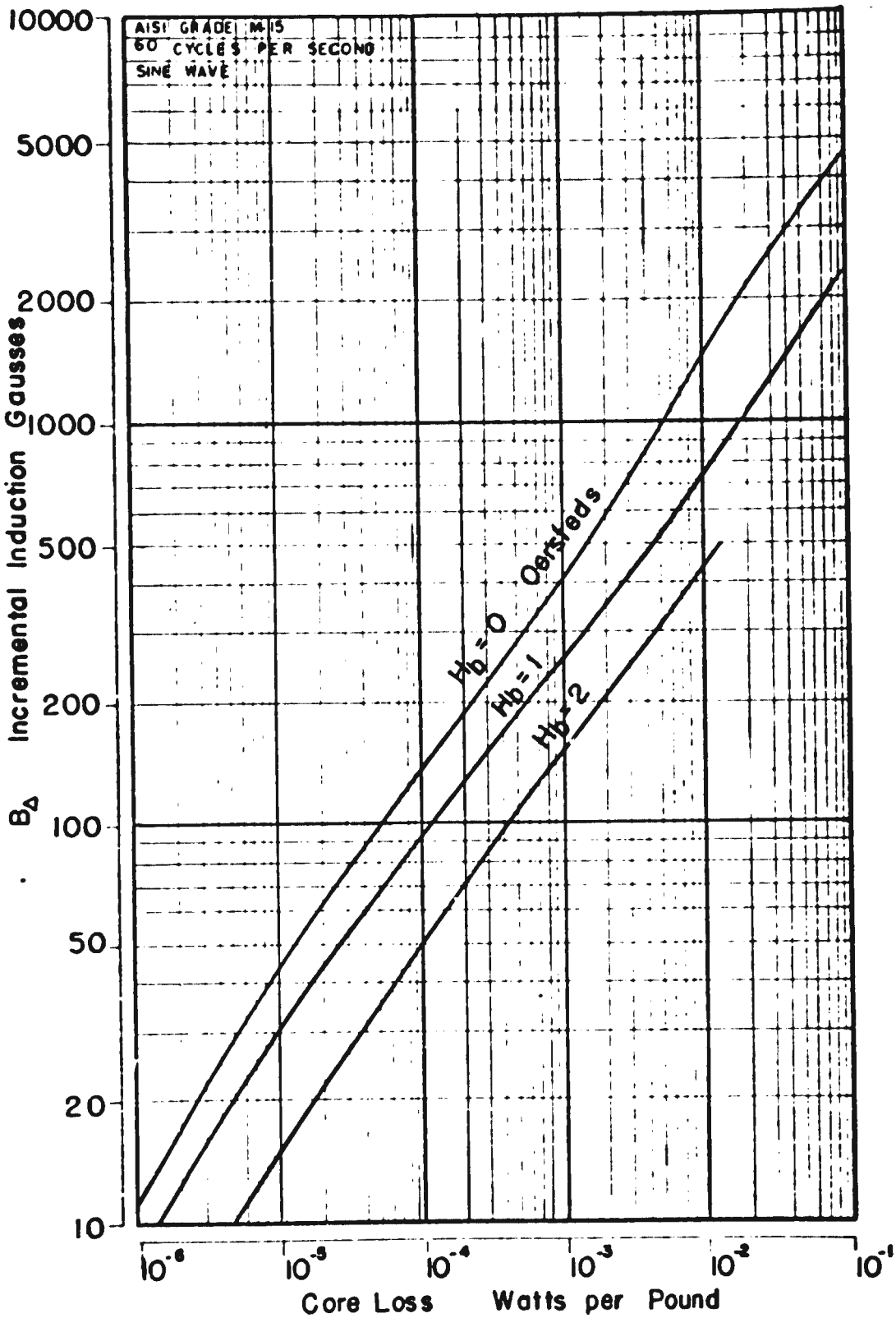


Fig. 8 Core loss with biasing magnetizing force as a parameter.

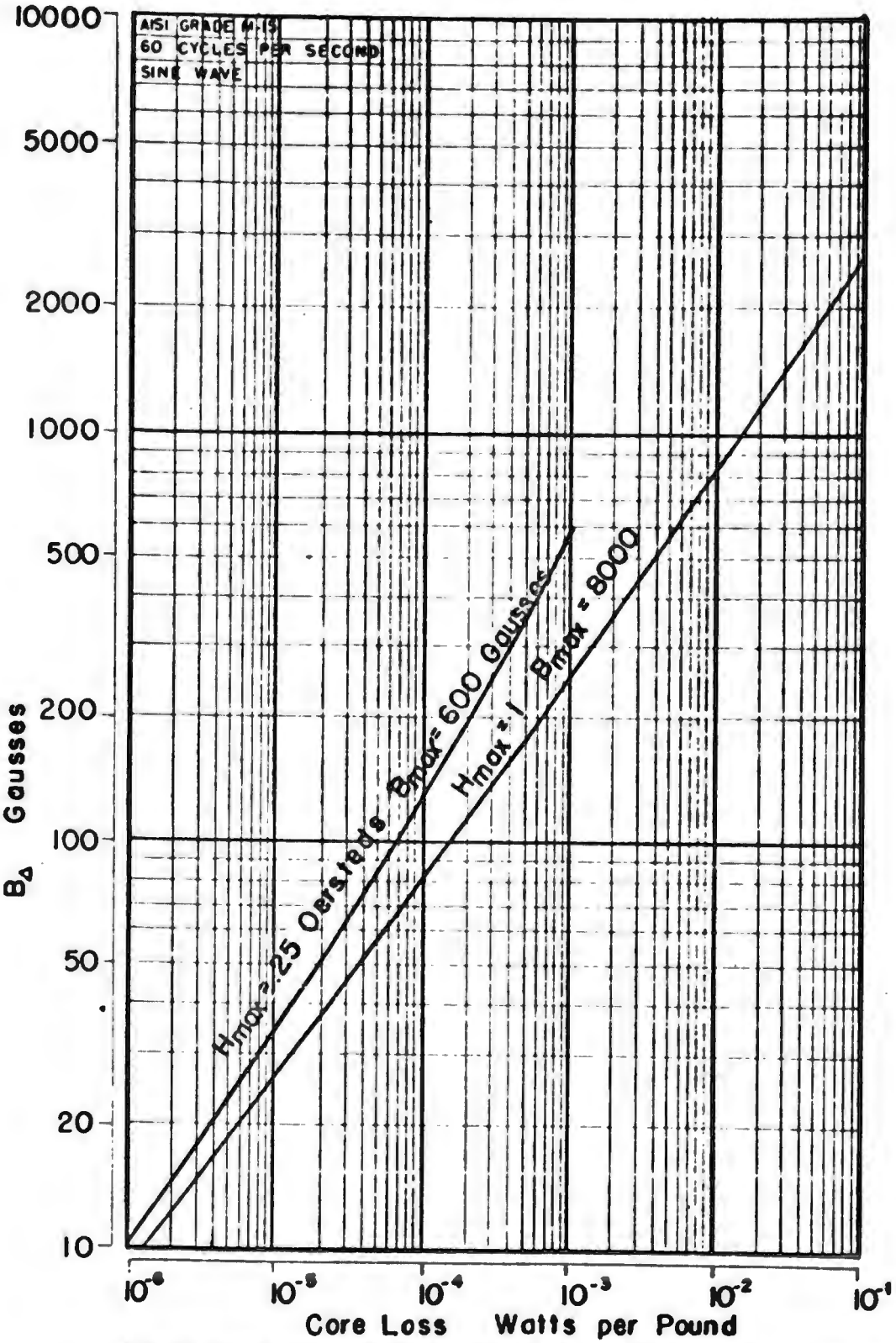


Fig.9 Core loss with maximum magnetizing force as a parameter.

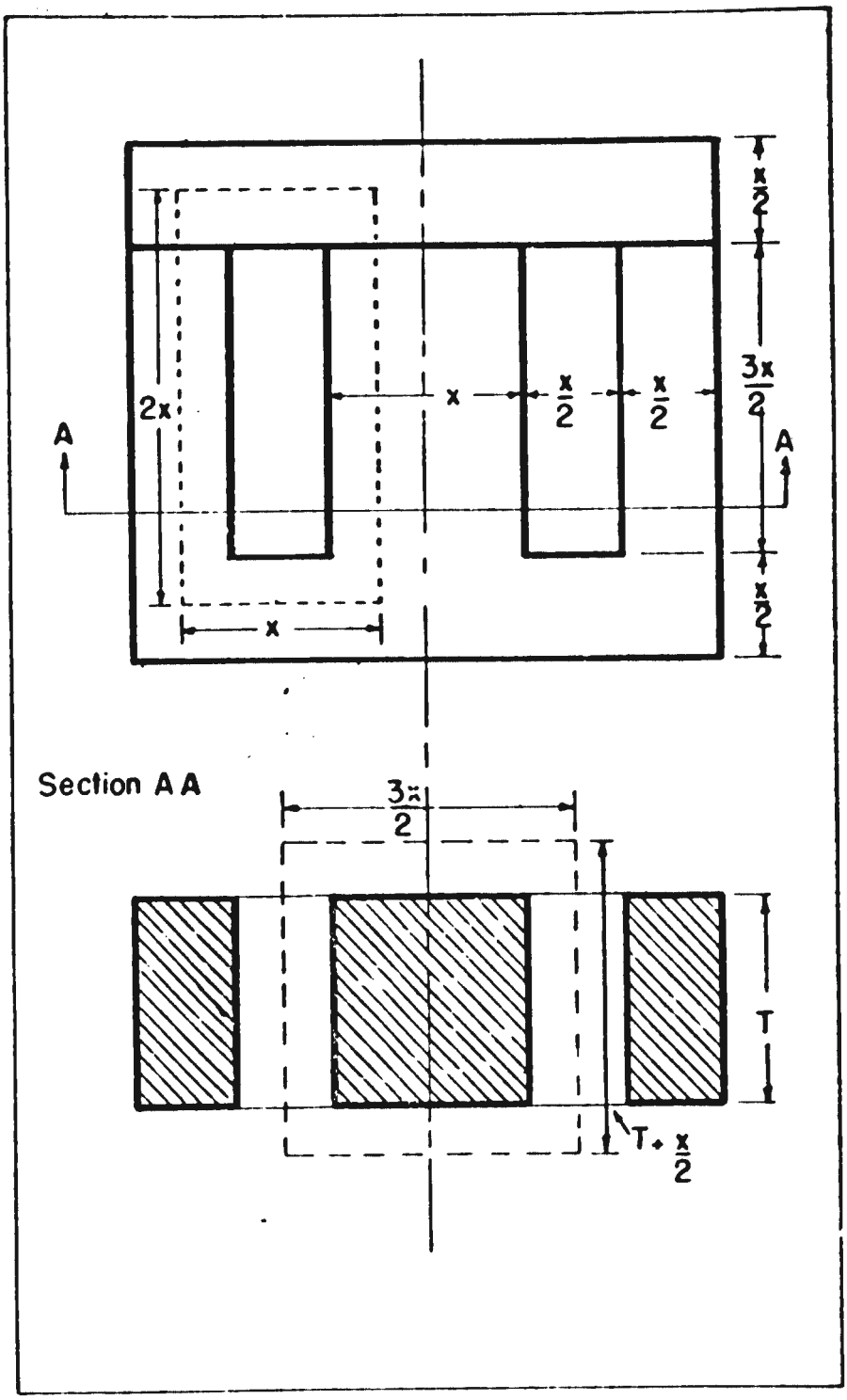


Fig. 10 Scrapless E I lamination.

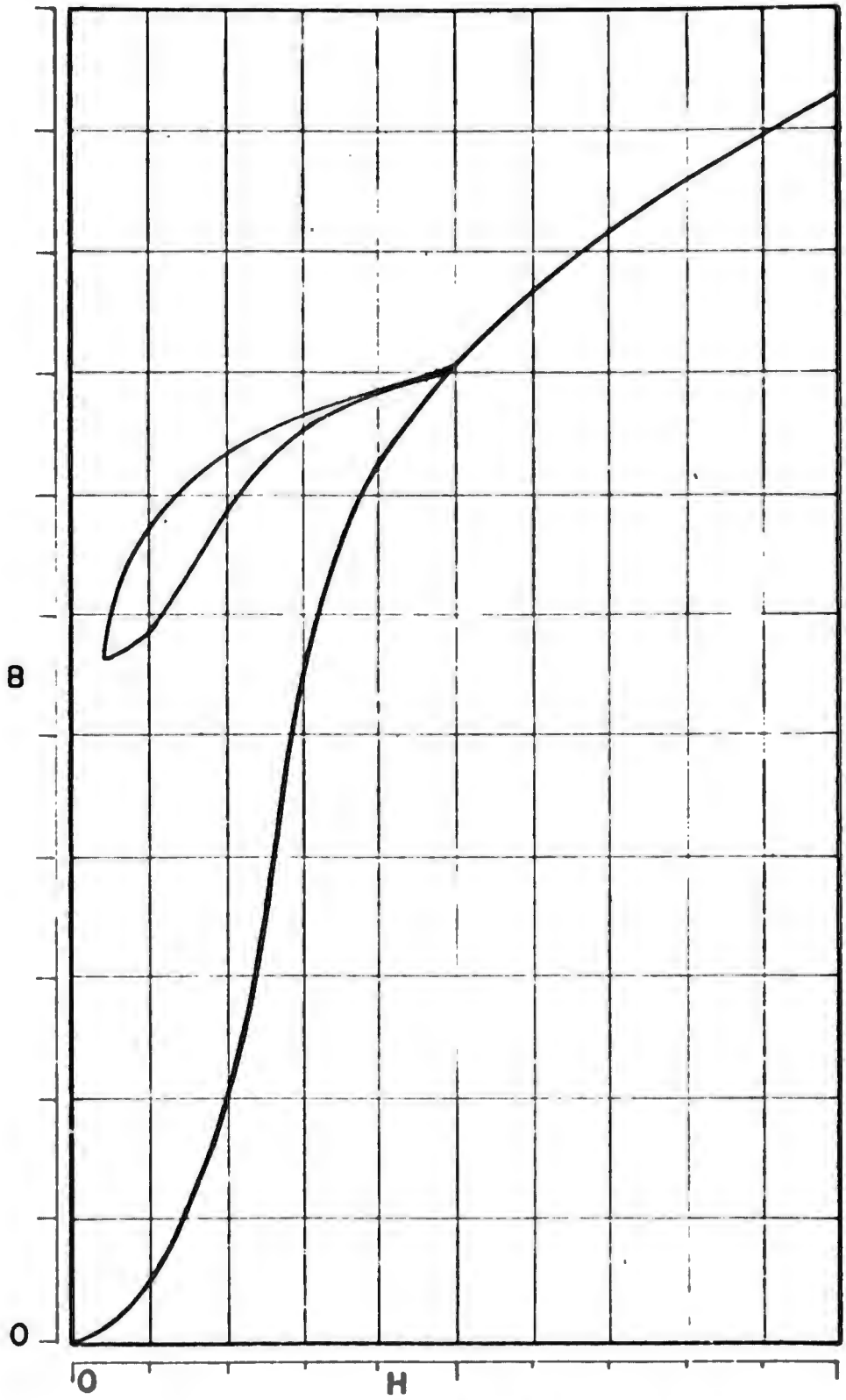


Fig. 11 Normal induction curve with a minor loop extending above the "knee".

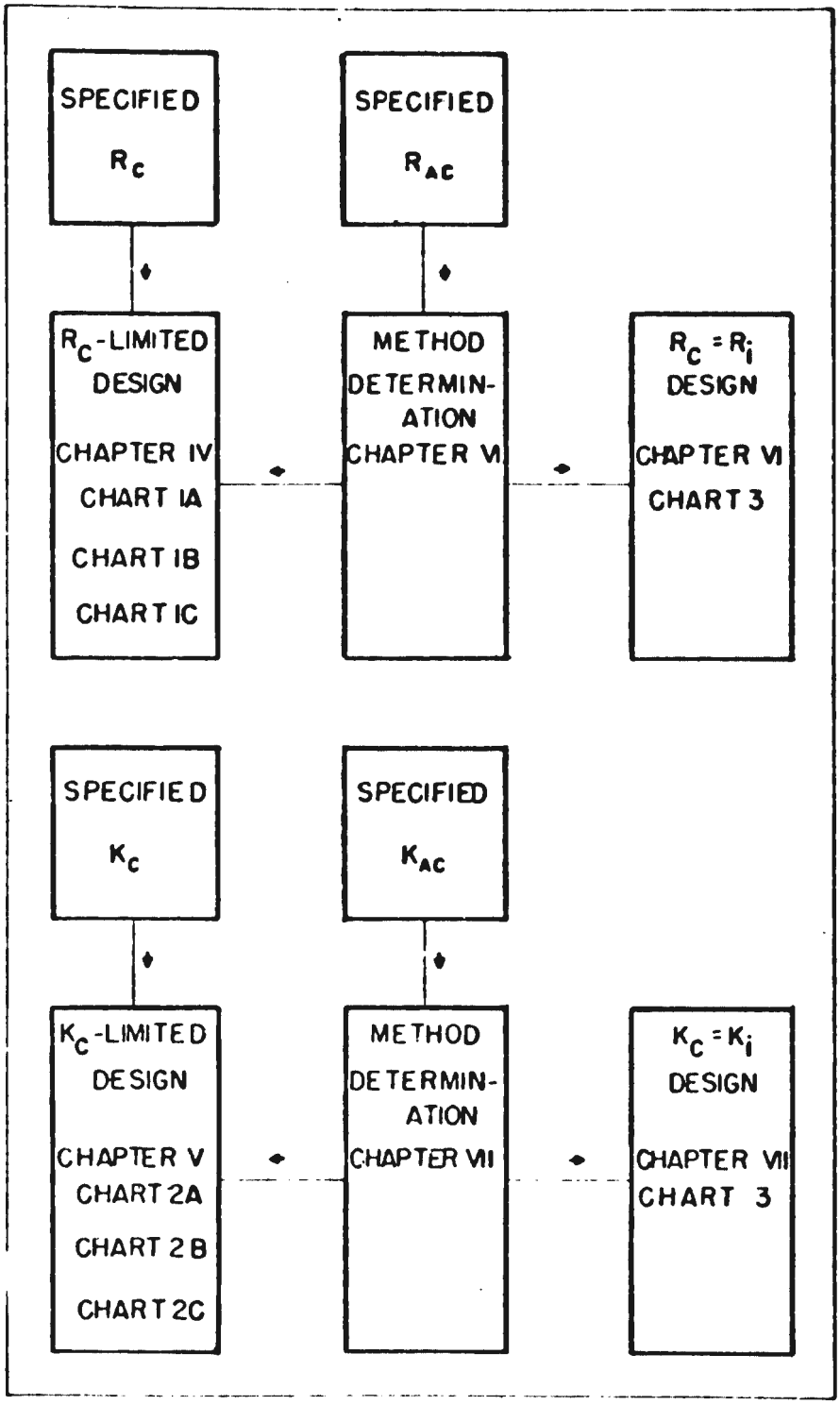


Fig. 12 Map of synthesis method.

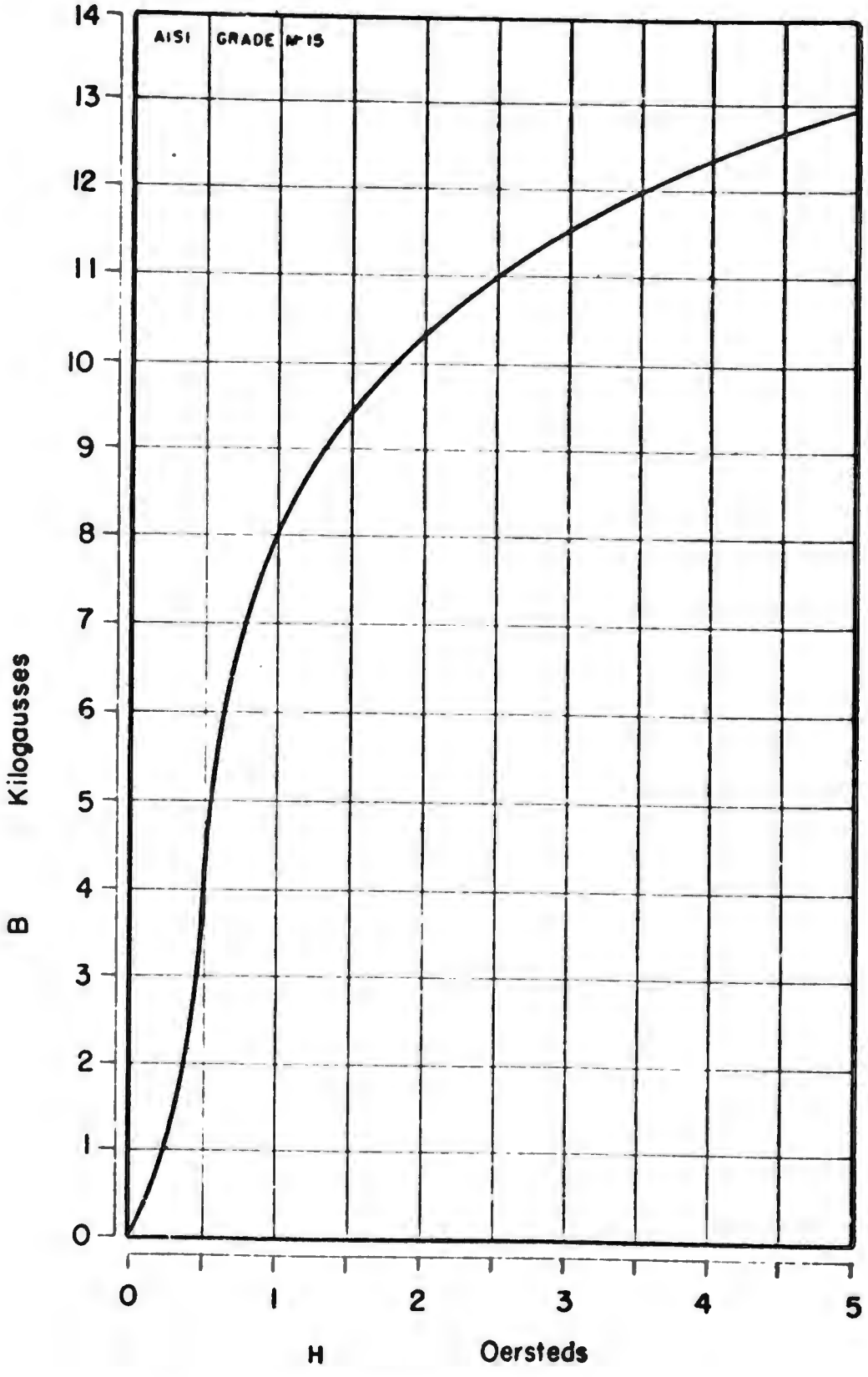


Fig. 13 Normal Induction Curve

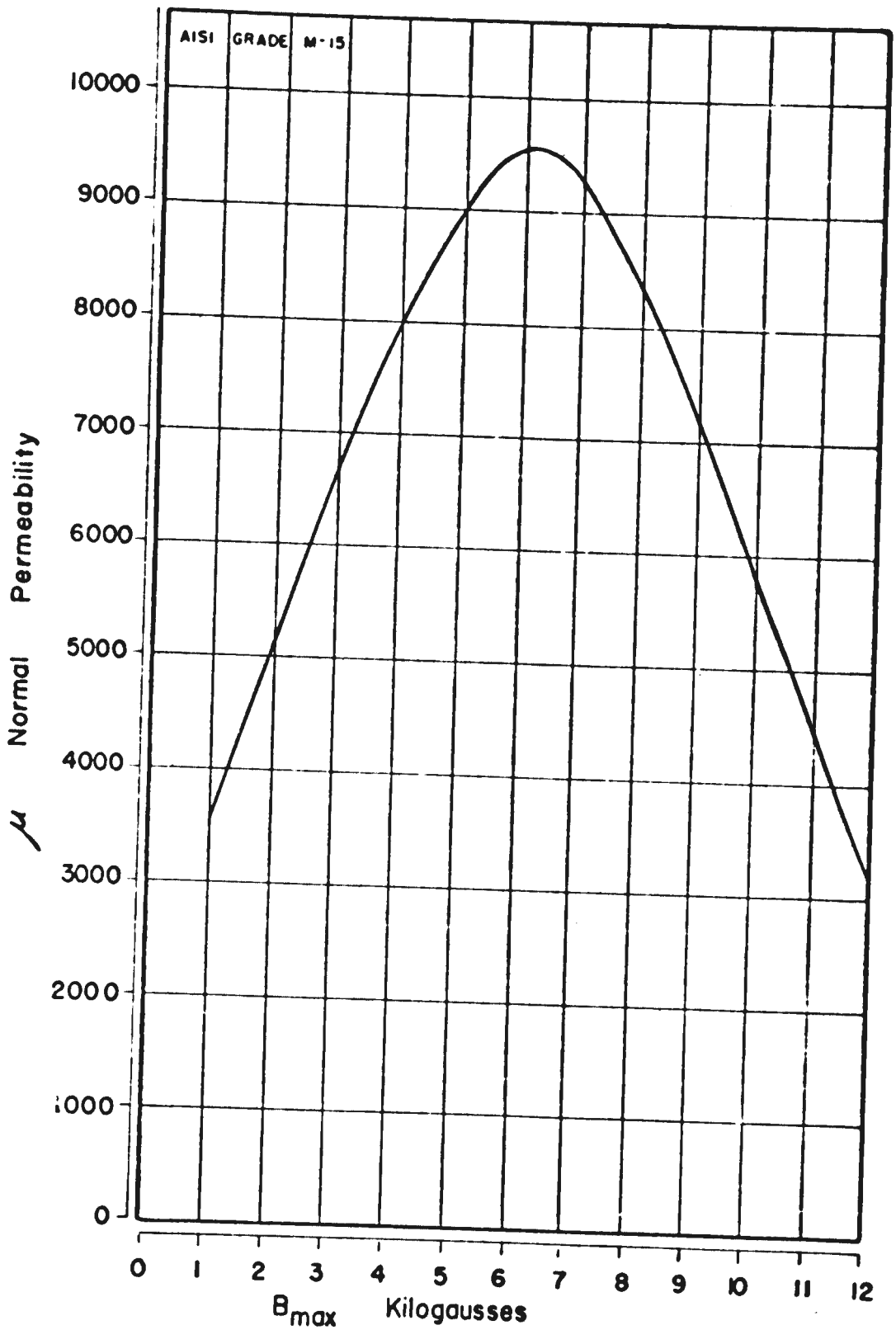


Fig. 14 Normal Permeability Curve

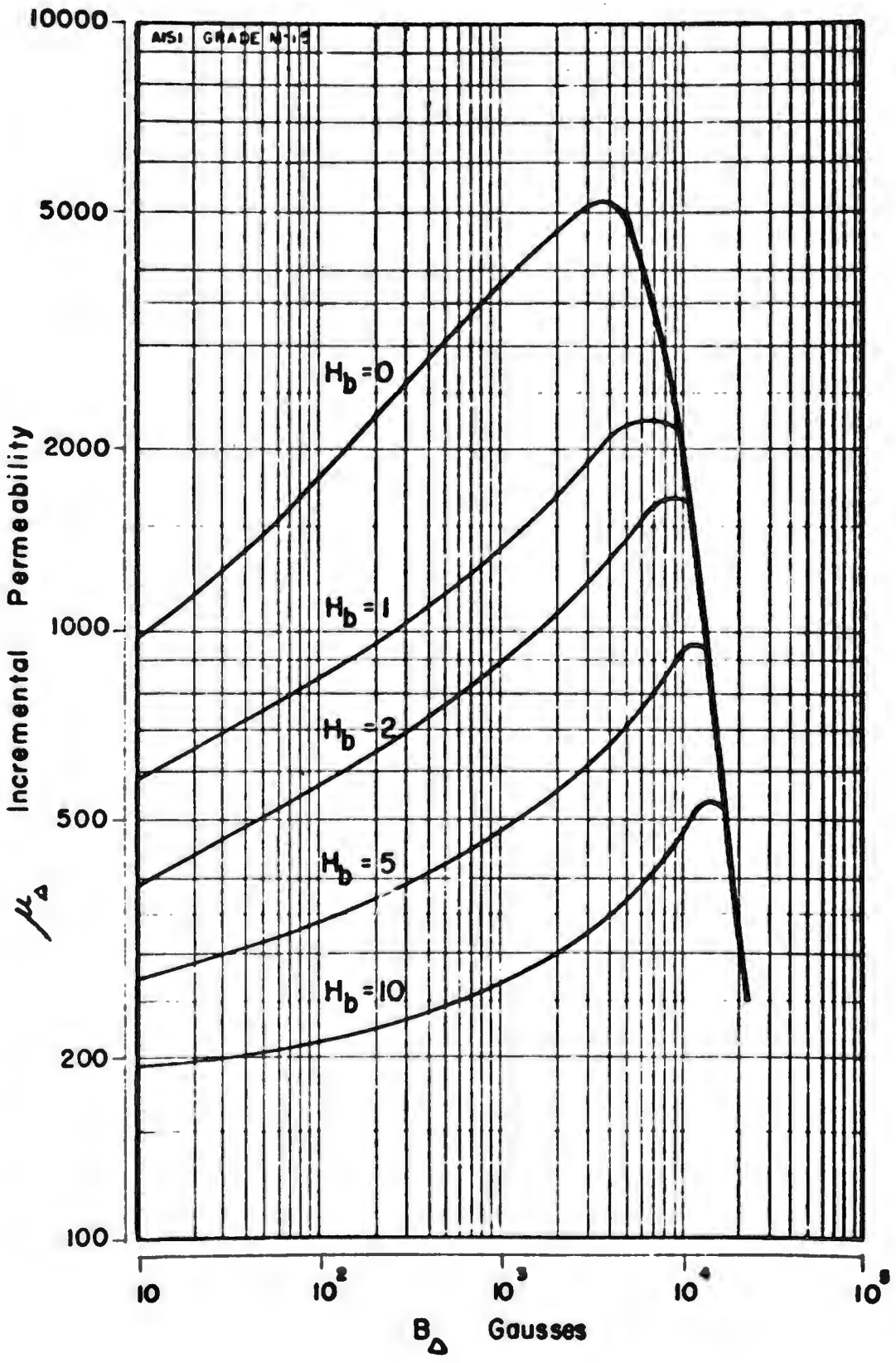


Fig. 15 Incremental Permeability Curves

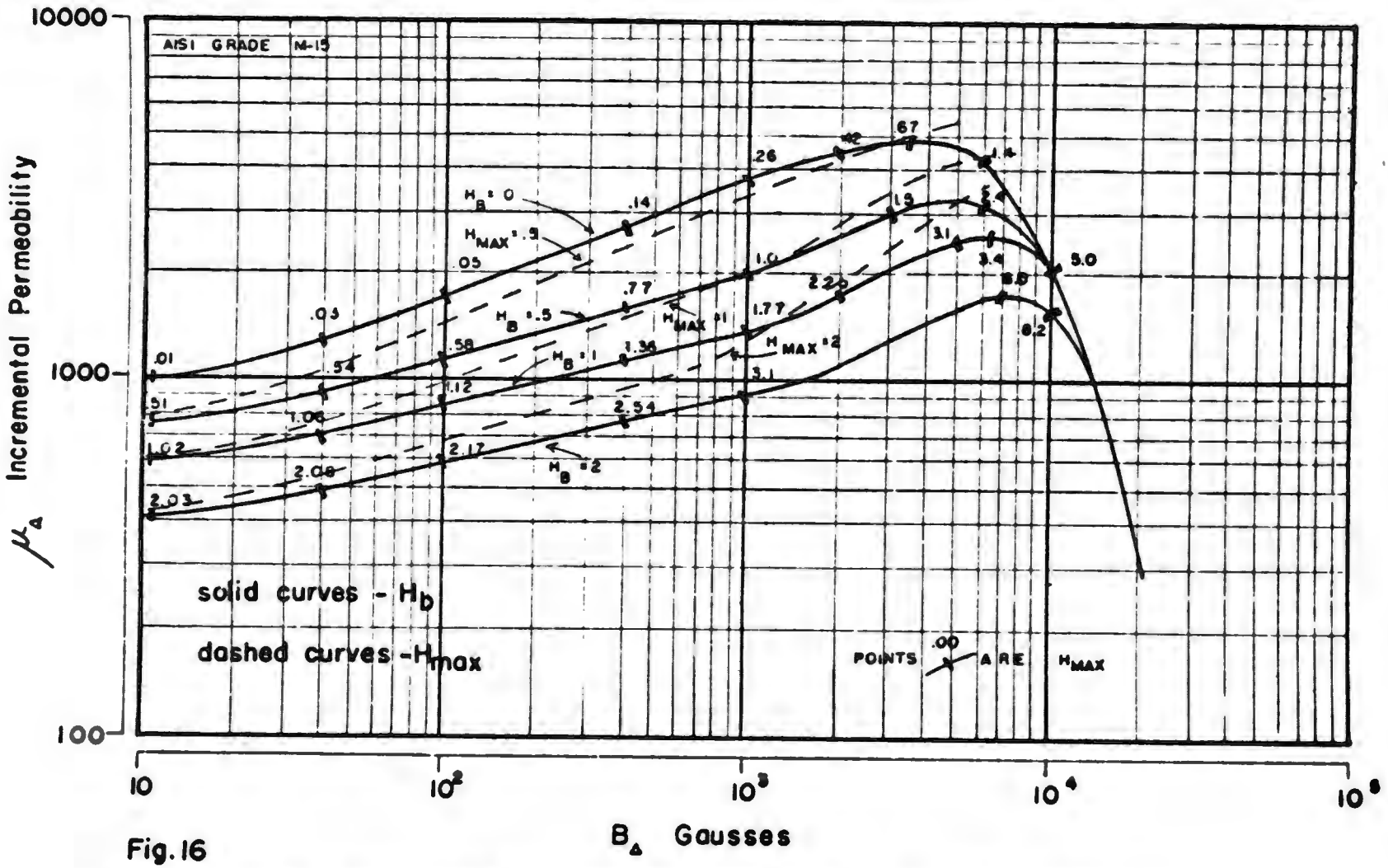


Fig. 16

Construction of incremental permeability curves with H_{max} as parameter.

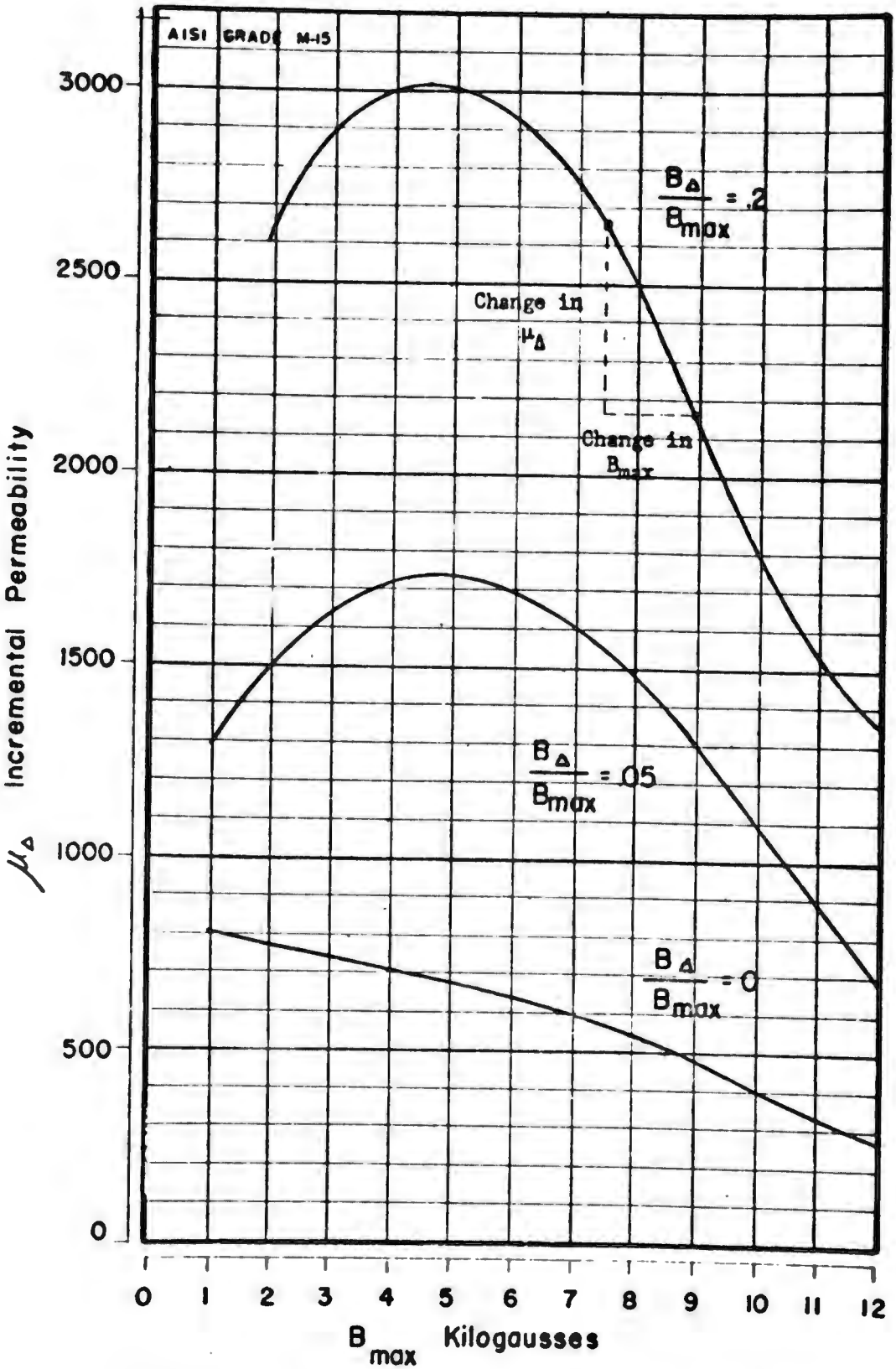


Fig.17 Incremental permeability vs B_{max} with B_Δ/B_{max} as parameter.

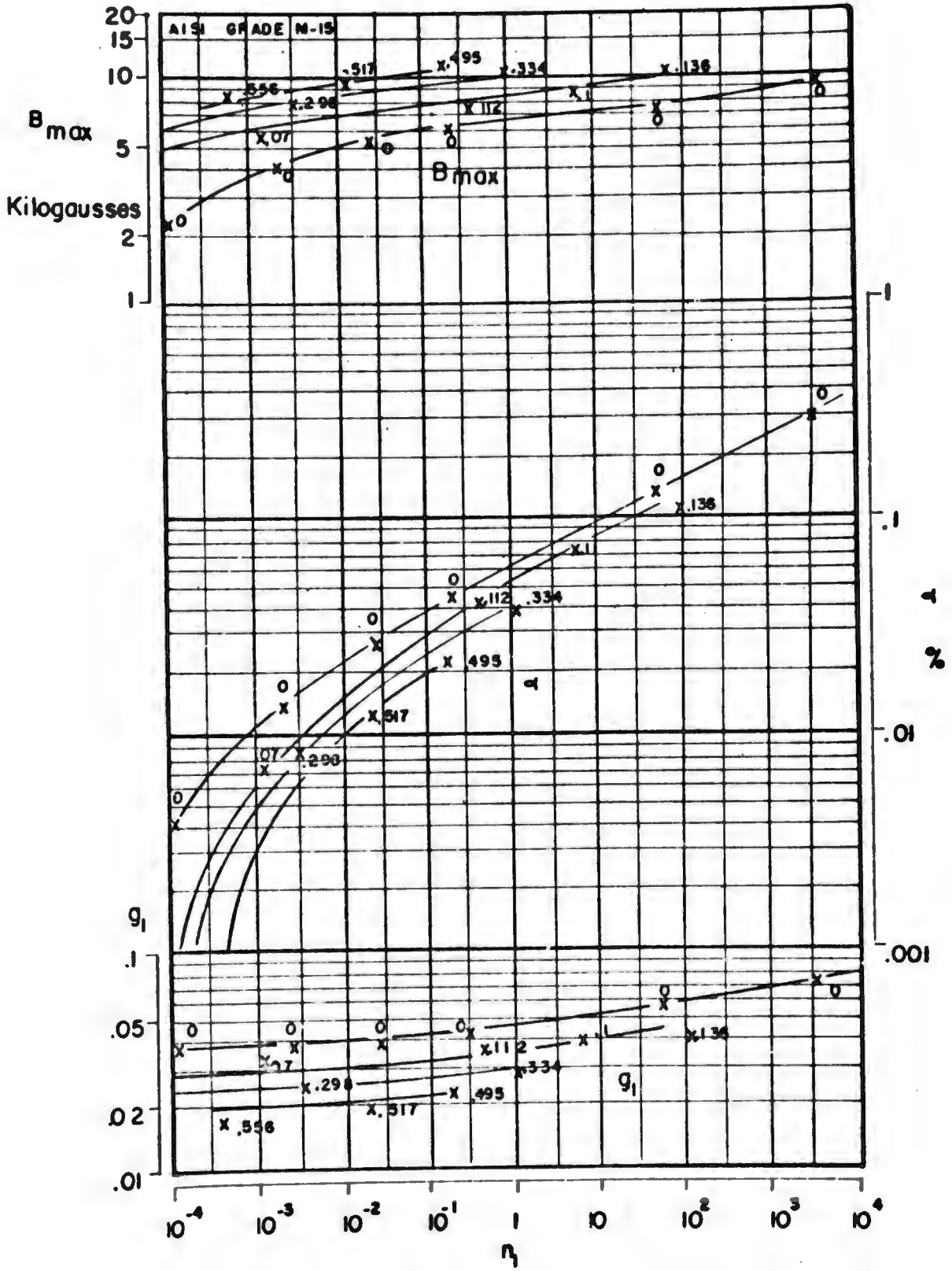


Fig. 18 Incomplete chart IA showing I_Δ/I_{max} points.

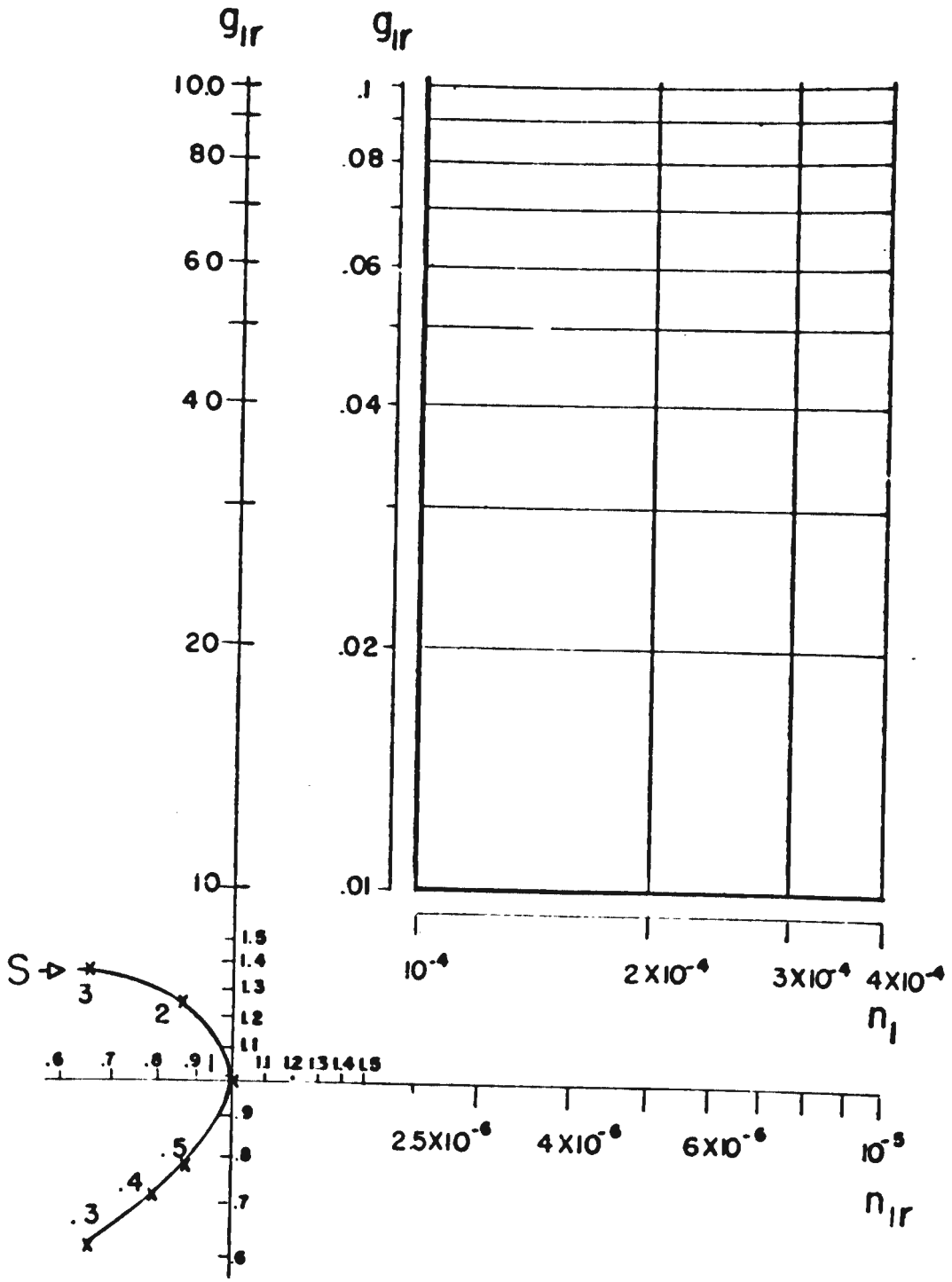


Fig. 19 Construction of g_{lr}, n_{lr}, and s axes.

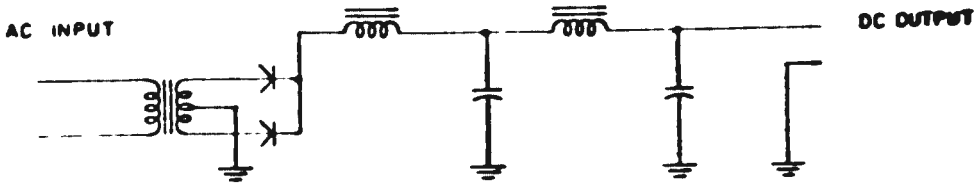


Fig. 20 Choke input filter

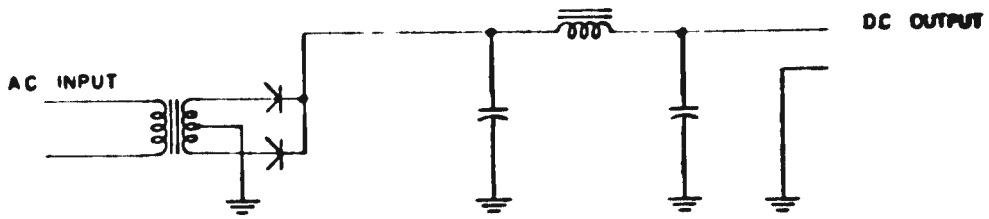


Fig. 21 Capacitor input filter

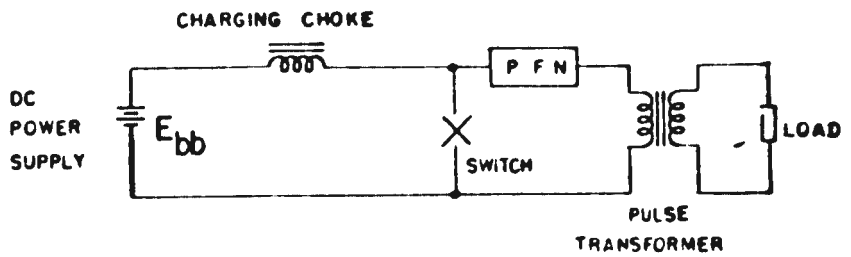


Fig. 22 Simplified pulser circuit

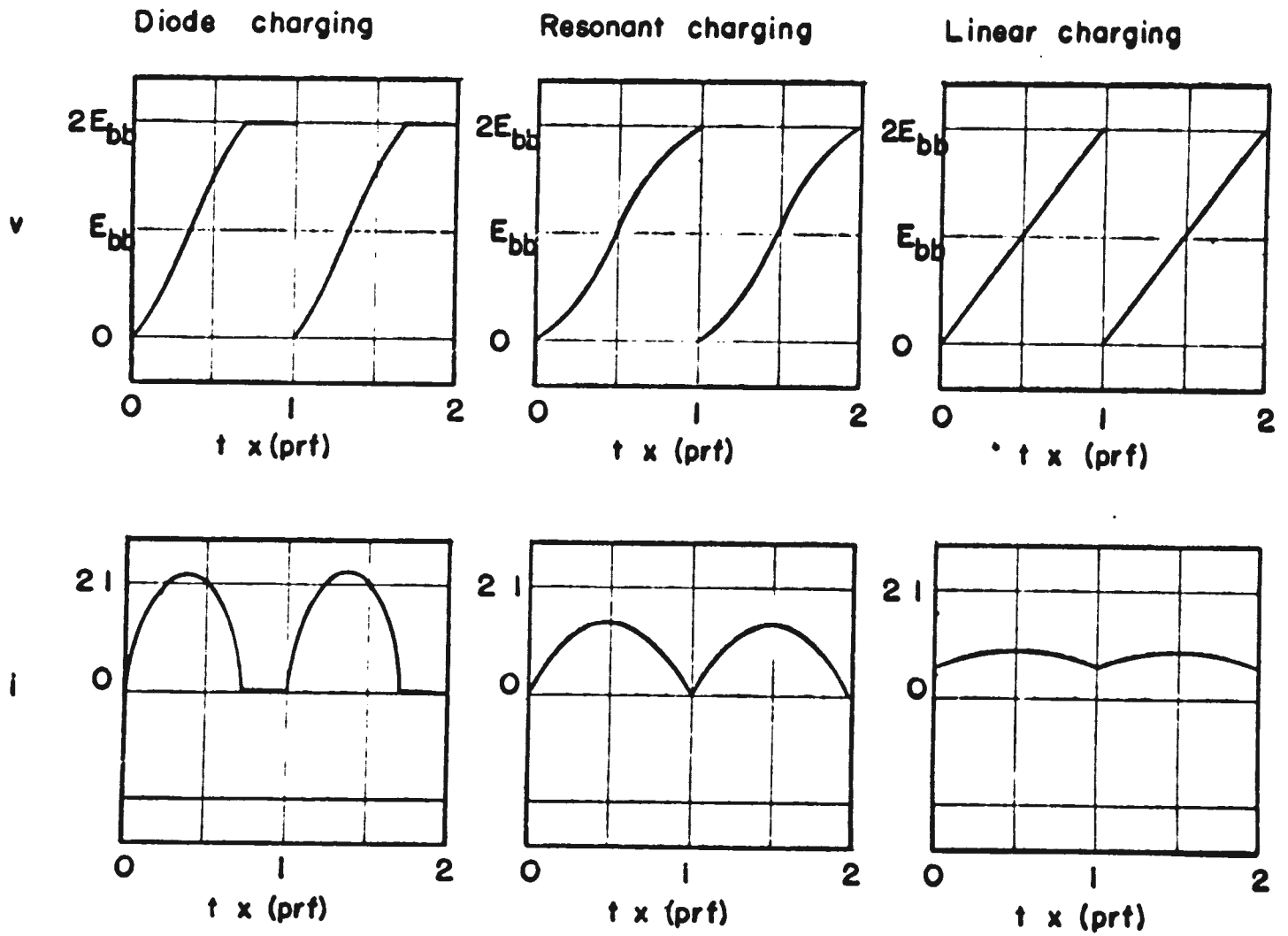


Fig. 23 Charging inductor waveforms for circuit of fig. 22.

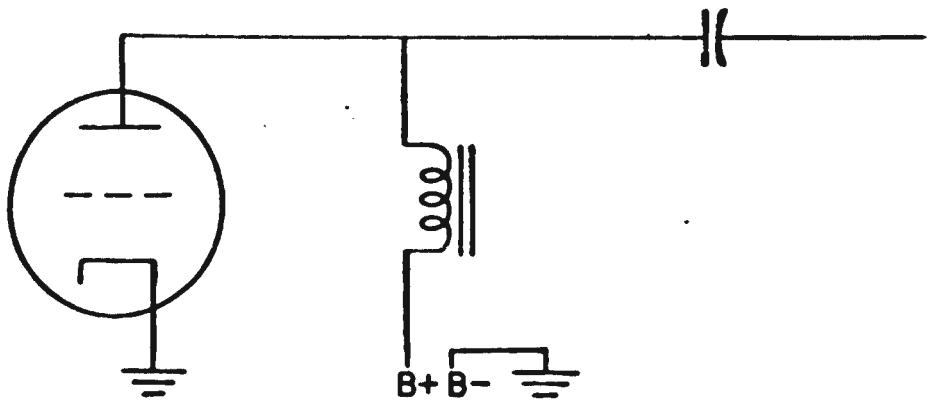


Fig. 24 Shunt fed amplifier

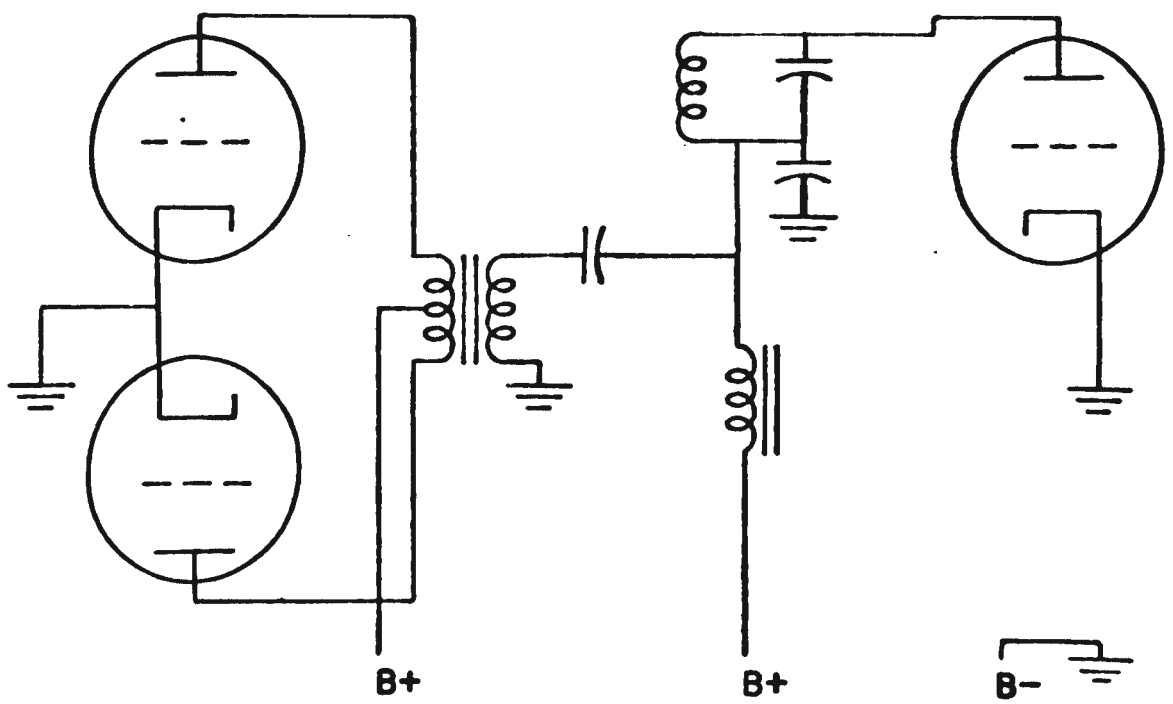


Fig. 25 Push-pull modulator

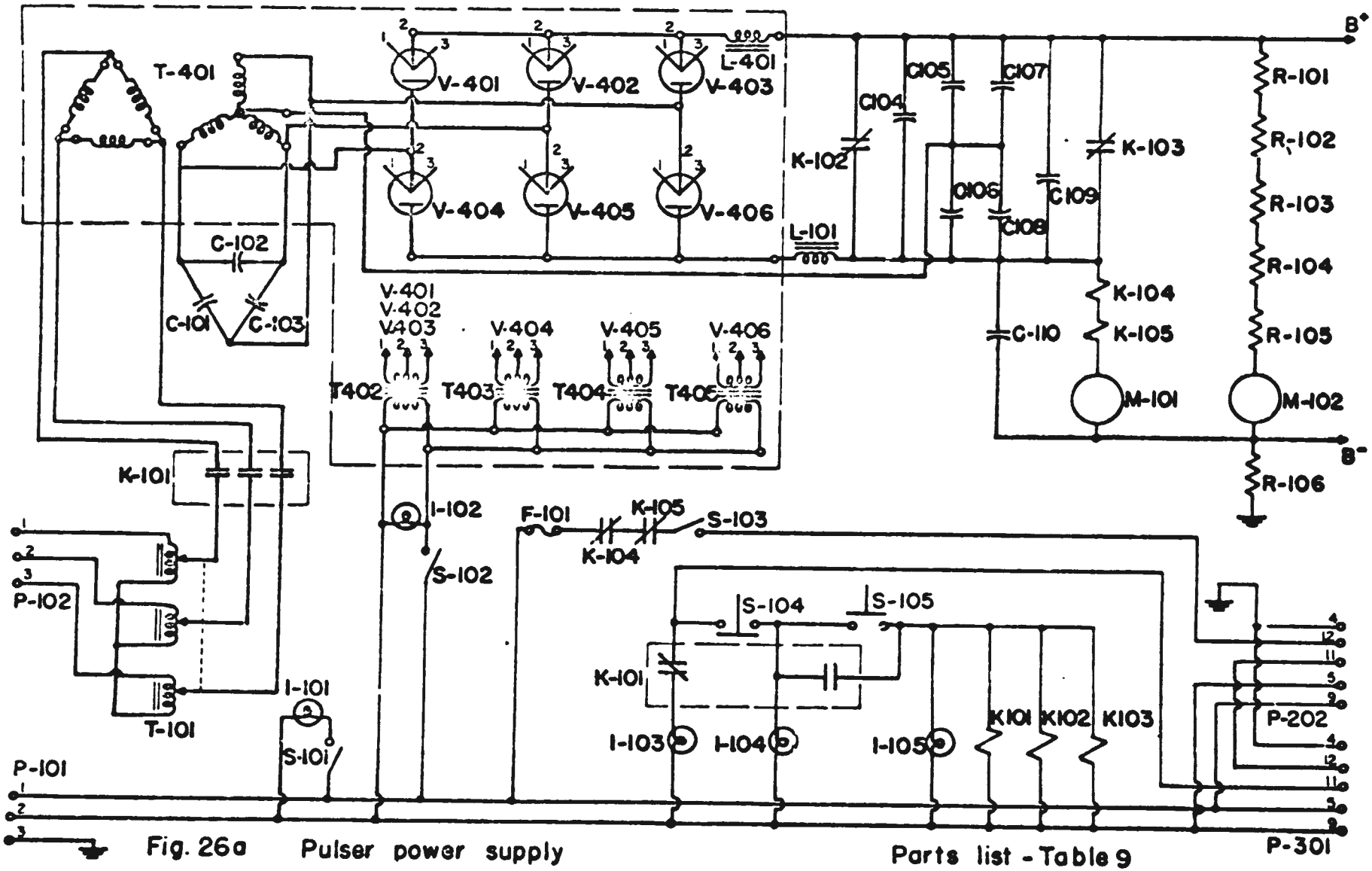


Fig. 26a Pulser power supply

Parts list - Table 9

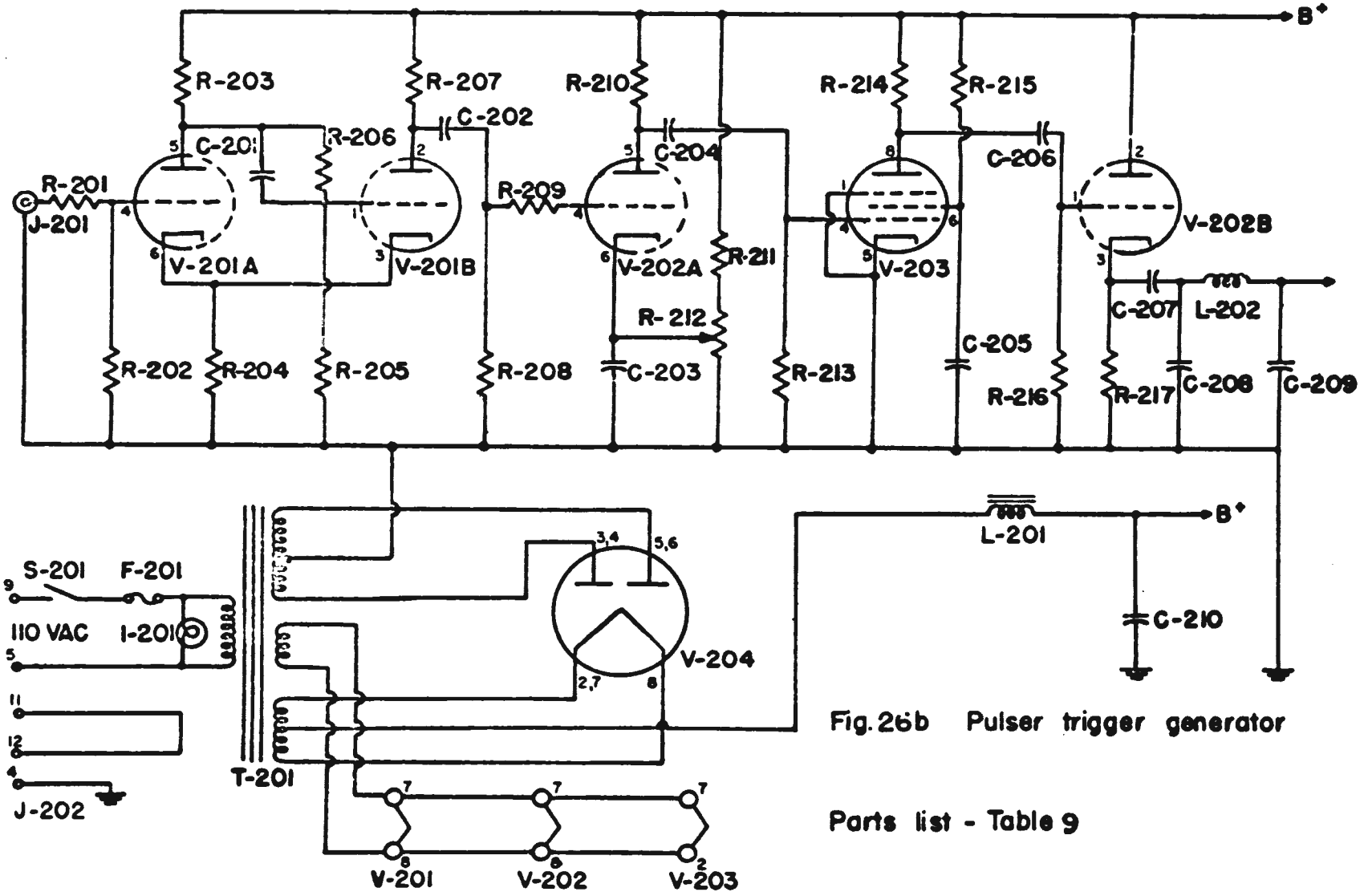


Fig. 26b Pulser trigger generator

Parts list - Table 9

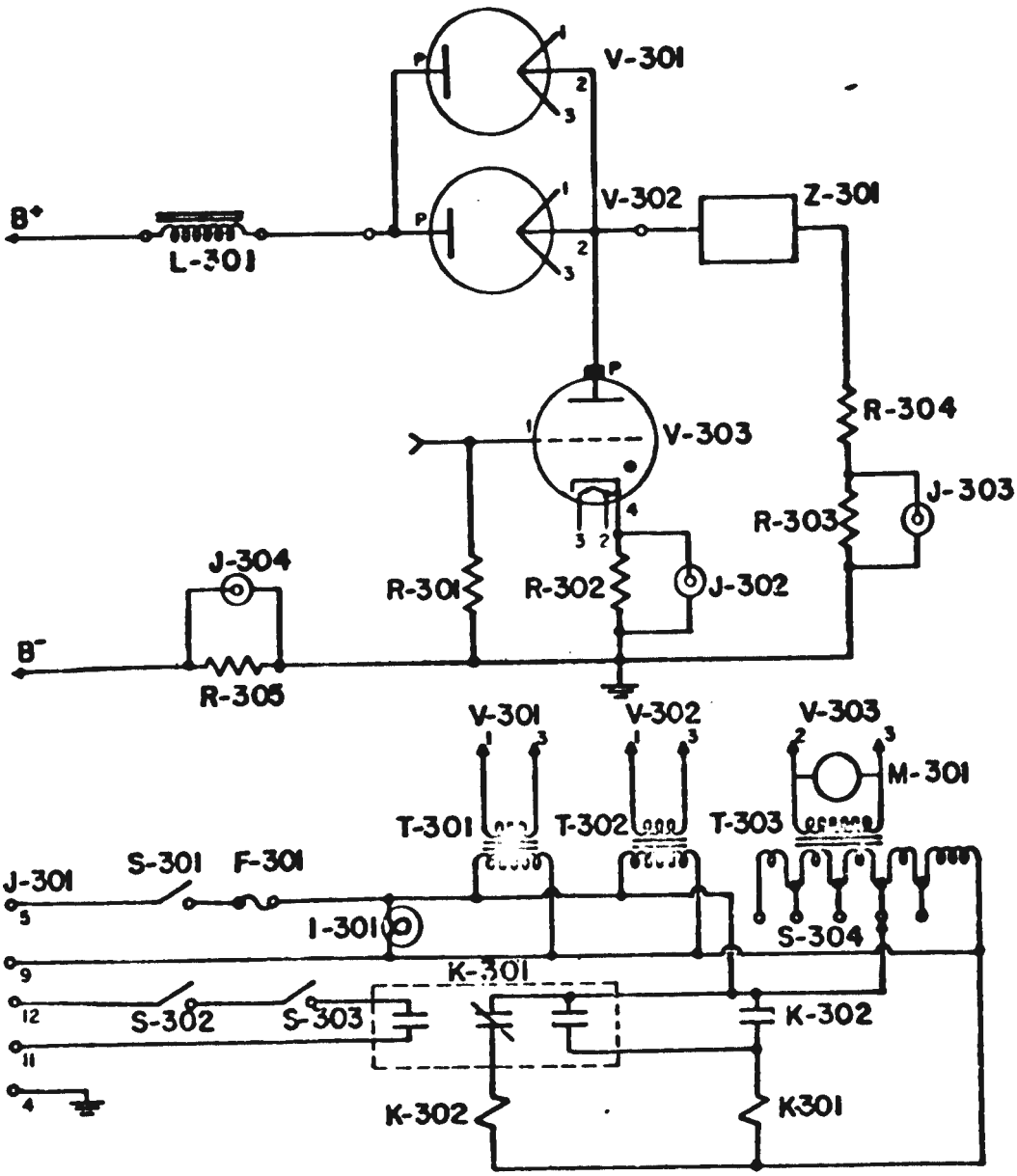
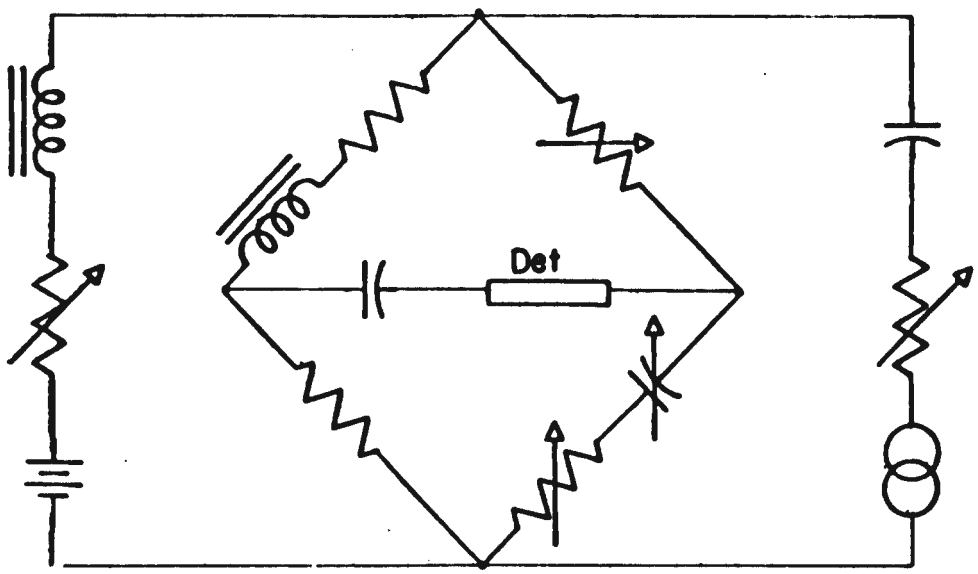


Fig. 26c Pulser

Parts list - Table 9



Det = Hewlett Packard harmonic wave analyzer model 300A

Fig. 27 Hay Bridge

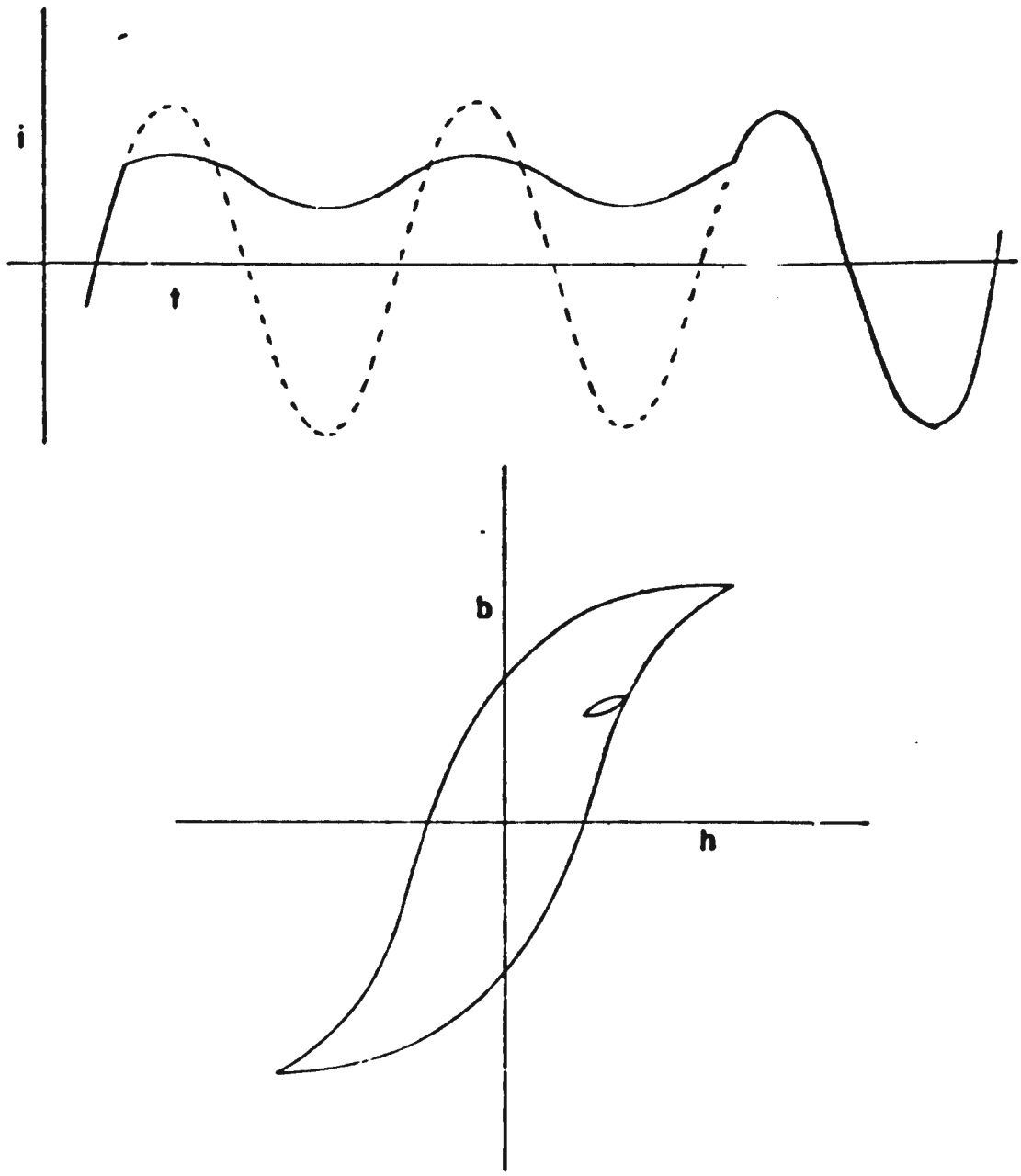
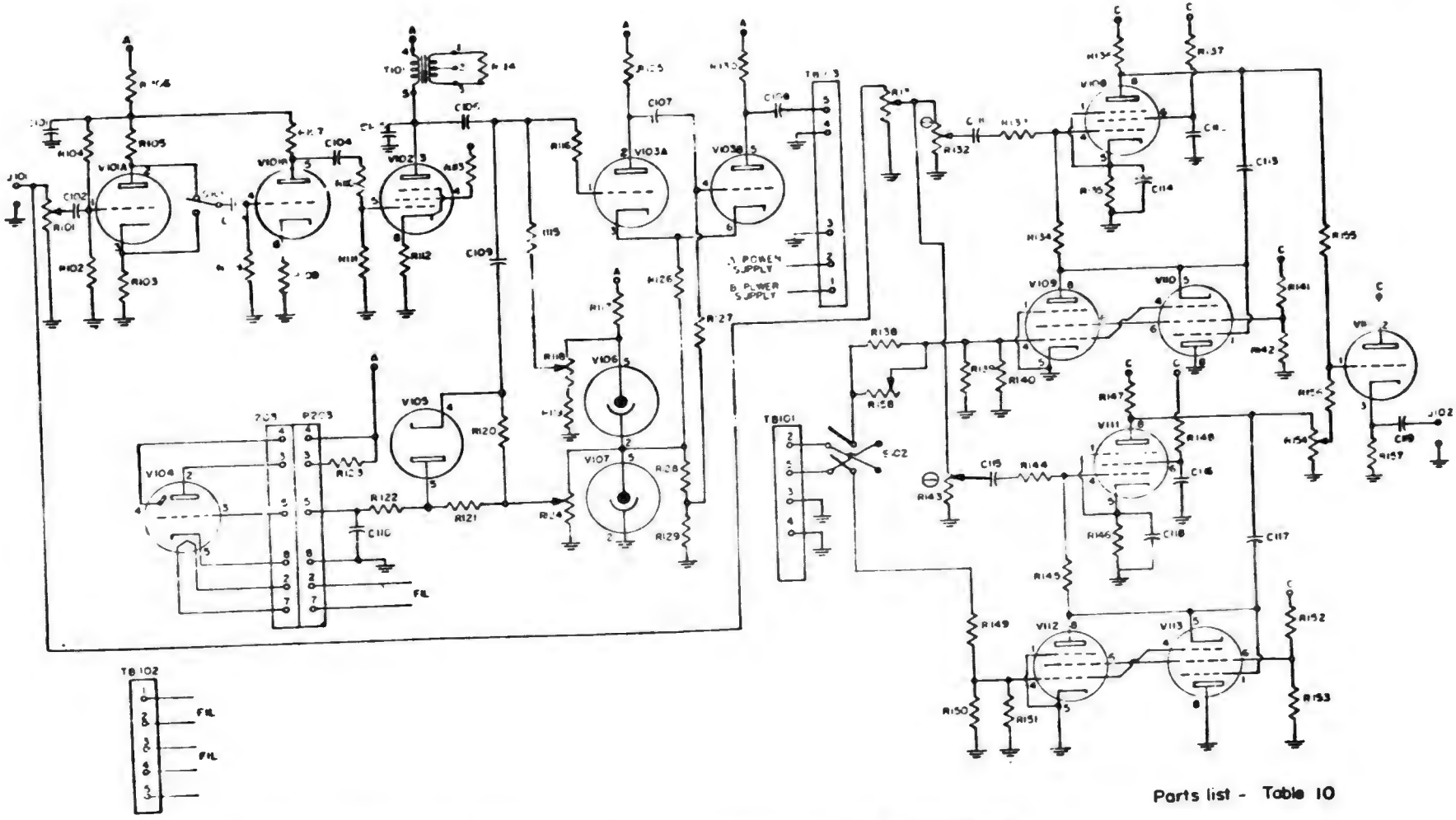


Fig. 28 Major minor wave form and loop.



Parts list - Table 10

Fig. 29a HIGH FREQUENCY B-H LOOPER, UPPER CHASSIS

REPRODUCED AT GOVERNMENT EXPENSE

REPRODUCED AT GOVERNMENT EXPENSE

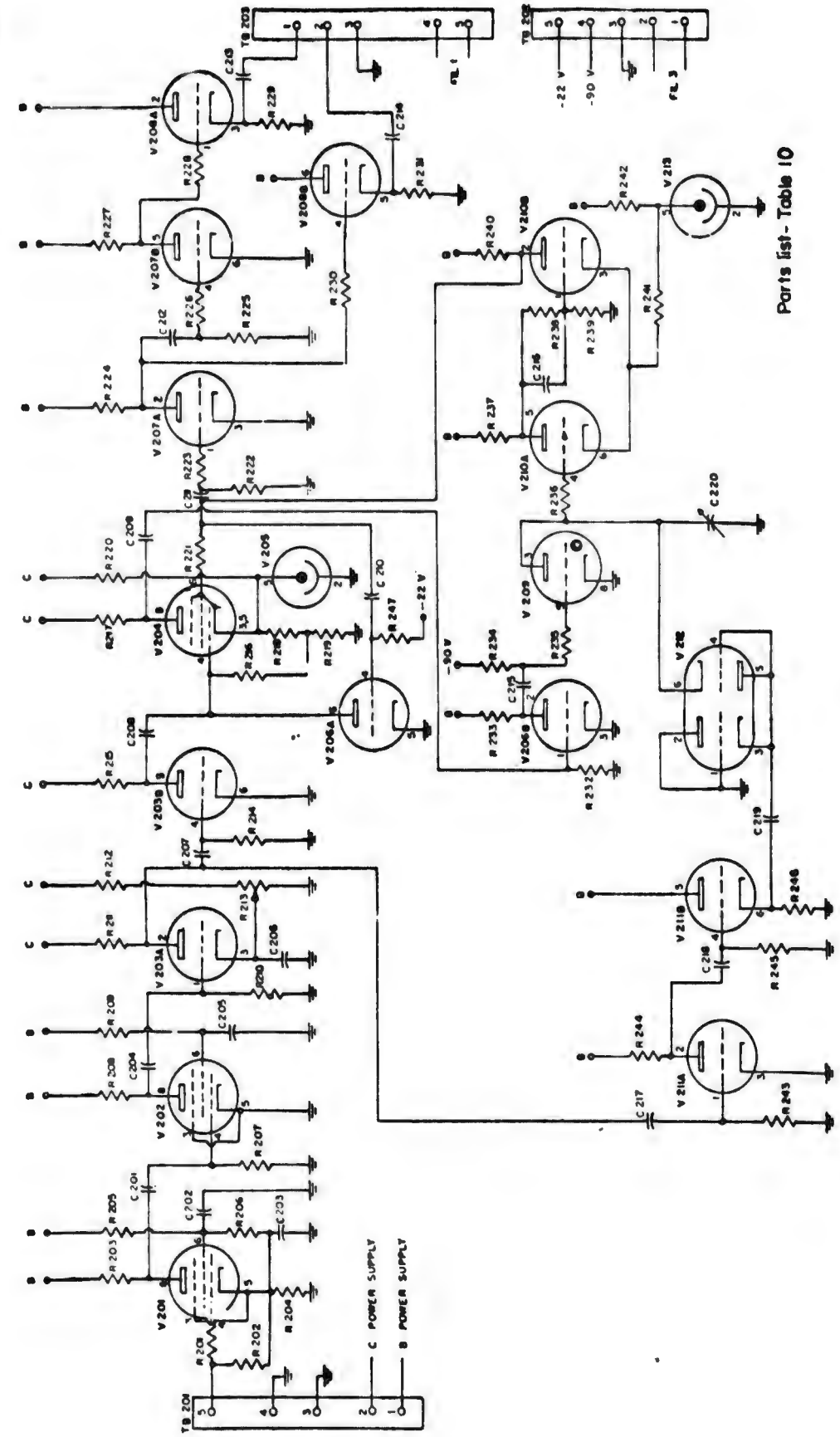


Fig. 29b HIGH FREQUENCY B-H LOOPER, LOWER CHASSIS

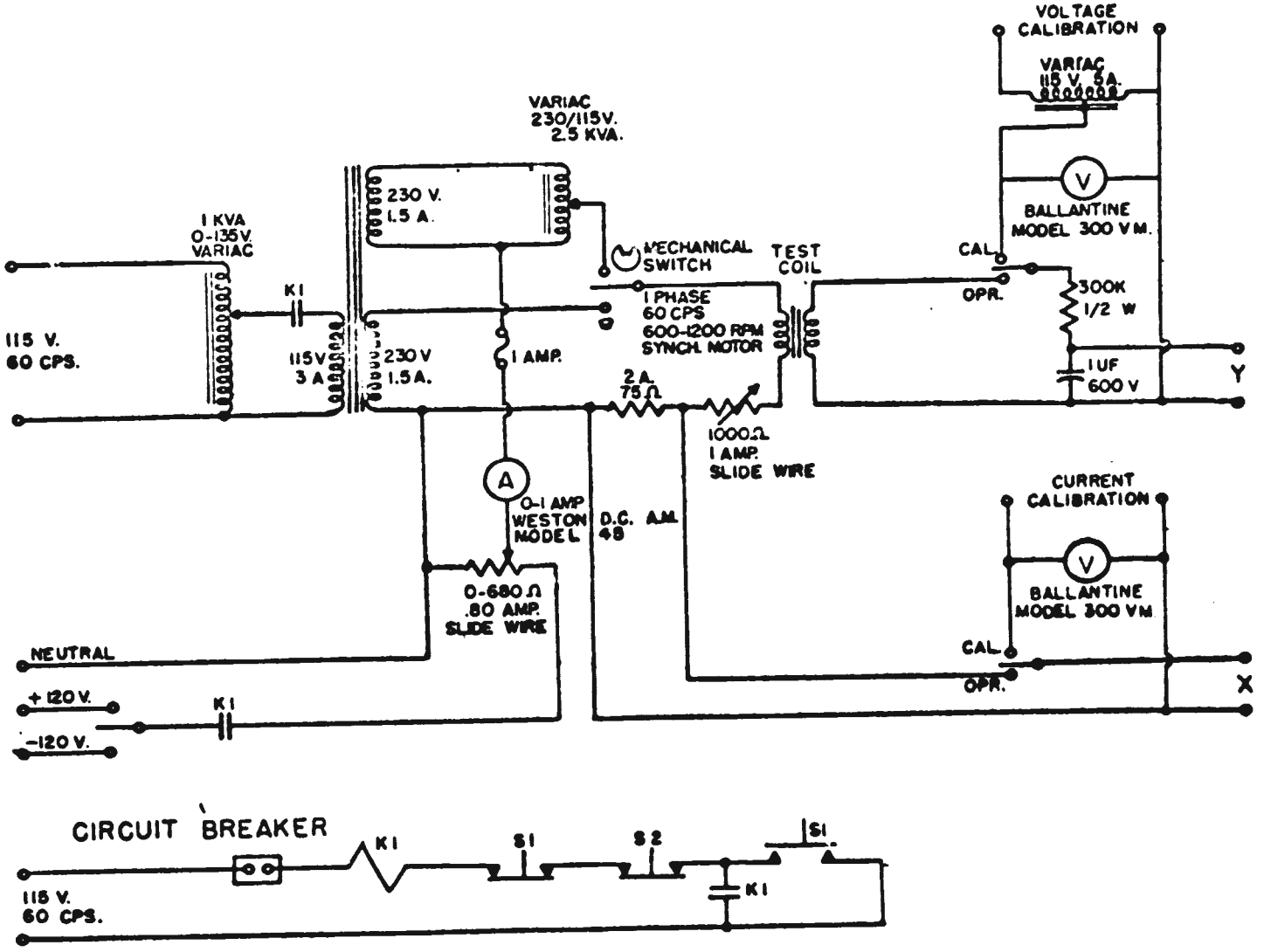
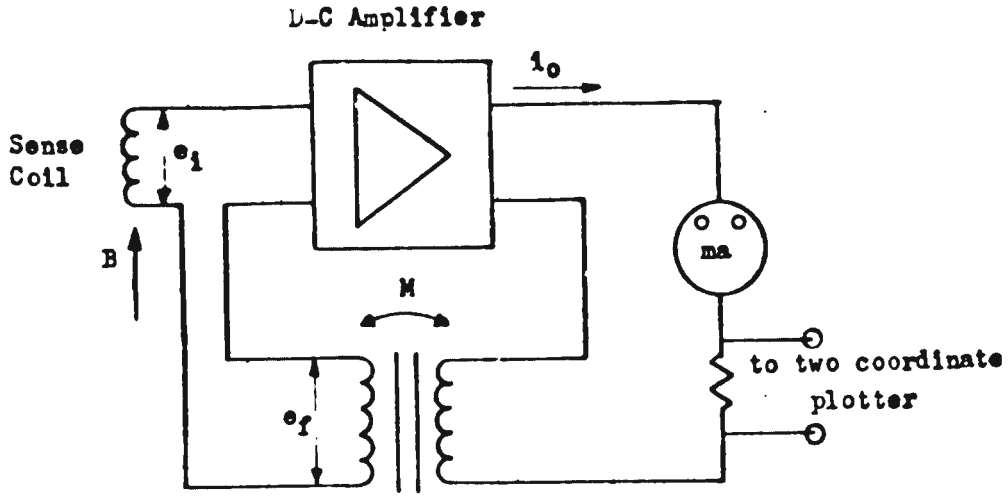


Fig. 30 MECHANICAL MAJOR–MINOR LOOP GENERATOR



$$e_i = K \frac{dB}{dt}$$

$$e_f = M \frac{di_o}{dt}$$

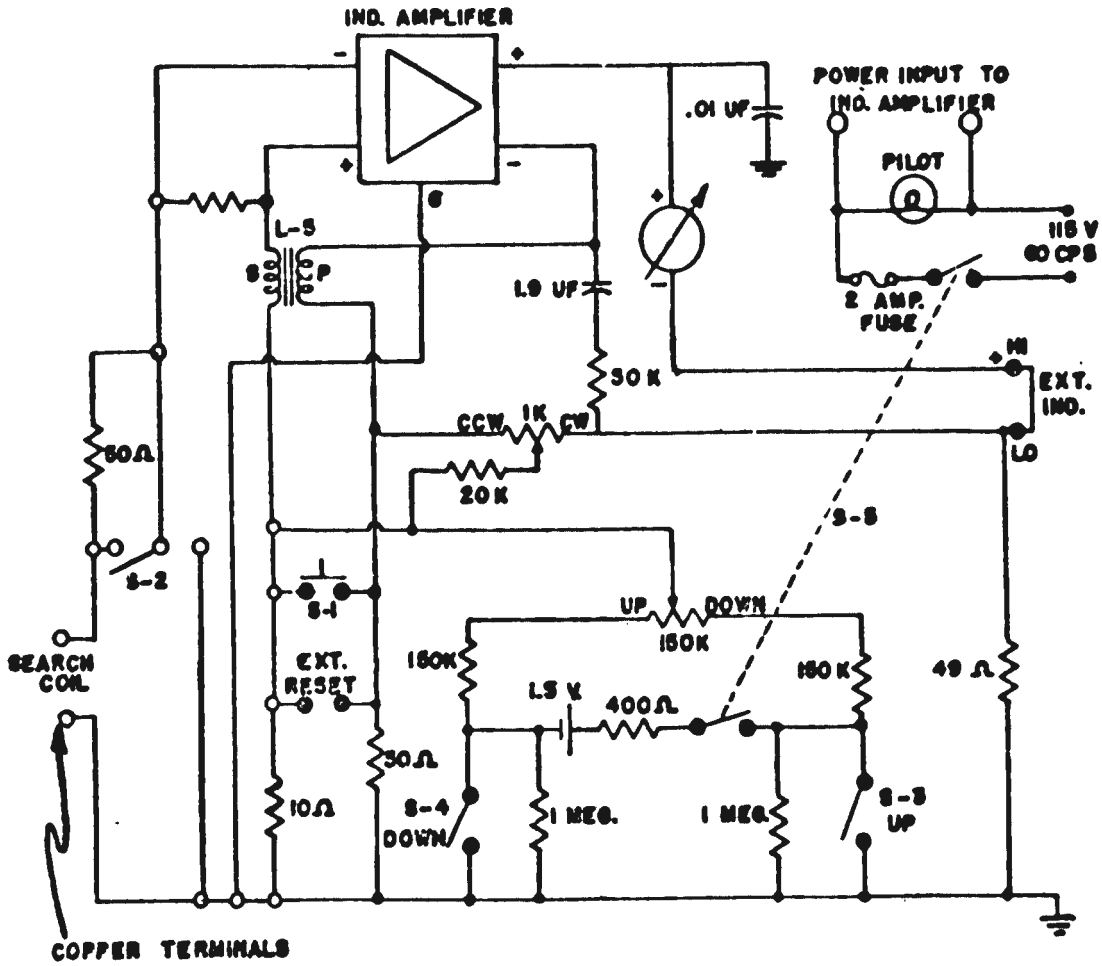
Since $e_f \cong e_i$

$$K \frac{dB}{dt} = M \frac{di_o}{dt}$$

$$\frac{K}{M} \frac{dB}{dt} = \frac{di_o}{dt}$$

$$\frac{K}{M} B + (\text{constant of integration}) = i_o$$

Fig. 31 Integrator.



NOTE. ALL JUNCTIONS INDICATED BY —o— ARE PRESSURE CONNECTIONS TO REDUCE THERMAL E.M.F.S.

FIG. 32 LOW FREQUENCY INTEGRATOR

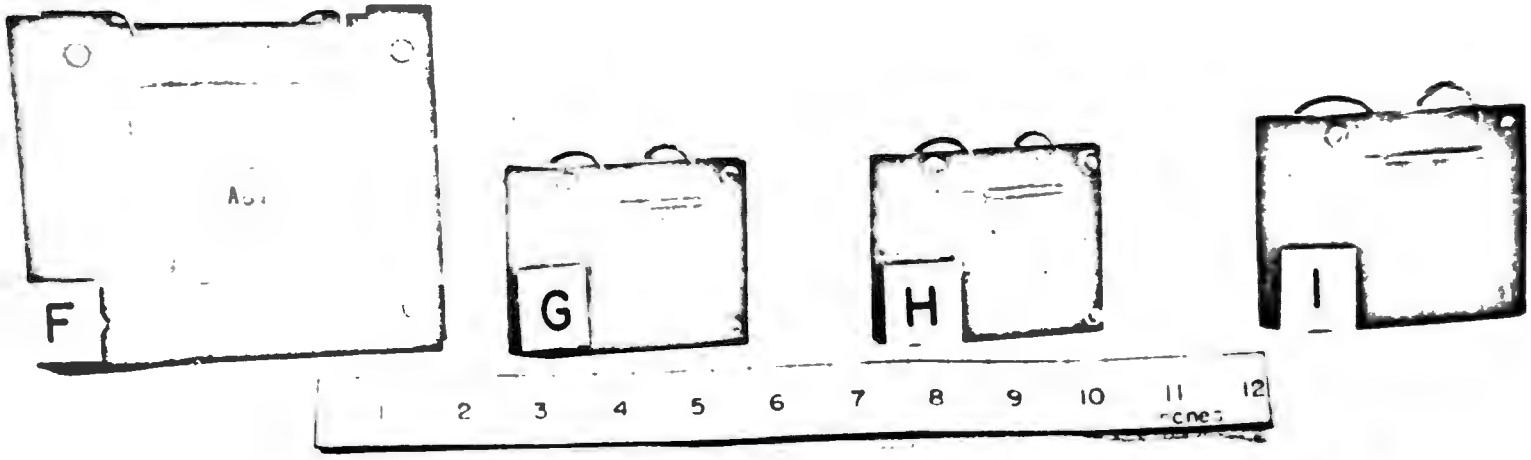
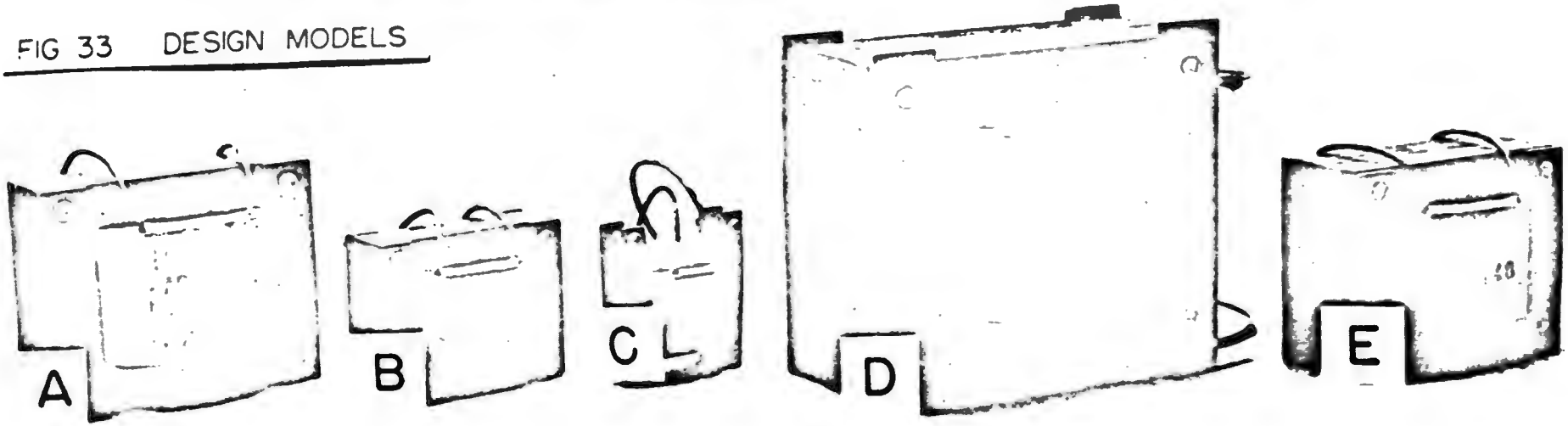


FIG 33 DESIGN MODELS



Simplified Procedure for Use of Curves

1. Calculate

$$n_1 = \frac{(.4\pi)^5 \nu^3 w I_{max}^4 R_c^3}{u^3 \rho^3 10^8 L} \qquad (4\text{-}32)$$

or

$$n_{1r} = \frac{I_{max}^4 R_c^3}{L} \qquad (4\text{-}44)$$

(only for low voltage scrapless EI construction)

2. Enter chart at this n_1 or n_{1r} point.

3. If the value of n_1 or n_{1r} is smaller than that at the left hand limit of the curves, use Chart 1B.

4. Read B_{max} and α from their respective curves for the required I_Δ/I_{max} ratio.

5. If B_{max} is too large, use Chart 1C.

6. Read g_1 (and g_{1r}) from the g_1 curve for the required I_Δ/I_{max} ratio.

7. Calculate δ_i from

$$\delta_i = g_1 \sqrt{\frac{u \rho 10^8 L}{.4\pi \nu w R_c}} \qquad (4\text{-}38)$$

or

$$\delta_i = g_{1r} \sqrt{\frac{L}{R_c}} \qquad (4\text{-}47)$$

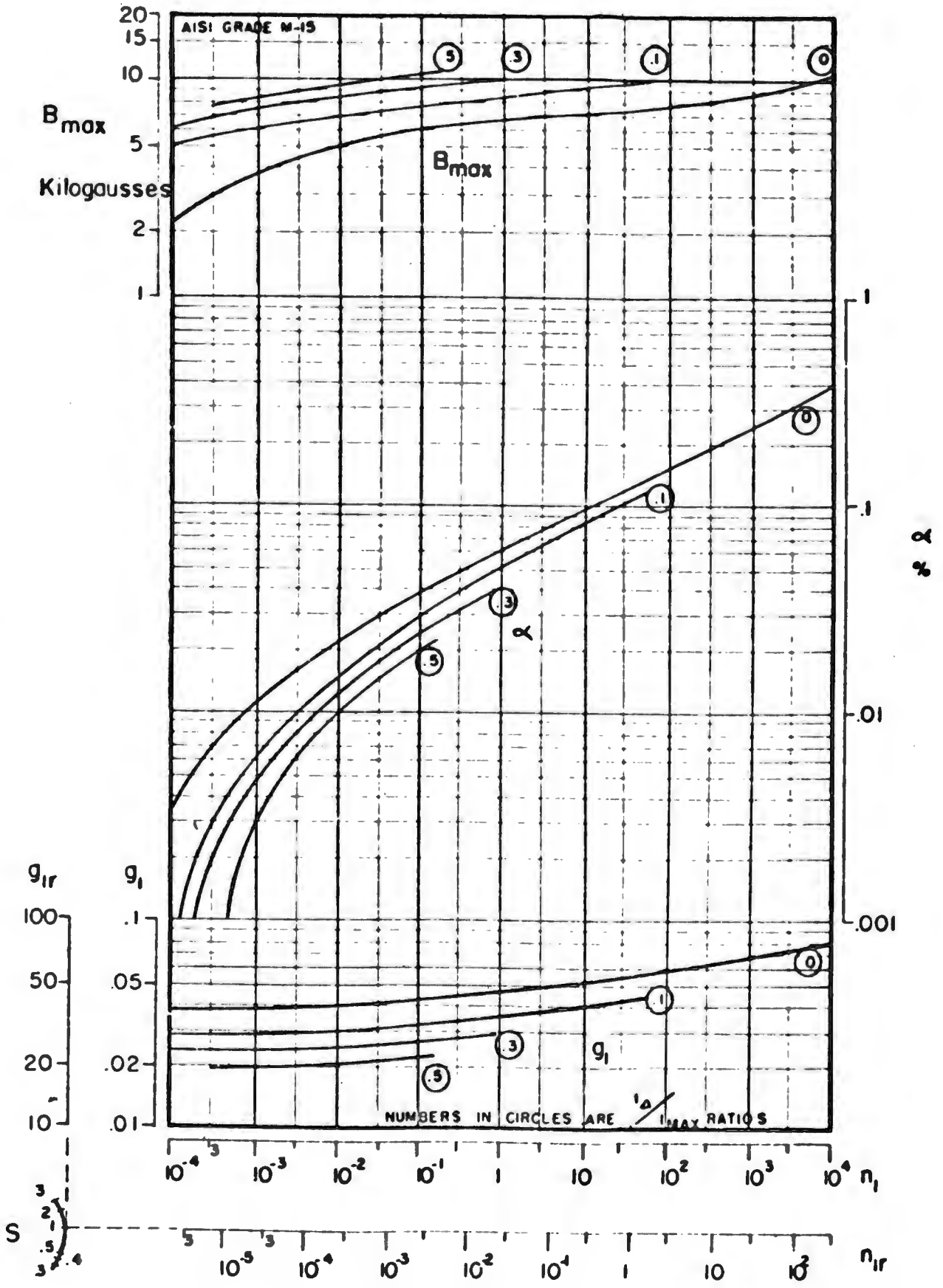
(only for low voltage scrapless EI construction)

8. If δ_i lies between standard laminations, see text.

9. Calculate N from

$$N = \sqrt{g_1 \sqrt{\frac{\nu 10^8}{.4\pi w \rho}} \sqrt{L R_c}} \qquad (4\text{-}41)$$

Chart 1A


AISI GRADE M-15
B_{max}
Kilogausses
20
15
10
5
2
1
.5
.3
.1
0
B_{max}
α
α %
1
.1
.01
.001
g_{ir}
g_i
100
50
20
10
.1
.05
.02
.01
g_i
NUMBERS IN CIRCLES ARE I_Δ / I_{MAX} RATIOS
10^{-4} 10^{-3} 10^{-2} 10^{-1} 1 10 10^2 10^3 10^4 n_i
S
3 2 1 .5 .4
10^{-5} 10^{-4} 10^{-3} 10^{-2} 10^{-1} 1 10 10^2 n_{ir}

Simplified Procedure for Use of Curves

1. Calculate

$$n_1 = \frac{(.4\pi)^5 \, v^3 \, w \, I_{max}^4 \, R_c^3}{u^3 \, \rho^3 \, 10^8 \, L} \qquad (4\text{-}32)$$

or

$$n_{1r} = \frac{I_{max}^4 \, R_c^3}{L} \qquad (4\text{-}44)$$

(only for low voltage scrapless EI construction)

2. Enter chart at this n_1 or n_{1r} point.

3. Read B_{max} from the B_{max} curve having the required I_Δ / I_{max} ratio.

4. Read g_1 (and g_{1r}) from the g_1 curve having the required I_Δ / I_{max} ratio.

5. Calculate δ_i from

$$\delta_i = g_1 \sqrt{\frac{u \, \rho \, 10^8 \, L}{.4\pi \, v \, w \, R_c}} \qquad (4\text{-}38)$$

or

$$\delta_i = g_{1r} \sqrt{\frac{L}{R_c}} \qquad (4\text{-}47)$$

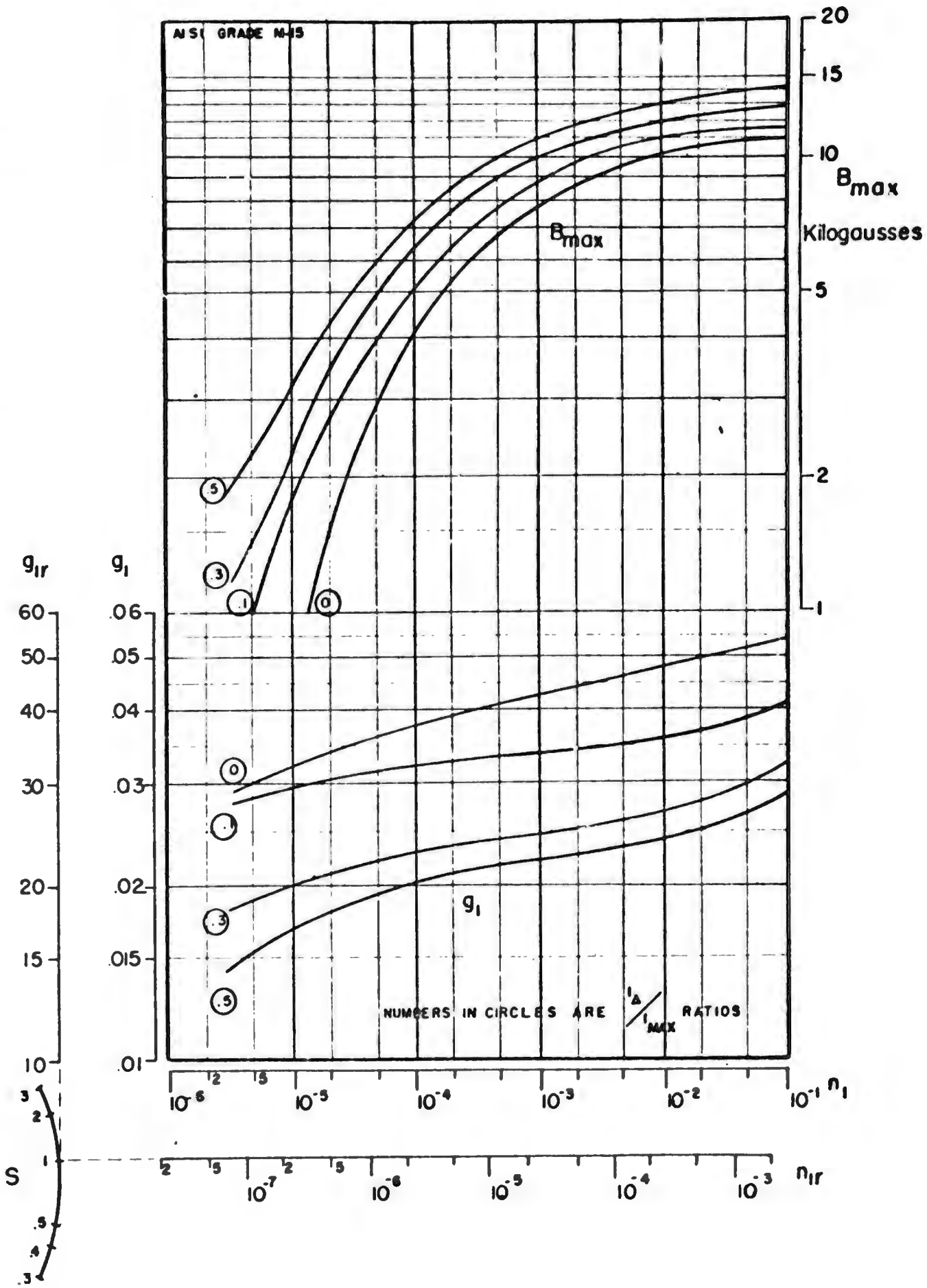
(only for low voltage scrapless EI construction)

6. If δ_i lies between standard laminations, see text.

7. Calculate N from

$$N = \sqrt{g_1 \sqrt{\frac{v \, 10^8}{.4\pi \, u \, w \, \rho}} \sqrt{L R_c}} \qquad (4\text{-}41)$$

Chart 1B ($\alpha = 0$)



Simplified Procedure for Use of Curves

1. Calculate

$$n_1 = \frac{(.4\pi)^5 v^3 w I_{max}^4 R_c^3}{u^3 \rho^3 10^8 L} \qquad (4\text{-}32)$$

or

$$n_{1r} = \frac{I_{max}^4 R_c^3}{L} \qquad (4\text{-}44)$$

(only for low voltage scrapless EI construction)

2. Enter chart at this n_1 or n_{1r} point.

3. Read α from the α curve having the proper I_Δ/I_{max} ratio.

4. Read g_1 (and g_{1r}) from the g_1 curve having the proper I_Δ/I_{max} ratio.

5. Calculate ℓ_i from

$$\ell_i = g_1 \sqrt{\frac{u \rho 10^8 L}{.4\pi v w R_c}} \qquad (4\text{-}38)$$

or

$$\ell_i = g_{1r} \sqrt{\frac{L}{R_c}} \qquad (4\text{-}47)$$

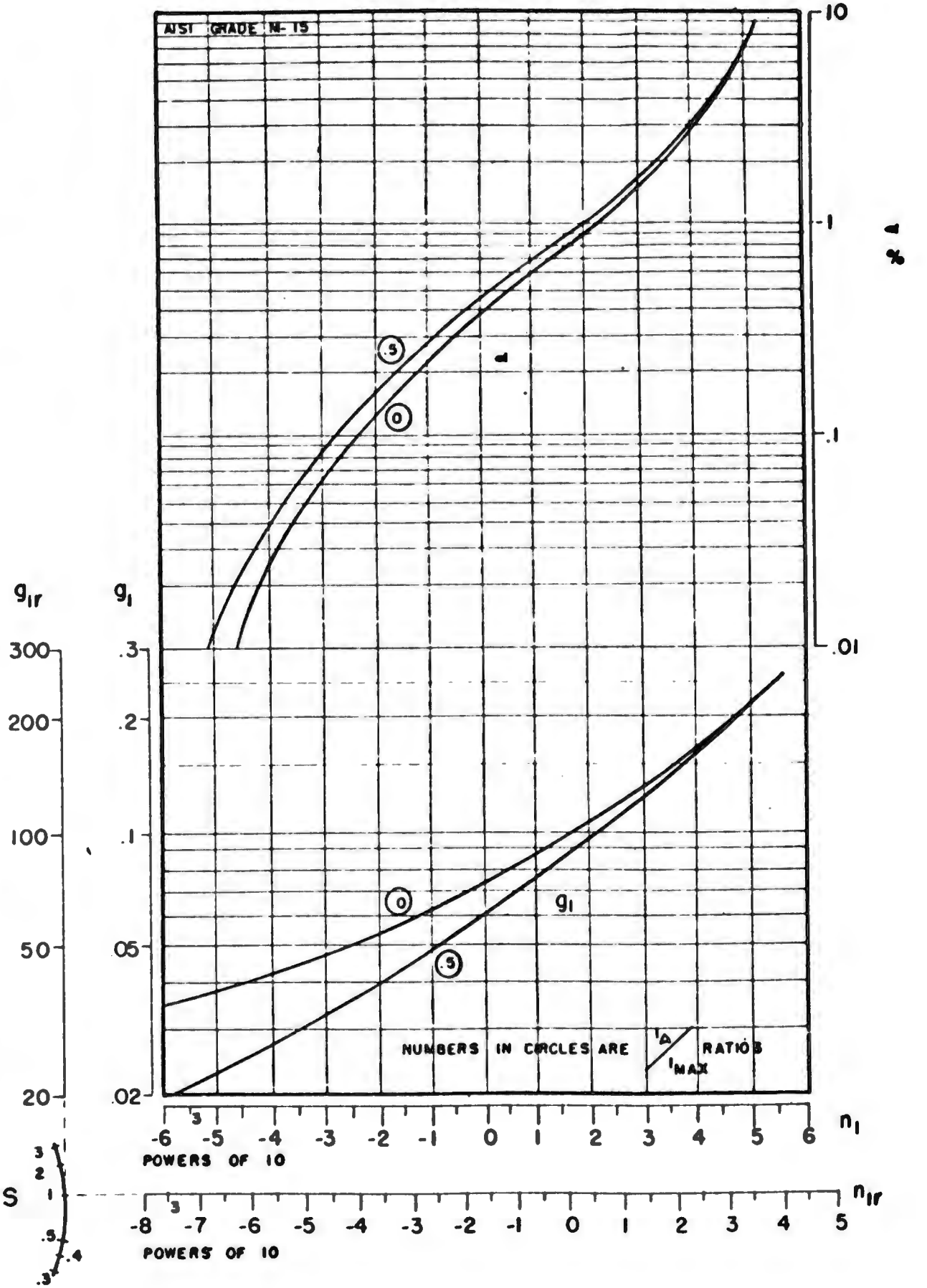
(only for low voltage scrapless EI construction)

6. If ℓ_i lies between standard laminations, see text.

7. Calculate N from

$$N = \sqrt{g_1 \sqrt{\frac{v 10^8}{.4\pi u w \rho}} \sqrt{2R_c}} \qquad (4\text{-}41)$$

Chart IC (B_{max} = 1 Kilogauss)



Simplified Procedure for Use of Curves

1. Calculate

$$n_1 = \frac{(.4\pi)^5 v^3 w I_{max}^4 R_c^3}{u^3 \rho^3 10^8 L} \qquad (4\text{-}32)$$

or

$$n_{1r} = \frac{I_{max}^4 R_c^3}{L} \qquad (4\text{-}44)$$

(only for low voltage scrapless EI construction)

2. Enter chart at this n_1 or n_{1r} point.

3. Read α from the α curve having the proper I_Δ / I_{max} ratio.

4. Read g_1 (and g_{1r}) from the g_1 curve having the propor I_Δ / I_{max} ratio.

5. Calculate δ_1 from

$$\delta_1 = g_1 \sqrt{\frac{u\rho\, 10^8 L}{.4\pi\, v\, w\, R_c}} \qquad (4\text{-}38)$$

or

$$\delta_1 = g_{1r} \sqrt{\frac{L}{R_c}} \qquad (4\text{-}47)$$

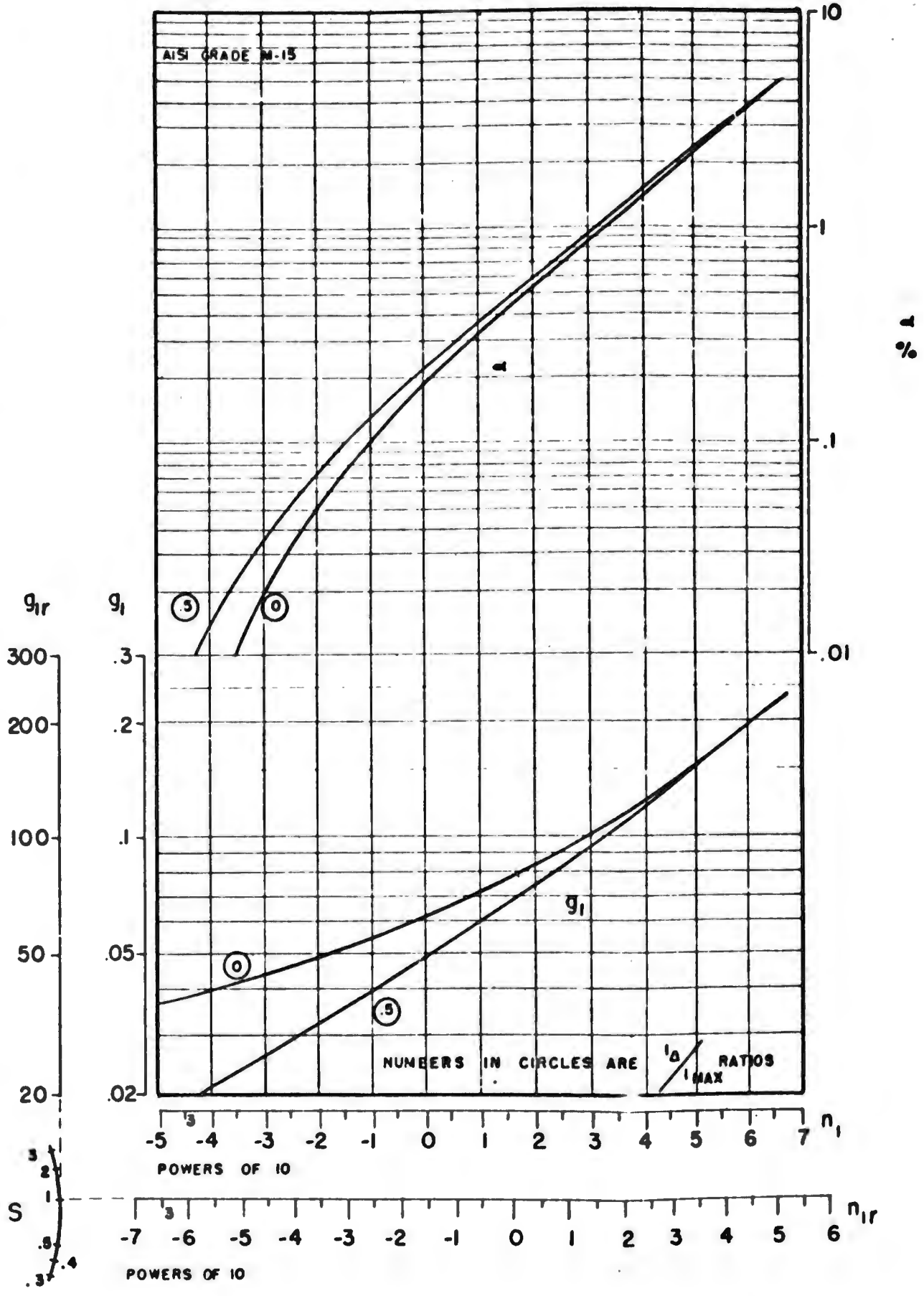
(only for low voltage scrapless EI construction)

6. If δ_1 lies between standard laminations, see text.

7. Calculate N from

$$N = \sqrt{g_1 \sqrt{\frac{v\, 10^8}{.4\pi\, u\, w\, \rho}} \sqrt{L R_c}} \qquad (4\text{-}41)$$

Chart IC (B_{max} = 2 Kilogausses)



Simplified Procedure for Use of Curves

1. Calculate

$$n_1 = \frac{(.4\pi)^5 \, v^3 \, w \, I_{max}^4 \, R_c^3}{u^3 \, \rho^3 \, 10^8 \, L} \qquad (4\text{-}32)$$

or

$$n_{1r} = \frac{I_{max}^4 \, R_c^3}{L} \qquad (4\text{-}44)$$

(only for low voltage scrapless EI construction)

2. Enter chart at this n_1 or n_{1r} point.

3. Read α from the α curve having the proper I_Δ / I_{max} ratio.

4. Read g_1 (and g_{1r}) from the g_1 curve having the proper I_Δ / I_{max} ratio.

5. Calculate δ_1 from

$$\delta_1 = g_1 \sqrt{\frac{u \, \rho \, 10^8 \, L}{.4\pi \, v \, w \, R_c}} \qquad (4\text{-}38)$$

or

$$\delta_1 = g_{1r} \sqrt{\frac{L}{R_c}} \qquad (4\text{-}47)$$

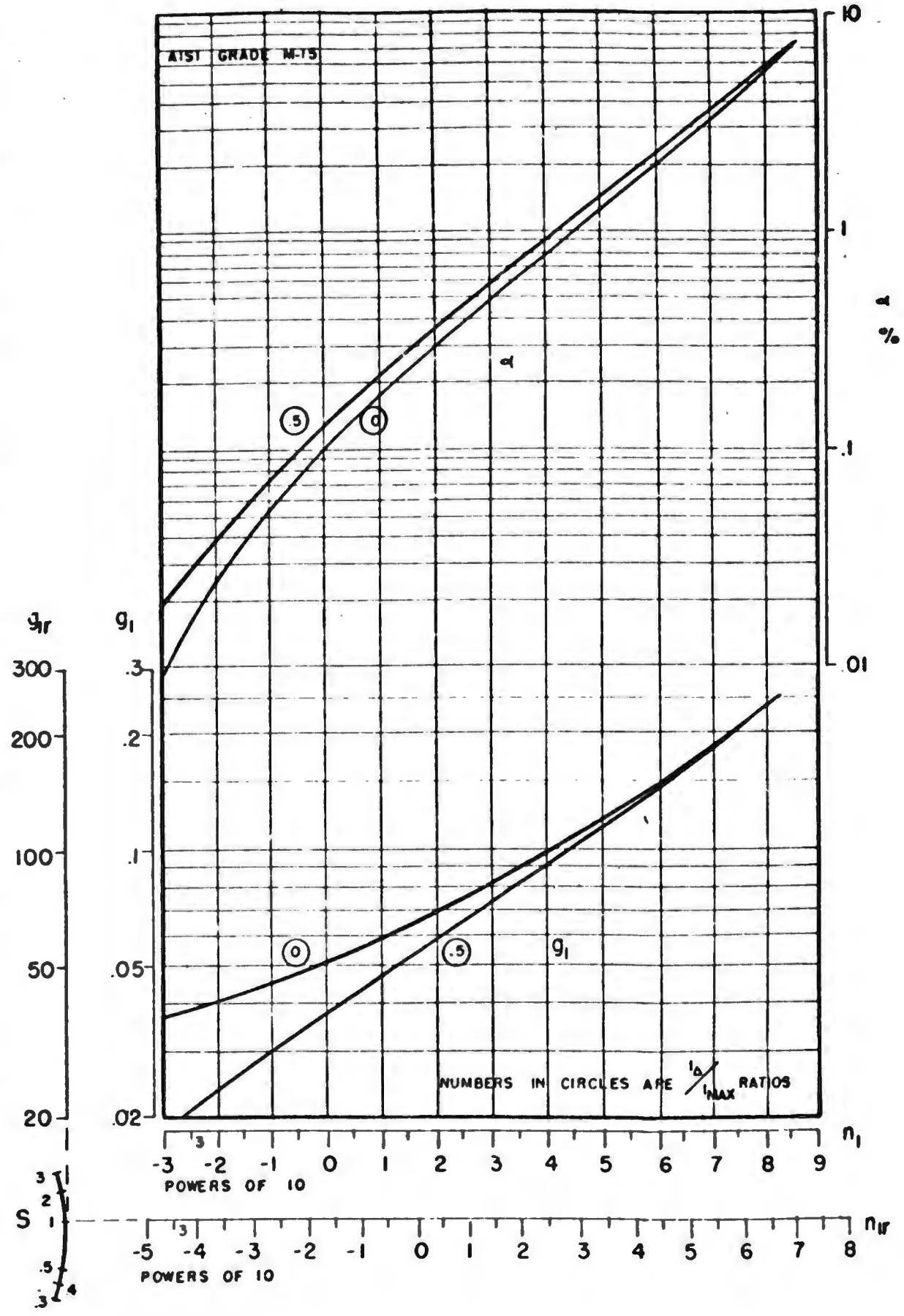
(only for low voltage scrapless EI construction)

6. If δ_1 lies between standard laminations, see text.

7. Calculate H from

$$H = \sqrt{g_1 \sqrt{\frac{v \, 10^8}{.4\pi \, u \rho}} \sqrt{I R_c}} \qquad (4\text{-}41)$$

Chart IC (B_{max} = 4 Kilogausses)



Simplified Procedure for Use of Curves

1. Calculate

$$n_1 = \frac{(.4\pi)^5 v^3 w I_{max}^4 R_c^3}{u^3 \rho^3 10^8 L} \qquad (4\text{-}32)$$

or

$$n_{1r} = \frac{I_{max}^4 R_c^3}{L} \qquad (4\text{-}44)$$

(only for low voltage scrapless EI construction)

2. Enter chart at this n_1 or n_{1r} point.

3. Read a from the a curve having the proper I_Δ / I_{max} ratio.

4. Read g_1 (and g_{1r}) from the g_1 curve having the proper I_Δ / I_{max} ratio.

5. Calculate ℓ_i from

$$\ell_i = g_1 \sqrt{\frac{u \rho 10^8 L}{.4\pi v w R_c}} \qquad (4\text{-}38)$$

or

$$\ell_i = g_{1r} \sqrt{\frac{L}{R_c}} \qquad (4\text{-}47)$$

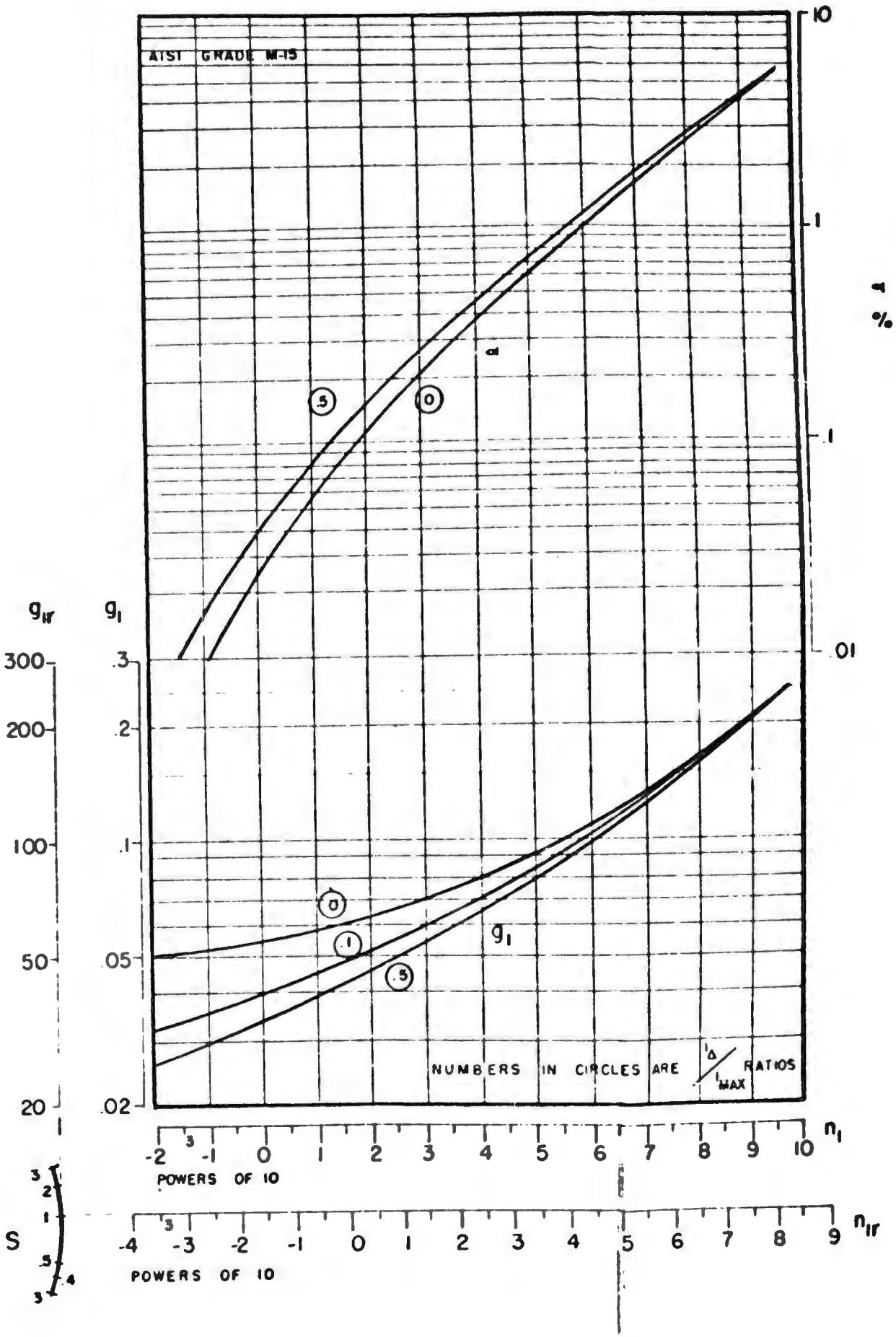
(only for low voltage scrapless EI construction.)

6. If ℓ_i lies between standard laminations, see text.

7. Calculate N from

$$N = \sqrt{g_1 \sqrt{\frac{v 10^8}{.4\pi uw\rho}} \sqrt{LR_c}} \qquad (4\text{-}41)$$

Chart 1C (B_{max} = 10 Kilogausses)



Simplified Procedure for Use of Curves

1. Calculate

$$n_2 = \frac{(.4\pi)^7 p^3 v^3 L I_{max}^8 K_c^3 10^8}{u^3 w \rho^3 I_{rms}^6} \qquad (5\text{-}9)$$

or

$$n_{2r} = \frac{L I_{max}^8 K_c^3}{I_{rms}^6} \qquad (5\text{-}21)$$

(only for low voltage scrapless EI construction)

2. Enter chart at this n_2 or n_{2r} point.

3. If the value of n_2 or n_{2r} is smaller than that at left hand limit of the curves, use Chart 2B.

4. Read B_{max} and a from their respective curves for the proper I_Δ/I_{max} ratio.

5. If B_{max} is too large, use Chart 2C.

6. Read g_2 (and g_{2r}) from the g_2 curve for the proper I_Δ/I_{max} ratio.

7. Calculate δ_1 from

$$\delta_1 = g_2 \sqrt[4]{\frac{u \rho 10^8 L I_{rms}^2}{.4\pi p v w K_c}} \qquad (5\text{-}15)$$

or

$$\delta_1 = g_{2r} \sqrt[4]{\frac{L I_{rms}^2}{K_c}} \qquad (5\text{-}24)$$

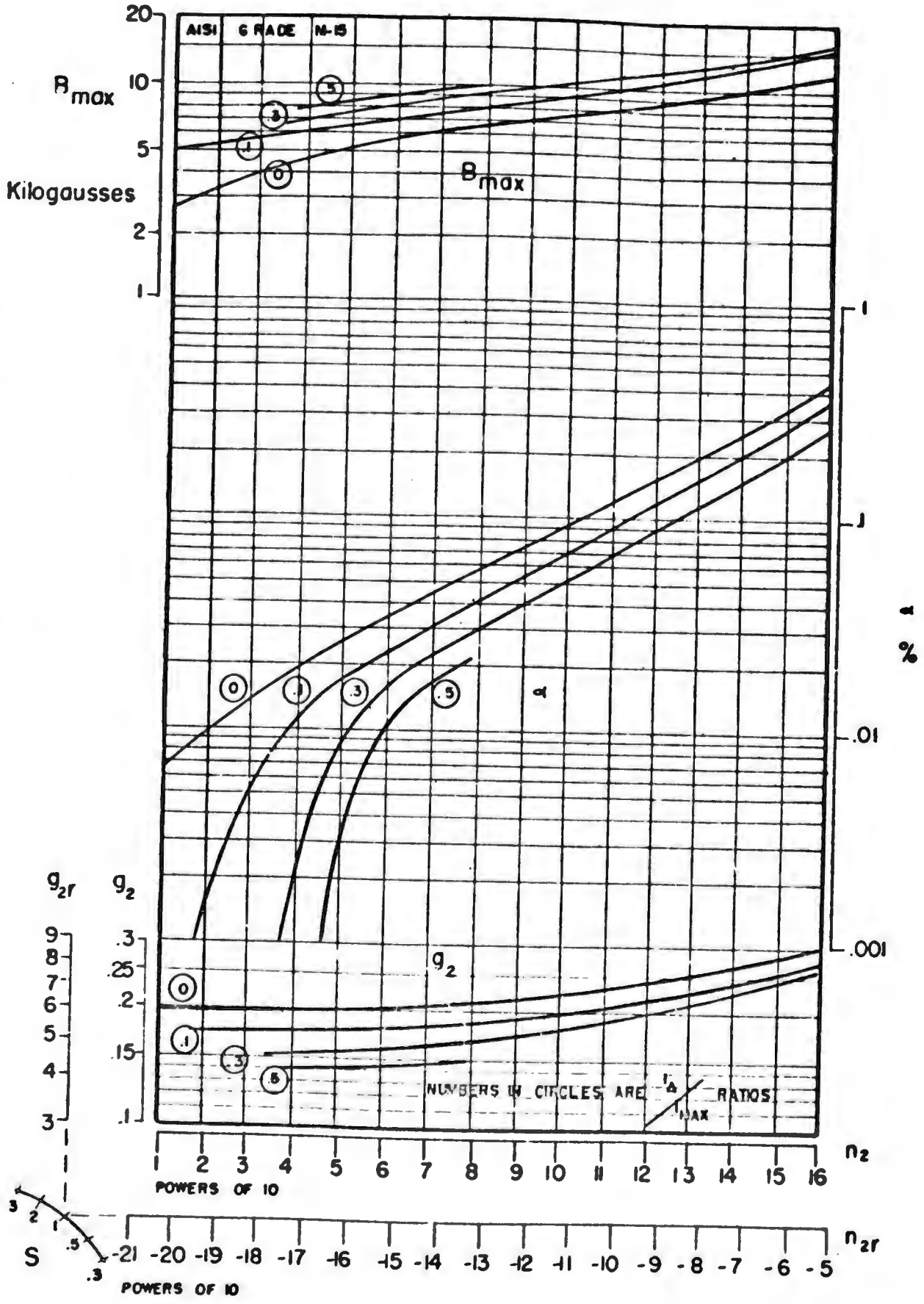
(only for low voltage scrapless EI construction)

8. If δ_1 lies between standard laminations, see text.

9. Calculate N from

$$N = (g_2)^2 \sqrt[8]{\frac{w 10^{-4} L^3 K_c}{(.4\pi)^3 u w^3 \rho I_{rms}^2}} \qquad (5\text{-}18)$$

Chart 2A


AISI GRADE M-15
B_{max}
Kilogausses
20
10
5
2
1
B_{max}
0
.1
.3
.5
α
1
.1
.01
.001
%
g_{2r}
g_2
9
8
7
6
5
4
3
.3
.25
.2
.15
.1
g_2
NUMBERS IN CIRCLES ARE $\frac{I_\Delta}{I_{MAX}}$ RATIOS
1 2 3 4 5 6 7 8 9 10 11 12 13 14 15 16
n_2
POWERS OF 10
S
3
2
1
.5
.3
-21 -20 -19 -18 -17 -16 -15 -14 -13 -12 -11 -10 -9 -8 -7 -6 -5
n_{2r}
POWERS OF 10

Simplified Procedure for Use of Curves

1. Calculate

$$n_2 = \frac{(.4\pi)^7 p^3 v^3 L I_{max}^8 K_c^3 10^8}{u^3 w \rho^3 I_{rms}^6} \qquad (5\text{-}9)$$

or

$$n_{2r} = L \frac{I_{max}^8 K_c^3}{I_{rms}^6} \qquad (5\text{-}21)$$

(only for low voltage scrapless EI construction)

2. Enter chart at this n_2 or n_{2r} point.

3. Read B_{max} from the B_{max} curve having the required I_Δ/I_{max} ratio.

4. Read g_2 (and g_{2r}) from the g_2 curve having the required I_Δ/I_{max} ratio.

5. Calculate ℓ_i from

$$\ell_i = g_2 \sqrt[4]{\frac{u \rho 10^8 L I_{rms}^2}{.4\pi p v w K_c}} \qquad (5\text{-}15)$$

or

$$\ell_i = g_{2r} \sqrt[4]{\frac{L I_{rms}^2}{K_c}} \qquad (5\text{-}24)$$

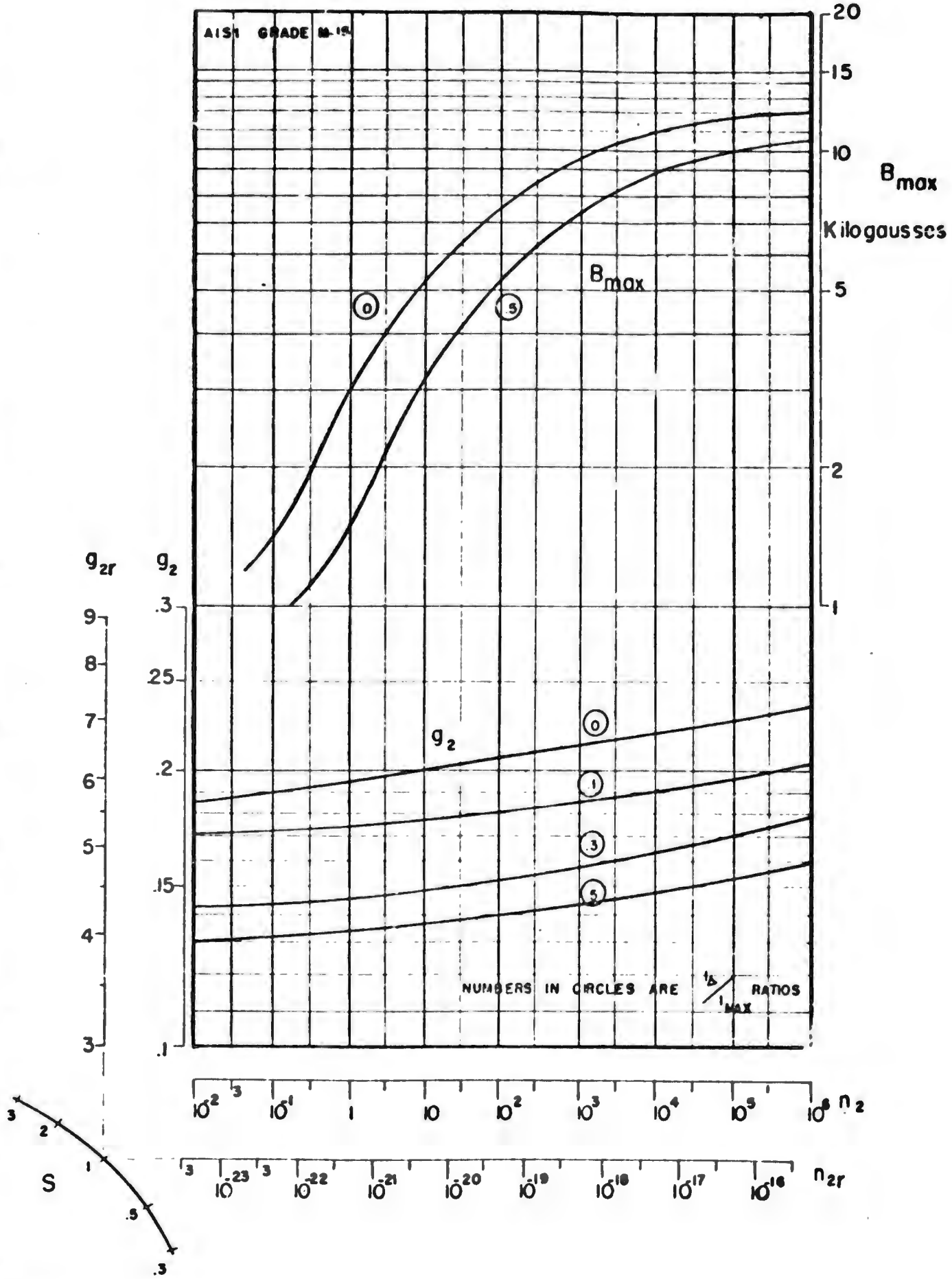
(only for low voltage scrapless EI construction)

6. If ℓ_i lies between standard laminations, see text.

7. Calculate N from

$$N = \left(\frac{B}{\quad}\right) \sqrt[8]{\frac{\rho 10^{-4} I \quad K_c}{(.4\pi)^3 w^3 \rho I_{rms}^2}} \qquad (5\text{-}18)$$

Chart 2B ($\alpha = 0$)



Simplified Procedure for Use of Curves

1. Calculate

$$n_2 = \frac{(.4\pi)^7 \, p^3 \, v^3 \, L \, I_{max}^{\,8} \, K_c^{\,3} \, 10^8}{w^3 \, w \, \rho^3 \, I_{rms}^{\,6}} \qquad (5\text{-}9)$$

or

$$n_{2r} = \frac{L \, I_{max}^{\,8} \, K_c^{\,3}}{I_{rms}^{\,6}} \qquad (5\text{-}21)$$

(only for low voltage scrapless EI construction)

2. Enter chart at this n_2 or n_{2r} point.

3. Read α from the α curve having the proper I_Δ/I_{max} ratio.

4. Read g_2 (and g_{2r}) from the g_2 curve having the proper I_Δ/I_{max} ratio.

5. Calculate δ_i from

$$\delta_i = g_2 \sqrt[4]{\frac{u \, \rho \, 10^8 \, L \, I_{rms}^{\,2}}{.4\pi \, p \, v \, w \, K_c}} \qquad (5\text{-}15)$$

or

$$\delta_i = g_{2r} \sqrt[4]{\frac{L \, I_{rms}^{\,2}}{K_c}} \qquad (5\text{-}24)$$

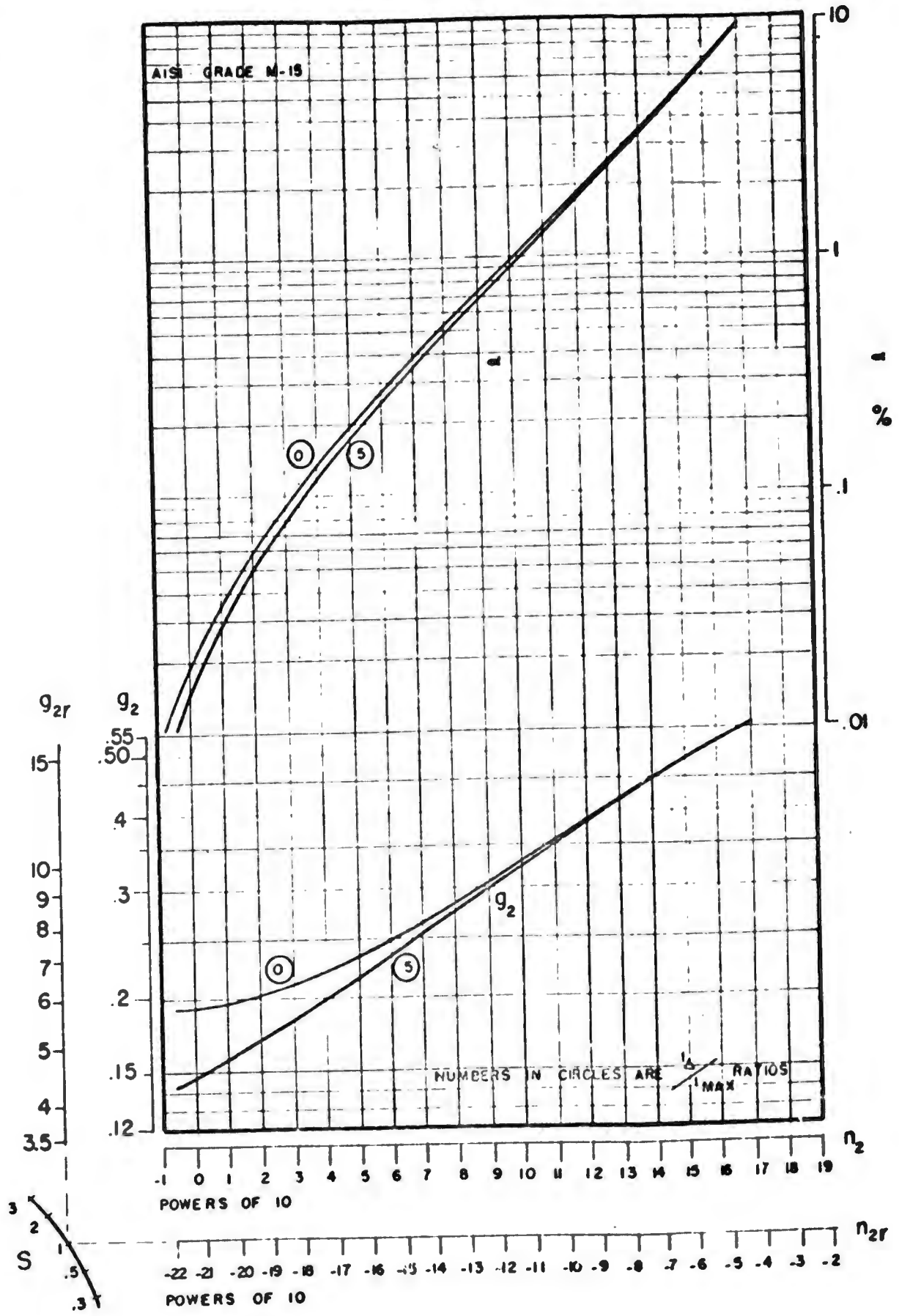
(Only for low voltage scrapless EI construction)

6. If δ_i lies between standard laminations, see text.

7. Calculate N from

$$N = (g_2)^{\frac{3}{2}} \sqrt[8]{\frac{p \, v \, 10^{24} \, L^3 \, K_c}{(.4\pi)^3 \, u \, w^3 \, \rho \, I_{rms}^{\,2}}} \qquad (5\text{-}18)$$

Chart 2C (B_{max} = 1 Kilogauss)



Simplified Procedure for Use of Curves

1. Calculate

$$n_2 = \frac{(.4\pi)^7 \rho^3 v^3 L I_{max}^8 K_c^3 10^8}{u^3 w \rho^3 I_{rms}^6} \qquad (5\text{-}9)$$

or

$$n_{2r} = \frac{L I_{max}^8 K_c^3}{I_{rms}^6} \qquad (5\text{-}21)$$

(only for low voltage scrapless EI construction)

2. Enter Chart at this n_2 or n_{2r} point.

3. Read α from the α curve having the proper I_Δ/I_{max} ratio.

4. Read g_2 (and g_{2r}) from the g_2 curve having the proper I_Δ/I_{max} ratio.

5. Calculate ℓ_i from

$$\ell_i = g_2 \sqrt[4]{\frac{u \rho 10^8 L I_{rms}^2}{.4\pi p v w K_c}} \qquad (5\text{-}15)$$

or

$$\ell_i = g_{2r} \sqrt[4]{\frac{L I_{rms}^2}{K_c}} \qquad (5\text{-}24)$$

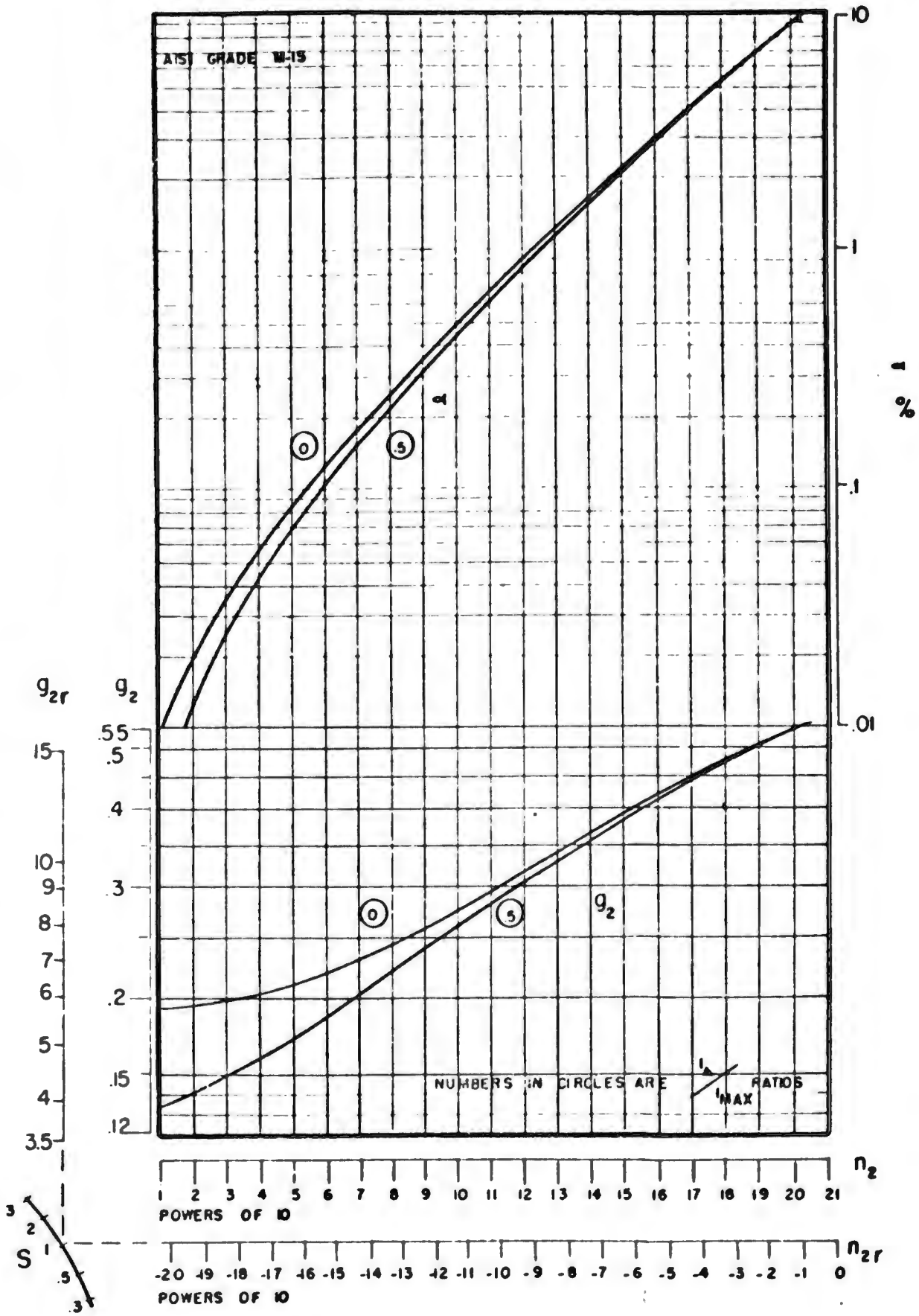
(only for low voltage scrapless EI construction)

6. If ℓ_i lies between standard laminations, see text.

7. Calculate N from

$$N = (g_2)^{\frac{3}{2}} \sqrt[8]{\frac{p v 10^{24} L^3 K_c}{(.4\pi)^3 u w^3 \rho I_{rms}^2}} \qquad (5\text{-}18)$$

Chart 2C (B_{max} = 2 Kilogausses)



Simplified Procedure for Use of Curves

1. Calculate

$$n_2 = \frac{(.4\pi)^7 \rho^3 v^3 L I_{max}^8 K_o^3 10^8}{u^3 w \rho^3 I_{rms}^6} \qquad (5\text{-}9)$$

or

$$n_{2r} = \frac{L I_{max}^8 K_o^3}{I_{rms}^6} \qquad (5\text{-}21)$$

(only for low voltage scrapless EI construction)

2. Enter chart at this n_2 or n_{2r} point.

3. Read a from the a curve having the proper I_1/I_{max} ratio.

4. Read g_0 (and g_{02}) from the g_2 curve having the proper I_1/I_{max} ratio.

5. Calculate δ_1 from

$$\delta_1 = g_2 \sqrt[4]{\frac{.4 \rho I_{rms}^3 L I_{max}^2}{.4 \pi \rho v u K_o}} \qquad (5\text{-}15)$$

or

$$\delta_1 = g_{02} \sqrt[4]{\frac{L I_{max}^2}{}} \qquad (5\text{-}24)$$

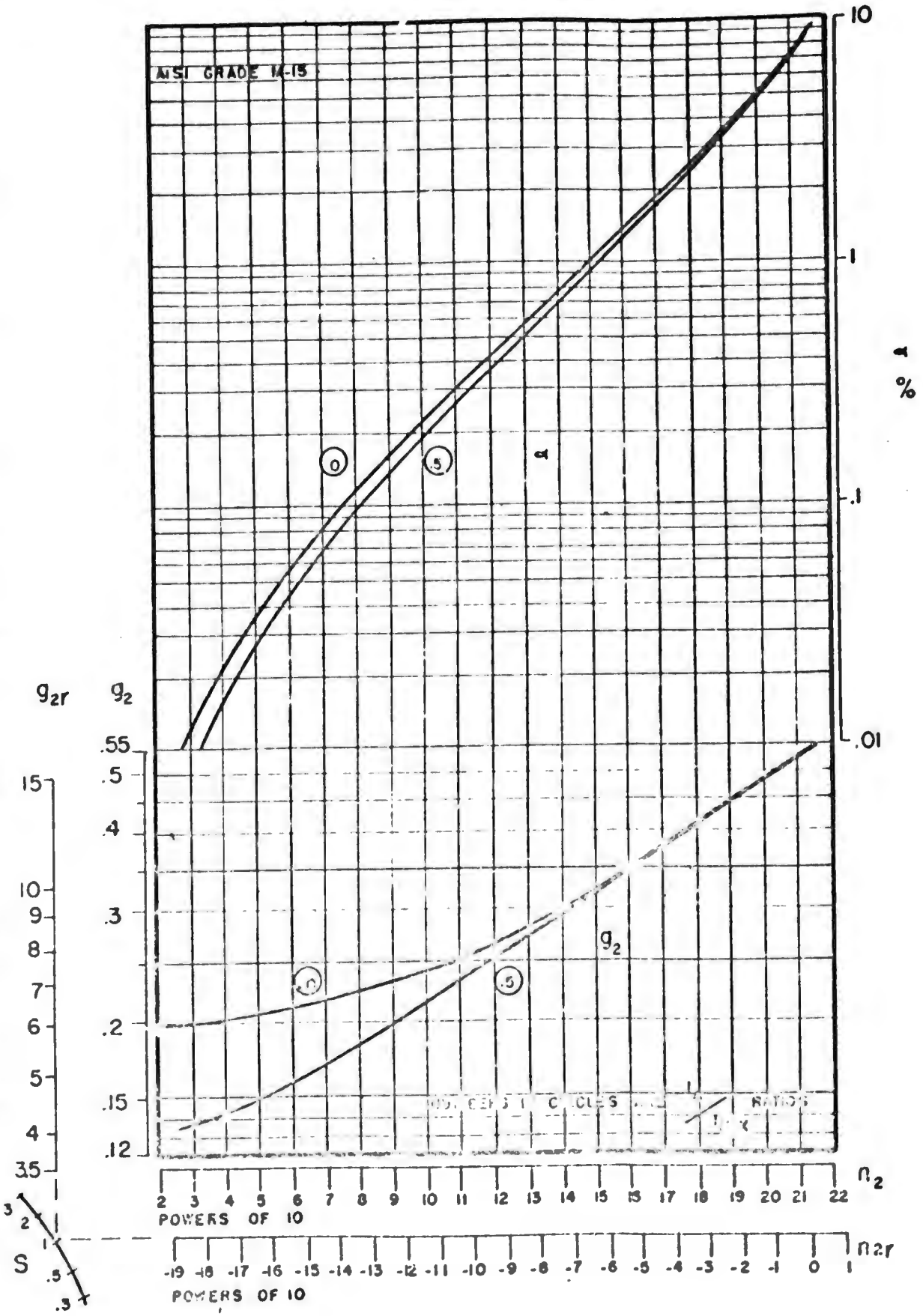
(only for low voltage scrapless EI construction)

6. [illegible] limitations, see text.

7. [illegible]

$$[illegible] = (g_2)^{\frac{3}{4}} \sqrt{\frac{[illegible] I^3 K_o}{(.4\pi)^3 \rho I_{rms}^2}} \qquad (5\text{-}18)$$

Chart 2C (B_{max} = 4 Kilogausses)



Simplified Procedure for Use of Curves

1. Calculate

$$n_2 = \frac{(.4\pi)^7 \, p^3 \, v^3 \, L \, I_{max}^{\,8} \, K_o^{\,3} \, 10^8}{w^3 \, w \, \rho^3 \, I_{rms}^{\,6}} \qquad (5\text{-}9)$$

or

$$n_{2r} = \frac{L \, I_{max}^{\,8} \, K_o^{\,3}}{I_{rms}^{\,6}} \qquad (5\text{-}21)$$

(only for low voltage scrapless LH construction)

2. Enter chart at this n_2 or n_{2r} point.

3. Read a from the a curve having the proper I_p/I_{rms} ratio.

4. Read g_2 (g_{2r}) from the g_2 curve having the proper I_p/I_{max} ratio.

5. Calculate f_1 from

$$f_1 = a \sqrt{\frac{g_2 \, \rho \, 10^3 \, L \, I_{rms}^{\,2}}{w \, \rho \, v \, w \, K_o}} \qquad (5\text{-}15)$$

or

$$f_1 = a \sqrt{\frac{g_{2r} \, L \, I_{max}^{\,2}}{K_o}} \qquad (5\text{-}24)$$

(low voltage scrapless construction)

6. Find f_2 from [illegible] curves, see text.

7. Calculate H from

$$H = (.4\pi)^{\frac{1}{2}} \sqrt{\frac{\rho \, v \, w \, L^3 \, K_o}{(.4\pi)^2 \, \rho \, I_{rms}^{\,2}}} \qquad (5\text{-}18)$$

Chart 2C (B_{max} = 10 Kilogausses)

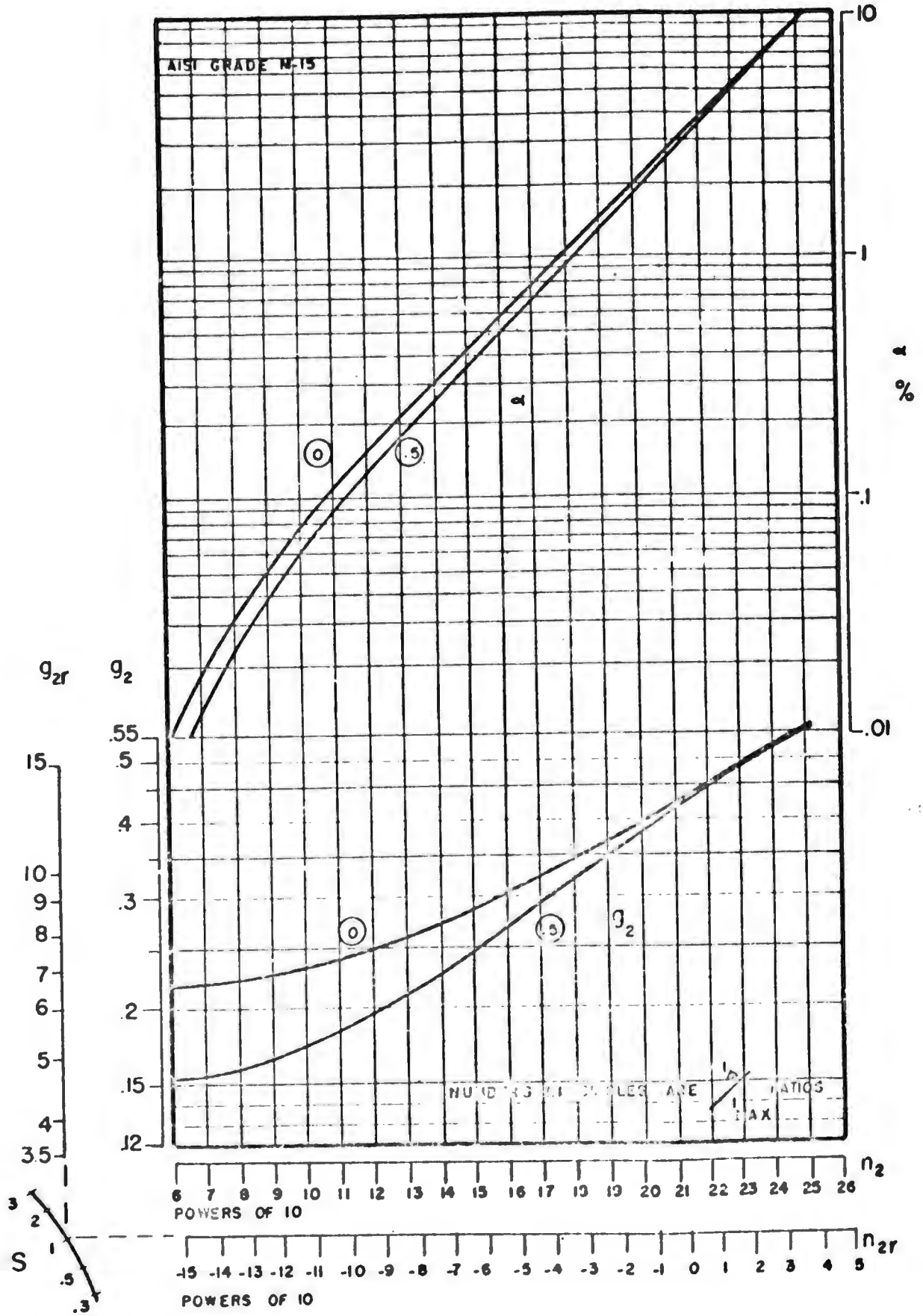


Chart 3

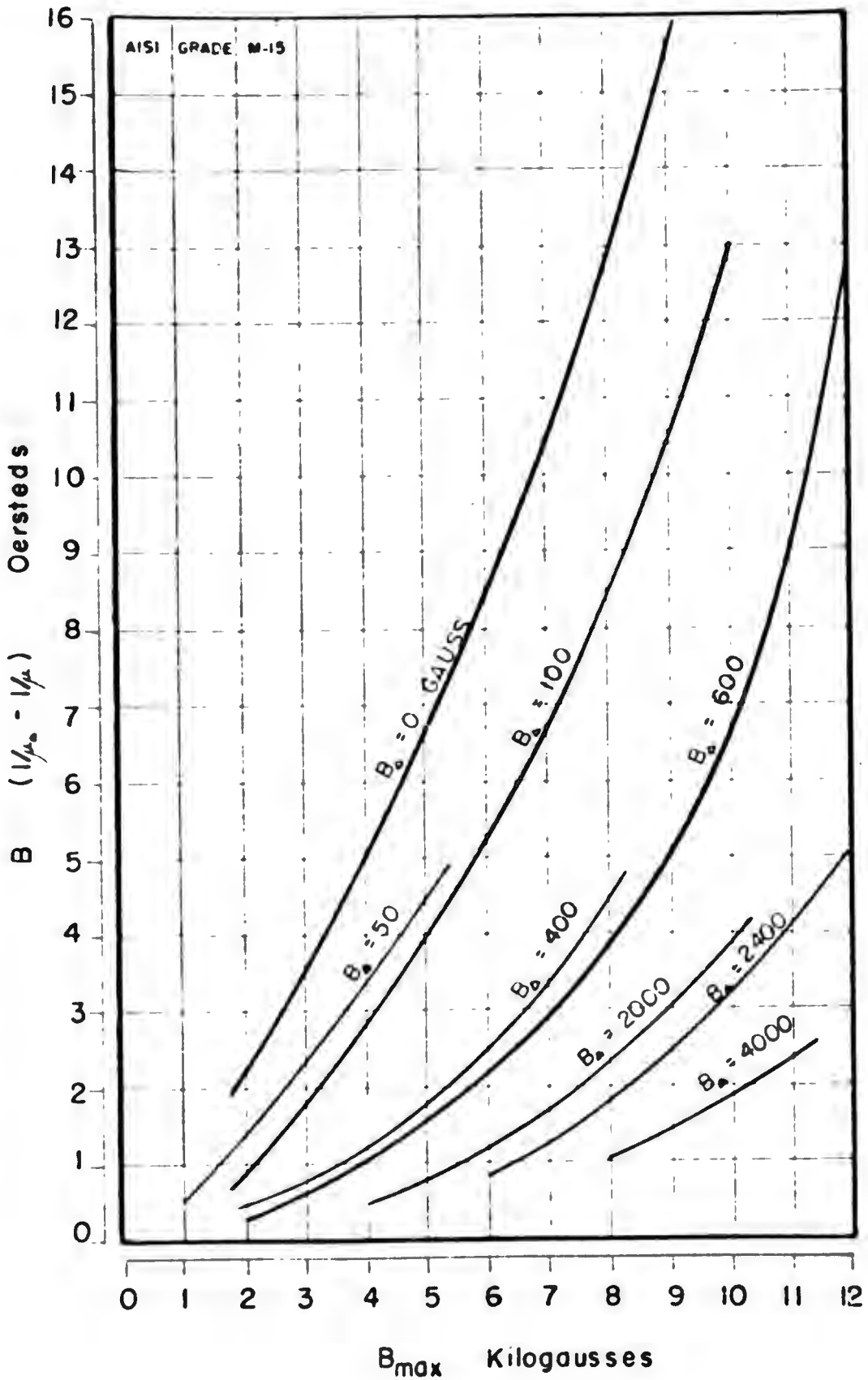
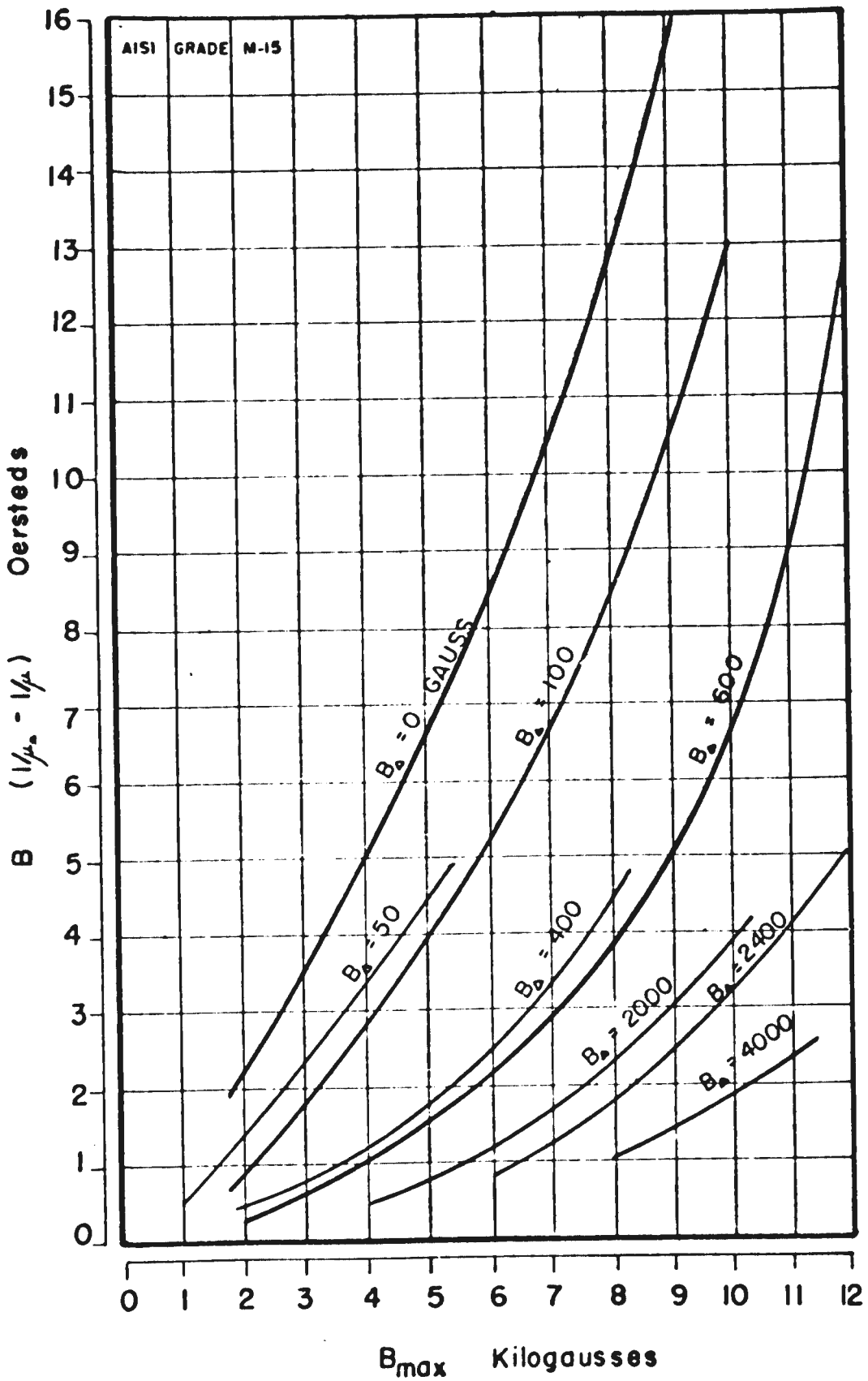

AISI GRADE M-15
B (1/μ₀ - 1/μ) Oersteds
Bmax Kilogausses
Bo = 0 GAUSS
Bo = 50
Bo = 100
Bo = 400
Bo = 600
Bo = 2000
Bo = 2400
Bo = 4000
0 1 2 3 4 5 6 7 8 9 10 11 12
0 1 2 3 4 5 6 7 8 9 10 11 12 13 14 15 16

Chart 3


AISI GRADE M-15
B (1/μa - 1/μ) Oersteds
Bmax Kilogausses
Ba = 0 GAUSS
Ba = 50
Ba = 100
Ba = 400
Ba = 600
Ba = 2000
Ba = 2400
Ba = 4000
0 1 2 3 4 5 6 7 8 9 10 11 12
0 1 2 3 4 5 6 7 8 9 10 11 12 13 14 15 16

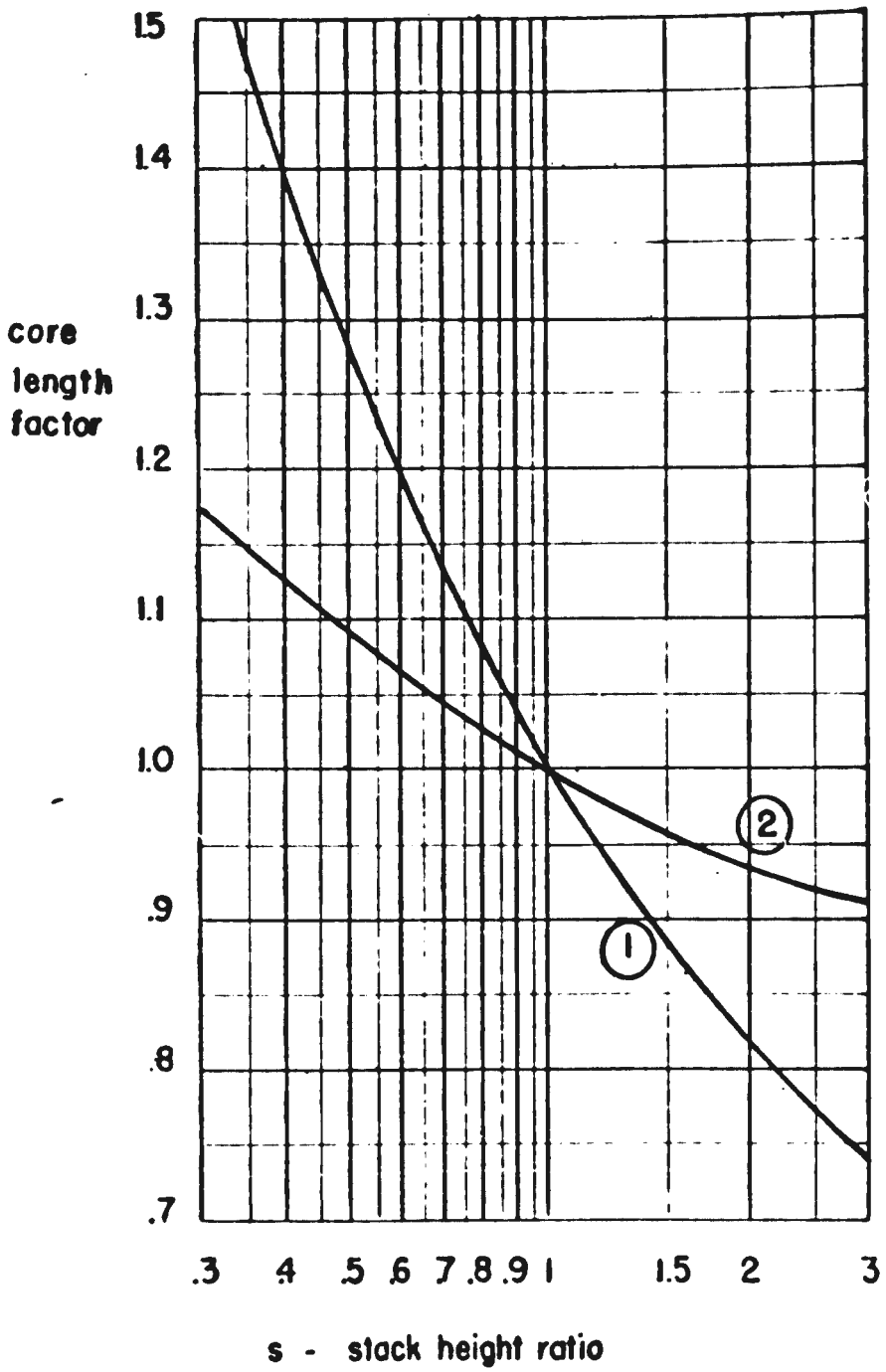
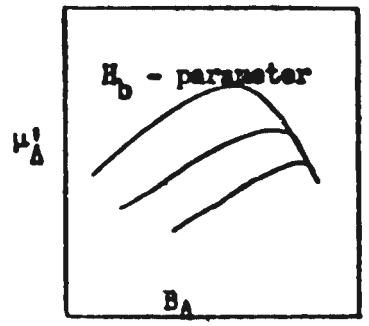


Chart 3a Scrapless E1 core length factors vs stack height ratio for cores with various stack heights.

Table 1

Construction of Figure 17

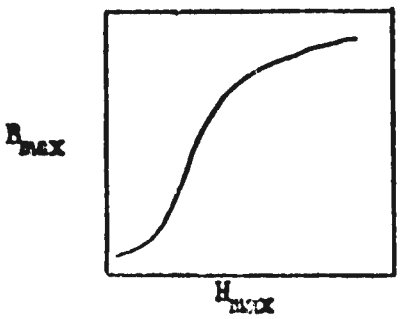
1. Choose a point from Fig. 15 and read B_Δ, H_b, and μ_Δ.



2. Calculate H_{max} from

$$H_{max} = \frac{B_\Delta}{\mu'_\Delta} + H_b \qquad (9\text{-}4)$$

3/ Read B_{max} from Fig. 13.



4. Calculate B_Δ/B_{max} knowing B_Δ from step 1, and B_{max} from step 3.

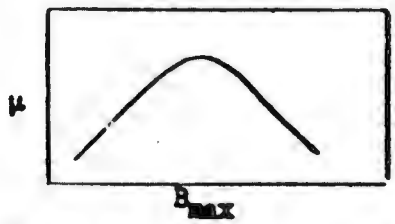
Table 2

Construction of Chart 1A

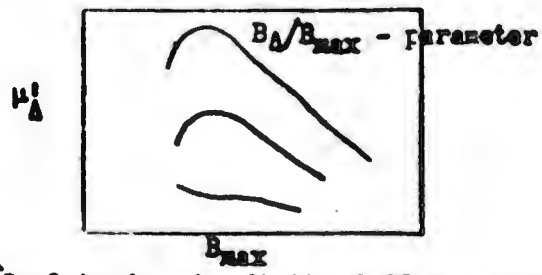
1. Choose a value of B_Δ/B_{max}.

2. Choose a value for B_{max}.

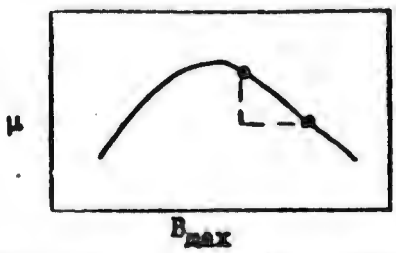
3. Get μ from Fig. 14, knowing B_{max}.



4. Get μ_Δ' from Fig. 17, knowing B_Δ/B_{max} and B_{max}.



5. Calculate $\frac{d\mu}{dB_{max}}$ by finite difference method, use Fig. 14.



6. Calculate $\frac{d\mu_\Delta'}{dB_{max}}$ by finite difference method, use Fig. 17.

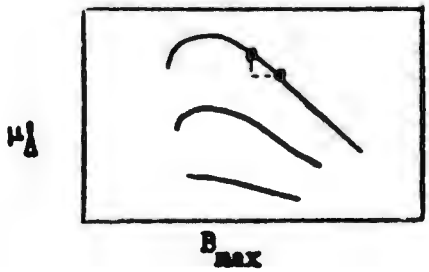


Table 2 (cont.)

7. Calculate D from

$$D = \frac{1}{\mu^2}\frac{d\mu}{dB_{max}} - \frac{1}{\mu_A^2}\frac{d\mu_A}{dB_{max}} \qquad (4\text{-}21)$$

8. Calculate α from

$$\alpha = B_{max} D - \frac{1}{\mu} \qquad (4\text{-}24)$$

9. Calculate n_1 from

$$n_1 = B_{max}^{\,8} B^4 \left(B_{max} D - \frac{1}{\mu} + \frac{1}{\mu_A}\right) \qquad (4\text{-}35)$$

10. Calculate g_1 from

$$g_1 = \sqrt{B_{max} D - \frac{1}{\mu} + \frac{1}{\mu_A}} \qquad (4\text{-}39)$$

11. Calculate I_A/I_{max} from

$$\frac{I_A}{I_{max}} = \frac{B_A}{B_{max}} \frac{1/\mu_A + \alpha}{1/\mu + \alpha} \qquad (4\text{-}43)$$

Table 3

Construction of Chart 1B

1. Choose a value for B_Δ/B_{max}.

2. Choose a value for B_{max}.

3. Get μ from Fig. 14, knowing B_{max}.

4. Get μ'_Δ from Fig. 17, knowing B_{max} and B_Δ/B_{max}.

5. Calculate n_1 from

$$n_1 = \frac{B_{max}^4}{\mu^4 \mu'_\Delta} \qquad (4\text{-}73)$$

6. Calculate ϵ_1 from

$$\epsilon_1 = \frac{1}{\sqrt{\mu'_\Delta}} \qquad (4\text{-}74)$$

7. Calculate I_Δ/I_{max} from

$$\frac{I_\Delta}{I_{max}} = \frac{B_\Delta \mu}{B_{max} \mu'_\Delta} \qquad (9\text{-}8)$$

Table 4

Construction of Chart 1C

1. Choose a value for B_Δ/B_{max}.

2. Choose a value for B_{max}.

3. Get μ from Fig. 14.

4. Get μ_Δ' from Fig. 17.

5. Choose a value for g_1.

6. Knowing μ, μ_Δ', B_{max}, and g_1 calculate n_1 from

$$n_1 = B_{max}^4 \, g_1^2 \left(g_1^2 - \frac{1}{\mu_\Delta'} + \frac{1}{\mu}\right)^4 \qquad (4\text{–}79)$$

7. Calculate α from

$$\alpha = g_1^2 - \frac{1}{\mu_\Delta'} \qquad (4\text{–}80)$$

8. Calculate I_Δ/I_{max} from

$$\frac{I_\Delta}{I_{max}} = \frac{B_\Delta \, (1/\mu_\Delta' - \alpha)}{B_{max} \, (1/\mu + \alpha)} \qquad (4\text{–}43)$$

Table 5

Construction of Chart 2A

1. Choose a value for B_Δ/B_{max}.

2. Choose a value for B_{max}.

3. Get μ from Fig. 14.

4. Get μ'_Δ from Fig. 17.

5. Calculate D from

$$D = \frac{1}{\mu^2}\frac{d\mu}{dB_{max}} - \frac{1}{\mu'^2_\Delta}\frac{d\mu'_\Delta}{dB_{max}} \qquad (4\text{-}21)$$

6. Calculate n_2 from

$$n_2 = \frac{B_{max}^{16}\, D^8}{B_{max} D - \frac{1}{\mu} + \frac{1}{\mu'_\Delta}} \qquad (5\text{-}12)$$

7. Calculate ε_2 from

$$\varepsilon_2 = \sqrt[4]{B_{max} D - \frac{1}{\mu} + \frac{1}{\mu'_\Delta}} \qquad (5\text{-}16)$$

8. Calculate α from

$$\alpha = \varepsilon_2^4 - \frac{1}{\mu'_\Delta} \qquad (5\text{-}14)$$

9. Calculate I_Δ/I_{max} from

$$\frac{I_\Delta}{I_{max}} = \frac{B_\Delta\,(1/\mu''_\Delta + \alpha)}{B_{max}(1/\mu + \alpha)} \qquad (4\text{-}43)$$

Table 6

Construction of Chart 2B

1. Choose a value for B_Δ/B_{max}.
2. Choose a value for B_{max}.
3. Get μ from Fig. 14.
4. Get μ_Δ' from Fig. 17.
5. Calculate n_2 from

$$n_2 = \frac{B_{max}^{\,8}\,\mu_\Delta'}{\mu^8} \qquad (5\text{-}34)$$

6. Calculate g_2 from

$$g_2 = \sqrt[4]{1/\mu_\Delta'} \qquad (5\text{-}35)$$

7. Calculate I_Δ/I_{max} from

$$\frac{I_\Delta}{I_{max}} = \frac{B_\Delta\,\mu}{B_{max}\,\mu_\Delta'} \qquad (9\text{-}8)$$

Table 7

Construction of Chart 20

1. Choose a value for B_Δ/B_{max}.

2. Choose a value for B_{max}.

3. Get μ from Fig. 14.

4. Get μ'_Δ from Fig. 17.

5. Choose a value for g_2.

6. Calculate n_2 from

$$n_2 = \frac{B_{max}^8 \left(g_2^4 - \frac{1}{\mu'_\Delta} + \frac{1}{\mu}\right)^8}{g_2^4} \qquad (5\text{-}34)$$

7. Calculate α from

$$\alpha = g_2^4 - \frac{1}{\mu'_\Delta} \qquad (5\text{-}35)$$

8. Calculate I_Δ/I_{max} from

$$\frac{I_\Delta}{I_{max}} = \frac{B_\Delta \left(1/\mu'_\Delta + \alpha\right)}{B_{max} \left(1/\mu + \alpha\right)} \qquad (4\text{-}43)$$

Table 8

Construction of Chart 3

1. Choose a value for B_Δ to be used as a parameter.
2. Choose a value for B_{max}.
3. Get μ from Fig. 14.
4. Get μ'_Δ from Fig. 17.
5. Calculate the value of $1/\mu$.
6. Calculate the value of $1/\mu'_\Delta$.
7. Calculate the value of $1/\mu'_\Delta - 1/\mu$.
8. Calculate the value of $B_{max}\ (1/\mu'_\Delta - 1/\mu)$.
9. The value of step 2 is the abcissa and the value of step 8 is the ordinate.

Table 9 page 1
Parts list for Figures 26a, 26b, and 26c.
Main Rack (Fig. 26a)

C-101 0.02 uf, 8 KV.

C-102 0.02 µf, 8KV.

C-103 0.02 µf, 8KV.

C-104 0.25 µf, 50 KV.

C-105 15KVA, 6900V, 60 cps. (0.835 µf).

C-106 15KVA, 6900V, 60 cps. (0.835 µf).

C-107 15KVA, 6900V, 60 cps. (0.835 µf).

C-108 15KVA, 6900V, 60 cps. (0.835 µf).

C-109 0.5 µf.

C-110 7 µf.

F-101 250 V, 6 amp

I-101 60 Watt, 120 V, Work light.

I-102 6 Watt, 120 V, Green, Rectifier filament pilot.

I-103 6 Watt, 120 V, Green High voltage OFF pilot.

I-104 6 Watt, 120 V, Green, Ready pilot.

I-105 6 Watt, 120 V, Red, High voltage ON pilot.

K-101 Main HV contractor.

K-102 Condensor discharge relay.

K-103 Condensor discharge relay.

K-104 Overload relay.

K-105 Overload relay.

L-101 19 Hy., 0.20 amps. D.C., 8750 R.M.S volts.

M-101 0-200 D.C. Milliamperes.

M-102 0-1 D.C. Milliamperes.

P-101 Power input.

P-102 Power input for variable auto transformer.

R-101 6 Megohms, Wire wound.

Table 9 page 2

R-102 6 Megohms, Wire wound.

R-103 6 Megohms, Wire wound.

R-104 6 Megohms, Wire wound.

R-105 6 Megohms, Wire wound.

R-106 33 ohms.

S-101 Push-button switch, Work light OFF-ON switch.

S-102 DPST, Rectifier filament OFF-ON switch.

S-103 Push-button switch, Relay contact.

S-104 Push-button switch, High voltage OFF switch.

S-105 Push-button switch, High voltage ON switch.

T-101 Variable auto transformer.

Table 9 page 3

Continental X-Ray Corporation Power Supply

Model FW-5

L-401 36 Hy., Filter choke.

T-401 High-Voltage transformer.

T-402 Rectifier filament transfofmer.

T-403 Rectifier filament transformer.

T-404 Rectifier filament transformer.

T-405 Rectifier filament transformer.

V-401 705A, High-voltage rectifier tube.

V-402 705A, High-voltage rectifier tube.

V-403 705A, High-voltage rectifier tube.

V-404 705A, High-voltage rectifier tube.

V-405 705A, High-voltage rectifier tube.

V-406 705A, High-voltage rectifier tube.

Table 9 page 4

Timer Chassis (Fig. 26b)

C-201	13-58 μμf, Ceramic disc.	R-213	4700, 1/2 watt.
C-202	100 μμf.	R-214	9 K, 6 watt.
C-203	0.1 μf.	R-215	22 K, 4 watt.
C-204	0.1 μf.	R-216	100 K, 1/2 watt.
C-205	0.25 μf.	R-217	10 K, 2 watt.
C-206	0.1 μf.	S-201	Power OFF-ON switch.
C-207	0.1 μf.	T-201	Stancor P4081.
C-208	200 μμf.	V-201	6SN7.
C-209	200 μμf.	V-202	6SN7.
C-210	16 μf.	V-203	6AQ7.
F-201	250 V., 5 amp.	V-204	5Y3.

I-201 6 Watt, 120 V., White, Power OFF-ON switch.

J-201 Coaxial jack, Signal input.

J-202 Coaxial jack, Trigger output.

L-201 28 Hy.

L-202 100 Millihenry.

R-201 12 K, 1/2 watt.

R-202 100 K, 1/2 watt.

R-203 220 K, 1/2 watt.

R-204 3300, 2 watt.

R-205 33 K, 1/2 watt.

R-206 180 K, 1/2 watt.

R-207 12 K, 2 watt.

R-208 39 K, 1/2 watt.

R-209 100 K, 1/2 watt.

R-210 18 K, 2 watt.

R-211 68 K, 2 watt.

R-212 10 K pot., 2 watt.

Table 9 page 5

Pulser Chassis (Fig. 26c)

F-301	250 V., 5 amps., Power fuse.
I-301	6 Watt, 120 V., Green, Power OFF-ON pilot.
J-301	Power cable.
J-302	Thyratron current jack.
J-303	Load current jack.
J-304	Choke current jack.
K-301	Auxiliary relay (5022 starting).
K-302	5 min. thermal time delay relay (5022 starting).
L-301	Charging choke under test.
M-301	AC-DC voltmeter.
R-301	20K, 100 watt, wire wound.
R-302	Thyratron current shunt.
R-303	Load current shunt.
R-304	50 ohm pulseload resistor, (two 25 ohm, 160 watt non-inductive wire wound resistors in series oil bath, water cooled).
R-305	Choke current shunt.
S-301	DPST, Power OFF-ON switch.
S-302	Interlock switch.
S-303	Interlock switch.
S-304	Filament transformer tap switch.
T-301	50-60 cycle, 115 V. input; 5.1 V., 5 amps output.
T-302	50-60 cycle, 115 V. input; 5.1 V., 5 amps output.
T-303	50-60 cycle, 115 V. input; 5.1 V., 5 amps output.
V-301	705A
V-302	705A
V-303	5022 Thyratron.
Z-301	Pulse forming network.

Table 10 Parts list for figures 29a and 29b.

Upper Chassis Parts List (Fig. 29a)

C-101	8 µf	450 v
C-102	.1 µf	400 v
C-103	.05 µf	400 v
C-104	.05 µf	400 v
C-105	2500 µµf	Mica Capacitor
C-106	.5 µf	400 v
C-107	25.5 µµf	Mica Capacitor
C-108	.25 µf	400 v
C-109	.25 µf	400 v
C-110	.1 µf	400 v
C-111	.01 µf	400 v
C 112	8 µf	450 v
C-113	.001 µf	600 v
C-114	100 µf	50 v
C-115	.01 µf	400 v
C-116	8 µf	450 v
C-117	.001 µf	600 v
C-118	100 uf	50 v
C-119	.5 µf	400 v
J-101	Input Jack	
J-102	Output Jack	

Table 10 page 2

R-101	500 K	Potentiometer
R-102	1 Meg	1/2 watt
R-103	22 K	1 watt
R-104	2.7 Meg	1 watt
R-105	22 K	1 watt
R-106	2 K	1 watt
R-107	15 K	2 watt
R-108	1 Meg	1/2 watt
R-109	1 K	1 watt
R-110	33 K	1/2 watt
R-111	1 Meg	1 watt
R-112	390	2 watt
R-113	15 K	2 watt
R-114	18 K	1 watt
R-115	100 K	1/2 watt
R-116	560 K	1/2 watt
R-117	4 K	2 watt
R-118	50 K	Potentiometer, General Radio Type 471
R-119	5600	1 watt
R-120	1 Meg	1/2 watt
R-121	4.7 Meg	1/2 watt
R-122	1 Meg	1/2 watt
R-123	1 Meg	1/2 watt
R-124	50 K	Potentiometer (353-5101)
R-125	180 K	1 watt
R-126	4700	1 watt

Table 10 page 3

R-127	330 K	1/2 watt
R-128	22 K	1 watt
R-129	100 K	1 watt
R-130	43 K	1 watt
R-131	100 K	Potentiometer
R-132	500 K	Potentiometer
R-133	470 K	1/2 watt
R-134	270 K	1/2 watt
R-135	330 ohms	1 watt
R-136	8 K	IRE Type DG
R-137	27 K	2 watt
R-138	100 K	1/2 watt
R-139	33 K	1/2 watt
R-140	470 K	1/2 watt
R-141	47 K	2 watt
R-142	10 K	1 watt
R-143	500 K	Potentiometer
R-144	470 K	1/2 watt
R-145	270 K	1 watt
R-146	330	1 watt
R-147	8 K	IRE Type DG
R-148	27 K	2 watt
R-149	100 K	1/2 watt
R-150	33 K	1/2 watt
R-151	470 K	1/2 watt
R-152	47 K	2 watt

Table 10 page 4

R-153	1 K	1 watt
R-154	1 Meg	Potentiometer
R-155	470 K	1/2 watt
R-156	1 Meg	1/2 watt
R-157	60 K	5 watts
S-101	S.P.D.T.	
S-102	D.P.D.T.	
T-101	Input Transformer, Push-Pull, Type B, Sangamo Elect Co.	
TB-101	5 Pin	Terminal Block
TB-102	5 Pin	Terminal Block
TB-103	5 Pin	Terminal Block
V-101	6SN7	
V-102	6V6	
V-103	6SL7	
V-104	6E5	
V-105	6H6	
V-106	VR 105	
V-107	VR 105	
V-108	6AG7	
V-109	6AG7	
V-110	6AG7	
V-111	6AG7	
V-112	6AG7	
V-113	6AG7	
V-114	6SN7	

Table 10 page 5

Lower Chassis Parts List (Fig. 29b)

C-201	.25 µf	400 v
C-202	8 µf	450 v
C-203	25 µf	25 v
C-204	27 µµf	Mica Capacitor
C-205	8 µf	450 v
C-206	5 µf	450 v
C-207	100 µµf	Mica Capacitor
C-208	.01 µf	400 v
C-209	.01 µf	400 v
C-210	100 µµf	200 v
C-211	.25 µf	400 v
C-212	.25 µf	400 v
C-213	.5 µf	400 v
C-214	.5 µf	400 v
C-215	.01 µf	400 v
C-216	23 µµf	Mica Capacitor
C-217	.01 µf	400 v
C-218	1600 µµf	Mica Capacitor
C-219	.005 µf	600 v
C-220	.001-.015 µf	(in 12 steps)
J-203	Octal Plug	
P-203	Octal Socket	
R-201	100 K	1/2 watt
R-202	470 K	1/2 watt
R-203	30 K	2 watt

Table 10 page 6

R-204	1 K	1 watt
R-205	15 K	2 watt
R-206	30 K	1 watt
R-207	1 Meg	1/2 watt
R-208	22 K	4 watt
R-209	39 K	1 watt
R-210	100 K	1/2 watt
R-211	39 K	2 watt
R-212	30 K	4 watt
R-213	10 K	Potentiometer
R-214	330 K	1/2 watt
R-215	25 K	4 watt
R-216	1 Meg	1/2 watt
R-217	220 K	1/2 watt
R-218	100 K	1/2 watt
R-219	220 K	1/2 watt
R-220	39 K	1 watt
R-221	100 K	1/2 watt
R-222	1 Meg	1/2 watt
R-223	100 K	1/2 watt
R-224	25 K	4 watt
R-225	1 Meg	1/2 watt
R-226	100 K	1/2 watt
R-227	25 K	4 watt
R-228	10 K	1/2 watt

Table 10 page 7

R-229	30 K	4 watt
R-230	10 K	1/2 watt
R-231	30 K	4 watt
R-232	1 Meg	1/2 watt
R-233	20 K	4 watt
R-234	1 Meg	1/2 watt
R-235	220 K	1 watt
R-236	47 K	1/2 watt
R-237	160 K	1 watt
R-238	1 Meg	1/2 watt
R-239	1 Meg	1/2 watt
R-240	30 K	4 watt
R-241	2700	1 watt
R-242	30 K	4 watt
R-243	1 Meg	1/2 watt
R-244	20 K	4 watt
R-245	82 K	1/2 watt
R-246	22 K	2 watt
R-247	470 K	1/2 watt
S-201	12 position wafer switch (for variable condenser)	
TB-201	5 Pin	Terminal Block
TB-202	5 Pin	Terminal Block
TB-203	5 Pin	Terminal Block
V-201	5SH7	
V-202	6SH7	
V-203	6SH7	
V-204	6SJ7	

V-205	VR-150
V-206	6SN7
V-207	6SN7
V-208	6SN7
V-209	884
V-210	6SN7
V-211	6SN7
V-212	6SN7
V-213	VR 75

Appendix C

The balance of the material in this report is extracted from the report of the Armour Research Foundation - Research and Development of New Design Methods for Power Transformers (Contract No. DA 36-039 SC-5519).

Appendix C
Extracts from Armour Report

III. TYPES OF TRANSFORMER CONSTRUCTION

To meet the multitude of diverse transformer requirements, a designer has many alternatives open for selection. The features of a specification usually serve to guide the choices regarding construction. Other practical considerations such as material availability, past manufacturing experience, available tools and machines limit the types still more. The designer must first select a basic type of core and winding configuration. Then there is sometimes latitude in the choice of winding construction. The core and coil unit are then usually treated in some manner to provide mechanical strength, protect against environmental conditions, and sometimes to improve dielectric strength. Some transformers are used with core and coils exposed; others have coverings for the windings only; and still other units are placed in a container with some filling material. The filling material may be one of many solids or oils. The container itself may be sealed to protect the unit from the environment, or the filling solid may be left partially exposed. Bushings are to be selected for bringing the transformer terminals to the outside. Other details such as mounting provisions for the core and coil unit and for the container are to be taken care of.

Factors in the Selection of Core Type

The types of core construction commonly employed for power transformers in the sizes being considered are the core type, the shell type, and the "simple" type as illustrated in Figure 5. For many transformer applications, there will be no compelling reason for selection of one in preference to the other two, although each has certain advantages and disadvantages.

It should be recognized that selection of a core type, similar to Figure 5a, does not imply a selection of design details of the core. For example, the core type may be made with various proportions; it may be a wound core or a stacked core; if wound it may be cut in various ways or not at all; if stacked, the laminations may be "L" shaped, "I" shaped, "U" shaped, or any of several possible combinations. Similar freedom of design may be had within the bounds of either of the other types. Selection of a type of construction then, is only one step in the design of a core, though obviously one of the first steps.

Examination of the three basic core types reveals certain differences which might become important in making a selection. The core type transformer should, for minimum leakage reactance, have the primary winding divided equally between legs and the secondary windings divided likewise. In case there are tapped windings, this maintenance of balance could become a serious complication. The necessity for winding two coils instead of one is an important cost factor. On small transformers particularly, the space used up by insulation in two coils can be appreciably greater than that required for a single cell.

On the other hand the core type permits low leakage reactance, low coil build, and good dissipation of heat from the coils. When creation of, or susceptibility to, stray fields is a factor of importance, balanced core-type construction is distinctly superior to either of the single coil types. Balanced construction is that which has thorough, systematic and symmetrical intermingling of the primaries and secondaries. Occasionally in transformer design there is need for a great deal of coil area for terminals and leads. Core type construction is good in this respect, although not necessarily better than the simple single coil core type, since more terminals will generally be required in the former type.

The shell type contruction of Figure 5b provides good exposure of the core surface to the cooling medium. Even though the usual problem is that of cooling the coil, a cool core can provide an excellent path for flow of heat from the coil. The shell type construction is simple to assemble, clamp, and mount, and in general is economical. Where protection of the coil is required, the shell type is readily adaptable to use with simple end bells; and where hermetic sealing is required it may be simply mounted by means of through bolts for combination core clamping and mounting. There are probably more standard sizes of E-I laminations available to transformer manufacturers for use in shell type cores than there are other laminations for the two-leg cores. This might be particularly important to small businesses. Occasionally it is desirable to get half-turn voltages--a feat easily accomplished with a shell type design, but usually quite impractical for either of the others.

The simple type of Figure 5c permits maximum utilization of window space, an important factor in small transformers. There is only the insulation for one coil using up window space; and all the clearance

between coil form and core can be taken on the outside so that the window space is entirely usable. Neither of the other types has both these advantages. Construction is simple and economical, coil cooling is good, and there is a large coil surface available for terminals. From an academic point of view it would appear that a unit of this type could always be changed to core type with a saving in copper simply by using the same identical core. From a practical point of view, this may not be economical, or even possible in some cases. It might also appear that conversion to shell type, using the same coil, would save iron. But this is not necessarily true when coil area is needed for terminals or for cooling.

In summary of the above discussions of construction types, there follows a list of questions to be answered in selecting the basic construction.

1. What kinds of cores are available? This will in many cases be the major consideration.
2. What available cores are best proportioned to meet the space and mounting requirements?
3. Will space for terminals and leads be a problem?
4. Is lowest leakage reactance required?
5. Are stray fields important?
6. Is mechanical protection of coils required?
7. Are there twin secondaries requiring precise matching?
8. Will half-turn voltages be required?
9. Are insulation requirements such that absolute maximum use must be made of window space?

Winding Construction

The conductor of the winding must supply the required ampereturns without voltage breakdown, either to external points or as short-circuited turns within the winding. Breakdown is considered to include both

complete electrical breakdown and corona whenever the latter is a problem.

The general types of windings which are used for power transformers are: precision-wound (Fig 6a), random-wound on bobbins (Fig 6b), and wound with layer insulation (Fig 6c). Each general type of winding has its advantages and disadvantages. The advantages and disadvantages can best be discussed if the applications of each type are considered.

Precision-wound windings have the highest possible space factor. Although precision winding need not be limited strictly to the use of round conductors, higher space factor is realized than for other types of construction when using a round conductor. In practice, the conductor is wound on a form with side supports. When using round conductors, each layer, except the first, is so wound that the conductors lie in the grooves formed by the round conductors of the preceeding layer. A method must be provided for obtaining taps when required. Precision-wound windings have relatively high thermal conductivity because the only material with relatively high thermal resistivity in the winding is the small amount of insulation on the conductor. Among the disadvantages or limitations are the following factors. There is no insulation other than the conductor coating, which must be adequate for the voltage between layers. Precision-wound windings will also have a relatively high distributed capacitance, but this will usually not be a problem with power transformers.

Very small transformers are sometimes wound on bobbins. A bobbin consists of a tubular form, which is usually rectangular for transformer applications, plus flanges or end supports. The bobbin provides support of the winding as well as insulation to the core. It may be molded from an insulating material such as nylon, or fabricated from paper or other insulating material. Windings may be wound on bobbins or in layers with the precision-wound lay shown in Fig 6a, but a common practice is to random-wind on bobbins without having controlled layers. When this is done, the conductor insulation must be adequate to provide for any portion of the winding voltage that may occur between turns. The volts between turns of such random-wound windings may be as much as the full winding voltage. Random-wound windings are thus limited to the voltages permissible for the conditions which may exist. The space factor of random-wound windings on bobbins may be better than the space factor of

windings wound with layer insulation but poorer than the space factor of windings wound with a controlled lay. The amount of control, and whether or not layer insulation is used, has some effect on the winding speed of windings wound on bobbins. The relatively good space factor of most fine wire windings wound on bobbins without layer insulation is perhaps the greatest advantage of such windings. Currently, the greatest application of transformer windings wound on bobbins is small audio transformers.

For power transformers the most common type of winding is the layer-insulated type. This type of construction usually has the disadvantage of giving a poorer space factor than for precision or random-wound coils with the resulting increase in size and weight of the transformer. The dissipation of heat from the internal surfaces of the winding is also much poorer because the electrical insulation between layers is a good thermal insulator. However the necessity for adequate insulation means that these disadvantages must be tolerated. The use of layer insulation improves the voltage breakdown strength between layers. The flexibility in the choice of materials and thickness of materials provides a valuable tool in the hands of the design engineer. Not only does the use of layer insulation increase the puncture breakdown strength at points of relatively high voltage stress, but layer insulation also provides a means for increasing the creepage breakdown voltage. In recent years the increased number of materials has greatly increased the utility of layer-insulated construction. Layer insulation may be used with any size transformer in the size and temperature range covered by this project. Taps are more easily placed in windings wound with layer insulation than for the other types of windings.

Mechanical and electrical properties of transformer insulation may be adversely affected by moisture, industrial vapors and foreign materials in general. Impregnation of the windings with a suitable compound helps exclude these undesirable substances. The impregnant, in addition to being a good insulator, should not be so brittle as to crack under temperature strains or rough handling, and must not chemically attack conductor or insulating materials used in the transformer. Small transformers are most conveniently impregnated assembled with the windings in place on the core. This practice avoids the possibility of cracking or otherwise penetrating the seal effected by the impregnant when inserting the laminations or core.

Although simpler and cheaper processes such as dipping the transformer into molten wax are sometimes used, vacuum impregnation provides the most effective protection. In this process the windings are heated in a vacuum until nearly all moisture has been removed. Before atmospheric pressure is again admitted to the vacuum chamber, the windings are immersed in the impregnating medium. Upon release of the vacuum, atmospheric pressure forces the impregnant into the evacuated spaces inside the windings. After a suitable interval the assembly is removed from the chamber and excess impregnant is drained. If the impregnating material was introduced in a solvent, vacuum baking is necessary to drive off the solvent.

There is a large variety of materials available for use in winding impregnation. The broad classes of these materials are the varnishes, waxes, asphalts, polyester resins, and oils. An oil impregnation treatment is limited to units mounted in oil-filled containers. Properties and applications of specific impregnates are discussed in a following chapter.

Open and Enclosed Construction

There are three principal classes of construction with regard to open or enclosed assembly of the transformer. These are the open, the compound-filled, and the oil-filled types. Units having a shell-type, partially-exposed core and end caps to protect the winding are to be considered as an open type. Also to be considered as open type are the so-called "encapsulated" transformers, which are coming into wider use at the present time. The transformers have a fairly heavy coating of material over the core and coil unit to provide resistance to environmental conditions. Some of these transformers have successfully passed military requirements for Grade I, Specification MIL-T-27, or those units most resistant to moisture, in effect, hermetically sealed. Compound-filled types include those with both hermetically sealed and unsealed cases, containing the core and coils immersed in some solid material. Oil-filled types considered here are hermetically-sealed. Due to certain special features of high-temperature materials a comparison will first be made for low-temperature transformers. Major considerations of the properties of the different types of construction that affect the performance of the transformers are: cooling and temperature limitations, size, voltage limitations, altitude, and

manufacturing problems. References to physical sizes by KVA are based on the equivalent physical size of 60 cycle transformers.

The cooling properties of a transformer depend upon the amount of heat that must be dissipated, and upon the thermal resistance of the paths that this heat must travel to leave the transformer. In the determination of the amount of cooling necessary for the usual application of a transformer, it is the usual practice to disregard the amount of cooling due to heat being conducted from the transformer through the mounting surface. The material on which the transformer is mounted may vary on different installations, and its ability to conduct the heat from the transformer is unpredictable. Some ASA and Underwriters' Laboratories specifications for temperature measurements on transformers recognize this possibility for variation in installation conditions by making temperature tests in a heat-run box made of asbestos material and specified dimensions. The transformer is supported a short distance above the base of the enclosure by wooden cleats, making contact only at the mounting flanges on the transformer. There may be instances where it is desirable to take advantage of known applications where the transformer will be installed on a heat-conducting surface. In such instances the design may be made such that the path through the mounting surface may be considered a major heat-flow path. Except for special applications it is assumed that all of the heat passes from the external surfaces of the transformer to the surrounding atmosphere by convection and radiation only. For all types of transformer construction the heat travels to the surfaces of the core and coil, including internal coil ducts, by conduction.

In the compound-filled construction, the heat travels from the core and coil surfaces to the external transformer surfaces by conduction through the compound. For oil construction, the heat travels from the core and coil surfaces o the tank walls by conduction through, and convection of the oil. While in very small oil-filled transformers a considerable portion of the heat will travel through the oil by conduction, in larger transformers most of the heat from the core and coil surfaces is carried to the tank walls by the convection of the oil. Since the thermal conductivity of the common "loaded" compounds is higher than that of oil, small transformers may advantageously be filled with loaded compound instead of oil when the voltage requirements can be satisfied.

Compound-filled types may need to be operated at lower losses than open types, in order to keep the temperature rise within limits, if low thermal-conductivity compounds are used. It may also be necessary when there are air voids in the case, when the core and coil unit is poorly impregnated, or when the case is inadequately filled with compound. Since heating is more of a problem with large units than with small units, it is particularly important that larger compound-filled units be well impregnated and adequately filled with a high thermal conductivity compound. In large units it may be desirable to use oil filling to provide more effective cooling. This will reduce the tendency toward increased size of compound-filled 60 cycle transformers larger than approximately 1 KVA. Open types of transformers, which do not have the additional thermal resistance caused by either the compound or the oil, may be efficiently cooled up to the maximum sizes being considered.

Oil-filled types may be efficiently cooled over all transformer ratings and voltages. However, in the voltage range where insulation is determined by mechanical rather than dielectric strength requirements, oil-filled construction offers limited cooling advantages over other types in the sizes of interest here. When high voltage insulation is necessary, the insulating advantages of oil-filled construction will give relatively better proportion of insulation to copper. This may permit more efficient overall cooling. All types of construction using low-temperature materials are limited to the same maximum operating temperature and are required to operate over the same range of ambient temperature . The temperature limitations affect transformer size required to insure adequate cooling so that the temperature rise over the ambient will not result in excessive operating temperatures. Related to cooling is the ability of a transformer to withstand reasonable overloads (not short-circuit conditions) for short periods of time without overheating. Oil provides a highly effective thermal capacity which may be advantageous for some short-period overload operating conditions. There may be an undesirable effect of deterioration of the oil if excessively high localized temperatures occur too often, or for too long periods of time.

Ventilating ducts may be placed in the coils and between core and coil to improve transformer cooling. This increases effective cooling surface areas, but at

the expense of space. Ducts can sometimes be utilized to reduce transformer size for a particular temperature rise. At the higher voltages (10 KV test and above) and at very high KVA power ratings, regardless of voltage, oil-filled transformers have less weight and volume than the other types. In general, oil-filled, 60 cycle transformers rated below 2 KV and 10 KV test voltage usually will not require ducts, while units rated approximately 20 KV test and above usually will require ducts.

Oil filled transformers must include some method for accommodating the expansion of the oil. (Oil has an expansion of 8% for 100° C. temperature change). A gas-filled space over the oil may be used. With this method, the gas volume must be selected such that the internal pressures are within limits over the entire range of temperatures that the oil may undergo. This method, however, is usually not satisfactory for transformers of high voltage ratings that must operate in any position. An expansion device, such as a metal bellows assembly, which is capable of maintaining the case or tank completely filled with oil is often applied. Both of these methods increase the overall volume. To keep size to a minimum, the oil in a transformer may be displaced by materials such as sand, gravel, glass marbles, or clay pellets. By these means, it is sometimes possible to reduce the total expansion and contraction requirements to the extent that they may be accommodated by flexure of the tank walls. These filling materials impede the circulation of the oil and reduce the internal cooling efficiency. In addition, the higher densities of these materials may increase the overall weight of the transformer even though the volume is reduced. For small units the oil volume may be so small that no filling material is required. Despite the expansion problem, the higher internal cooling efficiency and dielectric strength of oil give a size advantage over other types of construction in the larger KVA and voltage ratings. The addition of an enclosing case with oil are in these instances offset by savings in size of core and coils due to higher permissible voltage stresses and higher current densities.

The number of manufacturing problems are related to the complexity of the type of construction. Open units, being the simplest, are usually accompanied by the fewest manufacturing problems. Compound and oil-filled types requiring a case, bushings, and other items have the greatest number of problems. Leaks are

probably the greatest curse to manufacturers of oil-filled transformers and are likely to occur at any seam or joint of the case or between the case and the bushings. Proper soldering or welding techniques are necessary for all joints to keep leaks to a minimum. Sealing of the tank must be carefully done. The volume of oil in the tank must be the proper amount for the temperature at which the filling is done. For units with an air space, this involves careful adjustment of the oil level. In completely filled units, it involves clamping the bellows at the proper stroke. If the cushion is to be an inert gas, care must be taken that all air is excluded. For units that are completely filled with oil, it is important that no small void or bubble be left. While the oil will absorb some of the gas, excessive amounts will appear as bubbles, and corona may occur.

For otherwise equivalent transformers, open core and coil construction is usually the least costly, followed by compound-filled and oil-filled construction. Oil-filled units must have an enclosing case, and bushings must be carefully treated, filled and sealed to avoid oil leaks. High-voltage transformers in the sizes considered by this project may often be made smaller and less costly with oil-filled construction by taking advantage of the better cooling and insulating properties of oil for such applications. In general, however, the cost of oil-filled transformers will always be greater than other types which can be built in similar overall sizes.

High Voltage Problems

The low dielectric strength of air, together with susceptibility to internal corona, limits the use of open and compound construction to the lower voltage designs. While the division point is not clearly defined, transformers with test voltages over 10,000 are usually of oil filled type regardless of volt-ampere rating. Oil construction has been applied to transformers of much higher operating voltages than the 50 kilovolts considered here. Nevertheless, certain precautions are necessary. It is desirable that the core and coils and all internal leads be under oil. The higher dielectric strength of oil permits short clearances. Corona is prevented more easily if small

diameter leads are under oil. Completely filled transformers, with a bellows to provide for expansion fulfill these conditions, and transformers with a gas space above the oil may be so constructed by placing the bushings beneath the oil level. It is often advantageous for bushings to be mounted on the cover of high voltage units even though a gas space above the oil is used. For such units, proper selection of bushings and insulation of the leads will prevent corona and voltage-breakdown difficulties. Corona may not only be a source of radio interference, but may be the cause of insulation deterioration which eventually results in a voltage breakdown. It is, therefore, desirable that corona be maintained below a tolerable level. One of the greatest advantages of oil construction is its low corona level.

Open and compound-filled transformers are most susceptible to corona. After the treating and impregnating processes, small pockets of trapped air may remain in the insulation where corona may begin. Oil construction, however, gives much lower levels of corona at high voltages. Since the dielectric strength of oil is considerable greater than that of air, much higher voltage stresses are permissible. The usual treating and oil impregnation processes normally do not give rise to the trapped-air pockets which induce corona. Except for unusual conditions, corona is not present in oil until breakdown is approached.

To eliminate corona requires that bushings or terminals be carefully selected. Many bushings which pass high-voltage tests show considerable corona at the operating voltages. Two types of bushing construction which have been successfully applied to high voltage designs are the "draw-through-lead" and "through-stud" types shown in Figures 7a and 7b. Both may be designed to eliminate highly stressed fields in regions of low dielectric constant and to give satisfactory performance as regards corona. The type of Figure 7c must be designed so that internal corona is not present during operation.

Construction for High Temperatures

The use of high temperature insulating materials has attained wide-spread use in recent years for reducing the size of transformers. For units which must operate in very high ambient temperatures, their use is required. Since this is a rather recent development, it is reasonable to assume that full

advantage of these materials have not been made and that all of their disadvantages have not been encountered. Disadvantages of these materials as compared with low temperature materials are: higher cost, lower dielectric strength, and mechanical properties not as well adapted to transformer construction. The advantage of obtaining a smaller transformer justifies a higher cost in many cases. However, the higher cost tends to limit the use of high temperature materials to those applications where their properties are necessary. The high temperature materials, in general, have lower dielectric breakdown strengths than most low temperature materials (transformer oils, kraft papers, wire enamels). Therefore, a high-temperature design requires more care. In low voltage units, insulation is often determined by mechanical requirements instead of voltage. Where there is no special insulation problem, as in low-voltage units, the greatest advantages in using high-temperature insulation may be realized. In high voltage units, it is possible that the increase in insulation required for dielectric strength will not permit a saving in size, particularly in small ratings. In general, it can be stated that high-temperature insulations are limited to the lower voltage and larger capacity designs when the purpose of using them is to save size through higher temperature rises. Disadvantages due to poorly adapted mechanical properties can usually be eliminated by design, by manufacturing techniques, and by increased care in construction. These do not prevent the use of high temperature insulation, but rather increase the cost of using them.

Comparing open and liquid construction for high temperatures, it is found that open core and coil construction will permit smaller sizes. Silicone oil filled units for high temperature application, as for low temperature oil-filled units, require that a means be provided for expansion. High temperature units must generally operate over a wider temperature range of the liquid, and this together with the greater coefficient of expansion for the silicone oils (10% to 12% for a 100°C temperature change compared to 8% for oil) increase the expansion problems. The necessity of keeping the liquid volume small is indicated. When a gas cushion is used to provide for expansion in place of an expansion device it is important to consider the possibilities of corona at low internal pressures. Completely covering the coils and leads is one solution.

The problems of high-voltage design using high temperature insulations should be mentioned. Some insulating materials show high initial values of dielectric strength, but exhibit short life when subjected to high temperatures and high voltage stresses simultaneously. Other materials exhibit good dielectric strength and long life if tested alone, but when used in combinations, for example, the filling liquid and the layer and turn insulation in coils at relatively high voltage stresses, the life is short. Therefore, as promising new materials become available, they should be used with caution.

Extensive development and construction of high-temperature transformers has been carried out in recent years by the Bell Telephone Laboratories, under Contract No. W33-038 ac 13939, and by the Chicago Transformer Company under Contract No. W36-039 sc44500. Hermetically sealed and open types of construction have been studied. Directions for the use of materials and techniques of production are reported for miniaturized high temperature units.

IV. ELECTRICAL INSULATING MATERIALS

The information contained in this section is intended to acquaint the design engineer with properties of representative types of electrical insulating materials most generally used in the design of insulation systems for transformers. It also includes suggested applications of each material and sources of supply. Data covering properties are based on averaged published values submitted by the different suppliers. These data are to be used onlyas aguide and not for specification pruposes. Data for each material or class of material are presented in the form most commonly used by manufacturers of the materials.

Electrical insulating materials are defined as materials which offer a very large resistance to flow of current, and for thet reason they are used to keep the current in its proper path along the conductor. The primary purpose of insulation is therefore electrical, and in the early days this was the only purpose. As service requirements have broadened, insulation has gradually assumed a thermal, mechanical and even chemical burden as well. Often properties to meet such secondary requirements are so necessary that they, rather than the electrical properties, limit the choice of material. But manufacturing methods can nullify the best materials. Proper care must be taken not to injure the insulation by tearing, abrasion or scorching. Insulation is probably more important than any other component in determining the conditions under which an electrical unit can operate without damage or rapid shortening of life. The thermal, mechanical, chemical, or electrical abuse that the insulation encounters and the insulation's resistance to these conditions, determine its usefulness. Most electrical equipment is designed to do a specific job, and the insulation should be suitable for that purpose. It is best to determine the insulation requirements first and then choose the most economical material.

Among the representative insulation materials which are at present in wide use, or which show promise for application to transformers are the following:

Magnet Wire Insulation
Electrical Insulating Papers
Varnished Tube and Saturated Sleeving
Varnished Insulating Paper
Varnished Glass Cloth

Silicone Varnished Glass Cloth
Teflon Coated Glass Fabrics, Tapes and Laminates
Industrial Laminates
Mica Products
Electrical Insulating Varnishes
Silicone Electrical Insulating Resins
Silicone Rubber Coated Glass Cloth
Polyester Resins
Potting and Treating Compounds
Untreated Cotton Cloths, Tapes and Sleevings
Untreated Glass Cloths, Tapes and Sleevings
Glass Yarns
Pressure Sensitive Electrical Adhesive Tapes
"Scotch-Weld" Electrical Insulating Film No. 70, Polyester Film

These materials are discussed in detail, and tables of important electrical and mechanical properties are given in Appendix A, along with partial lists of suppliers, from whom additional information can be obtained.

Insulation Classification

To adequately describe an electrical insulating material in terms of its application, it is desirable to define both its operating temperature and its life at that temperature. This necessarily means that a particular material will have several classifications, depending on the temperature at which it will be used.

The Signal Corps desires that the system of classification given below be used, and has expressed the conviction that this system will be generally adopted in preference to the commonly known AIEE-ASA (American Institute of Electrical Engineers, American Standards Association) classification system which assigns specific materials to temperature classes designated as O, A, B, H, and C.

The preferred classification system uses a two-letter designation for any material; it defines the maximum contemplated temperature (Table 4-1) by the first letter and the insulation life expectancy (Table 4-2) by the second letter.

Table 4-1

Insulation Temperature Classes

Symbol	Maximum Operating Temperature - °C
A	to 105
B	from 105 to 155
C	from 155 to 200

Table 4-2

Insulation Life Expectancy

Symbol	Life-hours
W	10,000 or more
X	1,000 minimum
Y	100 minimum
Z	10 minimum

An important difference between the systems is that in the Signal Corps system, specific materials are not necessarily assigned to only one class and life, while in the AIEE-ASA system, a specific material or combination of materials is assigned only one letter. Thus, for example, in the proposed Signal Corps system, a certain varnished paper might be classified AW, BY and CZ. It would be the task of the transformer user, the insulation manufacturer, and other interested parties to determine the different ways in which varnished paper, alone or in combination with other materials, might be used. The Signal Corps system seems to avoid many exceptions and inconsistencies of the AIEE-ASA classification.

There are several reasons why the AIEE-ASA

system of classification, with its associated terminology, is not suited for use by the Signal Corps and other military services. The major reason is that requirements for variable insulation life are not adequately included. A material which is expected to have a long life at one temperature is often quite suitable for an application where a much higher temperature is encountered, but where required life is shorter. Comparatively short-life requirements, compared to the usual 20-30 year life of commercial equipment, are satisfactory for many needs of the military services. Another objection to the AIEE-ASA system is that the terms "organic" and "inorganic" are used to characterize low-temperature and high-temperature materials, respectively. However, some chemically-organic materials are suitable for use at the highest temperatures to which insulation is normally subjected. Therefore, the terms organic and inorganic are not very suitable for separating low-temperature and high-temperature materials. With the introduction of new insulation materials in recent years, as well as new methods of application, there has been an increasing need for a different classification system, particularly for military requirements.

Magnet Wire Insulation

Magnet wire is one of the very important ingredients entering into the manufacture of any wound electrical product, and may be defined as any insulated wire (copper, aluminum, etc) that is used in the form of coils for the purpose of interchanging electrical and magnetic energy. General types of insulated magnet wire available are:

1. Film-coated magnet wire: vinyl acetal (known as "Formex"* or "Formvar"), oleo resinous (conventional enameled wire), nylon* (Polyamide), and teflon* (Polytetrafluoroethylene), ceramic insulation covered with silicone resin (Ceroc 200)* or teflon (Ceroc T,* Ceroc ST*). (* Trade name).

2. Fabric-covered magnet wire: Cotton yarn, silk yarn, nylon yarn, glass yarn, and asbestos fibers.

3. Combinations of film coated and fabric covered magnet wire. For example--Vinylacetal film coated wire plus glass yarn covering.

4. Paper insulated magnet wire.

The selection of a magnet wire is based upon: wire space factor, mechanical properties, electrical properties, chemical properties, and thermal properties.

Of greatest importance for transformer coils are enamel and formvar coated wires. These are very similar in electrical properties, but formvar coated wire is characterized by toughness, flexibility and a high resistance to mechanical abrasion. Enamel, formvar, nylon, cotton, silk and paper covered wires, assuming impregnation, can be used in Class AU transformers, while teflon, glass and asbestos are used in Class CW transformers. Nylon-enameled wire is similar to formvar in possessing toughness and ability to withstand abrasion. Cotton is used principally as a mechanical separator and to absorb binding impregnates. Paper covered wire gives a better (higher) space factor than cotton, is resistant to abrasion, and has a high dielectric strength. The film coated wires tend to have higher space factors than the fabric covered wires, a feature very desirable in transformers. Dielectric strengths of some types of magnet wire are given in Table A-1 of Appendix A. Other data on magnet wire properties are given in manufacturers literature listed in Appendix D.

Electrical Insulating Papers

There are many types and grades of electrical insulating papers. In general, they can be roughly classified into the several major categories given below.

1. Non-Chemical Papers: wood pulp or kraft papers, rag and part-rag papers, and rope papers.

2. Chemical Rag Papers: vulcanized fiber or fish paper.

Each of these has certain physical and electrical properties from which insulation systems can be designed to meet the necessary application requirements. For test methods of untreated paper used as electrical insulation refer to A.S.T.M. Standards D-202. For short time dielectric test method refer to A.S.T.M. Standards D-149.

Kraft electrical insulating paper is a paper made entirely from wood pulp produced by the "sulphate" process. It can be obtained in different densities or

types such as, "super calendered", "machine calendered", "medium finish" and "rough finish". Thicknesses available range from .00025 inch up to and including .030 inch. Super-calendered kraft is a high density paper having a highly-glazed surface finish. Rough-finish kraft is a low-density paper having a minimum amount of calendering. Machine-calendered kraft is a medium density and medium finish paper. Machine finish is a medium density and medium finish paper similar to a machine calendered kraft, except that in thicknesses below .005" it is slightly better mechanically.

The various types and thicknesses of kraft electrical insulating paper lend themselves to many electrical insulation systems and are widely used in all types of transformers. They are generally used for coil layer insulation, coil wrappers, in-between insulation (between primary and secondary windings), lead separators, ground insulation, insulating washers, spool bodies, etc where a good electrical insulating paper is desired but requirements indicate the suitability of a low cost electrical insulating paper. For physical and electrical properties of three typical types of kraft electrical insulating paper see Tables A-2, A-3, and A-4.

The all-rag type of electrical insulating paper is made from cotton fibers obtained from clean cotton rags, but receives no chemical treatment such as the vulcanized fiber material. Features of this type of paper include exceptional toughness, tensile strength, tear resistance and dielectric strength. Suggested applications--coil wrappers, layer insulation, coil flanges, in-between-insulation (between primary and secondary windings), etc. Properties are given in Table A-5

The part-rag type of electrical insulating paper is composed of cotton fibers from clean cotton rags and chemical wood pulp fibers of the highest quality. Physical characteristics such as toughness, elongation, tensile strength and tear resistance are good but are somewhat lower than the all-rag type paper. The part-rag type of paper is often used where a superior quality paper with good dielectric strength is desired but requirements indicate the suitability of a lower-priced electrical insulating paper. Suggested applications are similar to those for all-rag paper. For physical and electrical properties, see Table A-6.

Rope electrical insulating paper is made from rope fibers, producing a sheet having good tear strength, flexibility and extensibility. It is suitable for low-voltage insulation requiring extreme tear strength. Suggested applications--coil insulation, wrappers, core insulation, ground insulation, lead separators, washers, etc. (Table A-7).

The basis of vulcanized fiber (sometimes called fish paper) is cotton fibers obtained from clean cotton rags which are made into special types of paper. These various cotton cellulose papers are chemically treated so that the cellulose fibers gelatinize and form a homogeneous structure. After gelatinization the chemical is removed by a leaching process which displaces the chemical with water. The sheet of material then passes through a drying operation and as the water is removed, shrinks in thickness so that a dense, tough, resilient hornlike product results. Calendar rolls then provide the desired surface finish. Suggested applications are: coil wrappers, spool flanges, field coil insulation, slot insulation, end laminations, washers, arc shields, formed slot wedges, formed specialties, etc. It can be obtained in sheets, continuous rolls, tubes and rods. (Table A-8).

** (See next page)

Varnished Insulating Paper

Varnished paper proves both economical and satisfactory for applications where the higher mechanical strengths furnished by varnished fabrics are not required. The varnished papers in general possess a higher dielectric strength per unit thickness than the varnished textiles and, therefore, permit the use of thinner insulation for a certain desired dielectric strength. Four different types of paper are generally suitable to provide maximum versatility of characteristics. Thicknesses range from .00075 to .020 inches. For these reasons varnished paper can be used for a variety of electrical insulating applications in such apparatus as motors, electronic equipment, ignition and communication systems, transformers, and coils. It is frequently used as layer insulation in transformers, for lining capacitors, and as insulating washers. The thin thicknesses are ideal where clearances are small and high dielectric strength is needed. The heavier thicknesses are suited to work where higher mechanical strength is desirable. For properties see Table A-10.

**

Varnished Tubing and Saturated Sleeving

Varnished tubing is a flexible tubular product made from braided cotton, rayon, nylon, glass or other fibers, and coated, or impregnated and coated, with a continuous film of varnish, lacquer, a combination of varnish and lacquer, or other electrical insulating materials. Saturated sleeving is a flexible tubular product made from braided cotton, rayon, nylon, glass or other fibers, and coated or impregnated with varnish, lacquer, a combination of varnish and lacquer, or other electrical insulating materials. The impregnant or coating need not form a continuous film.

Grades of varnished tubing and saturated sleeving are identified according to their performance characteristics, as given in Table A-9. In all grade designations (for example, A-A-1 and H-C-1), the first letter designates the class and the second letter and the number designate the grade.

For further information covering the physical and electrical requirements and the testing of flexible varnished tubing and saturated sleeving used for electrical insulation, refer to "NEMA Standards for Varnished Tubing and Saturated Sleeving", Pub. No. VSI - 1950.

Varnished Glass Cloth

Varnished glass cloth, made in both full width cloth and straight cut tape, is impregnated with either yellow or black varnish baked to give a highly flexible, mechanically strong insulating material. The black or yellow varnish coating of the glass provides high dielectric strength for maximum electrical protection. The varnish treatment also makes varnished glass cloth moisture and abraision resistant. Electrical properties of varnished glass cloth are dependent chiefly on the nature of the varnish, the degree of impregnation between fibers, and the temperature which the varnish will stand. Electrical properties of glass cloth alone are only equivalent to the air gap of the interstices.

Transformers insulated with varnished glass cloth can operate at higher current densities than transformers insulated with ordinary materials. This assists in making possible the reduction in size and weight of electrical apparatus and at the same time saves critical materials. Varnished glass cloth has a high thermal conductivity. Typical uses of this material for transformers are: coil layer and primary-secondary separation, core and ground insulation, wrappers, lead insulation, taping, etc. (See Table A-11).

Silicone Varnished Glass Cloth

Silicone varnishes for high temperatures have been developed which coat exactly like low-temperature varnishes, but have much greater heat resistance. The unusual properties of silicone varnished glass cloth can be attributed to its unique composition, a combination of woven glass cloth and silicone varnish. Woven glass cloth is a very strong, flexible material having a higher heat conductivity than other common insulating textiles. By coating woven glass with silicone varnish, a continuous void-free material is formed. The silicone imparts dielectric strength and moisture resistance to the finished product, and has outstanding thermal properties. Its heat resistance and heat stability are far superior to most treating materials. Silicone varnished glass cloth and tapes are recommended for insulating all electrical equipment that is exposed to abnormally high operating and ambient temperatures, heavy overloads, and excessive moisture. Typical uses of this material for transformers are: coil layer and

primary-secondary separation, core and ground insulation, wrappers, lead insulation, and taping. Properties are given in Tables A-12 and A-13

Silicone Rubber Coated Glass Cloth

Silicone rubber coated glass cloth consists of selected glass fabrics completely impregnated and coated with silicone rubber. The coated fabric is processed at extremely high temperatures to insure complete curing throughout. It is recommended for uses such as gaskets, air ducts, a nd electrical insulation, wherever extremely high or low temperatures are encountered. Suggested uses as electrical insulation for transformers are: coil layer and primary-secondary separation, core and ground insulation, wrappers and taping. (Table A-14).

Polytetrafluoroethylene (Teflon) Coated Glass Fabrics, Tapes and Laminates

"Teflon", or polytetrafluoroethylene coated glass fabrics, tapes and laminates are products comprising woven glass fabrics impregnated and coated. For all grades the exposed surfaces consist of smooth homogeneous films of polytetrafluoroethylene. They possess a unique combination of desirable properties which suggests their value and use for a wide variety of applications. These products are expected fo find many uses in the electrical industry because of their high and low temperature resistance, good electrical properties, and good physical and handling properties. "Teflon" coated glass fabrics, tapes and laminates are more stable under compressive loads and more resistant to abrasion than "Teflon" unsupported sheeting. These fabrics, tapes and laminates provide electrical insulation meeting Class CW requirements. They may be used continuously at 250° - 270° C (482° - 518° F) or for short periods at somewhat higher temperatures. "Teflon" coated glass fabrics remain pliable at temperatures as low as -87.5°C (-100°F). The extremely low loss characteristics of these products make them of value in the construction of radar and electronic equipment. The laminates possess arc resistance of an exceptionally high order. Chemical and solvent resistance should also be of value in many electrical applications. The products as a class show a particularly important advantage in creasing characteristics.

Creasing parallel to the fibers or diagonally does not result in rupture of the film and consequent electrical failure. With respect to dielectric strength, recommended working stresses over long periods are much lower than shown in table of properties.

The properties of the material suggest the following uses for transformers and coils: Coil separators, core insulation, layer insulation, terminal boards, coil wrappers and tape. Properties are given in Tables A-16 and A-17.

Industrial Laminates

Industrial laminates comprise a group of plastics products in sheet, tube and rod form available in a variety of grades, properties and sizes. These products consist essentially of fibrous sheet materials, such as cellulose paper, asbestos paper, cotton fabric or mat, asbestos fabric or mat, nylon fabric and glass fabric which are impregnated or coated with a thermosetting resin binder and consolidated under high temperature and pressure into hard solid products of high mechanical strength.

The principal resins used in industrial laminates are phenolics. These are made by the chemical combination and partial polymerization of formaldehyde and phenolic bodies, such as phenols, cresols or cresylic acid under carefully controlled conditions. Another class of thermosetting resins includes the melamine resins. These are made by the chemical combination and partial polymerization of formaldehyde with melamine and with urea or urea derivatives or combinations. Copolymers of two or more of these resins may also be used. Still another class of thermosetting resins includes the silicones. These are generally alkyl phenyl silicone copolymers made by the condensation of hydrolytic products or organo silicon chlorides.

The resins are dissolved in suitable solvents to form varnish solutions with which the fibrous sheet materials may be impregnated or coated. After impregnation and drying, the material is cut into sheets which are stacked together between metal pressing plates and pressed under high temperatures and pressures to form laminated thermosetting sheets. Tubes are formed by rolling the impregnation sheet material upon

mandrels between heated pressure rolls and then either oven-baking or pressing the material in a heated mold until the curing or setting of the resin into the infusible form is completed. Molded rods are composed of laminations of impregnated sheet material which have been molded in cylindrical molds under high temperature and pressure, and then ground to size.

For a description of the chief characteristics of the NEMA grades of industrial laminates and the various forms available see Table A-18, and for physical and electrical properties, see Table A-19. For further information concerning manufacture, test procedures, and performance of laminated thermosetting sheets, tubes and rods refer to NEMA Standards Publication No. LP1.

Mica

Mica comprises a group of natural silicates distinguished by highly developed basal cleavage into thin, tough, flexible laminae. Properly selected and prepared, the mica used in electrical apparatus is the most generally satisfactory insulation known. Used as electrical insulation, it has exceptionally good electrical properties, such as dielectric strength and dielectric power loss, is stable under varying atmospheric conditions, and is particularly useful at elevated temperatures.

Natural mica is seldom used as electrical insulation, except in small pieces, such as capacitor insulation, mica washers, or other small spacers. This is because pieces of natural mica are usually too small, or cannot be formed to the desired shape. It is necessary, therefore, to split the mica as mined and re-assemble or re-laminate the "micasplitting" in order to use mica to best advantage in most insulating work. The re-laminated, or pre-formed mica is commonly termed "built-up mica", "pasted mica" or "mica plate". Built-up mica is a product consisting of superimposed layers of mica splittings about one mil in thickness assembled with thin coatings of insulating binder between each layer, and formed into composite sheets under heat and pressure. The thickness of the sheet is regulated by the number of layers assembled. Specific physical and electrical qualities are attained by the use of different grades of mica splittings and different compositions of binder. Shellac is chiefly used as a binder. Materials such as silicone resin,

alkyd resin and various other synthetic cements are also used as binders. Mica, or combinations of glass cloth and mica, or silicone varnished glass cloth and mica, cemented together with silicone binders are Class CW insulations intended for use where high heat and moisture conditions exist. Various types of mica products are produced.

Non-molding mica consists of mica splittings that are bonded with a synthetic or shellac binder to form a hard, rigid plate to be used in flat form. The binder content is lower than in other forms of pasted mica. In this type of mica, the binder is thoroughly cured and, although the built-up plate can be sanded, punched or cut to the desired shape and size, it cannot be bent or formed.

Molding mica consists of mica splittings that are bonded with a synthetic or shellac binder to form a hard, rigid plate to be used principally for forming or molding under heat and pressure. The binder content is appreciably higher than in non-molding mica, being in the order of 10 to 20 percent. In this type of mica, when in flat-sheet form, the binder is not thoroughly cured so that it is possible to be molded or formed when heated. During the final molding or forming process, the binder is further cured, the degree of cure depending upon the part and application.

Mica tape consists of mica splittings bonded with a special binder, usually between two layers of a special grade of tissue paper. The paper forms a support and provides the essential mechanical strength necessary for winding the tape in place. Thin cotton or glass cloth is also used to some extent in place of paper.

Cold flexible mica consists of mica splittings bonded with a special binder to form a sheet product having such flexibility as will permit of wrapping or winding into place without heating. This type is not as dense or as stable as the molding micas when cured, but is useful where it can be wrapped or formed into place without heating.

The term composite mica is used to designate a group of built-up structures in which mica is the most important insulating material but with which, in addition to the binder, there are included other materials

such as cotton cloth, glass cloth or paper. Most composite mica is produced in sheets to form a laminated structure, the supporting material providing the required mechanical strength for handling and the application of the material.

Mica tubing is generally made in five grades, classified by the percentage of mica and other material used in its fabrication. It is usually bonded with shellac to condenser paper, glass cloth, kraft paper or asbestos to give different characteristics. All grades of round tubing can be obtained in various inside diameters and wall thicknesses.

The standard grades of mica tubing are:

NEMA Grade 101 - 100% manufactured mica.
NEMA Grade 102 - 95% manufactured mica - 5% paper.
NEMA Grade 103 - 80% manufactured mica -20% paper.
NEMA Grade 104 - 50% manufactured mica -50% paper.
NEMA Grade 105 - 50% manufactured mica -50% asbestos.

Mica products containing materials such as shellac, alkyd or other ordinary binders or paper are classified as Class BW insulation, and those containing silicone as the binder, or combinations of glass cloth and mica, or silicone varnished glass cloth and mica cememted together with silicone binders, are classfied as Class CW. Properties are given by Table A-20.

Electrical Insulating Varnishes

An electrical insulating varnish consists essentially of a base and a solvent or thinner. The base may be a natural or synthetic resin blended or chemically combined with a drying oil. Drying oils commonly used are linseed, chinawood, soya and castor oils. Modern varnish bases may be of synthetic resins with or without a drying oil. The synthetic resins are usually of the alkyd and phenolic types. They may dry or harden by oxidation, by heat-setting or polymerization, or by combinations of these. Polymerization involves changing of a compound through the union of two or more similar molecules into another compound having the same elements in the same proportions, but a higher molecular weight and different physical properties. The present trend is toward varnishes of these types. Less generally used today are the bases of the oleoresinous type, using natural resins and asphalts blended with drying oils.

Air drying impregnating varnishes dry under normal atmospheric conditions. They are generally applied by dipping or brushing.

Baking impregnating varnishes are the most widely used electrical insulating varnishes since they usually have the best balance of characteristics. They can be separated into two groups:

1. Conventional, oil modified, or oleoresinous type. Excellent flexibility makes these varnishes ideal for parts subject to distortion. Most varnishes of this type are not suited to high speed rotating equipment, but they are used for field coils, stators, and fine wire coils where maximum mechanical strength is not a major consideration. Curing is accomplished largely through oxidation.

2. Thermosetting, synthetic, polymerizing or heat reactive type. Varnishes of this type cure mainly by polymerization and when they are heated at the proper temperature for a certain period of time, they "set" permanently. Even deep pockets of varnish are cured thoroughly since the synthetic resins "turn over" or cure almost simultaneously. Thermosetting varnishes are practically infusible with high resistance to heat. They are also characterized by excellent mechanical bonding properties.

Protective insulating coatings are used largely for the external physical and chemical protection they provide.

Most insulating varnishes are clear or black and derive their color from the materials of which they are composed. Choice of a varnish should be based on its performance not its color, since color is no indication of quality.

Insulating varnishes are used to perform four primary functions: to provide a mechanical bond to prevent electrical breakdown or other harm due to movement and abrasion of conductors, to provide electrical apparatus with adequate protection against oil, moisture, acids, alkalies, dirt and other harmful matter, to supplement or increase the dielectric strength of

other materials in the insulating system, and to compensate for deficiencies and limitations the insulating system or its parts may have.

In choosing the most suitable varnish for a particular application, determine which of the functions it must perform and to what degree. In addition to these functions check the following list of characteristics, considering those that the varnishes should have in order to perform the necessary functions:

1. Penetration-- The ability of varnish to reach and protect all parts of the unit.
2. Depth of drying--Incomplete drying has many disadvantages.
3. Binding and adhesive properties.
4. Heat endurance.
5. Dielectric Strength.
6. Insulation Resistance.
7. Chemical Stability or Permanence
8. Moisture Proofness.
9. Oil Proofness.
10. Alkali Resistance.
11. Acid Resistance.
12. Physical Toughness.
13. Flexibility.
14. High Softening Temperature.

The proper steps in using a varnish are often just as important as the qualities of the varnish itself. The processing cycle must be correct since it has a great deal to do with obtaining the desired balance of varnish properties. Usually the use of a baking impregnating varnish consists of pre-heating, maintenance of varnish condition dipping. draining and baking steps for the processing cycle. The chief methods of varnish treatment of windings are dipping, vacuum filling, pressure filling, and brushing or coating as coil is wound.

Pre-heating of units before dipping is advisable to dissipate moisture from the insulating system, thus permitting the varnish to replace this moisture so that improved electrical properties are obtained. It expands the conductors temporarily, allowing better varnish penetration as the conductors cool and contract. The rate of evaporation of the solvent is increased, reducing the time required for curing. Pre-heating diminishes the possibility of varnish pockets forming. The heat thins the varnish around the unit thus

permitting better flow of the excess varnish during draining. It also expands the air in and around the unit and when the unit is immersed in the relatively cool varnish the air contracts. This causes a suction or pulling of the varnish into the windings which gives more thorough impregnation. (Table A-21).

Silicone Electrical Insulating Resins

Silicone electrical insulating resins should be specified when electrical equipment is to operate at high temperatures or when it is subject to frequent overload conditions. An appreciable increase in power output per unit space is sometimes obtained with silicone-wound equipment. The resins have excellent resistance to water and to some chemicals but have rather limited resistance to steam. Where toxicity is an important design factor, silicones are recommended particularly at temperatures up to 230°C. In some cases, such as aboard ships, toxicity may be extremely important.

Several silicone insulating resins are available with a wide range of properties. Resins can be provided to give a hard, thorough curing insulation on coils and windings. Others are thermoplastic and sticky during initial bake at high temperatures. Silicone resins are also used to coat glass cloth or asbestos, and glass sleeving for insulated component parts. In general, silicone resins provide high temperature insulation as impregnating varnish for electrical coils, bonding varnish on asbestos and glass fibers for wire conductors, bonding varnish on mica sheets and mica tape, binder for glass cloth laminates, and coating varnish for glass cloth and sleeving.

In general, silicone resins are resistant to all commonly used inorganic reagents except sulphuric and nitric acids. They have a limited resistance to solvents, but are unaffected by lower aliphatic alcohols. They are slightly affected by glacial acetic acid and such aliphatics as gasoline. Silicones are strongly affected by chlorinated solvents, esters, light naphthas, aromatics and ketones. The principle advantages of the resins are high overload safety factor, excellent thermal stability, low water absorption high dielectric properties, excellent insulation and arc resistance, low toxicity, and low electrical loss factor.

Polyester Resins

Polyester resins are a group of synthetics whose basic products are thermosetting and which can be modified to produce a variety of materials ranging from soft gels, through rubbery elastomers, to hard tough solids. They are used in coils as filling and potting compounds, to leak proof porous materials against gases or liquids, for impregnating wood and other structural materials to impart greater dimensional stability and mechanical strength, for impregnating and bonding laminates, and as casting resins. Basically, in their clear, unmodified form, the polyester resin materials are fluids of low viscosities which when heated become transformed into solid, infusible materials. Their distinguishing characteristic is that, since they contain no solvents, the entire composition is converted, with the aid of catalysts, to a solid state during the curing cycle. This unique feature insures a complete utilization of the material and freedom from voids, in contrast to conventional varnishes which to one-half or more by weight are composed of inert, volatile solvents that must be expelled on baking.

The clear polyester resins may in general be used as conventional type insulating varnishes and, where applicable, may be applied by dipping, brushing, or vacuum-pressure technique. They have found particular applications for the impregnation of magneto coils and certain small transformer and control coils where freedom of voids is requisite for successful "dry" operation (i.e. without immersion in oil) at high voltages and severe conditions of temperature, humidity and altitude. Another benefit resulting from the complete filling of all voids is a substantially higher heat dissipation rate, which will either, for the same size coil, allow the output rating to be increased or, for the same rating, permit a reduction of the size of coil.

Other features of the polyester type resins are:

1. Oxygen is not required to effect cure.

2. No volatile products, such as water or ammonia, are formed during the curing cycle, and since they also contain no solvents, cure to a solid state with freedom from voids.

3. Excellent dielectric properties (dielectric strength, power factor at 125-150°C and its very slight change with increasing voltage being of particular importance in high voltage applications.

4. High mechanical strength.

5. Unusual moisture resistance.

6. Unaffected by mineral oils.

7. Outstanding resistance to most acids and alkalies.

The basic clear polyester type resins may be modified to fit them to a wide variety of applications. Some of the various physical forms available are clear liquids of low viscosity for impregnating coil structures, porous bodies, potting and filling, casting and similar applications; fluids containing large amounts of fillers for casting, sealing and cementing operations, and for coating applications; putties containing large quantities of fillers for cold molding operations; and varnishes for conventional coil treatment, fabric and paper coating for bonding and laminating. For data covering several typical unfilled polyester resins used for applications such as dipping, impregnation, and encapsulation of magnet coils and transformers, see Table A-2 3.

Potting and Treating Compounds

Potting or sealing compounds are those used for sealing by filling interstitial spaces in windings and between coil and case, as in transformers. They are neither intended nor suitable for penetrating the pores and capillaries of cotton, paper, or other porous materials, or impregnating of coil windings but only to fill up open spaces for producing greater rigidity of structure, excluding moisture and dirt, and gaining added insulation values and safety. The chief reason for the non-penetrating nature of potting compounds is that they usually contain mineral fillers, such as silica, flint, talc or cement, which is added for reducing shrinkage, raising the flow or softening point, or increasing the heat conductivity. The active bond in potting or sealing compounds is usually a solid, such as asphalt, resins (natural or synthetic),

pitch, or wax. A typical asphalt potting compound consists of a petroleum flux oil blown to a definite melting point and penetration, blended with a filler. Various types and grades of potting compounds are available to meet specific requirements.

Treating compounds are made specifically for the penetration of porous materials such as wood, asbestos board, cloth, paper and impregnation of coil windings, The purpose of treating compounds is to fill or nearly to fill the pores of insulating materials or coil windings in order to increase the dielectric strength, and to maintain much higher values by the exclusion of air, moisture or other deleterious material. They are asphaltic or waxy materials that are easily brought, by heating, to a liquid of uniform consistency.

The treating of transformer coils with treating compounds can be done either by the hot dip or vacuum-pressure methods. For good impregnation the vacuum-pressure treating method is recommended.

Typical properties of these materials are given by Tables A-24 and A-25

Untreated Cotton Cloths, Tapes and Sleevings

Untreated cotton products such as cloth, tape and sleeving are used primarily for the mechanical protection and separation they provide. The dielectric strength of untreated cotton products is equal to an equivalent thickness of air. The conversion of cotton fibers into cloth, tape and sleeving involves three major steps. First, the fibers must be spun into thread. Next, these threads are twisted together into yarn. If the thread is not twisted together with other threads to form yarn it is known as a "single ply" yarn. The major step is the actual weaving of the yarn into cloth, tape or sleeving. The weave consists of yarns running the length of the cloth or tape which are crossed by yarns running widthwise.

The use of cotton cloths in electrical insulation systems is very limited. Their major use is as a base for varnish treated fabrics. There are four general types of cotton cloth. These are: straight weave sheeting, bias weave sheeting, straight weave duck and drill. The straight weave duck is the same as straight weave sheeting, except heavier weight. Drill is a heavy cotton fabric having a diagonal weave.

For electrical purposes there are three general types of weaves for tapes. Plain weave tapes are the most widely used because they stretch sufficiently to permit snug conformance to irregular surfaces. Where greater thickness and strength are required, herringbone weave tapes are usually specified. This latter type of tape is also frequently called a webbing or stay binding. Non-elastic weave is the third type. It is a heavy tape used where stretch ability is not desirable. Specific applications for cotton tapes include lead and connection insulation, space filling, protective wrappings on transformer coils, binder insulation, and temporary or permanent tying and anchoring of leads or other components.

Cotton sleevings are made from cotton yarns which are braided to form a seamless, flexible, hollow cloth cylinder. They are characterized by extreme flexibility. This is due to the basic flexibility of the fibers plus the flexible nature of the braid. For most applications, flexibility is advantageous during assembly. The dielectric strength of untreated cotton sleevings is equal to that of air which exists in the interstices (open spaces) of the braid. For this reason the use of cotton sleevings is limited largely to mechanical applications where dielectric strength is not a primary requirement. They provide physical protection for all types of coil connections, motor leads, transformer leads, and wires on other electrical apparatus.

Untreated Glass Cloths, Tapes and Sleevings

Cloth woven of glass yarns is supplied by weavers in a wide range of specifications in regard to type of yarn, weave, treatment and finished thickness. The untreated base cloth is rarely used by electrical equipment manufacturers, without some form of treatment. It is usually impregnated with varnish, combined with mica, or further processed into glass cloth-base insulating materials. Glass cloths are woven from both continuous filament yarns and staple fiber yarns. In general, cloths made from continuous filament glass yarns are used as a base in varnished cloth and tape, and for glass-cloth baked pressure-sensitive adhesive tape. They are also used as a reinforcement in plastic laminates where high strength, low weight or minimum thickness is required. Cloths made from staple fiber yarns

are used only in making laminates, or for certain varnished applications where electrical characteristics and strength are secondary to bulk or padding requirements of the material.

Tapes woven of glass yarns are available in a wide variety of specifications regarding width, thickness, type of yarns and weave, and finished treatment. They are made of both continuous filament yarns (used in over 95 percent of all applications) and staple fiber yarns. The high tensile strength and dimensional stability of glass yarn tapes have warranted their use in the manufacture and repair of electrical equipment. Untreated tapes are generally used as coil wrappers, protective coverings, conductor insulation, mechanical reinforcements, etc. Whether applied in treated or untreated form, woven glass tapes are ultimately varnished--very rarely do they go into actual electrical service in an untreated form.

The requirements for the tape are usually mechanical in nature rather than electrical. Space savings are becoming more and more important in new designs. For these reasons there is an increasing requirement for thinner tapes with good mechanical strength. The use of thinner glass tapes is possible primarily because of their exceptionally high tensile strength, usually far in excess of all requirements. The thinner the tape the lower the price per yard. Generally, it is more economical to use the thinnest tape that is practical to meet the particular requirements of the application. The width of tape as well as the thickness, depends on the particular application for which it is used. For small coils or coils with complex curves, it is advisable to use a narrow tape in order to obtain a smooth wrap. Where a coil has a long straight section and only moderately severe bends, a wide tape is preferable.

Untreated glass-base braided sleevings or tubing are tubular fabrics of small inside diameter formed by braiding glass yarns. Most braided sleevings are available with continuous filament yarn construction although some special heavier wall sleevings are made with staple fiber yarns. The continuous filament sleevings are very smooth, have a silvery white sheen and realize a considerable savings in space over asbestos sleeving. They are characterized by extreme flexibility. This is due to the basic flexibility of the fibers plus the flexible nature of the braid. The dielectric strength of untreated glass sleevings is equal to that of air which exists in the interstices (open spaces) of the braid.

Glass yarns are made from very fine, highly flexible fibers of glass and provide the base for electrical insulating materials made of glass filament or staple glass fibers. Continuous filament yarns are made by twisting and plying strands of continuous filaments of varying diameters, ranging from .00023" to .00038". These filaments are mechanically drawn from molten glass and have a resemblance to natural silk or rayon in general appearance. Staple fiber yarns are made by drafting, twisting and plying slivers of fine staple glass fibers. The individual fibers may vary in length up to 15 inches, with an average length of about nine inches. They are produced by blast drawing of molten glass and resemble staple cotton or wool fibers in general appearances, although they are longer in length.

Pressure Sensitive Electrical Adhesive Tapes

Paper backed electrical adhesive tapes are adapted to the most modern coil winding machines and methods. They are widely used for such phases of coil construction as to hold coil windings in place, insulate pole positions and anchor insulated leads. Backings are purified crepe or flat-back paper unified by impregnation with an electrical grade saturating solution. The electrical grade adhesive is pressure sensitive--applied by moderate pressure. No heat, moisture or other treatment is required for firm adhesion. For physical and electrical properties see Table A-26.

Acetate backed electrical adhesive tapes have been designed for use on extremely fine wire coils and other applications which demand the ultimate in non-corrosive properties. Included in this group are the acetate film constructions with high dielectric strength, extremely good insulation resistance, excellent moisture resistance and non-corrosive under the most severe conditions. Because of the thinness, they are ideally suited for internal coil applications. The laminated acetate film construction is designed for greater tensile strength than the straight acetate film. It is composed of .00088" acetate film and .004" rope paper.

Electrical tapes with "thermo-setting" or "heat curing" adhesive were developed to overcome the tendency of conventional adhesives to become soft during

high temperature baking, preheating, or hot wax impregnating cycles. In addition, thermo-setting or heat curing adhesives provide increased resistance to the solvents present in varnishes during impregnation cycles. Softening of adhesives due to heat or solvents can result in decreased holding power and formation of undesirable pockets of soft, wet residue. Such pockets are especially objectionable in rotating electrical equipment due to a possible "throw-out" tendency during operation of equipment. Thermo-setting or heat curing electrical tapes are used for the same applications as tapes with conventional adhesives, but as a component of the complete insulating system they are more stable and their use minimizes possible volatiles in the system if exposure to heat or solvents is involved.

The rate at which electrical tapes with thermo-setting adhesive set is dependent upon the temperature to which they are subjected. After exposure to 250°F for 2 hours or 300°F for 1 hour the adhesive becomes firm and demonstrates greatly increased resistance to solvents. Maximum resistance to solvents is not obtained until the heat treatment period is approximately doubled. It is seldom necessary to extend the baking cycle beyond 2 hours at 250°F. Properties are given in Table A-27.

"Mylar" Polyester Film

"Mylar" polyester film is a highly durable, transparent, water repellent film. It is heat sealable only under special conditions. It is characterized by its high tensile strength and high impact strength even at low temperatures. The film shows good stability up to 150°C (302°F). The electrical properties of the film are such as to make it of interest for insulation and capacitor uses.

"Mylar A" and "Mylar B" are not water vapor proof. "Mylar B" is the same as "Mylar A" except it is treated to decrease static and improve surface characteristics. Properties are given in Table A-28.

"Scotch-Weld" Electrical Insulating Film No. 70

"Scotch-Weld" Electrical Insulating Film No. 70 is a 100% self-supporting film of synthetic resin materials.

It contains no plasticizers or fillers and converts by heating into a tough, high strength bonding material and insulator. After "Scotch-Weld" has been neatly wrapped around the coil or other electrical piece to be insulated it is subjected to heat high enough to produce complete curing action. The film softens as heat is applied, bonding to itself and adjacent materials to form a continuous, unbroken layer of insulation. The heat cycle chemically converts the "Scotch-Weld" film into a tough, moisture and solvent resistant insulator. When thermo-set it is resistant to heat, solvents, chemicals, moisture, and oil. Curing cycles may be varied (200° to 300°F) to suit the requirements of each particular job. Maximum hardness in the cured film is obtained by using maximum curing cycles. Tougher, more resilient films may be produced by using intermediate cycles of time and temperature. Care must be taken that the adhesive is not in contact with the conductor, because the adhesive carbonizes during curing. For properties see Table A-29.

INSULATION PROBLEMS OF TRANSFORMERS AND BUSHINGS

Factors Affecting Dielectric Strength

Experience has fairly well established the characteristics of most insulating materials as used in typical electrical apparatus which do not have to operate under extreme or unusual conditions of pressure, humidity, or temperature. The purpose of this chapter is to describe the changes in insulating properties under extreme conditions, with particular regard to the low pressures encountered at high altitudes.

Insulating materials may be classified into three braod groups: gases, liquids, and solids. Potential breakdown in all of these mediums is affected by some factors, such as the separation of two electrodes and shape of the electrodes. Some factors may be of great importance to one medium, but have little effect on other mediums.

Of the gaseous insulating materials, we are only concerned here with air. In an open-type transformer, air spaces may contribute to the insulation strength between the windings and from windings to core, although the paper and impregnating substance usually provide all of the dielectric strength needed. The dielectric strength of air has been expressed in terms of corona and breakdown potential measurements as found by test. Presence of corona without breakdown between two electrodes is usually associated with configurations having different voltage gradients at different points in the electric field. Corona has sometimes been considered as incomplete breakdown. A uniform electric field, that is a field in which the voltage gradient is constant, is exemplified by two infinite parallel plane, across which a potential difference is applied. For such electrodes the potential necessary to produce corona is commonly the same as the breakdown point. Current studies of corona phenomena in transformers and bushings have been made by Stanford University under Contract DA 36-039 SC 5552, "Corona dnd Dielectric Losses", and by the General Ceramics and Steatite Corporation under Contract AF 33(600) 18569, "High Altitude, High Voltage Terminals". Approximations of planes, spheres, rods and other electrode shapes have been used to test the dielectric strength of insulating materials. The dielectric strength of air depends principally on electrode shape, electrode separation, and pressure.

Other factors of importance are moisture, humidity, temperature, frequency (for an alternating voltage test), and the time duration of a potential stress. The effect of separation of electrodes on potential breakdown has been given by Montsinger[3] as a relation of the type:

$$V = At^n, \qquad (5\text{-}1)$$

where A = a constant,

t = separation,

n = a constant in the range of .5 to 1.0.

This empirical formula with proper constants has been found to correlate well with test data for many insulating materials and electrode types. For the usual case, in which the exponent n is less than one, the equation means that insulation strength is not proportional to distance. In other words a small spacing of test electrodes will withstand a greater gradient than large spacings. An example is the low-frequency insulation strength of air between two plane electrodes as given by Figure 8, for strength in RMS alternating kilovolts with varying gap, as adapted from Schumann[7]. The linearity of the curve over most of the range indicates correlation with equation (5-1) which for separations greater than 0.1 inch becomes

$$KV = 52\ t^{.9} \text{ kilovolts}$$

where t = separation in inches (5-2)

However, plane electrodes withstand a greater potential difference at a given separation than any other type, so the study of other configurations is important in design.

High voltage small power transformers are usually of the oil-filled type for improved winding dielectric strength, so the principal insulation problem is often the selection of a proper bushing, since a stress exists between the outside lead and the grounded transformer case. As an approximate guide to the choice of a bushing, breakdown voltages have been compiled from available trade literature and reference works for a few simple bushings. These data are given in Figure 9, with flashover as a function of effective flashover distance. Data on the largest size units

were obtained from Schweiger[8]. Data on other types were obtained from commercial literature of the Stupakoff and Sealtron companies. Breakdown values for each of the five largest type bushings are the same for two different diameters. Therefore, while all dimensions are doubtless of importance, it appears that the breakdown potential of typical bushings depends principally on the direct flashover distance. Bushings without skirts or unusual configurations were purposely chosen for simplicity. The equation of average breakdown is approximately:

$$KV = 17.5\ t^{.63} \text{ kilovolts RMS.} \qquad (5\text{-}3)$$

These data are all for dry clean bushings. Dirt and moisture greatly reduce insulation strength, although the amount of reduction is usually very erratic. Corona will ordinarily be present at potentials considerably less than breakdown, but corona measuring techniques have not been sufficiently standardized to evaluate insulating materials. To compensate for dirt and moisture, and to keep corona low, recommended working voltages for bushings of the types given in Figure 9 should be chosen at about one-fourth to one-third of the breakdown values given. The curve for operating level given is intended as an approximate guide for operation of bushings under standard pressures. It may be noted that insulation strength of bushings is much less than that of parallel planes with the same spacing. The percent difference is greater at the higher potentials and spacings, in accordance with the different exponents of the empirical formulas.

The effect of pressure is a next important consideration. Insulation strength of air is reduced for a decreased pressure. This characteristic must be accounted for in the application of transformers and other electrical equipment at high altitudes, such as in airplanes 9. It has been found that for two parallel electrodes a general relation exists between pressure, separation and breakdown potential. This relation, called Paschens' law, holds that for constant breakdown potential, as pressure and spacing are varied, the product of pressure and spacing is a constant. According to available literature, this characteristic holds from extremely low pressures up to about four atmospheres. Application of this principle to Figure 8 for dielectric strength between plane electrodes, allows replacing

the abscissa, the separation, with separation times pressure. If pressure is taken as number of atmospheres, the numbers are unchanged. Data for the strength of plane electrodes at low pressure-spacing product are given by Figure 10. The dashed curves are given by Schumann, and the solid portion gives the values of Figure 8, with a gap filled in, so that the data is quite complete over a wide range. Figure 10 shows another interesting characteristic of air insulation. There is a minimum breakdown potential, about 250 volts RMS, which any combination of pressure and spacing (except zero) will withstand. This minimum breakdown is believed to hold for different electrode shapes. It can be seen that this minimum breakdown occurs at a pressure-spacing product of about .0003. At lower values of this product the insulation strength increases. Theories which attempt to account for this strange behavior point out that breakdown is a function of the mass of air between the electrodes, and that a sufficiently small mass makes more difficult the mechanism of breakdown. Sometimes a curve of this sort is mistaken for values of gradients, but it is actually the total voltage between electrodes.

While Paschen's Law is applicable only to planes, a more general principle called the law of similarity may be used for different electrode shapes. This states that if proportions of electrodes are held constant, then breakdown potential is constant for a fixed product of pressure times some characteristic dimension. Often a line of bushings of various sizes will have proportions which are fairly constant. While the bushings of Figure 9 deviate greatly in proportions, it is generally true that smaller size insulators will have smaller size conductors. We may apply the similarity principle to these bushings as an approximate guide. The equation for breakdown as a function of pressure and spacing then becomes:

$$KV = 17.5\ (pt)^{.63} \qquad (5\text{-}4)$$

where p = pressure in atmospheres.

For constnat size, (t) in this equation, the breakdown as a function of pressure is obtained. For several pressures, these are given in the following table, with breakdown at sea level taken as 100 percent. Also given are values from a curve in Blackburn's

Components Handbook[10] (also Steinburg[11]), which shows that the two sets of values agree well, and verifies somewhat the usefulness of equation (5-4).

Table 5-1

DIELECTRIC STRENGTH OF BUSHINGS AT REDUCED PRESSURES

Altitude Feet	Pressure, Inches Hg	Pressure Atmospheres	Percent Breakdown From Equation (5-4)	Comp. Handbook
0	29.9	1.0	100	100
10000	20.6	.687	79	77
20000	13.7	.460	61	58
40000	5.54	.185	34	33
60000	2.13	.071	19	22
70000	1.32	.044	14	--

As the pressure-spacing product is reduced to very low values, equation (5-4) will no longer hold, since breakdown levels off at the minimum breakdown potential, then rises. Thus for very low values the equation is conservative.

Among other factors effecting breakdown potentials in air, humidity is one which has little effect. However, condensed moisture in the air, or along the surface of solid insulation reduces the insulation strength, and should be allowed for when a bushing is chosen. The presence of a "creepage" path along solid insulation in air reduces the strength, unless a wavy path is provided so that the actual surface distance is greater than the shortest flashover distance. Very little dirt, as well as moisture has a great effect, but results from tests attempting to measure these effects are usually erratic. An increase of temperature also tends to decrease breakdown strength. The effect of time on insulation strength for all types of materials is the same; namely, the insulation will withstand much higher stresses for very short periods than continuously. Montsinger[3,12] gives this analytically as

$$V = V_o \left(1 + \frac{C}{T^n}\right) \qquad (5\text{-}5)$$

where V_o = long time breakdown strength,

T = time,

C and n are constants.

There are many references on air insualtion giving data for many other types of electrodes than those presented here. Certain electrodes at carefully measured spacings, principally rods and spheres, are used to measure voltage, since breakdown values are considered sufficiently reliable to determine whether a test voltage has exceeded the standard breakdown potential for the configuration. For high-voltage design work much of this is directly applicable. In addition to those references already given, Peek[13] and Miner[14] have made important contributions to insulation and corona study. In the study of pressure and insulation strength, many more tests have been at high pressures than low, but these are not applicable to the present problem.

Insulation problems with oil and solids are similar to those for air, in that breakdown characteristics depend on electrode shape, spacing, and most of the other factors. Corona in oil and solids is a problem, but breakdown tests are more generally used to evaluate dielectric strength. The behavior of oil and solids is much more unpredictable than air, since tests show higher deviation from average test results. An empirical equation for typical breakdown voltage of transformer oil using parallel electrodes is

$$KV = 80\ t^{.75} \text{ kilovolts RMS} \qquad (5\text{-}6)$$

where t = spacing in inches.

Dielectric "puncture" strength of the many kinds of solid insulation range from about twice that of oil to much higher values. For electrodes other than parallel planes, insulation strength is always reduced because of higher local voltage gradients.

The reduction of dielectric strength with reduced pressures for air, and to a less extent for oil, is the primary cause for special considerations needed for high altitude designs. The lower ambient temperatures at high altitudes also must be considered. Transformers which have become cold at the low temperatures existing at high altitudes may, when moved rapidly to the temperature and relative humidity conditions at low altitudes, be subjected to considerable condensed moisture on the surface. Such transformers must be moisture resistant to a high degree.

For oil-filled units, the internal pressure will depend to a large extent upon the external pressure. The bellows, used for expansion devices in completely filled units, operate with little pressure difference between the internal and external parts of the tank. The internal pressure is, therefore, almost the same as the external. The internal pressure of an oil constructed unit with a gas cushion will vary with the temperature of oil as determined by the temperature and pressure at which the transformer was sealed. At lower than sealing temperatures, the oil contracts and the internal pressure of the tank is reduced.

The effect of varying pressure on strength of oil as given by Schwaiger[8] is

$$V = (59 + 41\,p) \text{ percent of strength at sea level,} \quad (5\text{-}7)$$

where p = pressure in atmospheres.

Montsinger[3] shows a decrease of oil dielectric strength with pressure until a minimum is reached; then as pressure is further reduced, dielectric strength increases. The pressure for minimum dielectric strength is shown to be about 1.75 inches of mercury, and the dielectric strength here is about 65 to 70 percent of the sea level value.

The decrease in oil strength with decreasing pressure is probably due to evolution of dissolved gases and formation of bubbles. Low pressure should have little effect on the strength of well impregnated solid insulation, but if gas voids exist, these might expand at low pressures. The leads that pass through the air space of partially filled oil-filled units are subject to the pressure conditions that exist there. Since the internal pressures may be much less than sea level, the designer must take proper precautions to

prevent both corona and actual voltage breakdown failures in these regions. The importance of keeping leads under oil is evident.

Impurities in transformer oil, may or may not reduce dielectric strength. It is known that large amounts of moisture considerably reduce the strength. Some other impurities such as oxidation products, carbon and sludge usually have little effect, although undesirable for other reasons. The effect of increased temperature is to decrease insulation strength, more particularly of solids. Miner, who treats the properties of solids extensively, gives data on this subject, although limited to low temperature materials. Increase in frequency also means a decrease in insulation strength. Montsinger[12], gives for the range of 25-420 cycles per second

$$V = V_o \frac{K}{f^{.137}} \qquad (5\text{-}8)$$

where K = a constant

V_o = insulation strength at some reference frequency within the range.

Miner associates the increased dielectric losses accompanying increased frequency with the reduction in strength, and claims frequency has little influence if resistivity of the material is high. Breakdown in oil by the process of creepage across solid insulation is not as important a consideration as for air. The dielectric strength along a creepage path (along a solid surface) in oil is about the same as an equal "strike" distance through the oil, for the range of voltages applicable here.

Design and Tested Voltage Stresses - Safety Factors

An insulation should be selected which will withstand the handling, processing and abuse to which it will be subjected during manufacture of the product, and which will provide the minimum dielectric strength necessary under operating conditions, (including temperatures) to which it will be subjected in service. In the selection of suitable insulating materials to be

used between coil winding layers, and between the coil winding and ground, or between different insulated coil windings, a safety factor must be used to make sure that the voltage encountered during field operating conditions and during factory test are sufficiently below the minimum dielectric strength of the insulating material to prevent failure. The minimum dielectric strength of an insulating material is usually based on a short time test, on a predetermined number of specimens, after the specimens have been conditioned to temperature and humidity limits. The voltage across the material is then raised gradually until failure occurs, and the RMS value of sine wave voltage at which failure occurs is recorded as the minimum dielectric strength of the particular sample. The standard method of test for dielectric strength of electrical insulating materials at commercial power frequencies is given in Standard No. D49 issued by the American Society for Testing Materials.

Actual insulating material safety factors to be used in design may be influenced by a wide number of circumstances. For example, more safety factor may be necessary if a material varies from time to time in consistency, or if it is extremely fragile. An insulation should be tough enough, or thick enough, to withstand the manufacturing processing to which it will be subjected during such operations as coil winding or core stacking without cutting, puncturing, shredding or other damage. If it is known that a transformer is to be short lived, a reduced safety factor may be found to be satisfactory.

It is usually good design practice, for most paper insulating materials, to select a material which has a minimum RMS dielectric strength of at least twice the maximum RMS test voltage to be induced between coil winding layers, or the RMS high potential test voltage to be applied between the coil winding and ground, or between the coil and other coil windings insulated from it. This suggested safety factor is based on the assumption that the insulating material will not be given rough handling during manufacture. For the induced test between winding layers, this is also based on the RMS operating voltage being one-half of the induced test voltage. If the working voltage wave will be distorted, the safety factor allowance should be increased to allow for the additional voltage stress in service.

Some insulating materials, such as varnished paper, have a relatively high dielectric strength, but are easily damaged during manufacture to an extent which will reduce this dielectric strength. A considerably higher safety factor is desirable for these materials. If a new material is to be used it is good practice to be conservative on the safsty factor allowance until experience indicates that a reduced safety factor is justified.

For high voltage transformers, sufficient insulation should be used to prevent ionization and corona, which will weaken it in service. If the insulating material is non-homogeneous, consisting of layers of insulating materials of different dielectric constants, the voltage stress on any layer will be proportional to its thickness divided by its dielectric constant. A layer of low dielectric constant material, such as air, may thus become overstressed and subject to ionization and local break-down. It is very important to exclude voids or air pockets from solid insulations when high voltages are involved.

Impregnation of coils, or of core and coils, is desirable to saturate insulating materials, to increase their dielectric strength and to retard the entrance of moisture and foreign matter which might corrode the wire and cause insulation deterioration. Impregnation also helps to fill in air voids in the coil, it helps to protect the wire from movememt and from possible mechanical damage, and if applied to the core it provides a mechanical binder to reduce noise.

It is the usual practice, before completed transformers leave the factory, to subject them to an induced voltage test and a high potential test. The time of application of these voltages affects the dielectric strength of the insulating material, and the usual length of each of these tests if for a one-minute period. Tests required for transformers for military use are described in specification MIL-T-27.

The purpose of the induced voltage test is to cause rejection of any transformer having insulation weakness within the coil, which might cause it to fail in service. Defective, shredded or omitted coil layer insulation, defective wire insulation, or coil turns which are crossed over each other due to defective winding may cause a short circuited coil during this test.

The induced voltage test is usually made by the application to the primary winding of an RMS value of sine wave voltage which will impress on the transformer windings, and between winding layers, a peak voltage of twice the peak operating voltage. At least double frequency is used for this test to prevent saturation of the transformer core at the abnormal voltage, and to prevent possible damage to the primary winding due to an excessive exciting current and overheating.

The purpose of the high potential test is to cause rejection of any transformer having insulation weakness between the coil winding and metal parts, from which it is insulated, such as the core, the case, and other coil windings. Defective, shredded or insufficient insulation may cause such insulation failure.

The high potential test is made by the application of a 60 cycle RMS value of sine wave voltage between the coil winding and metal parts from which it is insulated, such as the core, the case, and other coil windings. This test voltage is usually twice the normal RMS rated voltage of the particular transformer winding plus 1000 volts. However, there are variations in these requirements for particular applications, and the particular high potential test voltage selected should take into consideration the peak operating voltage to be encountered in service. Small audio frequency transformers for radio receivers usually require a high potential test voltage of only 500 volts RMS. Military Specification MIL-T-27, "Transformers and Inductors (Audio, Power and Pulse)," lists high potential test voltages for different ranges of working voltage. Working voltage is defined as the maximum d-c voltage plus the peak a-c voltage that may appear between a winding, or any part thereof, and any other winding or core and/or case, under the continuous operating conditions specified.

IX. WINDING PARAMETERS AND LAYOUT

Two winding parameters are of particular importance for use in the design method to be given in the next chapter. These are: the allowable winding loss dissipation, a quantity measured in watts per square inch; and the winding space factor. The first parameter is related to transformer temperature rise, the most important factor determining required size of the unit. Use of this parameter is, in effect, an attempt to predict temperature rise based only on winding losses and winding exposed surface before the design is made.

The Winding Dissipation Parameter

The power transformer is a fairly efficient device in that internal losses are usually a small fraction of the transferred power. However, the losses which are present must somehow be dissipated from the core and coils. The temperature rise of the core and coils depends on the losses, on the geometry of the heat flow paths and on the characteristics of the materials present between the source of heat and some external medium having a temperature relatively independent of the transformer losses. The operating temperature of the winding is of great importance because excessive values damage or shorten the useful life of transformer insulation. The core may be vulnerable to excessive temperatures if insulating enamel is used between laminations. At very high temperatures (approximately 800°C) iron becomes completely nonmagnetic, but these temperatures are far above any contemplated ranges of operation.

The three modes of heat transfer in various mediums, conduction, convection, and radiation, will not be discussed in detail, but principal types of transformers and the important factors effecting temperature rise will be considered. These principal types are the open, the compound-filled encased, and the oil-filled encased. The latter two are usually hermetically sealed to exclude moisture and dirt from the core and coils. Some so-called "encapsulated" open types, in which core and coils are impregnated with special compounds, have been found to pass military requirements for hermetically sealed units. Many open-type units having shell-type cores are provided with end cases to enclose the winding only, and leave the core partially exposed. For an open-type transformer

heat is transferred from core and coils directly to the surroundings through the air and mounting chassis. The presence of a thick layer of impregnating material or of end cases impedes this flow of heat to some extent. For the compound-filled and oil-filled types, most of the heat is transferred to the oil, or compound, then to the case, and finally to the outside. Thermal properties of compounds have been found to vary considerably. An impregnating base material transfers heat much more readily when mixed with a material such as silica, and results in a lower internal temperature than would be obtained with plain asphalt or with wax.

The outside of a transformer may be made to transfer heat more readily by the addition of fins for increasing exposed surface. The cooling problem increases with transformer size. This is because proper cooling depends so much on surface areas available for heat transfer. Generated heat for fixed working densities of the core and coils depends on volume. However for increasing size, the increases in percent volume are greater than increases in percent external area; consequently generated heat increases more rapidly than cooling surface. So the temperature problem with large units must be attacked either by reducing losses per unit volume or by providing special aids for cooling, internally as well as externally. Ducts are sometimes provided within a winding, or between winding and core to increase

heat transfer from a principal source. In the sizes being considered, up to 5 KVA, techniques such as the use of ducts and fins are seldom applied.

The next aspect of the heat transfer problem is the nature of the relation between quantity of heat flowing and temperature rise. We might consider two general cases where temperature differences exist with heat flowing: through a homogenous medium, such as an air, oil or compound path, and across a boundary between dissimilar materials. Temperature changes through on oil or compound path, or through the thickness of a case are small compared to the changes from winding to oil or compound, and from case to outside air. Final heat transfer to air is common to all types of units, and this transfer occurs with a comparatively high temperature change. Within a winding, of course, heat transfer occurs across boundaries between dissimilar matherials, but these adjacent surfaces are ordinarily in very intimate contact. Temperature changes within

most windings are found to be small fractions of the change from winding or case to outside air. Empirical tests available in literature on the subject show that temperature differences between mediums can be approximated as

$$\Delta T = K \left(\frac{W}{S}\right)^{0.8} \text{ degrees C,} \qquad (9\text{-}1)$$

where W = quantity of heat flowing per unit time, watts,

S = common surface area between the mediums, sq. inches,

K = constant.

Several writers have used functions of this kind, among them: Montsinger[3], Lee[4], Reed[2], Connelly[5], Still[6], and Morris[24]. The formulas are presented and discussed in Appendix B.

Estimates of K, in view of available data and literature are

K = 90 for heat transfer from a winding or case surface to air at standard pressure

K = 40 from a winding to a compound

K = 20 from a winding to oil

K = 10 from compound or oil to a transformer case.

These constants apply for total heat transfer, as made up of transfer by one or more of the three fundamental modes. Conditions for the constants as given are: sea-level pressure, about 40 degrees C ambient temperature. Variation of this and other factors such as size require different values of K.

The design approach which has been developed requires consideration of the heating problem from somewhat of a different angle. Since we are trying to work backward from temperature limitations, an approximate relation between temperature rise and other design quantities must be used.

The proposed relation is

$$\Delta T = K\left(\frac{W_c}{S_c}\right)^{0.8} \text{ degrees rise,} \qquad (9\text{-}2)$$

where W_c = winding losses watts,

S_c = winding exposed surface (not in contact with core) sq. inches,

K = constant.

Equation (9-2) can be expected to provide a value of allowable watts winding loss to winding surface for a certain maximum temperature rise which will be satisfactory much of the time. Temperature is the most nearly universal design limitation and any attempt to systematize design methods to eliminate repeated tr- ls requires some such assumption. Naturally it is not proposed to use the same equation for final calculation of temperature rise, but if it will yield a correct core size, and a fairly close wire size, its purpose is accomplished.

To account for factors found to have most important effects on temperature rise, different values may be used for K in equation (9-2). After considerable study of available test data, various designs, and theories of heat transfer a table of the parameter K has been made. These values are given by Table 9-1. The variables considered are: transformer type, that is, open, compound-filled, and oil-filled; type of core, simple, shell, or core:, frequency; and ambient temperature. Since the desired temperature rise is presumed known, allowable winding dissipation, the parameter to be used in a design, is:

$$\frac{W_c}{S_c} = \left(\frac{\Delta T}{K}\right)^{1.25} \text{ watts per sq. inch} \qquad (9\text{-}3)$$

The function is also given in Figure 37, which can be used to find W_c/S_c for a broad range of values of K. Values of K given for the different conditions have been worked out using test data for reference where such was available. Naturally data were not available for every table entry, but characteristics of heat transfer and typical design application of materials were used to make the estimates. It was found that most

of the transformers which have been tested are quite conservatively designed insofar as temperature is concerned. There has been an effort to make estimates which will yield a higher temperature rise, but still be sufficiently conservative so that temperature limits will seldom be exceeded. From equation 9-2 it may be seen that as K increases, predicted temperature rise increases, and therefore, a high K is conservative.

Test and design data were only available for frequencies of 60 and 400 cycles, and for ambients of 40 to 85 degrees centigrade. In extending the table for different frequencies, the effect of core loss is the principal consideration. This required a study of typical core materials, densities, and losses for the range of frequencies. In most low frequency designs, exciting current tends to limit the flux density to be used, and core losses are lower than could be tolerated for a given temperature rise. For frequencies in Table 9-1 above 60 cycles, core loss tends to become the limiting factor, and thin, better quality steels are often used to reduce this loss. At frequencies above about 800 cycles core loss is so high, relatively, that it must be kept about constant for further increase of frequency. From the loss characteristics of the core, values of K were obtained from sample calculations of temperature. Operation at different ambient temperatures is an important variable because heat transferred by radiation is dependent on the value of final temperature, not on the rise alone. Since the heat transferred by radiation is greater at the high temperatures, K as given by the table is lower at the higher ambients.

The effect of transformer construction, that is, open, compound-filled, or oil-filled, depends on several circumstances, such as type of filling material, and size of unit. Most generally a transformer with a good heat-conducting compound material will be somewhat cooler than an otherwise identical open type. An oil-filled unit will be cooler than an otherwise identical compound-filled type except in small sizes. For the latter, a K for compound-filling can be used instead. The values of K given assume about the same rise for the open and compound-filled types at low frequencies and ambients. Compound-filled units most commonly use a silica loaded potting material, but where only plain asphalt or wax is used the values of K should be increased about 15 to 20 percent. Type of core is another factor considered in the problem of temperature rise, and values of K are lowest for the

Table 9-1

VALUES OF K FOR APPROXIMATE TEMPERATURE-RISE EQUATION

Transformer Type	Open				Compound-Filled			Oil-Filled		
Type of Core	Shell	Shell (End Cases)	Simple	Core	Shell	Simple	Core	Shell	Simple	Core
Ambient Temp. -°C / Frequency C.P.S.										
25 / 25	76	90	92	107	70	84	98	58	69	80
25 / 60	79	94	95	110	74	88	103	62	74	86
25 / 200	89	107	107	123	85	101	117	73	87	101
25 / 400	99	122	119	137	98	117	136	85	101	117
25 / 800	108	132	129	149	107	128	149	95	113	131
25 / 2500	112	136	131	151	110	131	152	98	116	134
50 / 25	72	87	86	100	68	81	94	56	67	78
50 / 60	75	91	90	104	72	86	100	60	71	83
50 / 200	84	104	101	117	83	99	115	71	84	97
50 / 400	94	119	112	129	95	113	131	83	98	114
50 / 800	102	129	122	139	104	124	144	92	110	128
50 / 2500	106	132	125	143	107	128	149	95	113	131
85 / 25	66	83	79	92	65	78	92	53	63	73
85 / 60	69	88	83	96	69	82	96	57	68	79
85 / 200	78	99	93	107	80	96	112	67	80	93
85 / 400	87	114	103	119	91	109	127	79	94	119
85 / 800	94	123	112	128	99	118	137	87	103	120
85 / 2500	97	126	115	131	102	122	142	90	107	124

Table 9-1 (Contd.)

VALUES OF K FOR APPROXIMATE TEMPERATURE-RISE EQUATION

Transformer Type		Open				Compound-Filled			Oil-filled		
Type of Core		Shell	Shell (End Cases)	Simple	Core	Shell	Simple	Core	Shell	Simple	Core
Ambient Temp. -°C	Frequency C.P.S.										
125	25	62	79	74	86	63	76	88	50	60	70
125	60	65	84	78	90	66	79	92	54	64	74
125	200	72	96	86	99	76	91	106	64	76	88
125	400	80	108	96	111	87	104	121	75	89	103
125	800	87	118	103	119	95	113	131	83	99	105
125	2500	90	120	107	123	98	117	136	85	101	117
200	25	52	74	63	73	58	69	80	46	55	64
200	60	54	77	66	75	61	73	85	49	58	67
200	200	62	88	73	85	70	84	98	58	69	80
200	400	68	100	81	94	80	96	112	68	81	94
200	800	74	109	88	101	87	104	121	75	89	103
200	2500	76	111	91	104	90	107	124	77	92	106

shell type, higher for the simple-type, and highest for the core type. This is to offset the differences in exposed winding surface area. Those core types with higher exposed winding surface areas are more readily cooled, but not in proportion to the increased winding area. Units with less winding area, such as the shell type, dissipate some of their heat through the core.

Tests which have been made at Armour Research Foundation give some information about the effect of core loss on winding temperature rise. A transformer was tested in air at two ambient temperatures, 40 and 75 degrees C. Temperature rise at several values of load current was measured for conditions of normal loading and short-circuited secondary, or in effect, for conditions or normal core loss and no core loss. At load currents corresponding to equal winding loss for each condition, the difference in winding temperature rise was not significant, even at rises as low as 10 degrees C. Although made at 60 cycles, the core loss for small loads was about seven times the winding loss. In this case, it may be concluded, core losses had no effect on winding temperature rise. Roters[25] gives some information on the effect of the presence of the core on winding temperature rise. His data are for a winding excited with D.C. The results showed no difference in temperature rise when the core was not present or was in poor thermal contact with the winding. For good thermal contact, the presence of the core effected a reduction in winding temperature rise of about ten percent. The effect of the core, because of its presence and losses, appears to be limited for an open-type construction. For an oil-filled or potted unit another effect of the core is to raise the inside ambient.

These then are four factors which are accounted for in their effect on temperature rise. Other factors appear to be of lesser importance, but may be considered to decide whether a liberal or conservative K is preferable. Physical size is automatically accounted for by the design method in limiting winding losses per unit surface area. However, another characteristic is the effect of size on heat transfer by convection[26]. This is of significance, but has not been observed in the study of available temperature rise data. Type of winding probably has an effect on temperature rise, in that windings with a lot of insulation should impede heat transfer more than others. This may indicate the use of a high (conservative) K.

Other factors which may be of some importance are: varying core proportions within one of the types given, and impregnating material. Solid matter, such as sand, in an asphalt will improve thermal conductivity. Open types which are hermetically sealed, or encapsulated units, normally have a heavy coating of insulating material over the core and coils which can be expected to impede heat transfer. Temperature rise may be quite different for various materials and processes, but the effect might be estimated by increasing K by 15 to 25 percent.

Altitude is another important factor to be studied in relation to the temperature problem. At high altitudes there is less air to carry off dissipated heat by convection, and a unit will have a higher temperature rise. Radiation is not dependent on air pressure, and if the ambient temperature is sufficiently lower than that of the transformer, most of the generated heat will be dissipated by this mode of transfer. However, in aircraft, where high altitude heating problems occur, the transformer is often mounted near other components operating at about the same or greater temperatures. This makes heating a particularly severe problem, and for cooling, means other than natural convection and radiation must be utilized. Some methods rely upon forced-air cooling and conduction cooling. The heating of transformers in such applications is a problem which the transformer designer cannot solve alone. It must be studied along with adjacent electronic components and aircraft structure.

There are test data available for operation of transformers under somewhat idealized conditions at low pressures. Kiltie[27] gives test results for a 2 KVA, open-type, 400 cycle unit in a 30° ambient. Morris[24] gives results for an oil-filled unit in an ambient of about 30°C. Relative temperature rise from these sources has been plotted against air pressure in Figure 38, where temperature rise at sea level is taken as 100 percent. The two sets of results show reasonable agreement, and the extrapolated portion may be a good approximation. However, these data must be used with caution in view of the more realistic and more difficult problem usually present. Morris also remarks that high-altitude heating would present no problem if transformers were operated in prevailing high-altitude ambient temperatures. As altitude increases, ambient temperature decreases more rapidly than temperature rise increases because of reduced air

pressure. There may be some applications where the benefits of this principle can be realized. At very high altitudes, high aircraft speeds give rise to considerable adiabatic heating of outside cooling air and of aircraft surfaces which can cancel the benefits of a low ambient temperature.

The discussion of temperature rise would be somewhat incomplete without some comment on temperature rise and transformer life. Most of the available information on this subject is limited to low temperature insulation materials. Many low-temperature materials are normally assumed to have a life of about 20-30 years if operated at a hottest temperature of 95° Centigrade. Montsinger[3] and others have found that for each 8 to 10 degrees increase in operating temperature over 95, the life is roughly reduced by one-half. Insulation life is not measured by dielectric strength, since this has been found fairly constant over a long period. However, the mechanical resistance to tension and abrasion is gradually reduced throughout insulation life. This is used as a measure of life, because when mechanical strength remaining is small, a transformer can easily be so damaged by vibration or short-circuit stress that the dielectric strength of the insulation is lost. If the life at 95°C is taken as 25 years then an approximate relation between life and temperature is

$$\text{Life} = (25)\ (\tfrac{1}{2})^{\frac{T-95}{8}}\ \text{years}, \qquad (9\text{-}4)$$

where T is hottest spot operating temperature, degrees C. This equation can serve as a guide in the design of short-life units. Some transformers are built which need operate satisfactorily only a few hours or less, and the allowable temperature can be much higher than 95°C. Ordinary standard transformers designed for an allowable average winding rise of 105°C probably have a hottest spot temperature of about 110°C. From equation (9-4) this corresponds to a life of about six years. For very short life, charring or burning of insulation would become the limiting factor, since severe localized damage to insulation can cause very rapid failure.

Winding Space Factor

In the design procedure it is necessary for a designer to estimate winding space factor, F_c. This has been defined as the ratio of winding cross-sectional area to window area. Winding space factor is of great importance in any attempt to obtain minimum size and weight, since if the window is not well-filled, more material is being used than necessary. Similarly if insulation thicknesses can be reduced in any way, a reduction in window area is possible. Therefore, it is important that space factors chosen should be fairly high, although it is undesirable to design transformers too tight to be built. No values which might be given would be just right for all manufacturers, since it can be expected that some utilize window space better than others. Space factors given are a compromise between the highest and the average values.

It is desired to choose a winding space factor from specifications and information known before a design is begun. It has been found that the factors having principal influence on space factor are: physical size of the transformer, number of windings, and operating voltage. As physical size is increased, a smaller proportion of the window space is required for the winding tube and for clearances, so that space factors are higher. On the other hand, as number of windings, or operating voltage are increased, more space is taken by insulation and space factor is reduced. Insulation for higher voltage may be required because of a high potential from an entire winding to ground, or between ends because of a high potential difference of the winding. In both cases insulation from any part of the winding to ground must provide sufficient dielectric strength, and in the second case, extra insulation between parts of a winding is sometimes required. However, the latter condition will occur very infrequently, since layer insulation required for mechanical strength only gives sufficient dielectric strength except in larger transformer sizes or very small wire sizes. Hence, increased insulation for voltage usually appears as increased tube size, wrapper thickness or coil margins.

The physical size of a transformer is not known at the beginning of the design, but is a function of the rating in volt-amperes, the temperature class, and the frequency. If we consider standard those units of 60 cycles frequency and about 40°C temperature rise, then physical size is a function of volt-amperes

rating, W_r. A design for a higher frequency or temperature rise can be made smaller in size, or rather, the equivalent rating at standard conditions is less than that at the higher frequency or temperature rise.

Let us first consider temperature. An increased rating from a given transformer is obtained by increasing the current. An increase in voltage and therefore in flux density is not desirable because the magnetic material is already being operated near the knee of the magnetization curve. Therefore rating is proportional to load current, which is in turn proportional to the square root of copper loss. Therefore copper loss W_c is proportional to the square of output volt-amperes, W_r. Since temperature rise from (9-2) is approximately

$$\Delta T = K \left(\frac{W_c}{S_c}\right)^{0.8} , \text{ then}$$

$$\Delta T = K' (W_r)^{1.6} , \qquad (9\text{-}5)$$

where W_r is a rating in volt-amperes, K and K' are different constants. Rating as a function of temperature is evidently

$$W_r = K'' (\Delta T)^{1/1.6} = K'' (\Delta T)^{0.63} \qquad (9\text{-}6)$$

Next, the effect of frequency on rating can be estimated. Equation (2-12) implies that rating is proportional to frequency for constant flux density, but core loss would be too high if transformers were used in this manner. Flux density must be reduced to keep core loss within reasonable limits. To find the limits of rating variation, assume that core loss is to be kept constant. Core loss for a given transformer can be approximated as

$$Wi = kf^x B^y , \qquad (9\text{-}7)$$

where f = frequency,

B = flux density,

x and y are constants depending on the material.

An average x for a magnetic material is 1.5 and an average y is 2.0. Now the rating of a given unit as a function of core properties alone is

$$Wr = k' (f F_i B), \qquad (9\text{-}8)$$

where F_i is core space factor.

Substituting the value of B from (9-7) gives

$$Wr = k'' (Wi)^{1/y} f^{1-x/y}. \qquad (9\text{-}9)$$

If Wi is constant, and values for x and y are substituted then

$$Wr = k''' f^{0.25} \qquad (9\text{-}10)$$

The exponent 0.25 is lower than achieved in practice because higher core losses are allowed as frequency increases. Sheet width is reduced to decrease eddy currents, and better grades of material are sometimes used. At the same time reducing the sheet width decreases F_i, the core space factor. With typical flux densities, sheet thicknesses and space factors as given by Lee[4], the following formula is a fair approximation of the effect of frequency on rating.

$$Wr = k' f^{0.76} \qquad (9\text{-}11)$$

For example, we find that a 400 cycle transformer has a rating of 4.23 times that of a 60 cycle transformer of the same physical size. To convert the 400 cycle unit to equivalent 60 cycle, the rating is divided by 4.23.

The equivalent volt-ampere rating, W_r', based on 60 cycles frequency, and 40°C rise becomes

$$W_r' = \frac{W_r}{\left(\frac{f}{60}\right)^{0.76} \left(\frac{\Delta T}{40}\right)^{0.63}} \text{ equivalent}$$

volt-amperes, (9-12)

where W_r is the nominal rating at frequency, f, and rise, ΔT.

As frequency increases rating also increases, but core loss finally becomes limiting. The rating cannot be further increased with increased frequency. Instead of the factor $(f/60)^{0.76}$, the fraction given by the ordinate of Figure 39 shoud be used in (9-12).

Recommended values for winding space factor are given by the equation:

$$F_c = 0.08 \log_{10} (W_r') + F \qquad (9\text{-}13)$$

where W_r' = equivalent standard rating in volt-amperes,

F = a term given by Figure 40.

Values of F, from Figure 40 represent the effect of different numbers of transformer windings and operating voltages. It is recommended that each plate winding be considered as two windings rather than one. Peak working voltage, the abscissa, is self-explanatory, and is used rather than RMS voltage because a direct voltage on an entire winding may be present. The voltage of that winding which is a maximum is to be used. In Figure 41 is shown the principal range of space factor values, with two lines given for F equal zero and equal .15. It can be seen from Figure 41 that great accuracy in the calculation of W_r' is not at all necessary, since the slope of the lines is small. Use of these space factor values by one group may well show a need for revision, but such changes are not necessarily valid for others.

In a design the final value of space factor will doubtless be different from the particular recommended value used at the beginning, and will probably tend to be higher. Added turns for high voltage primary taps, and added turns to compensate for regulation increase space factor.

Among factors believed to have lesser effect on space factor than those considered are the type of core, and presence of a shield. In some cases the space factor must be made low to allow room for impregnating materials, and a conservative value is to be chosen at the beginning of the design. The test of satisfactory choices of space factor and other quantities is whether the window is well filled, but that the unit can still be built.

Wire Data

The conductors used in transformer windings are usually of copper but more recently there has been an increasing use of aluminum. Although the resistivity of aluminum is 64 per cent greater than that of copper, the fact that the specific gravity of aluminum is 30.5 per cent of that of copper makes aluminum more nearly competitive with copper with respect to transformer weight and cost than the relative resistivities of each would indicate. Although the heating effect resulting from the greater resistivity of aluminum is a primary problem to the design engineer, he must also consider the electrolytic corrosion problem resulting from contact with dissimilar materials as well as manufacturing problems which include soldering operations. Corrosion of a conductor may be due to chemical, electrolytic, or galvanic action. Particular care to prevent corrosion must be taken with small sizes of wire. A general discussion of this problem is presented in Appendix C.

Regardless of the material used for the conductor it is necessary to provide conductor insulation so that there will be no short-circuited turns in the winding. Often, as for precision windings, or for random-wound coils on a bobbin, the insulation on the conductor may also provide insulation between layers. Usually, however, power transformer designers will supplement the conductor insulation by including insulation between the layers of each winding.

The kinds of wire insulation are:

1. Enamel
2. Vinyl acetal - "Formex" or "Formvar"
3. Nylon
4. Silicone
5. Teflon
6. Varnish - (Electrical Insulating)
7. Cotton
8. Glass (fiber)
9. Silk
10. Asbestos
11. Paper
12. Miscellaneous, including various materials such as ceramic and some of the insulating oxides.

Except for electrical insulating varnishes, which are often used to impregnate the fibrous materials, these materials

may be used individually in various thicknesses. The thicknesses are identified by descriptive adjectives such as single, double, triple, or quadruple. The designation "heavy" may be used in lieu of the "double" designation for Formvar insulated wire. While the "single" designation may be used to describe either film types or fibrous types of insulation, the "double" designation is often confined to fibrous materials whereas the "heavy" designation is applied to film types of insulation. The fibrous materials may be used individually in single or double thicknesses, or over the film types of materials. Some of the fiber insulation coated materials, particularly the glass fiber-insulated materials, are treated with varnish to prevent fraying of the fiber insulation. Silicone varnish is used if the insulation is to be used in Class H apparatus.

The smaller size conductors are normally available in round wire in sizes from about .001" to .128" diameter (No. 50 to No. 8 AWG). One of the film types of insulation is usually used as insulation on the above sizes of round wire. The single thickness enamel or Formvar is usually used for the smaller conductor sizes. However, for the conductor sizes larger thanabout .0571" diameter (No. 15 AWG) heavy or double enamel or Formvar may be more satisfactory. This heavier insulation for the larger sizes is used to provide a stronger insulating film for larger conductors where the single insulation may not withstand the winding conditions. Triple and quadruple thicknesses of film type insulations may be used where higher voltage strength may be necessary. Typical conditions of such higher voltage stresses may be encountered when two windings are interwound or when a winding is subjected to surge or impulse voltages, as may be encountered with pusle transformers and some other electronic equipment applications. The heavier insulation films may also be desirable for some situations where it is possible to operate at temperatures above normal by using the heavier insulation.

The fibruous type of insulations, such as cotton and glass, or combinations of the film type plus the fibrous type of insulations are usually used on the larger size wound wires or on the rectangular cross-section conductors. The insulation on larger size conductors may include a film type coating underneath the fiber insulation or a film type of coating underneath the fiber insulation plus a varnish impregnation of the fiber insulation. Such insulation is usually not used on small wire conductors because of the low space factor

which would result from its use with small wire. Because rectangular wire has rounded corners to reduce corona, and to make it easier to handle without damage to insulation, its cross-sectional area will always be somewhat less than the product of its two dimensions.

Table 9-2 gives data for copper wire from sizes AWG No. 50 to No. 4. Areas in circular mils are tabulated for use in the design method. Diameters of the bare conductor and for single and double layers of enamel are also given. Other film-type coatings, such as Formvar and Nylon enamels have closely the same diameters. The fabric-coated wires tend to have higher variability in size, so that it is preferable to obtain dimensions from the supplier. Useful literature on magnet wire is listed in Appendix D.

Resistivity is a conductor material characteristic which depends on temperature of the winding. Resistivity values are plotted against temperature in Figure 42 for copper and aluminum. The familiar equation for copper resistivity as a function of temperature is

$$\rho = \rho_{20} \frac{T + 234.5}{254.5} \qquad (9\text{-}14)$$

where ρ = resistivity at the temperature, T degrees Centigrade,

ρ_{20} = resistivity at 20 degrees centigrade.

The values for copper in Figure 42 are based upon the standard for annealed copper, having a conductivity of 100 percent. The percent conductivity of magnet wire values somewhat, but may be taken as 98 percent of the standard. Therefore the resistivity of copper wire may be taken as about two percent greater than the standard.

Coil Layout

The winding design requires the selection of insulation materials, and the specification of proper clearances, for both mechanical and electrical considerations. In previous chapters on construction, insulating materials, and high voltage insulation problems, information is given to enable the designer to specify sufficient insulation, and to recognize any

Table 9-2 COPPER WIRE DATA

Size AWG	Area in Circular Mils	Diameter - inches			Turns/inch (1 Layer Enamel)	Ohms/1000 ft. at 20°C 100% Cond.	Lbs. per 1000 ft., bare
		Bare Wire	1 Layer Enamel	2 Layers Enamel			
4	41,740	.2043				.248	126.4
5	33,100	.1819				.313	100.2
6	26,250	.1620				.395	79.5
7	20,820	.1443				.498	63.0
8	16,510	.1285	.1305	.1324	7	.628	50.0
9	13,090	.1144	.1164	.1182	8	.792	39.6
10	10,380	.1019	.1039	.1056	9	.999	31.4
11	8,234	.0907	.0927	.0943	10	1.260	24.9
12	6,530	.0808	.0827	.0842	11	1.588	19.77
13	5,178	.0720	.0738	.0753	12	2.003	15.68
14	4,107	.0641	.0659	.0673	13.5	2.525	12.43
15	3,257	.0571	.0588	.0602	15	3.184	9.86
16	2,583	.0508	.0525	.0539	17	4.016	7.82
17	2,048	.0453	.0469	.0482	19	5.064	6.20
18	1,624	.0403	.0418	.0432	21	6.385	4.92
19	1,288	.0359	.0374	.0387	24	8.051	3.90
20	1,022	.0320	.0334	.0346	27	10.15	3.09
21	810	.0285	.0300	.0310	30	12,80	2.45
22	624.4	.0253	.0267	.0278	34	16.14	1.94
23	509.5	.0226	.0238	.0249	39	20.36	1.54
24	404.0	.0201	.0213	.0224	43	25.67	1.22
25	320.4	.0179	.0191	.0201	48	32.37	.970
26	254.1	.0159	.0170	.0180	54	40.81	.769
27	201.5	.0142	.0153	.0161	60	51.47	.610
28	159.8	.0126	.0136	.0145	67	64.90	.484
29	126.7	.0113	.0122	.0130	75	81.83	.384
30	100.5	.0100	.0109	.0116	84	103.2	.304
31	79.70	.0089	.0100	.0105	94	130.1	.241
32	63.21	.0080	.0088	.0095	104	164.1	.1913
33	50.13	.0071	.0078	.0085	117	206.9	.1517
34	39.75	.0063	.0070	.0075	131	260.9	.1203
35	31.52	.0058	.0062	.0067	146	329.0	.0954
36	25.00	.0050	.0056	.0060	162	414.8	.0757
37	19.83	.0045	.0050	.0055	183	523.1	.0600
38	15.72	.0040	.0045	.0050	204	649.6	.0476
39	12.47	.0035	.0040	.0043	227	831.8	.0377
40	9.89	.0031	.0035	.0038	261	1,049	.0299
41	7.84	.0028	.0031	.0036	296	1,323	.02374
42	6.22	.0025	.0028	.0032	326	1,668	.01882
43	4.93	.00222	.00237	--	384	2,103	.01493
44	3.91	.00198	.00213	--	426	2,652	.01184
45	3.10	.00176	.00188	--	483	3,334	.00939
46	2.46	.00157	.00169	--	538	4,217	.00745
47	1.95	.00140	.00151	--	603	5,320	.00590
48	1.55	.00124	.00135	--	674	6,710	.00468
49	1.227	.001107	.00121	--	742	8,460	.00371
50	.973	.000986	.00108	--	830	10,670	.00294

special conditions to be met. Equations have been given for typical dielectric strengths of air, oil and bushings. The design method of the following chapter yields winding wire sizes and number of turns, and is intended to yield sufficient space for necessary insulation.

The specific insulating parts of a winding besides wire insulation are: the winding tubes, layer insulation, coil wrappers, impregnating materials and filling materials for encased units. Representative materials for each of these components, for different classes, are listed in Tables 9-3, 9-4, and 9-5. The proposed Signal Corps classification for materials is discussed in Chapter IV.

Allowances for mechanical clearances are always necessary regar less of the operating voltages. To allow for tolerances in the bare diameter and insulation thickness of the wire it may be necessary to add a small percentage to the insulated wire dimensions unless dimensional data is specified in maximum dimensions. For calculating coil build, the actual thickness is use for coil forms (whether tubes, bobbins, or channels), layer insulation, and winding wrappers. The clearance allowed between the coil and the core leg, on which the coil is assembled, must be added to the coil build. This total sum of conductor plus all insulation build is usually held to about 85 percent of the core window height. The remaining 15 percent is necessary for lapping layer insulation, bulge of the winding as it lies on a rectangular form, and clearance for stacking. The 15 percent allowance for core window clearance was assumed to include an allowance for bulge. If a calculated allowance for bulge is added to the calculated coil build in the window area, it is permissible to reduce the calculated clearance allowance to a smaller percentage. The conductors of coils wound on square forms usually lie down with less bulge than do the conductors wound on coils which have one dimension that is much longer than the other. Since bulge depends on coil dimensions, wire material, wire diameter, winding speed, tension, and perhaps on insulation, it is difficult to set up an accurate rule for calculating bulge. For estimating the bulge on each side of a coil it may be satisfactory to allow about 5 percent of the winding form dimension on the respective side. Calculated dimensions for lead build should include the lead diameter plus an allowance for the insulating and structural materials used.

Table 9-3

CLASS AW* INSULATION MATERIALS FOR TRANSFORMERS

Type	Winding Tubes	Layer Insulation	Wrappers	Wire Insulation	Impregnating Materials	Filling and Potting
Open, or open with end cases	Kraft paper Fish paper Rag paper Rope paper Varnished paper	Kraft paper Fish Paper Rag Paper Rope paper Varnished paper Acetate	Kraft paper Fish paper Rag paper Rope paper Varnished paper Acetate	Varnish Formvar Paper Cotton Rayon Silk Nylon Acetate	Varnish Asphalt Polyester resins	None
Compound-filled	Kraft paper Fish paper Rag paper Rope paper Varnished paper	Kraft paper Fish paper Rag paper Rope paper Varnished paper	Kraft paper Fish paper Rag paper Rope paper Varnished paper	Varnish Formvar Cotton Paper Nylon	Varnish Asphalt Polyester resins	Asphalt Asphalt with Mineral Filler
Oil-filled	Kraft paper Fish paper Rag paper Rope paper	Kraft paper Fish paper Rag paper Rope paper	Kraft paper Fish paper Rag paper Rope paper	Paper Cotton Formvar	Mineral oil	Transformer Mineral oil

*AW class inclues materials which at 105°C (A-temperatures), will have a life expectance of 10,000 hours or more (W-life), in accordance with proposed classification of the Signal Corps. See Chapter IV.

Table 9-4 CLASS B/ INSULATION MATERIALS FOR TRANSFORMERS

Type	Winding Tubes	Layer Insulation	Wrappers	Wire * Insulation	Impregnating Materials	Filling and Potting	Remarks
Open, or open with end cases	Asbestos Mica Glass	Asbestos Mica Glass	Asbestos Mica Glass	Asbestos Glass	Varnish Polyester-resin	None	Insulating binders and impregnating materials must be good for use in Class B insulation systems.
Compound-filled	Asbestos Mica Glass	Asbestos Mica Glass	Asbestos Mica Glass	Asbestos Glass	Varnish Polyester-resin	Polyester-resin with mineral filler	
Oil-filled	Asbestos Mica Glass	Asbestos Mica Glass	Asbestos Mica Glass	Asbestos Glass	Silicone oil	Silicone oil	Insulation binders and impregnating materials must not be soluble in the liquid

Table 9-5 CLASS CW INSULATION MATERIALS FOR TRANSFORMERS

Open, or open with end cases	Asbestos Mica Glass Teflon	Asbestos Mica Glass cloth Teflon	Asbestos Mica Glass cloth Teflon	Asbestos Glass fibers Teflon	Silicone varnish	None	Insulation binders (such as silicone varnish) good for Class CW must be used.
Oil-filled	Asbestos Mica Glass cloth Teflon	Astestos Mica Glass cloth Teflon	Asbestos Mica Glass cloth Teflon	Asbestos Glass fibers Teflon	Silicone oil	Silicone oil	

* Formvar coated wire is sometimes used at temperatures near the low end of the Class B range.

Clearance must also be allowed for overbuild of the layers along the axis of the coil. It is common practice to hold winding width (axially) to about 90-93 per cent of the net space available for the coil, after an allowance for end margins has been made. Layer width is calculated using nominal diameter of the conductor including insulation. The values of Table 9-2 include the allowance for axial clearance.

For sufficiently low voltages, the thickness of the tube, the layer insulation, and the margins from ends of the layers of wire to the core are set by requirements for mechanical strength, rather than by insulation strength. In general such transformers include most of those with all operating voltages below 1000 volts, and some that have higher voltages. Below 250 volts RMS, construction will always be for mechanical strength only.

Tube thickness may be based on core size, as in Table 9-6. Within the ranges for tube thickness given in the table, the lower values are to be used for a square core cross section, and the larger values are to be used when the larger dimension is 2-3 times the smaller. Layer insulation and margins, for mechanical strength only, are generally chosen based on wire sizes The larger wire sizes require thicker paper to support the layers and to prevent damage to the coil as it is being wound. Values of layer insulation and margins are given in Table 9-7. References for winding construction giving coil layout data are Lee[4], Connelly[5], Blackburn[10], and Roters[25].

Higher voltage windings require additional insulation and spacing for electrical clearance. A typical design value for permissible stress on paper insulation is 50 volts RMS per mil of insulation thickness, based on the operating voltage. This figure is conservative for some materials. It is recalled that a safety factor of two or higher is recommended for dielectric strength over test voltage. Since test voltage is somewhat over twice operating voltage, the insulation stress during normal operation should be somewhat less than one-fourth of the dielectric strength of the material. Sufficient tube thickness should be allowed, according to this rule, to insulate the inside winding from the core. Insulation between two layers should be sufficient for twice the voltage of one layer, since it is seen that this is the maximum stress between the two.

Electrical clearances in windings are based on creepage breakdown voltages. For transformers in air, the data given by Lee[4] should give satisfactory results if applied with adequate factors of safety. This data, while based on different configurations of creepage paths, shows that creepage breakdown is approximately dependent only on the total length of the path. An approximate relation is

$$KV = 18t^{.7}, \qquad (9\text{-}15)$$

where KV = RMS breakdown voltage is kilovolts,

t = creepage path length in inches.

This is practically the same as equation (5-3) for bushing flashover. For small distances the permissible stress per mil can be greater than at larger distances. A commonly-used design value is 10 RMS volts per mil for small spacings. As spacing is increased above about one-fourth inch, a lower value should be used. When it is necessary to maintain a minimum margin for electrical clearances, coils are often wound with folded-edge layer insulation, or strips of insulation which can be wound in the margin parallel to the conductor. Manufacturing tolerances must, of course, be added to the required electrical clearance. Although the creepage voltage breakdown in compound-filled units may be higher than for open core and coil construction, the spacings for creepage voltage breakdown in compound-filled transformers are frequently about the same as for open core and coil transformers. Creepage spacings in air become very large for high voltages. This results in very uneconomical construction and some other design difficulties which may include high leakage reactance. This dictates the use of oil-filled construction for high voltage designs. For oil creepage paths a working stress of 30 volts RMS per mil based on operating voltage should be satisfactory. Lee[4] also gives applicable data for creepage paths in oil. Allowance for creepage and strike paths in oil should be about the same. Adequately long spark-over paths are obtained in either air or oil-filled transformers by spacing points of potential difference or by assembling between such points an insulating material having a higher dielectric strength than that of the surrounding medium, which is usually air or oil.

Frequently windings are made up of several series-connected coils which are called sections. High

Table 9-6

TUBE THICKNESS FOR MECHANICAL STRENGTH

Smallest Core Dimension, inches	Tube thickness, mils of paper
to 1/2	10-20
1/2 to 5/8	15-30
5/8 to 3/4	17-35
3/4 to 7/8	20-40
7/8 to 1	25-45
1 - up	30-50

Table 9-7

LAYER INSULATION AND MARGINS FOR MECHANICAL STRENGTH

Wire Size AWG	Layer Insulation, mils	Margins at each end, inches
10-16	10.0	5/32
17-19	7.0	"
20-21	5.0	1/8
22-24	3.5	"
25-27	2.2	"
28-31	1.5	"
32-33	1.3	3/32
34-38	1.0	"
39-41	.7	1/16
42-44	.5	"

voltage windings are divided into narrow sections so as to reduce the turns per layer. The creepage voltage from one layer to any other layer of the section is then also lower than it would be for a wider single coil winding. High-voltage oil-filled transformer windings are usually divided into sections to make a more economical design. High voltage windings for air-cooled transformers are sometimes designed with section voltages as low as about 1500 volts but seldom are they designed with section voltages higher than about 5000 volts. For high-voltage windings, 5000 volts per section is also about the maximum in oil-filled construction.

Winding taps and leads should be taken off the winding outside of the part which fits into the core window. The start lead may be placed on the coil form and insulated. The coil turns are then wound on top. Tap leads can be arranged in the same manner giving a mechanically strong method of lead take off. Finish leads should be fastened with tape or string, since there are no turns of wire to hold them in place. Insulation is placed under the joint, and layer insulation is wound over the joint and entire coil to hold the lead in place. Electrical grade adhesive tape is widely used to anchor leads, since it is important to avoid the use of non-corrosive adhesive.

Leads must be large enough to keep the voltage drop low, and insulated well enough to withstand maximum voltage. Leads and joints must also be mechanically strong enough to withstand winding, impregnating, and handling stresses without breakage. Windings with wire sizes from AWG 17 to AWG 30 are best tapped by taking out the wire at the connecting point and bringing it back along the same path to start the next section. The two wires forming the tap can be twisted together to improve the mechanical strength. For wires smaller than AWG 27, heavier flexible leads should be soldered to the winding in the proper place.

When coils are to be wound on a multiple winding machine, it is desirable to design them so that the taps are to be made at the ends of certain layers. Otherwise the machine must be stopped while the tap is made manually. Sometimes the location of taps at the ends is undesirable because a larger coil is obtained.

A static shield is often used in coils to prevent high-frequency signals from being transmitted through the transformer from the secondary circuit to

the primary power source. This signal transfer can occur due to interwinding capacitance. The shield is a thin, one-turn strip of metal between the primary and secondaries, and is grounded. The turn must be open, or it will act as a short-circuited secondary. Typical shields are made of .002 to .004 inch thick copper, and are assembled with insulated, overlapping ends.

APPENDIX A: INSULATION DATA

Table A-1

TYPICAL DIELECTRIC REQUIREMENTS FOR MAGNET WIRE

Type	Size AWG	Dielectrid strength between 2 layers - RMS volts
Enamel* or Single Formvar	8 - 11	1500
	12 - 15	1300
	16 - 20	1100
	21 - 24	900
	25 - 28	650
	29 - 32	500
	33 - 36	400
	37 - 40	300
	41 and smaller	200
Heavy enamel* or enamel covered with single paper bonded, or Heavy (Double) Formvar	8 - 11	3000
	12 - 15	2650
	16 - 20	2300
	21 - 24	1900
	25 - 28	1500
	29 - 32	1100
	33 - 36	800
	37 - 40	500
	41 and less	300
Triple Formvar*	8 - 11	3900
	12 - 15	3500
	16 - 20	2900
	21 - 24	2500
	25 - 28	2000
	29 - 32	1600
	33 - 36	1100
	37 - 40	800
Glass Insulated** (Single)	to 9	500
	10 - 24	400
	25 - 40	250
Glass**	to 9	900
	10 - 24	600
	25 - 40	450

* NEMA "twist" test
** NEMA "layer" test
NOTE: Permissible working voltage is a fraction of the dielectric strength. See discussion of safety factors, Chapter V.

Table A-1 (Cont.)

TYPICAL DIELECTRIC REQUIREMENTS FOR MAGNET WIRE

(HIGH TEMPERATURE TYPES)

Type*	Dielectric strength,** volts per mil at 60 cycles	Power factor at 1 mc, %	Dielectric Constant Maximum
Ceroc ST, Single Teflon and Ceramic	900	1.5	3
Ceroc T, Double Teflon and Ceramic	1400	.8	3
Ceroc 200*** Silicone and Ceramic	600	2	3

* Trade names of Sprague Electric Co.
** Twist test
*** Use only in enclosed units

Sources of supply for magnet wire include:

The Acme Wire Company, New Haven, Conn.
American Steel and Wire Company, Cleveland, Ohio
Anaconda Wire and Cable Company, Chicago, Illinois
Belden Mfg. Company, Chicago, Illinois
Electric Auto-Lite Company, Port Huron, Michigan
Essex Wire Corporation, Fort Wayne, Indiana
General Cable Corp., New York, New York
General Electric Company, Bridgeport, Connecticut
Hudson Wire Company, Winsted, Connecticut
Kennecott Wire and Cable Co., Phillipsdale, R.I.
Phelps-Dodge Copper Products Corp., Fort Wayne, Indiana
Philadelphia Insulated Wire Co., Philadelphia, Penn.
John A. Roebling's Sons Co., Trenton, New Jersey
Rome Cable Corporation, Rome, New York
Rea Magnet Wire Co., Fort Wayne, Indiana
Sprague Electric Co., North Adams, Mass.
Warren Wire Co., Pownal, Vermont
Wheeler Insulated Wire Co., In., Waterbury, Conn.

Table A-2

PHYSICAL AND ELECTRICAL PROPERTIES* OF TYPICAL TYPES OF KRAFT PAPER

**Type	**Thickness in Inches	Density Grams/ Cu. Cm.	Tensile Strength (lbs) MD	CMD	Tear Strength (Grams) MD	CMD	Dielectric Strength (Short Time) Volts/Mil (Min. Ave.)
Super Calendered	.003	0.95-1.05	40	22	45	55	300-350
"	.005	1.0 -1.10	100	25	85	130	250-300
"	.015	0.95-1.15	395	60	470	960	200-250
Machine Calendered	.005	0.74-0.85	40	20	--	--	200-250
Machine Finish	.005	0.65-0.75	35	20	--	--	150-200
"	0.015	0.65-0.75	100	55	--	--	120-150

* The above data are to be used only as a guide and not for specification purpose.

** Other types and thicknesses are available. Thicknesses from .00025" to .030" can be obtained.

NOTE: Permissible working voltage is a fraction of the dielectric strength. See discussion of safety factors, Chapter V.

Sources of supply for the various types of Kraft paper include:

Case Brothers, Inc., Manchester, New York
Central Paper Company, Muskegon, Michigan
Claremont Paper Company, Claremont, New Hampshire
Hartford City Paper Company, Hartford City, Indiana
Hollingsworth and Vose Company, East Walpole, Mass.
Mosinee Paper Mills Company, Mosinee, Wisconsin
Riegel Paper Corp., New York City, New York
Peter J. Schweitzer Inc., New York City, New York
Stevens Paper Company, Windsor, Connecticut.

Table A-3 PROPERTIES* OF SUPER CALENDERED KRAFT PAPERS

Thickness										
Nominal	.00025"	.0003"	.0004"	.0005"	.0006"	.00075"	.001"	.0015"	.002"	.003"
Maximum	.00027"	.000325"	.000425"	.000525"	.00063"	.00079"	.00105"	.00157"	.0021"	.00315"
Minimum	.00024"	.000275"	.000375"	.000475"	.00057"	.00071"	.00095"	.00143"	.0019"	.00285"
Apparent Density										
Nominal	1.00	1.00	1.00	1.00	1.00	1.00	1.00	1.00	1.00	1.00
Maximum Avg.	1.07	1.05	1.05	1.05	1.05	1.05	1.05	1.05	1.05	1.05
Minimum Avg.	0.95	0.95	0.95	0.95	0.95	0.95	0.95	0.95	0.95	0.95
Moisture Content										
Average	6.5%	6.5%	6.5%	6.5%	6.5%	6.5%	6.5%	6.5%	6.5%	6.5%
Dielectric Strength										
Volts Per Mil	1250	1150	850	700	600	550	500	425	400	350

Table A-4 PROPERTIES* OF MACHINE CALENDERED KRAFT PAPERS

Thickness									
Nominal	.001"	.0015"	.0017"	.002"	.0025"	.003"	.004"	.005"	.006"
Maximum	.00105"	.00157"	.00178"	.0021"	.00262"	.00315"	.0042"	.00525"	.0063"
Minimum	.00095"	.00143"	.00162"	.0019"	.00285"	.00285"	.0038"	.00475"	.0057"
Apparent Density									
Nominal	0.775	0.775	0.775	0.775	0.775	0.775	0.775	0.775	0.775
Maximum Avg.	0.805	0.805	0.805	0.805	0.805	0.805	0.805	0.805	0.805
Minimum Avg.	0.735	0.735	0.735	0.735	0.735	0.735	0.735	0.735	0.735
Moisture Content									
Average	6.5%	6.5%	6.5%	6.5%	6.5%	6.5%	6.5%	6.5%	6.5%
Dielectric Strength									
Volts Per Mil	400	380	365	350	325	300	275	250	225

* These data are a guide to properties and are not to be regarded as specifications.

Table A-5 PROPERTIES OF ALL-RAG PAPER

Thickness Inches	Tear Strength (Grams) CMD	MD	Mullen Bursting Strength (lbs)	Tensile Strength (lbs/sq.in)	Dielectric Strength (Short time) Volts/mil (Min. Ave.)	Density Grams/ Cu. Cm.
.005	220	180	90			
.007	380	280	130			
.010	700	550	190	13,000-16,000	300	1.25-1.40
.012	900	675	240			
.015	1200	850	360			
.020	1700	1400	450			
.025	2200	1600	625			

Sources of supply include:

Cottrell Paper Company, Rock City Falls, New York
John A. Manning Company, Troy, New York
Spaulding Fiber Company, Tonawanda, New York

Plus manufacturer's representatives.

Table A-6 PART-RAG PAPER

Thickness Inches	Density Grams Per cc	Tensile Strength (lbs) MD	CMD	Elongation (%) MD	CMD	Tear Strength (Grams) MD	CMD	Dielectric Strength (Short time) Volts/mil (min. Ave.)
.007	1.2-1.4	70-80	25-35	3-4	8-9	300-350	350-400	300-450
.015	1.2-1.4	175-185	50-60	3.5-4.5	10-11	650-700	900-950	300-400

Sources of supply include:

Hollingsworth and Vose Company, East Walpole, Mass.
John A. Manning Paper Company, Troy, New York.

Table A-7 ROPE INSULATING PAPER

Thickness	Elongation (%) MD	CMD	Tensile Strength (lbs.) MD	CMD	Tear Strength (Grams) MD	CMD	Dielectric Strength (Short time) Volts per Mil (Min. Ave.)
.007	2.6	10.0	76	26	312	358	200

Table A-8 PROPERTIES OF VULCANIZED FIBER (FISH PAPER)

Tensile Strength (lbs/sq. in)

(Lengthwise)- - - - - - - - - - - - - - - - - - -8,000 min.
Crosswise)- - - - - - - - - - - - - - - - - - - 6,000 min.

Mullen Bursting Strength (lbs./sq. in.)

0.005" thick - - - - - - - - - - - - - - - - - - - 75 min.
0.007" thick - - - - - - - - - - - - - - - - - - - 105 min.
0.010" thick - - - - - - - - - - - - - - - - - - - 150 min.
0.015" thick - - - - - - - - - - - - - - - - - - - 225 min.
0.020" thick - - - - - - - - - - - - - - - - - - - 325 min.

Elmendorf Tearing Strength (grams)

	Lengthwise	Crosswise
0.005"	100	120
0.007"	190	220
0.010"	250	300
0.015"	375	450

Water Adsorption (%)

	2 hr.	24 hr.
.015" to .125" incl.	50-55	60-65

Density

Under .010" thick - - - - - - - - - - - - - - - - - .90 min.
.010" to 1/8" - - - - - - - - - - - - - - - - - - - 1.15 min.
Cubic inches per pound - - - - - - - - - - - - - - 20-25

Dielectric Strength (volts/mil)

Short time test .004" - .005" incl. - - - - - - - - 200 min.
over .005" - .015" incl. - - - - - - - - 300 min.
over .015" - .040" incl. - - - - - - - - 250 min.
over .040" - .125" incl. - - - - - - - - 175 min.

For information regarding test methods refer to ASTM-D-710.

Sources of supply include:

Continental-Diamond Fibre Company, Newark, Delaware
National Vulcanized Fibre Company, Wilmington, Delaware
Spaulding Fibre Company, Tonawanda, New York
Taylor Fibre Company, Norristown, Pennsylvania.

Table A-9 IDENTIFICATION OF GRADES AND SUMMARY OF PERFORMANCE CHARACTERISTICS
(NEMA STANDARDS FOR VARNISHED TUBING AND SATURATED SLEEVING)

NEMA Designations	Dielectric Strength, Volts C-48/25/50 Minimum Average	C-48/25/50 Minimum Individual	C-96/25/96 Minimum Average	C-96/25/96 Minimum Individual	Heat Aging	Transformer Oil Immersion (48 Hours at 105C, - 0C + 5C)	Heat Endurance, 15 Min. at 225C + 7C	Burning Rate Min. Sec. to Burn 1 Inch
A-A-1	7000	5000	2100	1500	No Failure	No disintegration or swelling	Shall not soften, blister or flow	45
A-A-2	7000	5000	2100	1500	No Failure	.....	.....	45
A-B-1	4000	2500	1200	750	No Failure	No disintegration or swelling	Shall not soften, blister or flow	45
A-B-2	4000	2500	1200	750	No Failure	.....	.....	45
A-C-1	2500	1500	....	....	.....	No disintegration or swelling	Shall not soften, blister or flow	45
A-C-2	1500	800	....	....	.....	.....	Shall not soften, blister or flow	45
A-C-3	....	....	....	....	.....	.....	.....	45
B-A-1	7000	5000	2800	2000	No Failure	No disintegration or swelling	Shall not soften, blister or flow	45
B-A-2	7000	5000	2800	2000	No Failure	.....	.....	..
B-B-1	4000	2500	2000	1250	No Failure	No disintegration or swelling	Shall not soften, blister or flow	45
B-B-2	4000	2500	2000	1250	No Failure	.....	.....	45
B-C-1	2500	1500	....	....	.....	No Disintegration or swelling	Shall not soften, blister or flow	45
B-C-2	1500	800	....	....	.....	....	Shall not soften, blister or flow	45
B-C-3	....	....	....	....	.....	.....	.....	..
H-A-1	7000	5000	2800	2000	No Failure**	.....	.....	45
H-B-1	4000	2500	2000	1250	No Failure**	.....	.....	45
H-C-1	2500	1500	....	....	.....	.....	.....	45
H-C-2	1500	800	....	....	.....	.....	.....	45
H-C-3	....	....	....	....	.....	.....	.....	..

Conditioning - 48 hours at 25°C and 50% Relative Humidity. Conditioning - 96 hours at 25°C and 96% Relative Humidity.
**If failure occurs after 96 hours at 200C ± 5C (392F ± 9F), the test shall be continued for an additional 96 hours. (Failure after the initial 96 hours may be due to temporary embrittlement which does not constitute failure if flexibility is recovered after an additional 96-hour period.)

Table A-10

PROPERTIES OF VARNISHED INSULATING PAPERS

Thickness (Nominal)	Color	Base Paper	Average Short-time Dielectric Strength V.P.M.	Approximate Weight lbs. Per 100 Sq. Yds.
.00075"	Yellow	Condenser	2500	4.8
.001"	Yellow	Condenser	2000	6.3
.0015"	Yellow	Condenser	1900	9.4
.002"	Yellow	Condenser	1900	12.5
.003"	Yellow	Condenser	1500	--
.0015"	Yellow	Bond	2000	9.4
.002"	Yellow	Bond	1800	12.8
.0025"	Yellow	Bond	1800	15.5
.003"	Yellow	Bond	1800	19.2
.004"	Yellow	Bond	1500	25.6
.005"	Yellow	Bond	1200	32.0
.006"	Yellow	Bond	1200	38.0
.004"	Yellow and Black	Kraft	1500	23.0
.005"	Yellow and Black	Kraft	950	27.0
.006"	Yellow and Black	Kraft	950	33.0
.007"	Yellow and Black	Kraft	950	38.0
.008"	Yellow and Black	Kraft	950	43.7
.010"	Yellow and Black	Kraft	950	53.0
.012"	Yellow and Black	Kraft	900	60.0
.015"	Yellow and Black	Kraft	900	77.0
.020"	Yellow and Black	Kraft	830	100.0
.007"	Yellow	Rope	770	40.0
.010"	Yellow	Rope	630	57.0
.012"	Yellow	Rope	700	68.0
.015"	Yellow	Rope	570	85.0

Note: The above technical data figures are averaged values and should not be used in writing definite specifications. Permissible working voltage is a fraction of the dielectric strength. See discussion of safety factors, Chapter V.

Table A-11

PROPERTIES OF VARNISHED GLASS CLOTH

Base Cloth Thickness (Nominal)	Finished Thickness (Nominal)	Approx. Wgt. lbs. per 100 sq. yds.	Tensile Strength lbs. per 1" Width	Dielectric Strength 2" Electrodes V.P.M. Black	Yellow
.002"	.003"	18.9	70	1200	1100
.002"	.004"	26.5	--	--	--
.002"	.005"	31.5	--	--	--
.003"	.005"	35.5	100	1200	1050
.003"	.007"	44.9	100	1200	1050
.003"	.010"	59.0	100	1200	1050
.007"	.010"	65.0	250	1170	1025
.007"	.012"	89.2	250	1170	1025
.007"	.015"	90.5	--	--	--
.010"	.015"	103.0	400	1000	900
.010"	.020"	142.0	400	900	800
.015"	.025"	171.0	550	800	700
.015"	.030"	179.0	550	700	600

Note: Permissible working voltage is a fraction of the dielectric strength. See discussion of safety factors, Chapter V.

Table A-12 PROPERTIES SILICONE VARNISHED GLASS CLOTH TYPICAL TEST DATA*

Nominal Thickness	.003"	.004"	.005"	.007"	.010"	.012"	.015"	.020"	.025"
Base Glass Cloth	.002	.002	.002	.003	.005	.006	.007	.010	.015
Tensile Strength Lbs. Per Sq. In. Width.	70	70	70	100	190	225	275	400	525
Lbs. Per 100 Sq. Yd.	20	34	34	47	69	85	109	132	160
Specific Gravity	1.44	1.44	1.44	1.43	1.40	1.39	1.39	1.39	1.38
	DIELECTRIC STRENGTH V.P.M.								
1/4 Electrodes A-ASTM-25°C	1200	1400	1400	1350	1250	1200	900	900	800
1/4 Electrodes A-ASTM-175°C	800	1000	1000	1000	900	900	600	600	500
2" Electrodes A-ASTM-25°C	950	1075	1075	1075	950	925	600	600	500
2" Electrodes A-ASTM-175°C	600	700	700	700	650	600	300	300	250
	POWER FACTOR - 100° C								
Conditioned 3 hours at 105°C	1.0	1.0	1.0	1.0	1.0	1.0	1.0	1.0	1.0
Conditioned 24 hours at 65% RH	1.3	1.3	1.3	1.4	1.4	1.5	1.5	1.7	1.7
	DIELECTRIC CONSTANT - 100°C								
	3.5	3.5	3.5	3.4	3.4	3.4	3.4	3.4	3.4
	MOISTURE RESISTANCE								
% H_2O Absorbed- 24 hours at 65% RH	.01	.01	.01	.015	.015	.02	.02	.025	.03
%H_2O Absorbed- 24 hours Immersion	.70	.70	.70	.60	.55	.55	.55	.55	.50

* Based on average of published data.

NOTE: The above technical data figures are averaged values and should not be used in writing definite specifications.

Table A-13 PROPERTIES OF TYPICAL TYPES OF SILICONE VARNISHED GLASS CLOTHS

(BASED ON PUBLISHED INFORMATION)

This table presents additional test data of typical types of silicone varnished glass cloth

TEST			.004"	.007"
Tensile Strength - Pounds Per Inch Width (after 96 hours at 25°C and 50% Relative Humidity)		Warp	80	125
		Fill	36	80
Tear Strength - Grams (after 96 hours at 25°C and 50% Relative Humidity)		Warp	192	350
		Fill	125	250
Dielectric Strength - Volts Per Mil	After 96 hours at 25°C and 0% Relative Humidity		2000	1700
	After 96 hours at 25°C and 96% Relative Humidity		1450	1200
Power Factor at 60 cycles	After 96 hours at 25°C and 0% Relative Humidity		.010	.010
	After 96 hours at 25°C and 96% Relative Humidity		.060	.060
Dielectric Constant at 60 cycles	After 96 hours at 25°C and 0% Relative Humidity		4.0	4.0
	After 96 hours at 25°C and 96% Relative Humidity		4.2	4.2
Approximate Weight Per Square Yard in Pounds			.27	.47
Low Temperature Bend			-51°C (-60°F.)	
Heat Aging at 200°C (392°F)			over 1500 Hours	
Solvent Resistance	Hot Oil Resistance - 10C Oil at 150°C (302°F)		softens	
	Mineral Spirits		softens	
	Alchohol		fair	
	Benzene		soluble	
	10% HCL Solution		good	
	10% NAOH		good	

.007" SILICONE VARNISHED GLASS CLOTH

Dielectric Strength Volts/Mil 1/4" Electrodes - Short Time			Dielectric Constant	
	Initially	1860	at 25°C	19
	After 28 days at 200°C	1586	100°C	24
	After 28 days at 240°C	1506		
	After 7 days at 275°C	1738		
60 Cycle Power Factor at	25°C	.0034		
	100°C	.0028		

Table A-14

PROPERTIES OF SILICONE RUBBER-COATED GLASS CLOTH

Thickness (Nominal)	.007"	.010"	.012"	.015"
Approximate Weight lbs./sq. yd.	0.60	0.90	1.07	1.31
Tensile Strength - P.I.W.	100/85	160/150	225/195	225/195
1/4" Electrodes - V.P.M.				
At 25 deg. C.	800	700	600	500
At 100 deg. C.	800	700	600	500
At 150 deg. C.	750	650	550	450
Power Factor				
At 25 deg. C.	0.7%	0.7%	0.7%	0.7%
At 100 deg. C.	1.80%	1.80%	1.80%	1.80%
At 150 deg. C.	3.20%	3.20%	3.20%	3.20%
Dielectric Constant				
At 25 deg. C.	3.30	3.35	3.35	3.35
At 100 deg. C.	2.80	2.85	2.85	2.85
At 150 deg. C.	2.80	2.84	2.84	2.84
Low temperature Flexibility	-60°C	-60°C	-60°C	-60°C
Heat Resistance	Silicone rubber coated glass cloth will retain its flexibility after 500 hours exposure to 200° C, indicating that it has a safe continuous operating temperature up to 175°C.			

NOTE: Permissible working voltage is a fraction of the dielectric strength. See discussion of safety factors, Chapter V.

Table A-15

SOURCES OF SUPPLY FOR ELECTRICAL INSULATION MATERIALS

Materials include:

Varnished Insulated Paper.
Varnished Tubing and Saturated Sleeving.
Varnish Glass Cloth.
Silicone Varnished Glass Cloth
Silicone Rubber Coated Glass Cloth

Manufacturers:

The Alox Mfg. Co, St. Louis, Mo.
Bentley Harris Mfg. Co., Conshohocken, Penn.
Dielectric Materials Company, Chicago, Ill.
William Brank and Company, Willimantic, Conn.
Electra Insulating Corp, Woodside, New York.
Electro-Technical Products Corp., Nutley, New Jersey
General Electric Company (Chemical Division) Pittsfield, Mass.
Irvington Varnish and Insulator Co., Irvington, New Jersey.
Frank L. Markel and Sons, Norristown, Penn.
Mitchell-Rand Insulation Co., Inc., Irvington, New Jersey
National Electric Coil Co., Columbus, Ohio.
National Varnished Products Corp., Woodbridge, New Jersey.
New Jersey Wood Finishing Company, Woodbridge, New Jersey.
Mica Insulator Company, Schenectady, New York.
Suflex Corporation, Woodside, New York.
Suprenant Mfg. Co., Boston, Mass.
Varflex Corporation, Rome, New York.
Westinghouse Electric Corporation, Pittsburgh, Penn.

Distributors or Sales Representatives:

Earl B. Beach Company, Pittsburgh, Pa.
Brooks Electrical Supply Company, Baltimore, Maryland.
Electrical Maintenance Equipment Company, Philadelphia, Penn.
J. J. Glenn and Company, Chicago, Illinois
The Huse-Liberty Mica Company, Boston, Mass.
Insulation Manufacturers Corporation, Chicago, Illinois.
Insulation and Wires Inc., St. Louis, Mo.
The Fred W. Kiemle Company, Toledo, Ohio.
C. D. LaMoree, Los Angeles, California.
Moore-Handley Hardware Company, Inc., Birmingham, Alabama.
Robert McKeown Company, Newark, New Jersey.
Summers Electric Company, Dallas, Texas.
Strance Products, Inc., Chicago, Illinois.
TriState Supply Corporation, Los Angeles, California.
Western Fiberglas Supply Ltd., San Francisco, California.
White Supply Company, St. Louis, Mo.

Table A-16 ELECTRICAL AND PHYSICAL PROPERTIES OF "TEFLON" COATED GLASS FABRICS-SINGLE PLY

Product		3 Mil	5 Mil	8 Mil	10 Mil	14 Mil	ASTM Method of Test
ELECTRICAL PROPERTIES*							
Surface arc resistance, sec		>240	>240	>240	>240	>240	D-495
Dielectric strength, short time, volts/mil		>500	>500	250 avg.	250 avg.	250 avg.	D-149
Dielectric constant, 60 to 100,000 cycles		2.8	2.8	3.0	3.0	3.3	D-150
Power Factor, 60 to 100,000 cycles		0.0005	0.0006	0.0007	0.0007	0.0007	D-150
Volume resistivity, ohm-cm., room conditions		$5x10^{11}$	$5x10^{11}$	$5x10^{11}$	$5x10^{11}$	$5x10^{11}$	D-257
Insulation resistance, ohms (96 Hrs. at 90% R.H., 35°C)		10^8	10^8	10^8	10^8	10^8	D-257 (Fig 2)
MECHANICAL PROPERTIES							
Tensile strength, lb./in. of width	warp	>40	>70	>215	>225	>250	D-39-39
	fill	>35	>65	>210	>165	>200	Grab Method
Approx. minimum breaking strength lb./in. of width	warp	70	100	250	250	400	.....
	fill	40	70	200	200	290	.....
Tear strength, lb./sq.in.	warp	720	750	1200	...	...	D-624
	fill	500	760	1360	...	...	....
Elmendorf tear strength, lbs.	warp	>0.30	>0.55	>2.7	>2.7	>2.8	....
	fill	>0.20	>0.40	>2.2	>2.2	>2.5	....
Elongation, %	warp	0	0	0	0	0	D-412
	fill	0	0	0	0	0	(modified)
Mullen hydrostatic, lb./sq.in. (Average Values - See Note 1)		55	100	75	100	130	....
Shear strength, 1" diam. punch, lb./sq.in.		7800	13,100	11,300	11,300	11,200	D-732
Stiffness, lb./sq.in. (modulus in flexure)	warp	Limp	Limp	130,000	132,000	168,000	D-747
	fill	Limp	Limp	....	97,000	113,000	....
Static tensile modulus, lb./sq.in.	warp	211,000	195,000	....	77,000	64,300	....
	fill	192,000	138,000	....	73,000	60,400	....

Note 1: Mullen Hydrostatic: The values shown are average pilot plant production. Occasional pin holes can be expected and wherever a pin hole occurs, a low hydrostatic value can be expected.

* Permissible working voltage is a fraction of the dielectric strength. See discussion of safety factors, Chapter V.

Table A-17 MISCELLANEOUS PROPERTIES OF "TEFLON" COATED GLASS FABRICS - SINGLE PLY

Product	3 Mil	5 Mil	8 Mil	10 Mil	14 Mil	ASTM Method of Test
THERMAL PROPERTIES						
Specific heat, cal./g./°C	0.189	0.218	0.194	.....	.....	.....
Thermal conductivity Btu./hr./°F/sq.ft./in.	0.1245	0.100	0.298	.....	.....	.....
t.cal./sec.sq.cm/°C/cm.	.43x10^{-4}	.34x10^{-4}	.92x10^{-4}	.....	.....	.....
Service temperatures, max. and min.	See Note 3.					
MISCELLANEOUS PROPERTIES						
Moisture permeability, g./100m.^{2}hr.	36	55	56	.....	.....	DuPont Cellophane method D-570 (modified)
Water absorption, %	0.30	0.26	0.30	.....	.....	
Appearance	Waxy					
Color	Colorless to Pale Amber					
Flammability	Non-flammable					
Weathering	Excellent					
Anti-sticking and anti-friction	See Note 4.					

Note 2: Chemical Resistance: Attacked slowly by molten alkali metals, and under special conditions by flourine and chlorine trifluoride. Unaffected by any other corrosive chemicals, except possibly at cut edges by chemicals which attack glass.

Note 3: Service Temperatures: "Teflon" Coated Glass Fabrics are extremely stable at elevated temperatures. Under prolonged storage at 250°C (482°F) there is no appreciable loss in weight. "Teflon" Coated Glass Fabrics remain pliable at temperatures as low as -87.5°C (-100°F). Samples thoroughly flexed at -87.5°C show no visible signs of cracking.

Note 4: Anti-Sticking and Anti-Friction: The surface of any "Teflon" Coated Glass Fabric or Laminate exhibits remarkable anti-adhesive and anti-friction qualities. In general, sticky, resinous or moist materials do not readily adhere, making it unnecessary to use anti-blocking agents, or lubricating release agents.

Table A-18 INDUSTRIAL LAMINATES

Paper-Base Laminates (Phenolic Resin)

NEMA Grade (Military Spec. and Type)		Forms Available
X	Primarily intended for mechanical applications where properties are of secondary importance. Should be used with discretion when high-humidity conditions are encountered. Not equal to fabric-base grades in impact strength.	Sheets Tubes
P	Primarily intended for punching hot. More flexible and not as strong as Grade X. Intermediate between Grade X and XX in moisture resistance and electrical properties.	Sheets
PC	Primarily intended for cold punching and shearing. More flexible and lower in flexural strength than the P grade but higher in cold flow.	Sheets
XX (MIL-P-3115B Type PBG)	Suitable for usual electrical applications. Good machinability.	Sheets Tubes Rods
XXP	Better than Grade XX in electrical and moisture-resisting properties and more suitable for hot punching. Intermediate between Grades P and XX in punching and cold flow characteristics.	Sheets.
XXX (MIL-P-3115B Type PBE)	Suitable for radio frequency work, for high-humidity applications and with minimum cold flow characteristics.	Sheets Tubes Rods
XXXP (MIL-P-3115B Type PBE-P)	Better in electrical properties than Grade XXX and more suitable for hot punching. Intermediate between Grades XXP and XX in punching characteristics. This grade is recommended for applications requiring high insulation resistance and low dielectric losses under severe humidity conditions.	Sheets.

Fabric-base Laminates (Phenolic Resin)

C (MIL-P-15035B, Type FBM)	Laminated from medium weave and weight cotton fabric. A tough, strong material suitable for gears and other applications requiring high impact. The weight of fabric is determined by the thickness and applications: heavier fabric giving better impact strength; lighter	Sheets Tubes Rods

Table A-18 (Continued)

	offering better machinability. This grade does not have controlled electrical properties and its use for electrical applications is not recommended.	
CE (MIL-P-15035B, Type FBG)	This grade is made from the same fabrics used in Grade C. Suitable for electrical applications requiring greater toughness than provided by Grade XX or for mechanical applications requiring greater resistance to moisture than provided by Grade C. This Grade is not recommended for primary insulation* for electrical applications involving commercial power frequencies at voltages in excess of 600 volts.	Sheets Tubes Rods
L (MIL-P-15035B, Type FBI)	This grade is made from a very fine weave and light weight cotton fabric. It is suitable for small gears and other fine mechining applications, particularly in thicknesses under 1/2 inch. Not quite so tough as Grade C. This grade does not have controlled electrical properties and its use for electrical applications is not recommended.	Sheets Tubes Rods
LE (MIL-P-15035B, Type FBE).	Made from the same cotton fabrics as Grade L. Suitable for electrical applications requiring greater toughness than provided by grade XX. Better machining properties and finer appearance than Grade CE and available in thinner sizes. Good in moisture resistance. This grade is not recommended for primary insulation for electrical applications involving commercial power frequencies at voltages in excess of 600 volts.	Sheets Tubes Rods
	Asbestos-base Grades (Phenolic Resin)	
A	Asbestos paper base. More resistant to heat and slightly more resistant to heat than the cotton fabric and paper base grades because of the high inorganic content. More difficult to machine than the cotton fabrics and paper base grades. Not recommended for primary electrical insulation at commercial power frequencies in excess of 250 volts.	Sheets Tubes
AA	Asbestos fabric base. More resistant to heat and tougher than Grade A. Not recommended for primary electrical insulation. Machining properties are better than Grade A but not as good as Grade C.	Sheets Tubes

* "Primary insulation" means insulation which is in direct contact with terminals, conductors, or other current-carrying members.

Table A-18(Continued)

Glass-base Grades

G-1	Staple-fibre-type glass cloth with phenolic resin binder. General purpose, heat-resistant grade. Higher impact strength than cotton-fabric and asbestos grades. Good dielectric loss properties and insulation resistance under dry conditions. Low dimensional change under humid conditions. Difficult to machine. Suitable for class BW insulation.	Sheets Tubes Rods
G-2	Staple-fibre-type glass cloth with phenolic resin binder. Electrical and heat-resistant grade. Good electrical properties under high humidity conditions. Mechanically it is the weakest of the glass-base grades. Lower in dielectric losses than other glass-base grades excepting silicone. Good dimensional stability.	Sheets Tubes Rods
G-5 (MIL-P-15037B, Type GMG)	Continous-filament-type glass cloth with melamine resin binder. Highest mechanical strength and hardest laminated grade. Good flame resistance, and second only to silicone laminates in heat and arc resistance. Good electrical properties under dry conditions. Low insulation resistance under high humidities. Good dimensional stability.	Sheets Tubes Rods
G-6	Staple-fibre-type glass cloth with silicone binder. Extremely low dielectric loss and high insulation resistance properties under dry conditions. Good electrical properties under high humidity. Excellent heat and arc resistance. Good impact strength. Other mechanical properties fair. Good dimensional stability and machining properties similar to Grade G-7. Recommended as insulation where high temperature resistance, arc resistance, and low losses are needed such as radio transmitter insulation and Class CW transformers.	Sheets
G-7 (MIL-P-997B Type GSG)	Continuous-filament-type glass cloth with silicone resin binder. This grade combines the excellent electrical and heat resisting properties of Grade G-6 with somewhat higher tensile and flexural strengths. Bond strength slightly lower than for Grade G-6. Meets Class CW insulation requirements. Recommended for similar applications to G-6 but where higher mechanical strength is required.	Sheets
N-1 (MIL-P-15047A, Type NPG)	Nylon cloth base with phenolic resin binder. Excellent electrical properties under high humidity conditions. Good impact strength, but subject to flow or creep especially at temperatures higher than normal.	Sheets Tubes Rods

Table A-19 PROPERTIES OF INDUSTRIAL LAMINATES

NEMA Grade	Water Absorption % After 24 Hours Thickness 1/32"	1/16"	1/8"	Specific Gravity	Specific Volume Cu in/lb	Tensile Strength lbs per sq in L.W.	C.W.	Dielectric Strength Perpendicular to Laminations Volts/Mil. Short Time 1/16"	1/8"	Step by Step 1/16"	1/8"
X	5.9	3.3	1.8	1.37	20.25	15,000-20,600	12,000-16,000	700-750	500-600	500-530	360-400
P	3.0	2.8	1.7	1.36	20.4	10,000-13,500	8,000-10,000	575-700	470-500	400-500	320-360
PC	5.5	3.3	2.0	1.34	20.3	9,000-12,000	8,000- 8,700	600-775	425-675	400-600	290-475
XX	2.0	1.4	0.90	1.36	20.3	10,000-14,500	10,000-11,100	675-700	500-615	500-550	360-425
XXP	2.3	1.6	1.0	1.34	20.5	10,000-16,400	8,000-12,900	700-775	500-675	500-625	360-500
XXX	1.5	0.86	0.60	1.34	20.5	11,000-13,100	10,000-10,500	650	470-575	450-575	320-425
XXXP	1.3	0.80	0.42	1.31	20.7	9,000-15,400	7,500-11,800	650-725	470-575	450-675	320-550
C	4.0	3.4	1.3	1.36	20.25	10,000-12,100	9,000- 9,800	200-440	--	120-300	--
CE	2.5	1.54	1.0	1.35	20.5	9,000-13,400	8,000- 9,800	380-525	360-400	265-325	220-240
L	4.6	1.9	1.2	1.36	20.3	11,000-14,000	9,500-10,000	200-475	--	120-325	--
LE	3.3	1.4	0.80	1.35	20.5	10,000-15,000	8,000-10,600	450-525	360-400	290-320	140-220
A	2.1	1.3	0.80	1.68	16.0	10,000	6,000- 8,000	225-325	160-225	135-200	95-140
AA	--	2.0	1.0	1.64	16.1	10,000-12,000	6,500-10,000	85	70	65	40
G-1	2.5	1.7	0.87	1.57	16.7	12,500-15,000	9,500-12,000	250-450	200-300	150-390	120-210
G-2	--	1.7	0.87	1.57	16.7	12,500-15,000	9,500-12,000	250-450	200-300	150-390	120-210
G-3	2.0	1.7	0.82	1.68	16.0	23,000-28,000	15,000-22,000	575-700	450-600	390-500	375-450
G-5	2.4	2.2	1.7	1.91	14.43	25,000-38,200	22,000-35,000	375-600	275-500	250-350	175-300
G-6	--	0.30	0.30	1.67	16.8	16,000	10,500	150-250	--	100-220	--
G-7	0.35	0.30	0.20	1.69	16.5	23,000	18,500	250-400	--	170-350	--
N-1	0.55	0.26	0.16	1.15	24.0	8,500-9,250	8,000-9,000	600-650	450-550	425-450	300-375

NOTE: Permissible working voltage is a fraction of the dielectric strength. See discussion of safety factors, Chapter V.

Table A-19 (Continued)

PROPERTIES OF INDUSTRIAL LAMINATES

NEMA Grade	Power Factor 10^6 Cycles 1/16" Thickness As Received	Power Factor 10^6 Cycles 1/16" Thickness After 24 Hours in Water at 25°C	Dielectric Constant 10^6 Cycles 1/16" Thickness As Received	Dielectric Constant 10^6 Cycles 1/16" Thickness After 24 Hours in Water at 25°C	Insulation Resistance Megohms After 96 Hours at 90% Relative Humidity at 35°C	Heat Resistance Degrees F Continuous	Heat Resistance Degrees F Short Time	Loss Factor 10^6 Cycles As Received
X	.039-.046	.050-.052	5.1-5.8	6.0	90-100	225-275	275-300	0.20-0.24
P	.036-.043	.040-.046	4.6-5.3	5.2-6.0	100-200	230-275	275-300	0.17-0.19
PC	.041	.050	--	--	100-200	200-250	250-275	0.23
XX	.038-.045	.039-.050	5.0-5.5	5.4-6.0	500	250-275	275-300	0.20-0.21
XXP	.030-.040	.034-.045	4.3-4.8	4.5-5.2	500	250-275	275-300	0.13-0.17
XCX	.032-.038	.033-.047	4.7-5.4	5.0-5.9	800-1000	250-275	275-300	0.16-0.17
XXXP	.026-.030	.027-.035	4.0-4.6	4.4-4.6	2000	250-275	275-300	0.11
C	.065-.075	0.218	5.8-6.5	--	20-25	200-225	225-275	0.36-0.50
CE	.045-.060	.049-.070	5.2-5.5	5.5-5.6	50-100	200-250	225-300	0.26-0.33
L	.065-.070	0.72	6.0	6.3	20-25	200-225	225-275	0.39-0.45
LE	.045-.055	.050-.070	4.8-5.8	5.2-6.0	30-100	200-250	225-300	0.22-0.29
A	.090-0.179	0.223	5.2-7.0	7.3	--	270-290	290-400	0.54-0.60
AA	.44-.059	0.73	6.8-7.5	12.5	--	275-325	325-400	2.99
G-1	.011-.02	.02-.05	4.2-5.2	4.3-6.8	200-500	290-325	325-410	0.046-0.10
G-2	.011-.02	.02-.05	4.2-5.2	4.3-6.8	200-500	290-325	325-410	0.046-0.10
G-3	.017-.025	.035-.04	4.8-4.9	5.1-5.3	25-200	290-325	325-410	0.09-0.13
G-5	.011-.020	.03-.08	6.1-7.4	7.9	50-200	300-325	325-425	0.094-0.11
G-6	.0015-.0022	.015-.0227	2.9	3.7	--	400-482	500+	--
G-7	.0015	.012-.015	3.2	3.3	--	400-492	500+	--
N-1	.015-.038	.017-.039	3.3-3.9	3.9	50,000-400,000	165-225	210-235	0.05

For information concerning "test procedures" refer to NEMA Standards Publication No. LP1. NOTE: Permissible working voltage is a fraction of the dielectric strength. See discussion of safety factors, Chapter V.

Table A-20

ABSTRACTS FROM NEMA MANUFACTURED ELECTRICAL MICA STANDARDS (PUBLICATION NO. 46-117, MAY 1946)

NEMA No.	Type of Material	Bond Content Percent (ASTM) (D 352-49)	Splittings NEMA Grade	Nominal Thickness Inches	Variation in Avg. Thickness From Nominal, Inches		Variation of Individual Measurements from Nominal, Inches		Avg. Dielectric Strength, VPM ASTM D 149-44	
					Plus	Minus	Plus	Minus	Short Time Method "A"	Step-by Step Method "B"
1	Molding Plate, Milled	Not over 16	E	0.020 up to 0.036	0.002	0.002	0.003	0.003	500	390
2	Molding Plate, Unmilled	Not over 16	E	Up to 0.015	0.003	0.003	--	--	500	390
			E	0.015 up to 0.063	0.005	0.005	0.008	0.008	350	250
6	Cold Flexible Mica, Sheet	Not over 20	C	Up to 0.010	0.003	0.001	0.007	0.003	525	350
		Not over 20	D	0.010 up to 0.020	0.003	0.003	0.008	0.005	350	250
		Not over 20	E	0.020 and over	0.005	0.005	0.010	0.008	300	200

Principle Uses, No. 1 and 2: Formed parts of various shape, commutator cones, slot cells and troughs, end bell insulation, coil forms and spools, tubes of various cross-section, angles, channels, bushings, washers, etc.

No. 6: Insulation in armature slots, under end windings, at cross-overs, under terminals of field coils, core insulation, etc.

NOTE: Permissible working voltage is a fraction of the dielectric strength. See discussion of safety factor, Chapter V.

Table A-21 PROPERTIES* OF TYPICAL TYPES ELECTRICAL INSULATING VARNISHES

Type Varnish / Properties / Type base	Clear Air-Drying Modified Phenolic Drying Oil	Clear Air-Baking and Baking Oil Modified Alkyd	Black Air-Drying Asphalt Drying Oil	Clear Baking Oil Modified Phenolic Thermosetting	Clear Baking Alkyd	Black Baking Asphalt Drying Oil
Percent solids	50-51	49-51	37-39	49-51	50	50
Thinner	Petroleum Spirits	Xylol	VM and P Naphtha or Toluene	Petroleum Spirits or VM and P Naphtha	Pet. Spirits	Pet. Spirit or VM and P Naphtha
Viscosity at 25°C Centipoises	--	--	200-400	375-425	900	200-300
Specific Gravity at 21°C	--	--	.845-.850	.925-.935	0.910	--
Flash Point - Degrees F	95°	78°	--	--	95	--
Dielectric Strength(Dry)Volts/mil	1540	1450	1300	2200	1480	2500
Dielectric Strength-Volts/mil (After 24 hrs. water immersion)	570	505	500	1200	900	900
Build Relative	Good	Good	Excellent	Excellent	Fair	Good
Adhesion	Good	Excellent	Good	Excellent	Good	Good
Toughness	Good	Good	Fair	Good	Good	Good
Hardness	Good	Excellent	Fair	Excellent	Good	Good
Flexibility	Good	Fair	Fair	Good	Excellent	Good
Penetration	Good	Poor	Fair	Excellent	Excellent	Fair
Water	Excellent	Fair	Excellent	Excellent	Good	Excellent
Acid	Excellent	Excellent	Excellent	Excellent	Good	Excellent
Alkali	Good	Fair	Excellent	Excellent	Fair	Excellent
Oil	Good	Excellent	Poor	Excellent	Good	Good

* The above data are to be used as a guide and not for specification purposes.

Table A-22 SUPPLIES

Teflon Laminates and Film:

E. I. DuPont de Nemours and Company, Wilmington, Delaware (Laminates and Film.)

Continental Diamond Fiber Company (Laminates).
Minnesota Mining and Manufacturing Company (Tapes and Film).
Dielectrix Company, New York, New York (Film).

Industrial Laminates

Continental Diamond Fiber Company, Newark, Delaware.
The Formica Company, Cincinnati, Ohio.
General Electric Company (Chemical Division,)Pittsfield, Massachusetts.
Mica Insulator Company, Schenectady. New York
National Vulcanized Fiber Company, Wilmington, Delaware.
The Richardson Company, Melrose Park, Illinois.
Synthane Corporation, Oaks, Pennsylvania.
Taylor Fiber Company, Norristown, Pennsylvania.
Westinghouse Electric Corporation, Trafford, Pennsylvania.

Mica Products

Continental-Diamond Fiber Company, Newark, Delaware.
General Electric Company (Chemical Division), Pittsfield, Massachusetts.
The Macallen Company, Boston, Massachusetts.
Insulation Manufacturers Corporation, Chicago, Illinois.
Mica Insulator Company, Schenectady, New York.
National Electric Coil Company, Columbus, Ohio.
New England Mica Company, Waltham, Massachusetts.
J. J. Glenn and Company, Chicago, Illinois.

Electrical Insulating Varnishes:

Acme Wire Company, New Haven, Connecticut.
Bakelite Division, Union Carbide and Carbon Corp., New York, New York.
Geo. C. Borthig Co., Inc., East Rutherford, New Jersey
E. I. DuPont de Nemours and Company, Wilmington, Delaware
Brooklyn Varnish Mfg. Company, Brooklyn, New York.
Durez-Plastic and Chemicals Inc., New York, New York
John C. Dolph Varnish Company, Monmouth Junction, New Jersey
General Electric Company (Chemical Division), Schenectady, New York
P. D. George Company, St. Louis, Mo.
The Glidden Company, Cleveland, Ohio
Hanna Industrial Finishes, Columbus, Ohio.
Irvington Varnish and Insulator Co., Irvington, New Jersey
Mica Insulator Company, Schenectady, New York
Mitchell-Rand Insulation Company, Inc., New York, New York
Schenectady Varnish Company, Schenectady, New York
Sherwin-Williams Company, Cleveland, Ohio.
Sterling Varnish Company, Sewickley, Penn.
M. B. Suydam, Pittsburgh, Penn.
Universal Varnish Company, Cleveland, Ohio.
Westinghouse Electric Corporation, Pittsburgh, Pennsylvania.

Table A-23 POLYESTER RESINS

Type	Viscosity	Dielectric Strength v/m	60 cycle P.F. % 25C	60 cycle P.F. % 125C	60 cycle Dielectric Constant at 125C	% Shrinkage Liquid to Solid Unfilled Resin	Arc Resistance Sec.
rigid	low	450-550	0.9	3.0	2.8	7.5	120-135
rigid	low	400-500	1.2	1.7	4.3	8.2	
flexible	low		0.5		4.2	8.5	125

Sources of Supply for Polyester Resins

	Trade Name
American Cyanamide (Plastics and Resins Div.) New York, N. Y.	"Laminac"
Bakelite Div.. Union Carbide and Carbon Corp., New York, N. Y.	"BRS" Resins
General Electric Company (Chemical Division), Pittsfield, Mass.	"Permafil"
General Tire and Rubber Co., Akron, Ohio	"Genpol"
Marco Chemical, Sewaren, New Jersey	"Marco" (MR)
Naugatuck Chemical (Div. of U.S. Rubber Co.), Naugatuck, Conn.	"Vibrin"
Pittsburgh Plate Glass Company, Pittsburgh, Penn.	"Selectron"
H. H. Robertson, Pittsburgh, Penn.	"Stypol"
Rohm and Haas Company, Philadelphia, Penn.	"Paraplex" (P)
Westinghouse Electric Company, Pittsburgh, Penn.	"Fosterite"

NOTE: Permissible working voltage is a fraction of the dielectric strength. See discussion of safety factors, Chapter V.

Table A-24 TYPICAL ASPHALT POTTING COMPOUND DATA

Softening Point (R and B) degrees F. (A.S.T.M. E-28-42T)	245-255
Penetration at 77°F. (A.S.T.M. D5-49)	18-22
Percent Filler	53-55
Recommended pouring temperature, °F	400-425
Cold Flow Point, degrees F.	215-225
Thermal Conductivity (BTU. $hr.^{-1}$ $°F^{-1}$ $ft.^{-2}$ $in.^{-1}$)	2.35+
Specific Gravity at 77°F.	1.45-1.55
Flash Point °F (A.S.T.M. D92-46)	585+
Stain	Excellent
Adhesion to metal, black japanned surfaces, and component parts	Excellent

Table A-25 TYPICAL ASPHALT TREATING COMPOUND DATA

Softening Point (R and B) degrees C -- 70-80
Penetration 100 grams/25°C/5 seconds -- 10-18
Viscosity at 150°C (Centipoises) -- 250-270

Sources of Supply for Potting and Treating Compounds:

Asphalt (Insulating)
Mitchell-Rand Insulation Co., Inc., New York, N. Y.
Pioneer Asphalt Div. Witco Chemical Co., Chicago, Ill.
H. H. Robertson Company, Pittsburgh, Penn.
Solar Compounds Corp., Linden, New Jersey
Trumbull Asphalt Company, Summit, Illinois
Witco Chemical Company, New York, N. Y.
Zophar Mills Inc., Brooklyn, N. Y.

Waxes (Insulating)
Bareco Oil Co., Tulsa, Olkahoma or Philadelphia, Penn.
BiWax Corporation, Skokie, Illinois
Cities Service Oil Company, New York, N. Y.
International Wax Refining Corp., Brooklyn, N. Y.
National Wax Company, Chicago, Ill.
Solar Compounds Corp., Linden, N. J.
Wax Corporation of America, Brooklyn, N. Y.

Table A-26 PROPERTIES OF ADHESIVE TAPES WITH TREATED BACKINGS

Type of Backing	Thickness in Mils	Tensile Strength lb./in.	Elongation %	Adhesion oz./in. Width	Insulation Resistance Megohms	Dielectric Strength Volts	Electrolytic Corrosion Factor
Yellow Crepe (Purified Kraft)	9.5-10.0	20	12.0-12.5	25-35	35-50	1,500-1,800	0.85-0.90
Black Crepe (Purified Kraft)	9.5-10.0	20	12.0-12.5	25-30	35-50	1,500-1,800	0.85-0.90
Yellow Flat back (.004" Rope)	6.0-6.5	40	4.0-5.0	40-50	50	1,500-1,800	0.95
Black Flat back (.004" Rope)	6.0-6.5	40	4.0-5.0	40-50	50	1,500 1,800	0.95
White Extra Strength (.006" Rope)	9.0	50	5.0	50	10	1,800	0,85
White Super Strength (.0135 Rope)	17.0	75	12.0	50	10	2,000	0,85
Cotton Cloth	11.0	45	10.0	35-50	50	1,800	0.90
Acetate Film (.002" Clear or Yellow).	3.5	20	10	35-50	50,000-67,000	5,500-6,000	1.0
Acetate Cloth - Film (.00088 Film)	9.0	50	15	40	50,000	5,000	1.0
Acetate Cloth (White, black, brown, ivory).	8.5	40	20	35-50	50,000	1,800	1.0
Acetate Film - Fiber. (.00088 Film - .004 Rope Paper).	8.0-10.0	50	4.0 - 6.0	50	50-250	5,000	.095

For test procedures refer to A.S.T.M. Spec. No. D-100-48T

Sources of supply:

Industrial Tape Corporation, New Brunswick, New Jersey

Minnesota Mining and Manufacturing Co., St. Paul, Minnesota.

Table A-27 PROPERTIES OF PRESSURE SENSITIVE ELECTRICAL ADHESIVE TAPES - THERMO-SETTING OR HEAT CURING -

Type of Backing	Thickness in Mils	Tensile Strength lbs./in.	Elongation %	Adhesion Oz./in. Width	Insulation Resistance Megohms	Dielectric Strength Volts	Electrolytic Corrosion Factor
Acetate Cloth Film (.00088" Film)	9.0-9.5	50	15	35	30,000-50,000	5,000	1.0
Glass Cloth	7.0	150	7	20	5,000	1,800	.95
Acetate Cloth (White)	8.0-8.5	40	20	30-35	30,000-50,000	1,800	1.0
Cotton Cloth	11.0	45	10-12	30	50	1,800	.90
Tan Crepe Paper	9.5-11.0	20	12	25-35	35-50	1,500-1,800	.85-.90
Tan Flat Back Paper	6.0-6.5	40	4-5	35-50	50	1,500-1,800	.73-.90
Acetate Film	3.5	20	10	40	50,000-67,000	5,500-6,000	1.0
"Mylar A" Film	2.5	20	50		100,000	5,000	1.0

NOTE: Permissible working voltage is a fraction of the dielectric strength. See discussion of safety factors, Chapter V.

Table A-28 PROPERTIES OF DU PONT "MYLAR A" POLYESTER FILM

Temp. °C	60 Cycles Per Second		1 Kilocycle Per Second		1 Megacycle Per Second	
	Dielectric Constant	Dissipation Factor - %	Dielectric Constant	Dissipation Factor - %	Dielectric Constant	Dissipation Factor - %
0	3.02	0.5	2.99	0.80	2.79	1.6
25	3.02	0.21	3.01	0.47	2.83	1.9
75	3.02	0.14	2.99	0.12	2.95	1.7
100	3.08	0.69	3.06	0.46	3.01	1.4
125	3.36	1.2	3.29	1.4	3.15	1.7
150	3.46	0.64	3.45	0.68	3.31	2.0

DIELECTRIC STRENGTH AT 60 CPS

(Between 2" Disc Electrodes in Air)

°C	Volts Per Mil *
0	4400
25	4500
75	4200
100	4300
125	3250
150	3150

FILM PROPERTIES VS. TEMPERATURE

°C	Tensile Strength p. s. i.	Elongation %
-18	26,000	135
25	26,000	130
50	10,200	71
100	6,800	68
138	4,500	63
150	4,000	62
160	3,300	62

* Permissible working voltage is a fraction of the dielectric strength. See discussion of safety factors, Chapter V.

Table A-29 TYPICAL PROPERTIES OF 6 MIL THICK "SCOTCH-WELD" ELECTRICAL INSULATING FILM NO. 70

Property		Units	Method *	Uncured	Cured
Physical	Tensile Strength	lbs./sq.in.	D-1000-48T	2750	9700
	Elongation	%	D-1000-48T	200	6
	Specific Gravity	---	D-792	1.29	1.02
	Water Absorption (24 hrs. immersion)	%	D-570-42	15	3
	Water Vapor Permeability	gms/100in^2/24 hrs.	Similar to D-697-42T	6.00	3.60
	Thermal Conductivity	cal/sec/cm^2/°C/cm	Similar to D-325-31T	8×10^{-4}	5×10^{-4}
Electrical	Dielectric Strength (Short time)	Volts/mil	D-149-44	725	1750
	Insulation Resistance	ohms (1" width)	D-1000-48T	10^{10}	10^{11}
	Dielectric Constant 60 cycles	---	D-150-46T	5.59	2.28
	Power factor 60 cycles	---	D-150-46T	.305	.006
Chemical	The cured film possesses excellent resistance to weak acids and alkalies, oils, askarels, and aromatic hydrocarbons. It swells but does not dissolve in aliphatic hydrocarbons. The uncured film has fair resistance to all of these materials except the aliphatic hydrocarbons, in which it is soluble.				

* Unless indicated otherwise, tests were conducted by A.S.T.M. methods at room temperature; 70°F and 50% R.H.

Source of Supply: Minnesota Mining and Mfg. Co.
St. Paul 6, Minnesota

NOTE: Permissible working voltage is a fraction of the dielectric strength. See discussion of safety factors, Chapter V.

APPENDIX C - CORROSION IN MULTIPLE LAYER WOUND COILS

Every engineer designing coils for use in controls, transformers, reactors, relays, chokes and solenoids does everything he can to prevent open circuits. Analysis of service complaints and test records indicates that in coils making use of small diameter magnet wire, corrosion is still a major cause of open circuits, although considerable progress has been made in the last ten years in overcoming the problem. Corrosion within a coil can be any one of three types, namely chemical, electrolytic, or galvanic; or it is possible to have a combination of any two or even all three.

Chemical Corrosion

Chemical corrosion is disintegration of a conductor by the straight chemical reaction of an acid or alkali (usually in dilute concentration) on the copper. It is usually detected by greening and piling up of disintegration products at a localized point of the conductor, such as at the lead joint or at some rupture point in the film insulation on the wire. It is most common in an area where ingress of moisture is greatest. Moisture is necessary to produce chemical corrosion. Potential on a coil is not necessary; thus corrosion can occur during shelf storage, especially if the location of storage is in humid atmosphere, or goes through cycles of high humidity.

Capillary wicking, the process by which most of the water gets into a coil is well known, however the rapidity with which a coil will reach equilibrium is surprising. Coils, which from the standpoint of appearance, are thoroughly impregnated and coated and would seem to be impervious, become moisture loaded to equilibrium within a week. Once moisture is inside a coil structure it can leach out, dissolve and/or combine with salts, which exist in the component materials to form corrosive compounds which readily attack any bare copper in the structure. It is very common thing to have salts from perspiration present in a coil just from normal handling of the construction materials. Probably the worst material offender in Class A coils is paper. Residual salts from digesting the wood, sizing, and buffering agents offer excellent possibilities of producing corrosive compounds. Cotton cloth, pressure sensitive tapes, varnishes, and the film on the magnet wire inself are all potential sources of chemical corrosion.

Varnish treatments are sometimes the cause of chemical corrosion. Varnishes containing resins with high acid number are corrosive to bare copper, and attack before they are oxidized or polymerized. Drying oils used in varnishes can become acid in reaction with age, which in turn may produce corrosion within a coil. The pH value of dried varnish films will lower with age, and when in combination with moisture can form small amounts of acids which attack and corrode the conductor. It has been demonstrated , however, that insulating varnishes can be formulated that will not exhibit a lowering of pH value of the dried film with age.

Perhaps the most common source of chemical corrosion is that caused by the careless use of corrosive soldering fluxes, such as those containing zinc chloride and the use of strippers in removing formex films. It is absolutely necessary that all remaining flux and stripping agents be thoroughly removed from all joints if corrosion is to be avoided. Many a coil stored in a humid atmosphere has had badly corroded terminals and lead connections when removed from its package just because the excess soldering flux was not thoroughly removed after soldering operations.

For prevention of chemical corrosion, paper and cotton materials should have a neutral acid number or pH. If the coils are varnish treated, the characteristics of the varnish film after aging must be known, and assurance established that any acids or soaps formed will not be corrosive. As pointed out, ingress of moisture plays a most important part and any treatment, potting in compound, or sealing up that can be done on a coil will help guard against chemical corrosion. Airborne impurities, such as CO_2, acid, or alkali, and other fumes in small quantities which combine with moisture to form corrosive solutions should be shielded out by treatment or potting whenever it is possible to do so.

Electrolytic Corrosion

By far the most troublesome and complicated corrosion problem in multiple layer-wound coils is that caused by electrolytic action. This type of corrosion is readily produced in coils carrying D. C. potentials; in fact, electrolytic corrosion can almost be forgotten in A. C. coils. However, A. C. operated coils with D. C. currents superimposed on them, and coils having interrupted D. C. impressed on them are easy victims of this type

of corrosion, and the smaller the wire diameter the more serious the problem becomes.

The exact cause of electrolytic corrosion has been debatable for a long time, but one important fact has been definitely established and accepted. That is, that moisture must be present. One of the commonly accepted theories is that the moisture dissolves the salts or bases existing in the coil construction materials as impurities, thus forming electrolytes and establishing leakage paths between potential gradients within the coil. The current flowing in these leakage paths produces the well known plating action, in which positive ions are discharged on the negative electrode or cathode and negative ions are discharged on the positive electrode or anode. For every negative ion which flows to the positive electrode, a chemically equivalent amount of copper is taken away from the positive and eventually migrates or flows to the negative electrode. Thus, the positive electrode becomes pitted and shows a definite weight loss. Not all of the copper torn away from the positive electrode flows to the negative electrode. A portion of it remains, and when this is in contact with the carbon dioxide of humid air, it forms basic copper carbonate. This is the greening usually seen and which forms the basis for visually judging the amount of corrosion. It should be thoroughly understood, however, there can be no ion migration without current flow.

Leakage paths may be established over the surface of the coils from terminal to terminal, or through insulation from one conductor to another where potential gradients exist, or between conductor and frame through the insulation. Many corrosion failures have been located deep in a coil structure, far from outside surfaces, where a leakage path had formed between the copper of the conductor and ground.

To have current flow between wires or between wire and ground or terminal in a coil, it is necessary that the insulating film on the magnet wire be broken so that it is no longer a barrier to the potential impressed on it. Corrosion is frequently caused by minute nicks, or cracks in the film or the wire. This explains why many opens in coils, resulting from this type of corrosion, appear as a broken wire.

It may be noted that the factors for producing electrolytic corrosion are essentially the same as those producing chemical corrosion.

In 1937 the theory of electrochemical oxidation of cellulose as a cause of electrolytic corrosion was introduced. Many tests seem to substantiate this as a fact. Electrolytic corrosion will take place in a coil, making use of the purest forms of cellulose insulation, if a D. C. potential and moisture are present. This corrosion is the result of electrochemical oxidation. Cellulose such as paper or cotton will oxidize at the particular spot, where they contact minute areas of bare copper wire that carry a positive potential in respect to other wires in the coil. The oxidation products will combine with the moisture to form complicated organic acids, which are good electrolytes. These organic acids migrate within the coil and are readily ionizable. Once these organic acids are present, electrolytic action can take place. Control of electrolytic corrosion has been a problem for years and while there is still no control technique universally recognized, definite progress is being made in that direction. One point definitely certain is that not all materials are subject to electrolytic corrosion and that materials produce electrolytic corrosion in varying degrees. These facts seem to be borne out by all the methods used in evaluating electrolytic corrosion. At the present time, it seems evident that materials which are not subject to electrochemical oxidation and are not ionizable, are not subject to electrolytic corrosion. This permits a choice of materials in many cases.

Some of the materials that do not produce electrolytic corrosion are cellulose acetate, methylamathaculate, polysterene, polyethylene, acetate butyrate and Nylon. Materials which do produce this type of corrosion are kraft paper, rag paper, cotton cloth, tapes and sleevings, phenolic compounds and animal glues. In the case of paper and cloth, varnish treatments do not guarantee against corrosion of the electrolytic type, and a neutral pH is not a guarantee against electrolytic corrosion.

Galvanic Corrosion

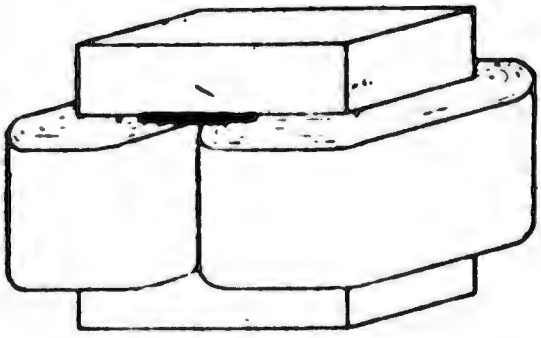
Galvanic corrosion is definitely significant and becomes of increasing importance with the introduction of aluminum wire as conductors. Galvanic corrosion can exist whenever a couple of dissimilar metals is made either by fusion or by use of a third metal such as solder. A necessary requirement is a bi-metal couple for producing galvanic corrosion is moisture, which

permits ion migration in the presence of a potential. A coil need not be energized to produce galvanic corrosion.

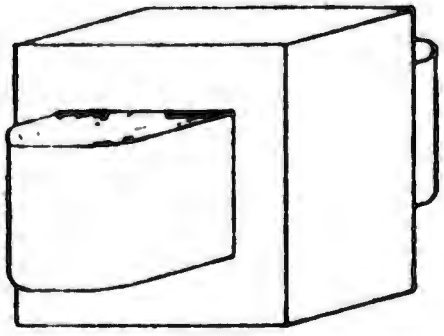
The degree of action depends on the relative position of one of the metals to the other in the electromotive force series of the elements. In the electromotive force series each element carries an electrode potential in respect to hydrogen which is referenced at zero. Any metal will replace any other metal in a salt below it in the series. The farther apart the metals are in the series the greater the potential is between them and in turn the greater the galvanic action if moisture is present. Thus a zinc-copper couple gives a greater E.M.F. than the zinc-lead couple or the iron-copper couple.

In all cases of bi-metal couples, potentials exist. With moisture present, an electrolytic cell is formed, and disintegration of one of the metals will take place. The amount and speed of disintegration depends on the electrolytes which the moisture forms and the potential difference between the two metals.

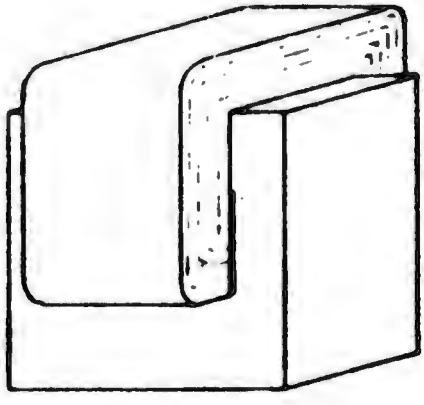
At the present time there is just one way to prevent galvanic corrosion in conductor couples: to shield moisture away from the actual joint by coating with a moisture proof varnish or compound. Varnish treatments on coils, while essentially put on for an entirely different purpose, has prevented much galvanic corrosion that might otherwise have been very troublesome.



a CORE TYPE

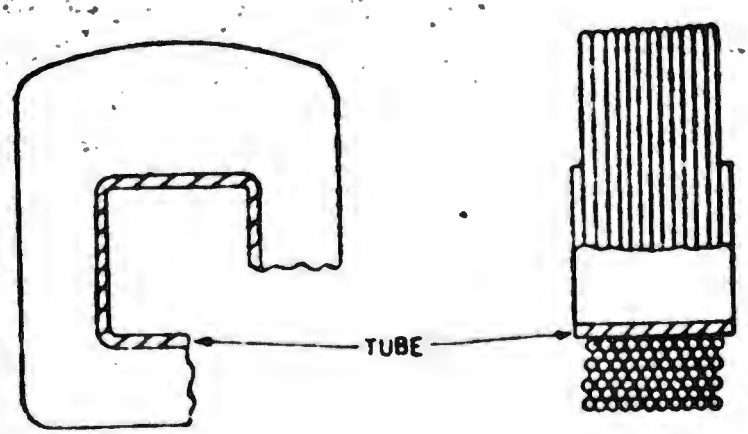


b SHELL TYPE

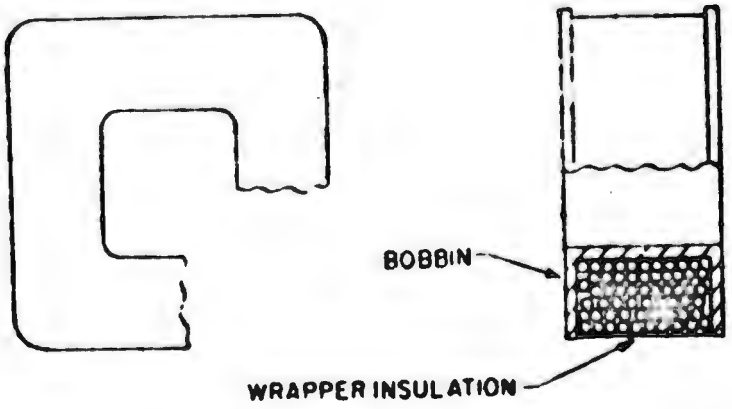


c SIMPLE TYPE

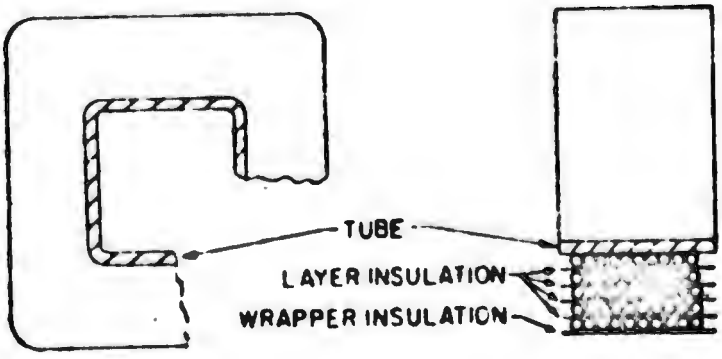
FIG 5 - BASIC TYPES OF CORE CONSTRUCTION



a. PRECISION-WOUND WINDING NOTE GREATER BUILD ON UPPER SIDE OF COIL RESULTING FROM CROSSOVER OF CONDUCTOR

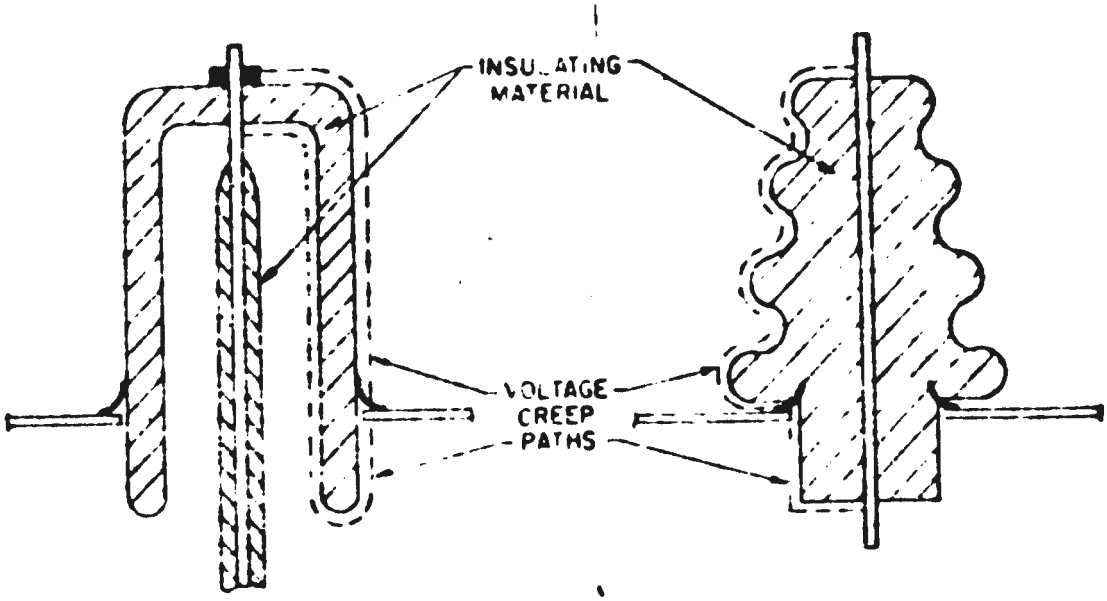


b. RANDOM-WOUND WINDING ON BOBBIN (NOTE RANDOM LAY OF CONDUCTOR)



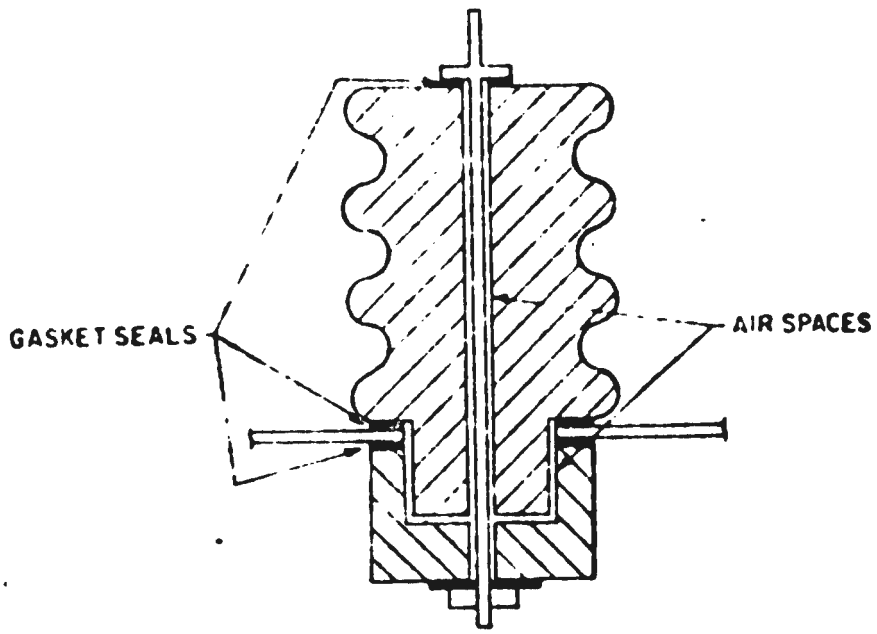
c LAYER-INSULATED WINDING

FIG 6 - TYPES OF WINDING CONSTRUCTION



a OIL-FILLED, DRAW-THROUGH LEAD BUSHING

b THROUGH-STUD BUSHING



c CERAMIC BUSHING

FIG 7 - TYPICAL BUSHINGS FOR HIGH VOLTAGE TRANSFORMERS

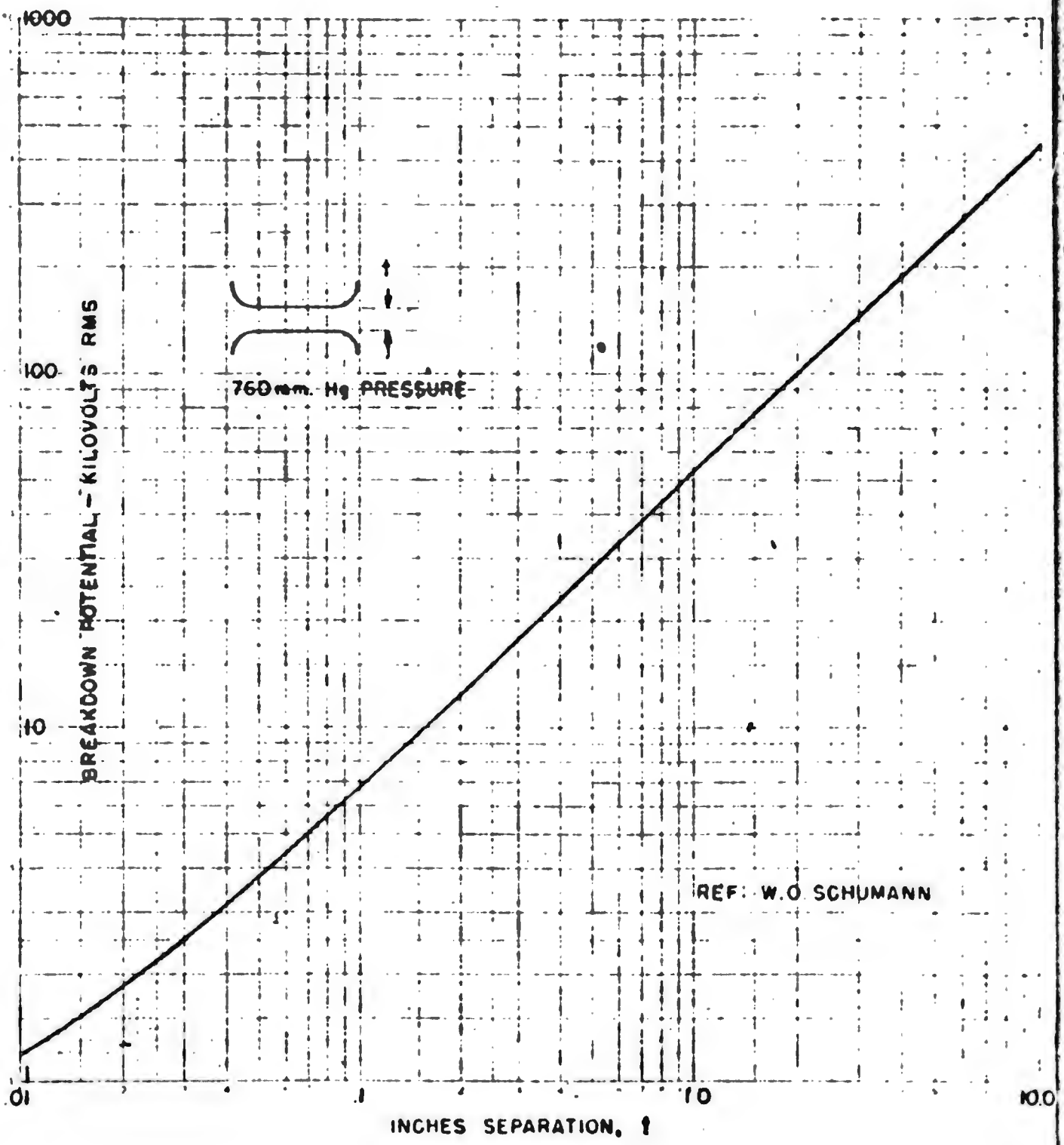


FIG. 8 - POTENTIAL BREAKDOWN IN AIR FOR PARALLEL PLANE ELECTRODES

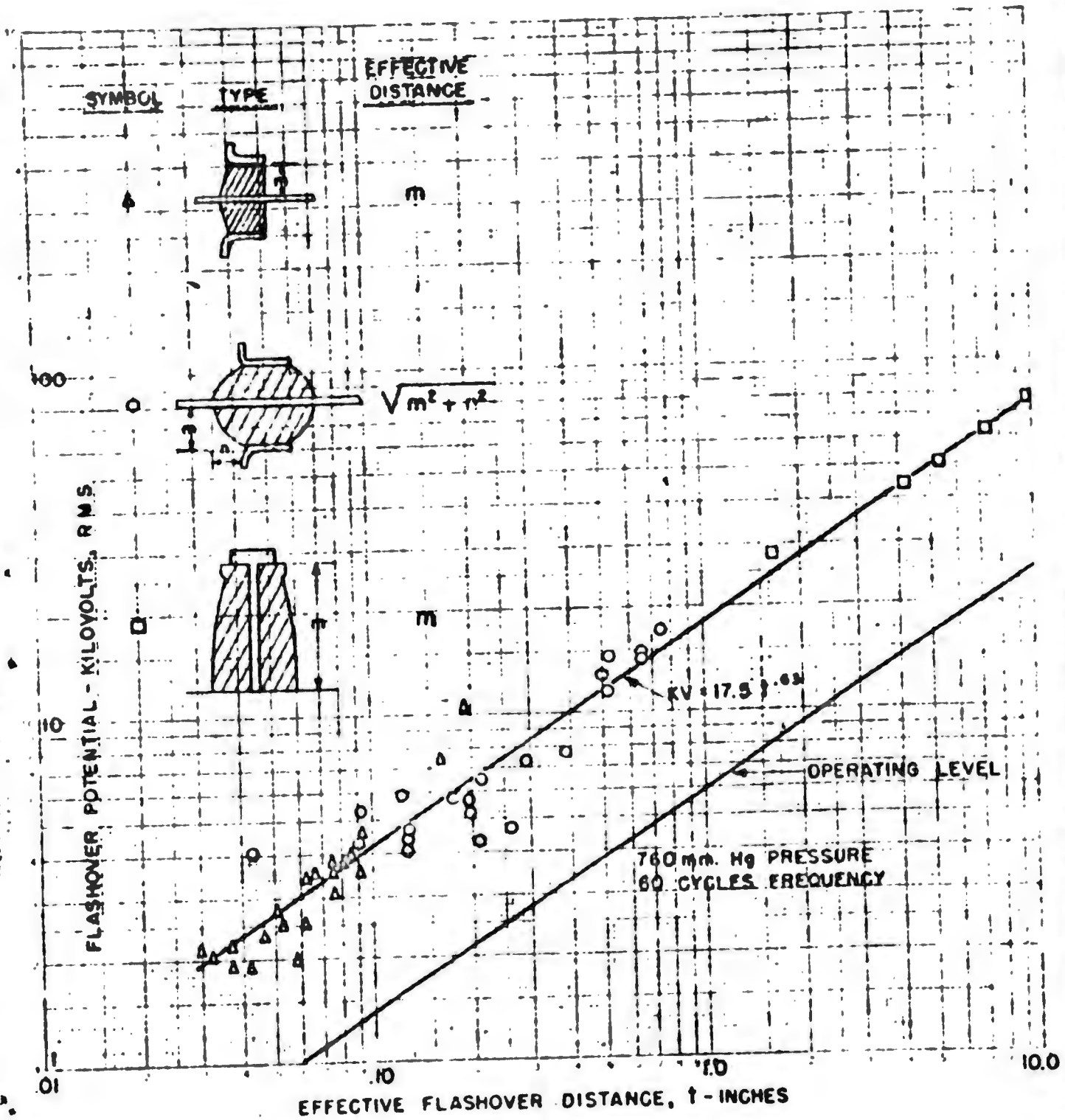


FIG 9 - INSULATION STRENGTH OF TYPICAL DRY BUSHINGS

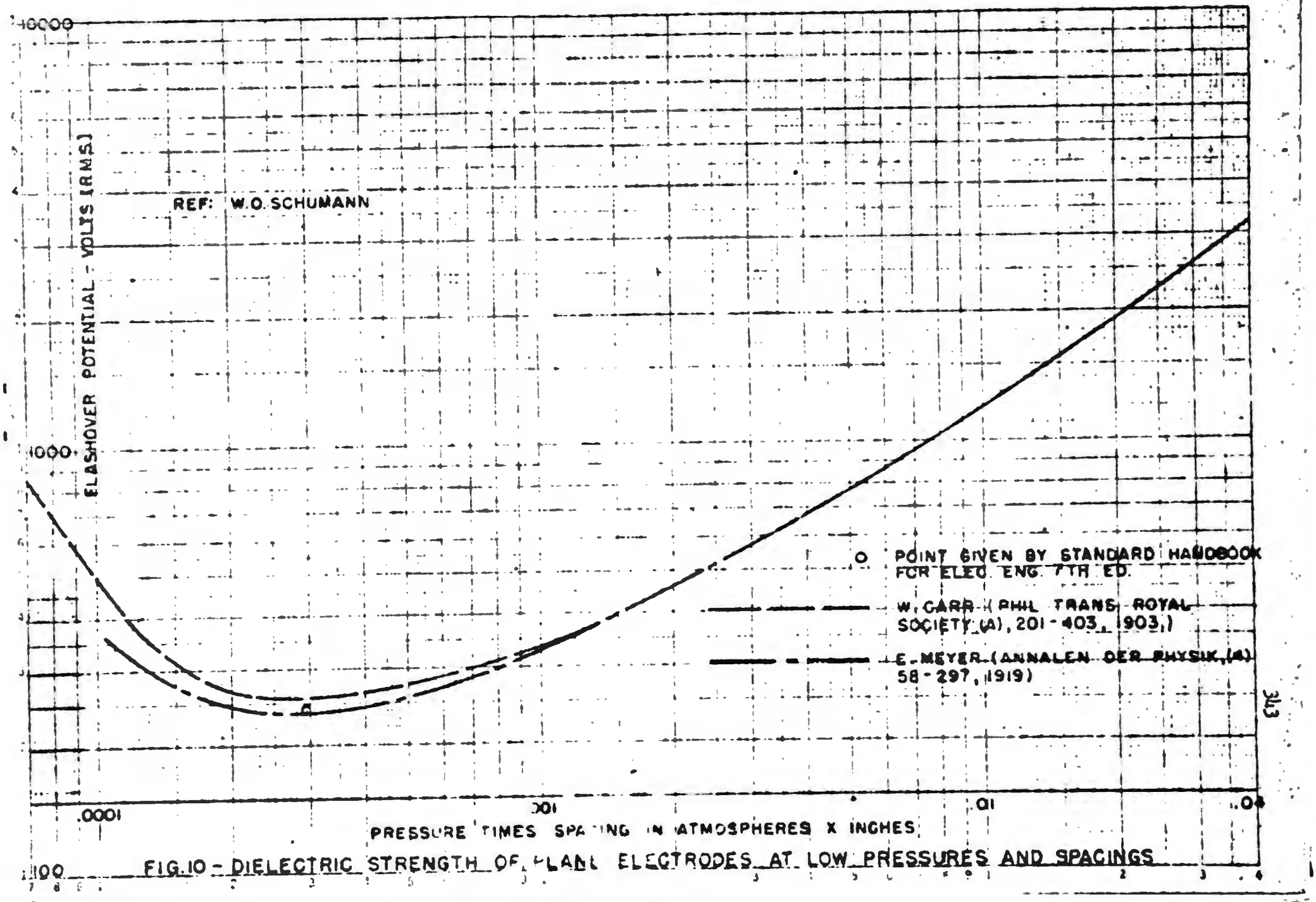


FIG. 10 - DIELECTRIC STRENGTH OF PLANE ELECTRODES AT LOW PRESSURES AND SPACINGS

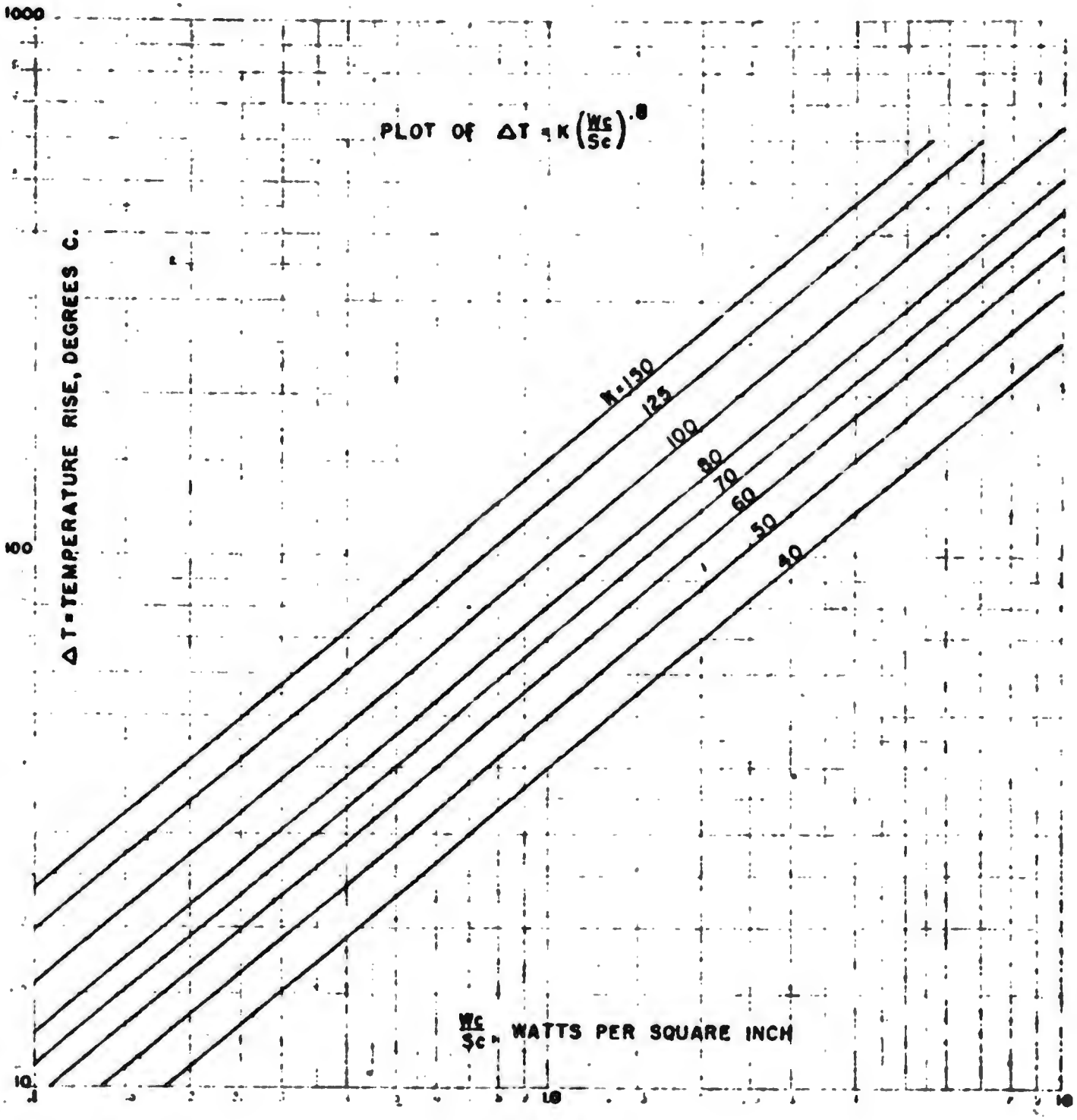


FIG. 37 – TEMPERATURE RISE AND WINDING DISSIPATION

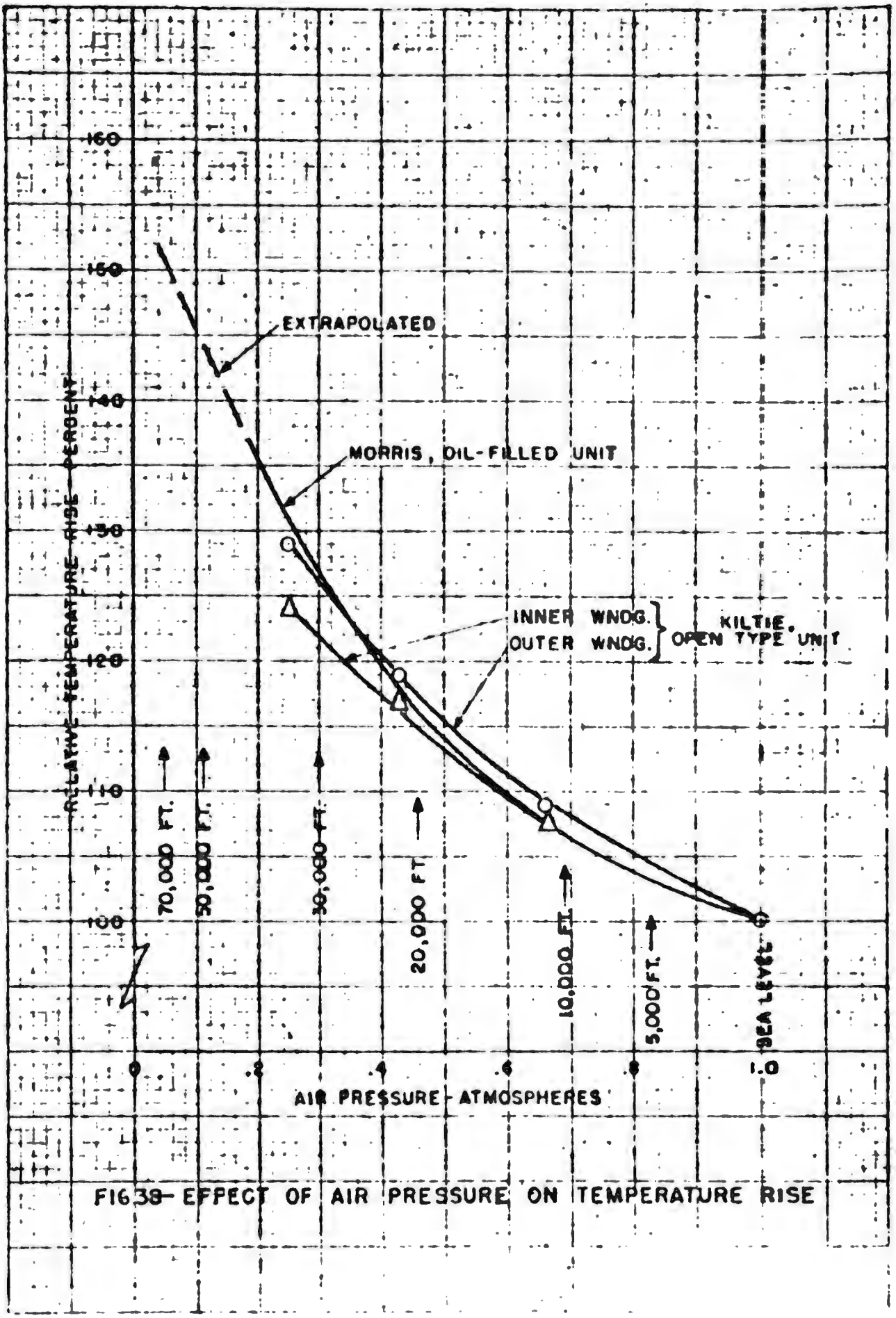


FIG 38- EFFECT OF AIR PRESSURE ON TEMPERATURE RISE

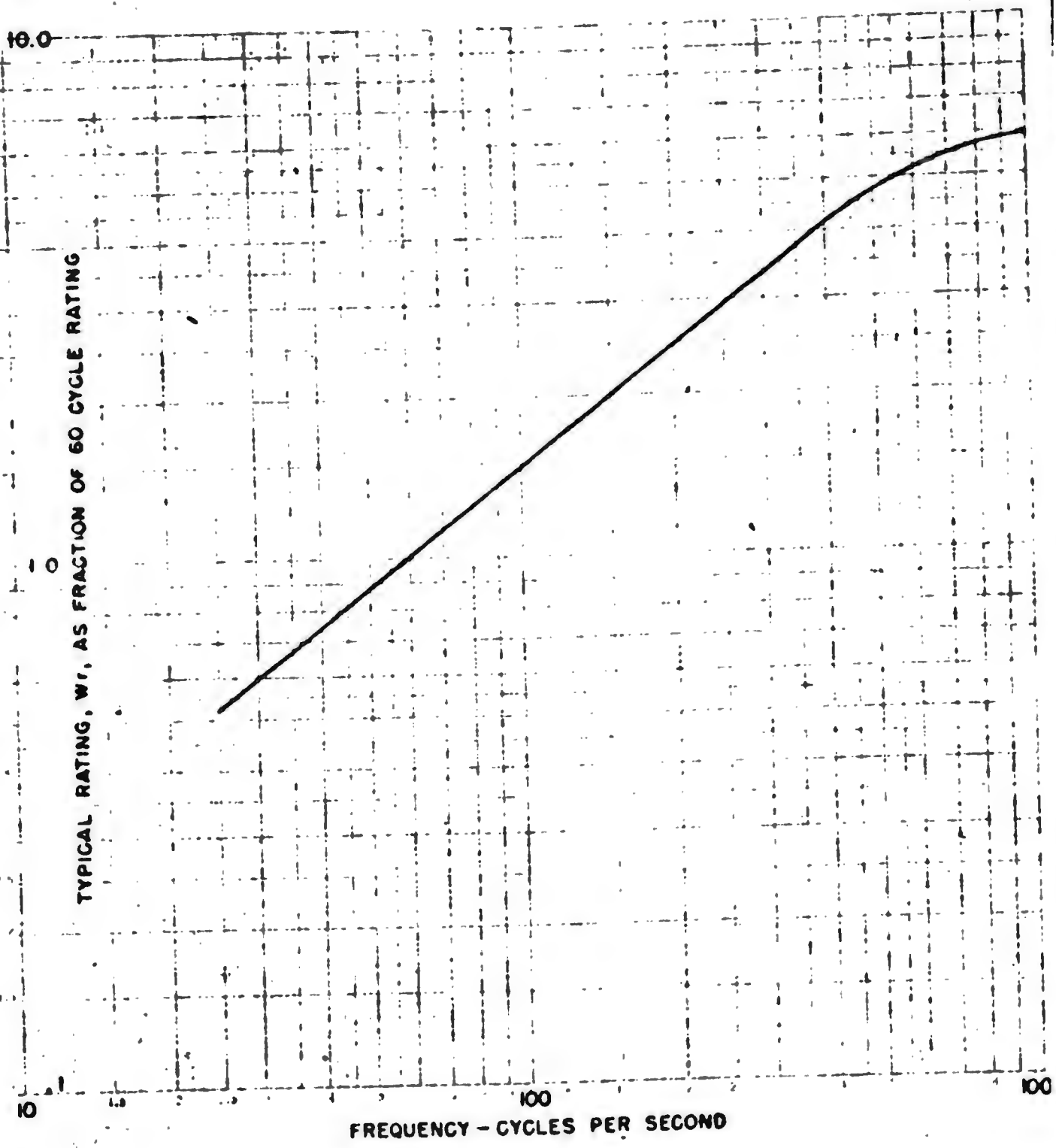


FIG. 39 - APPROXIMATE EFFECT OF FREQUENCY ON RATING FOR TRANSFORMERS HAVING THE SAME PHYSICAL SIZE

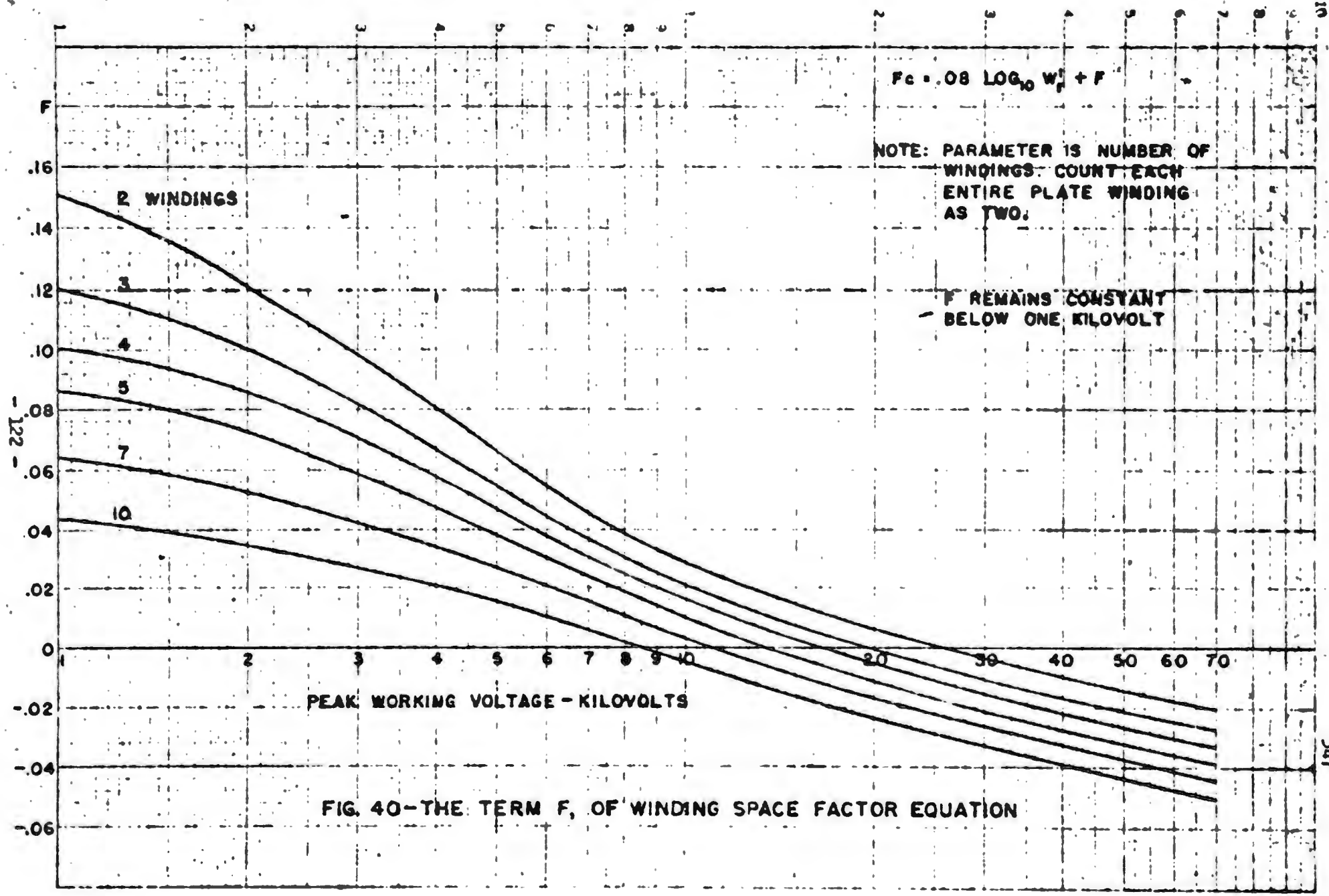
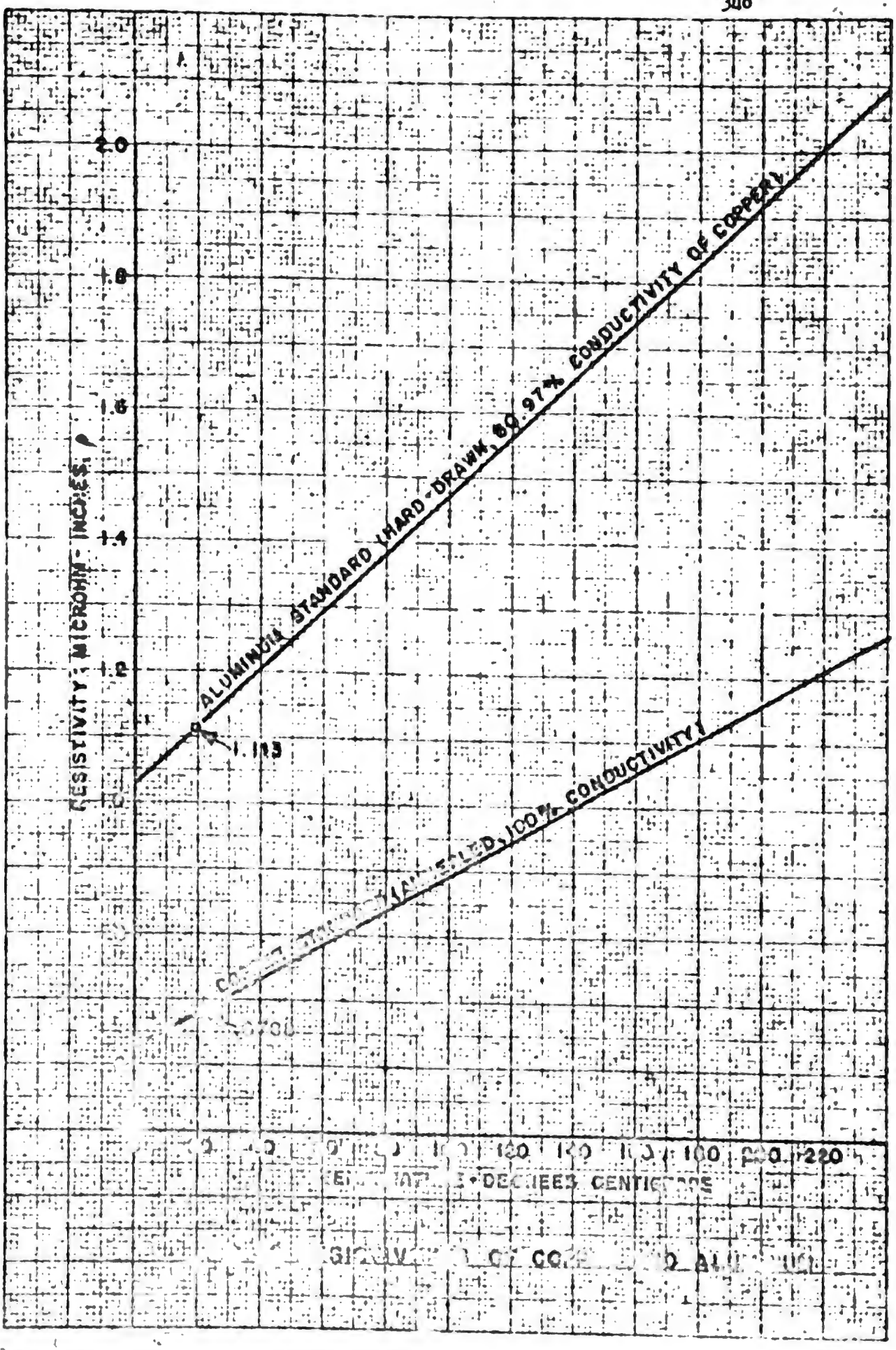
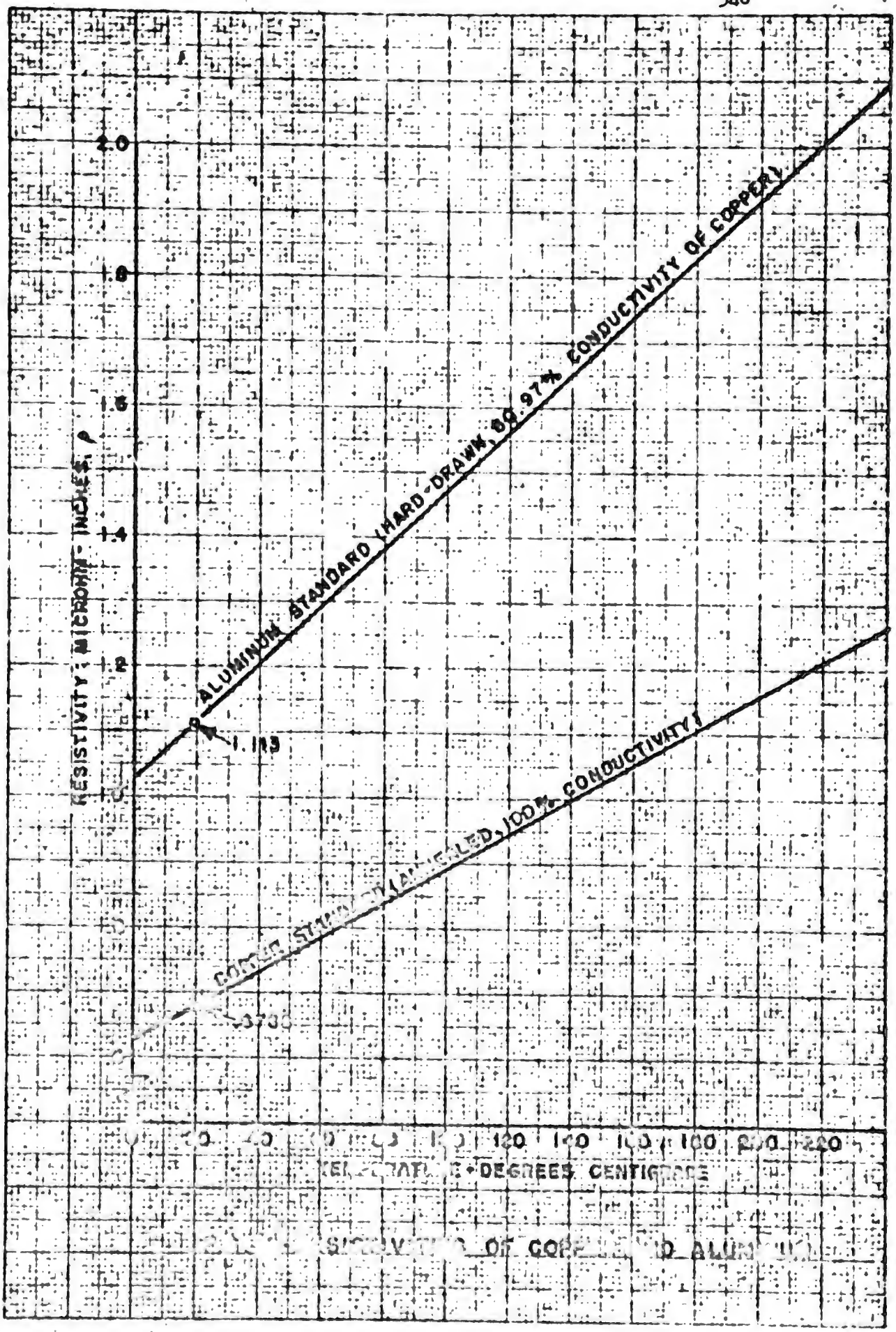


FIG. 40—THE TERM F, OF WINDING SPACE FACTOR EQUATION


RESISTIVITY, MICROHM-INCHES, ρ
2.0
1.8
1.6
1.4
1.2
ALUMINUM STANDARD HARD-DRAWN, @ 97% CONDUCTIVITY OF COPPER
1.113
ANNEALED, 100% CONDUCTIVITY
DEGREES CENTIGRADE



RESISTIVITY OF COPPER AND ALUMINUM

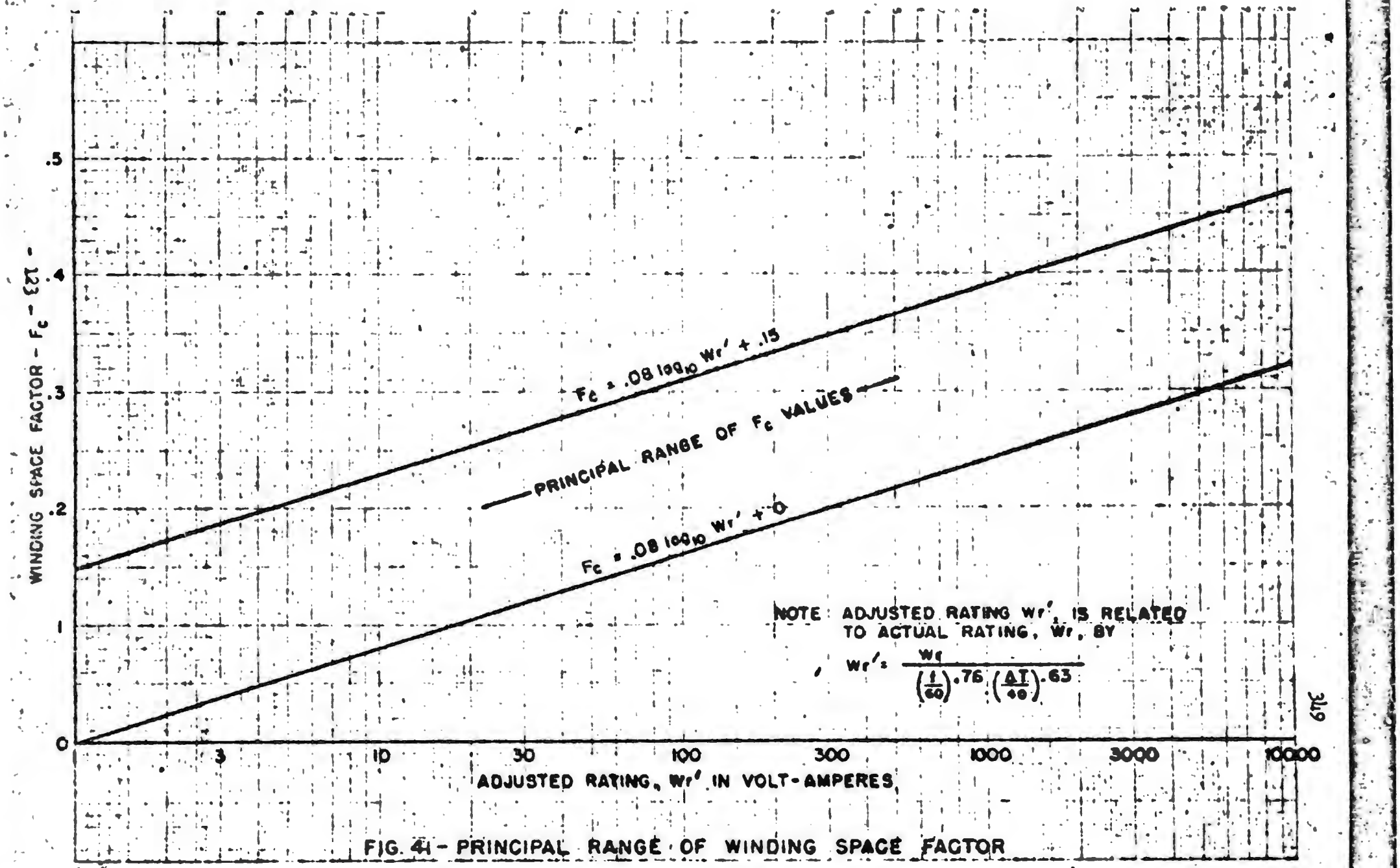


FIG. 41 - PRINCIPAL RANGE OF WINDING SPACE FACTOR

AD 64525

Armed Services Technical Information Agency

Reproduced by

DOCUMENT SERVICE CENTER

KNOTT BUILDING, DAYTON, 2, OHIO

Because of our limited supply, you are requested to
RETURN THIS COPY WHEN IT HAS SERVED YOUR PURPOSE
so that it may be made available to other requesters.
Your cooperation will be appreciated.

NOTICE: WHEN GOVERNMENT OR OTHER DRAWINGS, SPECIFICATIONS OR OTHER DATA ARE USED FOR ANY PURPOSE OTHER THAN IN CONNECTION WITH A DEFINITELY RELATED GOVERNMENT PROCUREMENT OPERATION, THE U. S. GOVERNMENT THEREBY INCURS NO RESPONSIBILITY, NOR ANY OBLIGATION WHATSOEVER; AND THE FACT THAT THE GOVERNMENT MAY HAVE FORMULATED, FURNISHED, OR IN ANY WAY SUPPLIED THE SAID DRAWINGS, SPECIFICATIONS, OR OTHER DATA IS NOT TO BE REGARDED BY IMPLICATION OR OTHERWISE AS IN ANY MANNER LICENSING THE HOLDER OR ANY OTHER PERSON OR CORPORATION, OR CONVEYING ANY RIGHTS OR PERMISSION TO MANUFACTURE, USE OR SELL ANY PATENTED INVENTION THAT MAY IN ANY WAY BE RELATED THERETO.

UNCLASSIFIED